Respiratory Monitoring in Mechanical Ventilation

Techniques and Applications

Jian-Xin Zhou
Guang-Qiang Chen
Hong-Liang Li
Linlin Zhang
Editors

Springer

Respiratory Monitoring in Mechanical Ventilation

Jian-Xin Zhou • Guang-Qiang Chen
Hong-Liang Li • Linlin Zhang
Editors

Respiratory Monitoring in Mechanical Ventilation

Techniques and Applications

Springer

Editors
Jian-Xin Zhou
Department of Critical Care Medicine
Beijing Tiantan Hospital
Capital Medical University
Beijing
China

Guang-Qiang Chen
Department of Critical Care Medicine
Beijing Tiantan Hospital
Capital Medical University
Beijing
China

Hong-Liang Li
Department of Critical Care Medicine
Beijing Tiantan Hospital
Capital Medical University
Beijing
China

Linlin Zhang
Department of Critical Care Medicine
Beijing Tiantan Hospital
Capital Medical University
Beijing
China

ISBN 978-981-15-9769-5 ISBN 978-981-15-9770-1 (eBook)
https://doi.org/10.1007/978-981-15-9770-1

This Springer imprint is published by the registered company Springer Nature Singapore Pte Ltd.
The registered company address is: 152 Beach Road, #21-01/04 Gateway East, Singapore 189721, Singapore

Contents

Part I
Techniques for Respiratory Monitoring

Chapter 1
Gas Exchange

Kun-Ming Cheng, Linlin Zhang, Xiu-Mei Sun, and Yu-Qing Duan

1.1 Partial Pressure of Oxygen and Derived Parameters

Respiratory gas exchange refers to the exchange of oxygen and carbon dioxide between alveoli and blood, blood and tissue. The former is lung ventilation, the latter is tissue ventilation. This exchange is a direct diffusion process, which refers to the transfer of gas molecules from the higher pressure side to the lower pressure side. The power of gas diffusion is the difference in gas partial pressure.

1.1.1 The Process of Gas Exchange

Under normal circumstances, the partial pressure of oxygen in the alveoli is higher than that in venous blood, while the partial pressure of carbon dioxide in the alveoli is lower than that in venous blood. Therefore, when the venous blood in the pulmonary artery passes through the pulmonary capillaries, oxygen diffuses from the alveoli to the blood, and carbon dioxide diffuses from the venous blood to the alveoli driven by the partial pressure difference. As a result, the content of oxygen in venous blood increases, the content of carbon dioxide decreases, and venous blood is transformed into arterial blood. The diffusion of oxygen and carbon dioxide between the blood and the alveoli can be balanced in 0.3 s. It usually takes about 0.7 s for blood to be available through the pulmonary capillaries. Therefore, when venous blood passes through the pulmonary capillaries, there is sufficient time to complete the gas exchange. When arterial blood passes through the

K.-M. Cheng · L. Zhang (✉) · X.-M. Sun · Y.-Q. Duan
Department of Critical Care Medicine, Beijing Tiantan Hospital, Capital Medical University, Beijing, China

J. Zhou et al. (eds.), *Respiratory Monitoring in Mechanical Ventilation*,
https://doi.org/10.1007/978-981-15-9770-1_1

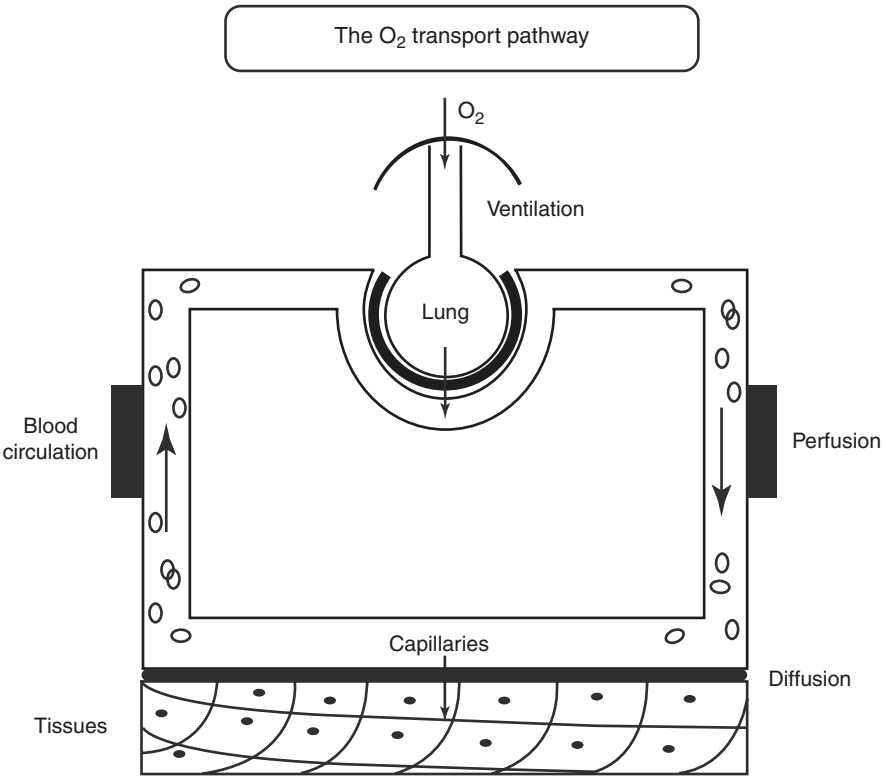

Fig. 1.1 Schematic of the O_2 transport pathway

pulmonary capillaries, tissue cells absorb and utilize oxygen and diffuse the resulting carbon dioxide into arterial blood, turning arterial blood into venous blood (Fig. 1.1) [1].

1.1.2 Partial Pressure of Oxygen and Derived Parameters

1.1.2.1 Transport of Oxygen

Oxygen can be transported in two ways: physical dissolution and chemical combination. Although oxygenated hemoglobin formed by the combination of oxygen and hemoglobin is the major transport mode of oxygen, the physical dissolution of oxygen directly determines the partial pressure of oxygen and affects the content of oxygenated hemoglobin. It also determines the difference of oxygen partial pressure between blood and tissue, which affects the absorption and utilization of oxygen by cells.

Partial Pressure of Oxygen (PO_2)

Oxygen partial pressure is an important factor in gas dispersion and transportation. Partial pressure refers to the partial pressure occupied by a certain gas in a mixed gas, or also the partial pressure produced by the physical dissolution of a certain gas in a liquid.

Partial Pressure of Oxygen in Inhaled Gas (PIO_2)

At sea level, the oxygen content in the air is 20.9%, the atmospheric pressure is 760 mmHg, and the water vapor pressure is 47 mmHg at 37 °C, so the PIO_2 of the human body is 149 mmHg($PIO_2 = (760–47)\times 20.9\%$).

Alveolar Partial Pressure of Oxygen (PAO_2)

It is impossible for a normal person to exhale all the gas in the alveoli. When exhaling, there is always some residual gas in the lungs. When inhaled gas enters the alveoli, it must be mixed with this residual gas, resulting in a decrease in the partial pressure of oxygen. Therefore, in order to estimate the partial pressure of oxygen in the alveoli, the following formula is used:

$$\mathrm{PAO_2} = \mathrm{FiO_2}\left(760 - 47\right) - 1/R\left(\mathrm{PACO_2}\right)$$

where R is the respiratory exchange ratio, which is equal to 0.8 most of the time [2].

Arterial Partial Pressure of Oxygen (PaO_2)

Partial pressure of oxygen in arterial blood refers to the pressure produced by physically dissolved oxygen molecules in plasma. It is an important index to reflect the oxygen situation of the body, and it can be used to judge hypoxia and its degree. However, when using PaO_2 for assessment, it is necessary to determine the inspired concentration of oxygen.

Reference value: Under normal circumstances (at sea level), it is equivalent to 80–100 mmHg (10.6 ~ 13.3 kPa). A variety of physiological factors affect PaO_2, such as age, body mass index, posture, altitude and so on. A prediction equation of PaO_2 for the population of life- long nonsmoking subjects, aged 40–74 years, with normal pulmonary function is given below [3]

$$\mathrm{PaO_2}\left(\mathrm{mmHg}\right) = 143.6 - \left(0.39 \times \mathrm{age}\right) - \left(0.56 \times \mathrm{BMI}\right) - \left(0.57 \times \mathrm{PaCO_2}\right) \pm 5.5$$

Clinical significance: Under normal circumstances, there is also a right-to-left physiological shunt in the lung, and the uneven distribution of intrapulmonary ventilation blood flow caused by gravity, PaO_2 is lower than PAO_2.

PaO_2 is mainly used to determine whether hypoxia exists, and helpful in evaluating the severity of hypoxia. Those whose PaO_2 is lower than the normal value of the same age is called hypoxemia. When the air is inhaled without extra oxygen, if PaO_2 <60 mmHg, the respiration may be decompensated, which is the criterion for the diagnosis of respiratory failure. If PaO_2 <40 mmHg, severe hypoxia occurs. If PaO_2 <20 mmHg, aerobic metabolism cannot be carried out normally, life is difficult to be supported.

Arterial Oxygen Saturation (SaO_2)

Arterial oxygen saturation refers to the ratio of the combined oxygen to the maximum amount of oxygen that can be combined in arterial hemoglobin, which reflects the actual combination of arterial oxygen and Hb.

$$SaO_2 = \frac{\text{Actual Hb combined with } O_2}{\text{Total Hb available for binding with } O_2} \%$$

Reference value: 95% ~ 98%

Clinical significance: The determination of SaO_2 is helpful for the differentiation of hypoxia. In anoxia, due to lack of oxygen supply, PO_2 decreased and SaO_2 decreased, which is common in pulmonary ventilation and pulmonary ventilation dysfunction.

If there is hypoxia and SaO_2 is normal, it suggests a decrease in effective hemoglobin, such as abnormal hemoglobin disease. Because at this time the effect hemoglobin itself, no longer anoxic conditions, can play the maximum oxygen binding capacity. Therefore, although the partial pressure of oxygen is low, the arterial oxygen saturation does not decrease. Therefore, use of SaO_2 to identify whether the body is anoxic has the potential risk of concealing hypoxia. Additionally, there is no obvious change of SpO_2 when PaO_2 is above 60 mmHg since the oxygen dissociation curve reaching the plateau. At this stage, even if there is a significant change in PaO_2, the increase or decrease of SaO_2 is very small. Therefore, during mild hypoxia, although PaO_2 has decreased significantly, SaO_2 may not change significantly [3].

PaO_2/FiO_2

Oxygenation index refers to the ratio of arterial blood oxygen partial pressure to inhaled oxygen concentration.

Reference value: Its normal range is 400 ~ 500 mmHg (53.13 ~ 66.67 kPa). The average normal value is 100/0.21 = 480 mmHg

Clinical significance: PaO_2/FiO_2 is commonly used for diagnosis of lung injury (acute respiratory distress syndrome (ARDS) and transfusion-related acute lung injury), the assessment of course and therapy in pulmonary disease, and the evaluation of donor lungs and clinical outcome pulmonary transplantation for [4].

To a certain extent, PaO_2/FiO_2 eliminated the effect of oxygen concentration on PaO_2, and reflect the ventilation function of the lung under the condition of oxygen therapy.

PaO_2/FiO_2 can be used to exclusive categories of ARDS [5]:

Alveolar-Arterial Oxygen Partial Pressure ($P_{(A\text{-}a)}\ O_2$)

Alveolar-arterial oxygen partial pressure difference refers to the difference between alveolar oxygen partial pressure and arterial oxygen partial pressure, also known as the alveolar-arterial oxygen difference. The alveolar-arterial oxygen difference of oxygen is a direct index for evaluating pulmonary gas exchange.

Calculating formula: $P_{(A-a)}O_2 = PAO_2 - PaO_2$

Reference value: The average value is 8 mmHg (1.07 kPa), ranging from 5 to 10, in healthy people younger than 30 years. It will reach 24 mmHg (3.20 kPa) at the age of 60–80 years. As age increases, $P_{(A\text{-}a)}\ O_2$ rises in a linear manner [6]

Clinical significance: $P_{(A\text{-}a)}\ O_2$ is an index to judge whether the function of gas exchange in the lung is normal or not. There are three main factors that affect $P_{(A\text{-}a)}\ O_2$: anatomical shunt, imbalance of ventilation and perfusion ratio, and diffusion disorder of alveolar-capillary barrier [7].

Therefore, the changes in oxygen concentration, intrapulmonary blood flow rate, prolonged inspiratory time, and positive end-expiratory pressure can result in the change of $P_{(A\text{-}a)}\ O_2$. The greater the difference of $P_{(A\text{-}a)}\ O_2$ is, the greater the difference of oxygen content between arterial blood and alveoli will be, which suggests the impaired diffusion function of the lung. Ventilatory dysfunction often results in an increase of $P_{(A\text{-}a)}\ O_2$ difference, such as chronic obstructive pulmonary disease. In all, the oxygen partial pressure difference of the alveolar artery comprehensively reflects the function of the ventilation and diffusion in the lung [8–11].

Arterial Oxygen Content (CaO_2)

The content of oxygen in arterial blood refers to the sum of the amount of physical solution and chemical binding of oxygen in each artery blood.

Reference value: 8.55 ~ 9.45 mmol/L

Clinical significance: CaO_2 is an index to reflect the content of red blood cells and plasma. The decrease of CaO_2 may be due to the decrease of hemoglobin, the decrease of blood oxygen saturation, or the decrease of PO_2. The normal content of oxygen in arterial blood cannot rule out tissue hypoxia.

1.2 Pulse Oximetry

1.2.1 Introduction

The pulse oximeter is one of the most widely used monitoring techniques in medicine to evaluate human health. Since the mid-1980s, when it began to be used in clinical practice, it has been widely used as a routine measure of arterial hemoglobin saturation in the fields of anesthesia, critical care, emergency, and respiratory medicine, because of its noninvasive, accurate, and real-time monitoring of pulse oxygen saturation (SpO_2) [12]. The reliability and accuracy of reflecting real arterial hemoglobin saturation (SaO_2) have been reliably verified. This technique contributes to the early diagnosis and treatment of hypoxia, which is lower in incidence and severity than in patients without an oximeter. Pulse oximetry has revolutionized modern medicine with its ability to continuously and transcutaneously monitor the functional oxygen saturation of hemoglobin in arterial blood. Pulse oximetry is so widely prevalent in medical care that it is often regarded as a fifth vital sign.

1.2.2 Principles of Pulse Oximetry

Pulse oximetry is commonly used to assess SpO_2 and heart rate, which is made up of an optical spectrometer and a plethysmograph. The working principle of the pulse oximeter is spectral analysis, that is, the unique light absorption characteristics of the solution are used to detect and quantify the components in the solution [13]. There is a significant difference between the absorption spectra of hemoglobin (Hb) and Oxygenated hemoglobin (HbO_2) in the range of red to near-infrared wavelengths. In the process of measuring blood oxygen saturation, the working principle of pulse oximetry is mainly divided into two kinds, which is mainly according to the type of light received by the photoelectric sensor, that is, transmitted light and reflected light, that is, light is emitted to the medium, and then reflected and transmitted respectively, propagate the signal, collect the signal through the photoelectric principle, and process the collected signal accordingly, and finally feedback the result. Two circuit schematic diagrams reflect the acquisition principles of these two methods (Fig. 1.2) [14].

In addition, the pulsation of the human arteries can cause changes in blood flow in the test site, which can cause changes in light absorption. Light absorption in non-blood tissues (skin, muscle, bone, etc.) is usually considered constant. Pulse oximetry measurement technology determines blood oxygen saturation by detecting changes in light absorption caused by blood volume fluctuations and eliminating the effects of non-blood tissues [15].

Fig. 1.2 Measurement setup for reflection and transmission

1.2.3 Method of Application

With the wide application of pulse oximetry in clinical practice, the methods of its application have gradually diversified. Although traditional finger-cuff or finger-type pulse oximetry is still commonly used at the bedside, other forms of pulse oximetry have been developed based on clinical requests, such as portable pulse oximetry, nocturnal oximetry, wearable pulse oximetry, hand-held pulse oximetry, and so on. Although the shapes of pulse oxygen monitors are different, the application methods are basically the same.

Although the pulse oximetry is easy to operate, there are still some details that we need to pay attention to. We need to connect the sensor to the appropriate position of the patient's body, preferably at the same height as the heart. We cannot place sensors on limbs with arterial or intravenous catheters and blood pressure cuffs. Meanwhile, the right adult, child, and newborn status should be set. Use in high humidity environments should be avoided as far as possible. It should be used in non-strong light. If you need to monitor under strong light such as surgical light, bilirubin light, sunlight, etc., cover the probe with an obstacle. It is best to change the measuring position every 3 h to avoid the disturbance of blood circulation caused by long-term wearing on the fixed fingers and affect the measurement accuracy.

Protect sensors and cables from sharp objects.

1.2.4 Clinical Application of Oximetry

Pulse oximetry can be performed by trained personnel in a variety of environments, including (but not limited to) hospitals, clinics, and families. The following is a summary of the application of pulse oximetry in different clinical conditions [16].

1. When the spot SpO_2 is checked in ED, primary care, outpatient observation (e.g., rehabilitation, oxygen clinic, preflight assessment, and others), those features or issues should be considered:
   1.1. Set long averaging times to minimize motion artifact.
   1.2. Pulsatile waveform display useful for checking signal quality.
   1.3. Select most appropriate sensor/site (e.g., finger/ear probe).

2. When the nocturnal breathing disorders are detected in the sleep laboratory, those features or issues should be considered:

    2.1. Use oximeter in “sleep” mode or with alarms disabled.
    2.2. Set averaging time to 3 s or less.
    2.3. Set date sampling and storage rate to minimum of 10 Hz.
    2.4. Ability to output date in real-time to capture on polysomnography system.

3. When nocturnal breathing disorders are detected in the home setting, those features or issues should be considered:

    3.1. Use oximeter in “sleep” mode or with alarms disabled.
    3.2. Set averaging time to 3 s or less.
    3.3. Set date sampling and storage rate to minimum of 1 Hz.
    3.4. Adequate date storage capacity (minimum of 8 h).
    3.5. Download/analysis software required for report generation.

4. Adult clinical monitoring in intensive or high-dependency care should consider those features or issues:

    4.1. Consider ABG sampling to assess $PaCO_2$, pH, and Hb status.
    4.2. Select oximeter with good motion artifact rejection.
    4.3. Consider using central sensor site.
    4.4. Set alarm levels appropriate for individual patient.

5. Pediatric clinical monitoring in neonatal intensive, high-dependency care should consider those features or issues:

    5.1. Select oximeter with good motion artifact rejection.
    5.2. Consider using central sensor site.
    5.3. Set alarm levels appropriate for individual patient.

6. When performing the screening or titration for supplemental oxygen in the outpatient clinic, domiciliary care, primary care, the pulse oximetry should set long averaging times to minimize motion artifact.
7. When detecting the exercise desaturation in an exercise laboratory or pulmonary rehabilitation, the following features or issues should be considered:

    7.1. Consider using central sensor site.
    7.2. Select oximeter with good motion artifact rejection.
    7.3. Set averaging time at medium to long (balance between motion artifact sensitivity and rapid desaturation detection).

8. When performing noncritical monitoring of hospital ward, the following features or issues should be considered:

    8.1. Set long averaging times to minimize motion artifact.
    8.2. Set alarm levels appropriate for individual patient.

9. When performing perioperative monitoring of oxygenation in the operating theater or recovery room, the alarm levels appropriate for individual patient should be set.

The use of pulse oximetry has revolutionized the monitoring of respiratory function, especially considering that multiple or continuous measurement results can be obtained quickly and noninvasively.

In general, pulse oxygen measurement plays an important role in the monitoring and treatment of respiratory diseases by detecting hypoxemia, guiding titration of oxygen supplementation and other treatments (such as stopping support ventilation), and reducing the need for blood gas analysis.

The monitoring of blood oxygen saturation during exercise is a standard part of pulmonary function rehabilitation. The easiest way to prove oxygen saturation during exercise is to use a pulse oximeter, which is usually done in the exercise lab during diagnostic tests. During exercise training, it is carried out in a physiotherapeutic environment (especially as part of a lung rehabilitation program).

Pulse oxygen saturation measurement plays a central role in the diagnosis of sleep-related respiratory disorders, especially obstructive sleep apnea (OSA), which is a key component of nocturnal polysomnography. OSA usually shows characteristic repetitive oxygen desaturation and then saturates again at night, so pulse oxygen saturation is increasingly used as a tool for screening OSA in family environments. Family nocturnal pulse oxygen measurement records can be analyzed and calculated [17].

In addition, pulse oximetry also has a unique position in pediatrics. Routine pulse oximetry has been reported as an additional screening test that can potentially improve the detection level of critical congenital heart defects (CCHD). During delivery, fetal pulse oxygen saturation can be measured using a probe inserted through the mother's vagina [18].

1.2.5 Limitations of Pulse Oximetry and Technological Update

The pulse oximetry cannot determine the adequacy of ventilation. In fact, there is evidence that patients with impaired ventilation may show normal saturation in the presence of life-threatening hypercapnia during oxygen inhalation. In order to correctly explain the results, it is necessary to recognize the inherent limitations of pulse oximeter in different clinical environments [19, 20]. Measurement artifact may occur for a variety of reasons, including motion artifact, nail polish, skin pigmentation, low perfusion state (e.g., low cardiac output, vasoconstriction, or hypothermia), use of intravenous dyes, and anemia [15].

1.2.5.1 Dyshemoglobin and Multiwavelength Pulse Oximetry

In addition to HbO_2 and Hb, adult blood may contain dyshemoglobin: hemoglobin derivatives, which do not work because they do not bind oxygen molecules inversely at the physiological level of PaO_2 in the blood, such as methemoglobin (MetHb) and carboxyhemoglobin (COHb). They are common in normal people, but at low concentrations. Functional SaO_2 is defined as the percentage of HbO_2 in the sum of

HbO_2 and Hb, while fractional SaO_2 is defined as the percentage of HbO_2 relative to the total number of four hemoglobin types. In low concentrations of methemoglobin, the difference between the two parameters is not significant, but at a high enough level, both functional and fractional readings may be compromised.

The traditional pulse oximeter uses two wavelengths of light to evaluate blood oxygen saturation, assuming that the only absorbers of these two wavelengths of light in the blood are HbO_2 and Hb. Because MetHb and COHb also absorb light within the wavelength range used in pulsed blood oxygen measurement, there will be errors in the measurement of SpO_2 in the presence of these hemoglobin. Some manufacturers have developed pulse oximeter with more than two wavelengths to estimate COHb and MetHb values (as well as total hemoglobin concentrations) in the blood [21].

1.2.5.2 Low Perfusion and Reflection Pulse Oximetry

In a transmissive pulse oximeter, light is detected after it is transmitted through the organ, so it is limited to the fingertips and earlobes. Because of its role in heat transfer, the blood flow to fingertips and earlobes is greater than that required by tissue metabolism, and their pulses have a high signal-to-noise ratio under normal conditions. However, these organs are strongly regulated by the autonomic nervous system, and their arteries contract when the ambient temperature is low or cardiac output is low. However, when the ambient temperature or cardiac output decreasing, vasoconstriction usually happens in these tissues to reduce heat loss or maintain an adequate blood supply to key core organs (heart, brain, and kidney) since they are strongly regulated by the autonomic nervous system. In this case, the signal is reduced thus reducing the accuracy of the pulse oximetry. The reflective pulse oximetry, that is, the light source and the photodetector are located on the same surface of the skin and can be used in any accessible position, so it has the advantage under the condition of low peripheral perfusion. The main part of the reflex pulse oximeter is the forehead. The reflective finger pulse oximeter has the advantage of low power consumption because it can shorten the distance between the light source and the detector thus reducing the absorption of light. Reflective pulse oximeter is also recommended for use in accessible internal structures such as esophagus, pharynx, and trachea. The researchers claim that measurements in these areas are more reliable when the surrounding perfusion is lower. The low perfusion caused by vasoconstriction leads to the decrease of signal, which is also related to the increase of SpO_2.

1.2.6 Future of Pulse Oximetry

The newer pulse oxygen saturation measurement technique can be measured with multiple wavelengths of light. In addition, studies have shown that pulse oximeter signals may be useful for applications other than SpO_2. However, the current technology is not yet mature and needs to be further improved. With the improvement of technology, the pulse oximeter may improve the method of using pulse oximetry

technology to detect SpCO, SpMet, SpHb, pulsus paradoxus, breathing frequency, and fluid responsiveness is likely to improve in the future [22].

Many reports focus on the use of pulse oximeter as a plethysmogram. Plethysmography analysis of peripheral pulse waves provides relevant hemodynamic information, which has been used in the diagnosis and follow-up of chronic cardiovascular diseases. However, this feature has not been further developed [23].

1.3 Venous Oximetry

1.3.1 Introduction

The imbalance of oxygen delivery (DO_2) and oxygen consumption (VO_2) can result in circulatory shock. It even develops multi-organ failure and increases morbidity and mortality if tissue hypoxia is unrecognized and uncorrected timely. Although physical examinations, such as vital signs, pulse oximetry, skin mottling, and urinary output, have somewhat distinct value, it is still insufficient to detect tissue hypoxia accurately. Venous oxygen saturation is a physiological parameter that has been introduced as an indirect index to assess the relationship between DO_2 and VO_2 both in the intensive care unit and in high-risk surgery [24]. The venous oxygen saturation is measured at the exit of any organ or tissue, the pulmonary artery and inferior vena cava or right atrium are easier to access. In 1970, Swan and Ganz developed a pulmonary artery catheter (PAC), also named as Swan and Ganz catheter, that can easily be inserted into the pulmonary artery to collect pulmonary arterial blood at the bedside, where blood is mixed from inferior and superior vena cava [25]. The oxygen content of pulmonary arterial blood is defined as mixed venous oxygen saturation (SvO_2), which reflects venous oxygen saturation of the whole body. But due to the high invasiveness of inserting PAC, its application remains under debate and less popular gradually. With the central venous catheter (CVC) of the superior vena cava being applied widely, central venous saturation ($ScvO_2$) has been advocated as a surrogate of SvO_2 to measure venous oxygen saturation, but it just contains venous blood from the upper body (brain) [26]. There is still debate about whether $ScvO_2$ can replace SvO_2.

1.3.2 Physiology

1.3.2.1 Oxygen Delivery

Oxygen Delivery (DO_2, mL/min) is the rate of oxygen being transported from the lungs to the microcirculation per minute, and it is also expressed by oxygen transport and oxygen supply. DO_2 is equal to the product of cardiac output (CO) and the oxygen content of arterial blood (CaO_2).

$$DO_2 = CO \times CaO_2 \tag{1.1}$$

The unit of CO is usually expressed as L/min and CaO_2 is mL/dL, so that value of CO should be multiplied by 10 to convert into the unit of dL/min. And CaO_2 depends on three parameters: the partial pressure of oxygen of arterial blood (PaO_2), the arterial oxygen saturation of hemoglobin (SaO_2, %), and hemoglobin concentration (Hgb, g/dL), expressed as

$$CaO_2 = \left(1.34 \times Hgb \times SaO_2\right) + \left(0.0031 \times PaO_2\right) \tag{1.2}$$

So, DO_2 can also be calculated by the following equation:

$$DO_2 = CO \times \left[\left(1.34 \times Hgb \times SaO_2\right) + \left(0.0031 \times PaO_2\right)\right] \tag{1.3}$$

where 1.34 (mL/g) is the Hufner constant and reflects the capacity of the hemoglobin carrying oxygen, but it varies with different species [27]. The 0.0031 is the coefficient of oxygen solubility in blood. The normal value of DO_2 is about 1000 mL/min.

1.3.2.2 Oxygen Consumption

Oxygen consumption (VO_2, mL/min) is the rate of oxygen being used by the tissues from the blood per minute. It can be calculated by the Fick equation [28]:

$$VO_2 = CO\,x\left(CaO_2 - CvO_2\right) \tag{1.4}$$

where CvO_2 (mL/dL) is short of the mixed venous blood oxygen content that is similar to CaO_2 and also related to three parameters, the partial pressure of oxygen of venous blood (PaO_2), SVO_2, and Hgb. It can be calculated by the following equation:

$$CaO_2 = \left(1.34 \times Hgb \times SvO_2\right) + \left(0.0031 \times PvO_2\right) \tag{1.5}$$

So, VO_2 can be calculated by the following equation:

$$VO_2 = CO\left\{\begin{array}{l}\left(1.34 \times Hgb \times SaO_2\right) + \left(0.0031 \times PaO_2\right) \\ -\left[\begin{array}{l}\left(1.34 \times Hgb \times SvO_2\right) \\ +\left(0.0031 \times PvO_2\right)\end{array}\right]\end{array}\right\} \tag{1.6}$$

The normal value of global VO_2 in resting status is about 250 mL/min. But it varies with different tissues. For example, splanchna is about 83 mL/min in resting status, skeletal muscle is 57 mL/min, the brain is 52 mL/min, the heart is 34 mL/min, kidney 19 ml/min, and skin 12 mL/min [29].

1.3.2.3 Oxygen Extraction and Oxygen Extraction Ratio

Oxygen extraction or oxygen extraction rate (O_{2ER}) is equal to the ratio of DO_2 and VO_2, that represents the percentage of arterial oxygen being used when it passes through the microcirculation:

$$O_{2ER} = \left(CaO_2 - CvO_2\right) / CaO_2$$

1.3.2.4 Venous Oxygen Saturation

According to Eq. (1.6), if dissolved oxygen is ignored, the formula can be simplified and converted as follows:

$$SvO_2 = \left[SaO_2 - VO_2 / CO\right]\left[1 / Hgb \times 1.34\right] \tag{1.7}$$

Therefore, SaO_2, VO_2, CO, and Hgb levels in blood all can affect SvO_2. The normal range is 70–75% in the resting status of healthy people [30].

The Interpretation of Venous Oxygen Saturation

In clinical, a variety of diseases can influence the values of SvO_2 (Fig. 1.3) that can reflect the relationship between DO_2 and VO_2. DO_2 decreases or VO_2 increase both results in low values of SvO_2 because the body initially increases O_{2ER} by feedback mechanisms to maintain adequate tissue oxygenation [29]. The patients with lung disease, the problem of circulation (e.g., Hypovolemia, heart failure, or arrhythmias

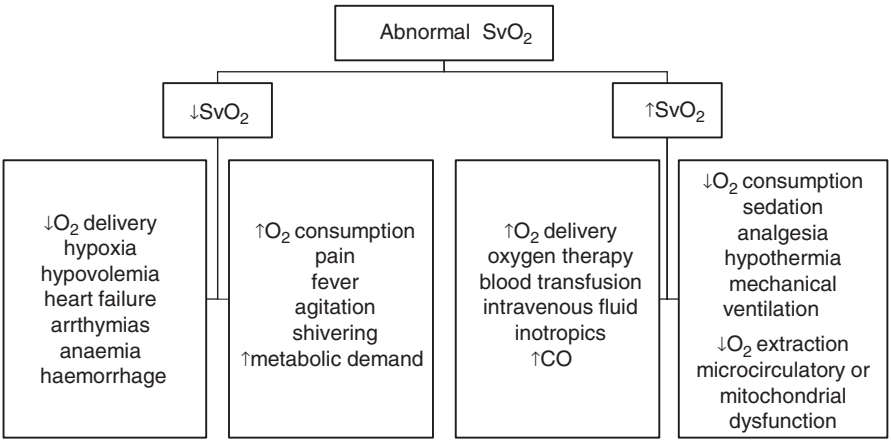

Fig. 1.3 Clinical common causes of abnormal mixed venous oxygen saturation. ↓ represents the values decreasing, and ↑ represents the values increasing

all results in the drop of CO), anemia, or hemorrhage all cause the decrease of DO_2 and SvO_2. And some conditions, such as pain, fever, agitation, shivering, can increase VO_2 and also reduce SvO_2 even if existing normal DO_2. Conversely, SvO_2 increases due to the increase of DO_2 (e.g., excessive oxygen therapy, blood transfusion, the application of inotropic) or the decrease of VO_2 (e.g., Sedation, analgesia, hypothermia, and mechanical ventilation) or the dysfunction of extracting oxygen (e.g., Microcirculatory or mitochondrial dysfunction). Secondary to microcirculatory and mitochondrial failure, high SvO_2 usually occurs in sepsis because of impairing oxygen utilization.

The Relationship Between Mixed and Central Venous Oxygen Saturation

The $ScvO_2$ monitoring has been considered to replace SvO_2 because inserting CVC is less expensive and simpler compared to PAC, but there is still debate. When CVC is placed into the superior cranial vein, it just can collect venous blood from the upper body (brain). In normal physiologic conditions, $ScvO_2$ can reflect SvO_2 well but is 2–5% less than SvO_2 due to high VO_2 of the brain [29]. However, the relationship between SvO_2 and $ScvO_2$ varies among different pathological conditions. There is a risk that $ScvO_2$ may poorly understand tissue perfusion of the lower body, especially for splanchna. In shock states, the blood is redistributed to maintain DO_2 of the brain at the expense of reducing the blood of splanchnic and renal. Therefore, venous oxygen saturation in the upper body increased while decreases in the lower body, causing that $ScvO_2$ might overestimate SvO_2. This relationship was also observed in other postsurgical and medical patients. Van Beest et al. performed a prospective observational study and compared $ScvO_2$ and SvO_2 in 53 patients (32 postsurgical and 21 medical patients). The study also found $ScvO_2$ was higher than SvO_2 [31]. To improve the correlation between $ScvO_2$ and SvO_2, Kopterides et al. suggested to further insert CAC to achieve the right atrium for drawing blood from the cranial and caudal vena cava. They found that $ScvO_2$ was higher than SvO_2 by only 1% after the tip CAC was placed into the right atrium, while $ScvO_2$ was higher than SvO_2 by 8% when CAC was inserted into normal location [32]. But it also increases the risk of formatting right atrial thrombus or other complications.

It is not denied that several studies supported the paralleled variations of $ScvO_2$ and SvO_2. The correlation coefficient between SvO_2 and ScvO2 was 0.97 in all different conditions (hemorrhage, hypoxia, resuscitation) in the experimental dogs. The difference between the SvO_2 and $ScvO_2$ remained less than 5% in 77% of all cases. A maximal difference was observed in hypoxic conditions, ranging from 6% to 20%. The SvO_2 and $ScvO_2$ were also compared in 70 neurosurgery patients, the bias of them was 6.8–9.3% and had a similar variation tendency in 75% cases [33]. It should be noted that a femoral central venous catheter is not suitable to measure $ScvO_2$ because of the anatomical conditions. A study compared the femoral venous oxygen saturation and central venous oxygen saturation in 160 patients and found that there was a lack of agreement in both stable and unstable medical conditions [34].

The Venous Oxygen Saturation Measurement

With the help of PAC or CVC, SvO_2 and $ScvO_2$ both can be measured by discontinuous or continuous methods. The discontinuous venous oximetry is accomplished by drawing blood from a catheter and performing blood gas analysis. And continuous venous oximetry needs a fiberoptics integrated into PAC or CVC that can display value by an external monitor continuously [35].

The Application of SvO_2 and $ScvO_2$ in Mechanical Ventilation

Venous oxygen saturation is mainly used in a variety of shock states and critical illness to provide information about oxygen delivery and consumption. The SvO_2 was recommended to remain higher than 65%, or $ScvO_2$ higher than 70% [29]. Low $ScvO_2$ is related to higher mortality of patients with septic shock. Meanwhile, high $ScvO_2$ (>90%) also reminds that patients might exist dysfunction of the O_2 utilization and also have a high rate of mortality. But recent studies also showed that using $ScvO_2$ as a goal to direct therapy of patients with septic shock did not improve mortality, compared with usual resuscitation [36].

For critical patients with mechanical ventilation, successful weaning and extubation are crucial procedures of treatment that is related to illness, hemodynamic stability, oxygenation, homeostasis, conscious, and cough reflex. A spontaneous breathing trial (SBT) should be met before extubation. SvO_2 and $ScvO_2$ have been reported to predict weaning success and failure accurately. In 1998, Jubran et al. monitored SvO_2 continuously in 19 medical and surgical patients who needed to perform SBT. As a result, eight patients failed to pass SBT and 11 patients passed SBT and were extubated successfully [37]. Although SvO_2 was similar in these two groups before SBT, SvO_2 dropped progressively in the failure group when the ventilator was disconnected, whereas it did not alter in the success group. It might be caused by a decrease in oxygen transport and an increase in oxygen extraction. Georgakas et al. also observed that the value of $ScvO_2$ also can predict the SBT outcome [38]. The study enrolled 77 patients who underwent a 30-min SBT, 63.6% of patients succeed in SBT according to standard criteria. And the difference between $ScvO_2$ at the before and the end of SBT lower than 4% was an independent index to predict successful weaning. However, in clinical, some patients who passed SBT still probably appear extubation failure. A prospective cohort study enrolled 73 patients who failed in the first SBT and continued mechanical ventilation until passed SBT, that was defined as difficult-to-wean patients [39]. Although difficult-to-wean patients all passed SBT, 31 patients (42.5%) still occurred extubation failure. Meanwhile, they monitored the change of $ScvO_2$ in these two groups. And $ScvO_2$ was 60 ± 8 in the extubation failure group and 70 ± 7 in the extubation success group ($p < 0.009$). The $ScvO_2$ decreased more than 4.5% during the SBT that might predict reintubation independently, with a sensitivity of 88% and specificity of 95% in this study.

Limitations

To obtain SvO_2 and $ScvO_2$, an invasive catheter needs to be inserted. There has been strong evidence to support routine use of them as an effective index to direct therapy so far. In clinical, PAC and SvO_2 becoming less and less popular recently, $ScvO_2$ just can reflect the venous oxygen saturation of the upper body, whether it can totally replace SvO_2 needs to be debated.

Conclusion

Venous oximetry can provide information about the balance between global oxygen delivery and consumption. Future studies should focus on the worth of SvO_2 and $ScvO_2$ to detect the different physiological situations and how to direct treatment.

1.4 Near-Infrared Spectroscopy

1.4.1 Definition

Near-infrared spectroscopy (NIRS) is a new technique to monitor the peripheral tissue oxygenation saturation (StO_2) noninvasively [40–43]. It measures cellular oxygen metabolism and microvascular dysfunction, especially in poor tissue perfusion conditions such as septic shock and other types of shock.

1.4.2 History

In 1937, NIRS was first introduced by Millikan [44], who developed a dual-wavelength oximeter for muscles. NIRS was introduced in the 1970s as a means of noninvasive monitoring of average hemoglobin oxyhemoglobin equilibrium by Jobsis, measured the absorption spectrum of near-infrared (NIR) (600 ~ 1000 nm) transilluminated through a neonate's head in 1977 [45]. The earlier work was described on the neonate's heads because the infrared light could pass through a neonate's skull. In 1985, Ferrari published the first description of the application of cerebral monitoring using NIRS [46]. In 1987, Ferrari et al. measured hemoglobin oxygen saturation in an adult cortex using NIR light that was reflected in the scalp [47]. In 1993, Somanetics invented the first commercially available NIRS device (INVOSÒ 3100).

Since then, NIRS has been used widely in clinical settings to obtain a mean value for mixed oxygenation in different tissues. Pulse Hb oxygen saturation, which uses similar technology in peripheral [48] (i.e., pulse oximetry), has been used globally in all acute clinical settings.

1.4.3 Physics and Principles

Near-infrared (NIR) is a term to define light with wavelengths varying from 600 ~ 1000 nm, with "true" infrared light of wavelengths less than 1 mm. In this range, the biological tissues seem almost translucent with the low molecular absorptivity of the tissue, a key "chromophore" constituent. In this range, the biological tissues seem almost translucent with the low molecular absorptivity of the tissue, a key "chromophore" constituent. The absorptivity of each chromophore is different so that the signals of the detector will not be mixed to quantify the signals of the specified chromophore in the target location, and this is the principle of NIRS. At 600–1000 nm, the absorption is relatively low so that scattering is the dominant tissue interaction process for NIR light. NIR light could be transmitted several centimeters into some organs or tissues so that it may be used as a noninvasive medical imaging and spectroscopy. Oxygenated and deoxygenated hemoglobin (Hb) are the most targeted chromophores and the signal substances to deliver biological information such as blood supply and oxygen transport in tissues.

The physics and mathematics of NIRS technology are based on a modified version of Beer-Lambert law, which describes that "a portion of the light transmitted through a solution containing a colored compound (chromophore) is absorbed by the compound," as a result, the intensity of the emerging light is attenuated. The Beer-Lambert law provides an equation between the absorption and concentration of a chromophore:

$$A = \log\left(I_0 / I\right) = \varepsilon cd,$$

where A is the optical density that represents the absorption of light (log of the ratio of the intensity of the incident and transmitted light), c is the chromophore concentration, d is the solution or media's thickness (optical path length), and ε is its extinction coefficient [49].

The working principle of NIRS is the differential absorption characteristics of oxyhemoglobin (HB-O) and deoxygenated hemoglobin (HB-r). At 800 nm, light is absorbed equally by HB-O and HB-r, whereas at 760 nm, light is absorbed primarily by HB-r [50]. This difference in light absorption of HB-O and HB-r reflects oxygen uptake in the tissue. Near-infrared light is directed on a tissue by placing probes. By measuring the quantity of returned photons, the spectral absorption of the underlying tissue can be characterized and the rSO_2 can be estimated. The measurement is termed as the regional oxygen saturation (rSO_2) [51].

NIRS signals are limited to vessels less than 1 mm in diameter, which might be explained by the Beer-Lambert law, due to the difference between light passing through large versus small blood vessels. If photons of NIR light pass through a single red blood cell, only a small portion of the light will be absorbed. However, if a photon passes through a 1 mm thick blood vessel with an extinction coefficient of 1, the absorbance will be 0.8 and thus only 10% of the impacting photons will

remain unabsorbed. Therefore, the NIRS absorption pattern mainly reflects small blood vessels [52].

Commercially available NIRS monitors provide oxyhemoglobin and deoxyhemoglobin scores for calculating StO_2 as well as total tissue hemoglobin (TTH) and absolute tissue hemoglobin index (THI), which are indicators of blood volume in the microvascular system sensed by the probe and expressed in arbitrary units. Each probe combines one light source and two detectors to detect tissue oxygenation at different depths. One path length measures the oxygenation of surface tissue, while the other measures the oxygenation of deep tissue.

The penetration of light tissue is directly related to the spacing between the illumination and detection fibers. At a distance of 25 mm, approximately 95% of the detected light signals are from a depth of 0–23 mm. NIRS monitors differ in wavelength selection, wavelengths numbers, photodiode pitch, and algorithms used to calculate data from absorption data. The currently used NIRS probe measures reflected light, so the NIRS light source is located next to the light sensor.

1.4.4 Vascular Occlusion Test

The vascular occlusion test (VOT) is performed to induce brief transient ischemia, applying a blood pressure cuff on the forearm to maintain 50 mmHg above the systolic blood pressure for 3 min, then the cuff was released for reperfusion. The VOT produces indicators on the descending slope after occlusion, representing local oxygen consumption, and the ascending slope, reflecting perfusion pressure and endothelial integrity at reperfusion. The VOT provides hemoglobin desaturation (DeO_2), followed by hemoglobin reoxygenation (ReO_2) following the release of the ischemia [53]. DeO_2 stands for the extraction of oxygen from the tissue when blood flow is excluded, while ReO_2 means the resaturation of hemoglobin reflecting the state of capillaries reactivity. Application of VOT improves the accuracy of StO_2 in detecting tissue hypoperfusion via "unmasking pre-existing vasoconstriction in blood vessels" [54].

Unfortunately, there is no guideline or consensus on the exact method or site to use is best for VOT [55]. It is still controversial to maintain ischemia for a specific time or to reduce StO_2 to a specific value.

1.4.5 Application

1.4.5.1 Monitoring the Real-Time StO_2 in Respiratory Failure

NIRS is being explored as a potential tool for weaning from mechanical ventilation. A lower ascending slope of StO_2 is a negative prognostic factor in patients with ARDS, and this change can be observed within 24 h after diagnosis [56]. A reduction of StO_2 can be observed in patients who fail the spontaneous breathing trial (SBT) and its value is significantly correlated with SaO_2 [57].

1.4.5.2 Monitoring the Real-Time StO_2 in Shock

As a useful tool to evaluate tissue oxygen saturation (StO_2), NIRS is extensively adapted to monitor tissue hypoxia and guide resuscitation in shock because it provides continuous monitoring of tissue perfusion.

In hypoperfusion status, the perfusion in muscles is decreased to warrant the blood supply to vital organs. By estimating the muscle perfusion via NIRS measured StO_2 noninvasively, the global saturation may be estimated. The bedside NIRS monitoring can be performed via lower extremity, brachioradialis muscle, and thenar eminence. Decreased thenar oxygen saturation indicates the possible presence of severe hypoperfusion. Identifying the real-time thenar StO_2 at the bedside may help to guide the early resuscitation of critically ill patients with hemodynamic instability.

In septic shock, Central venous oxygen saturation ($ScvO_2$) is a widely used indicator to guide early resuscitation but invasively. If there is a correlation between $ScvO_2$ and StO_2, noninvasive monitoring of sepsis may be feasible in intensive care units [58]. Based on the current literature and findings, insufficient evidence is available to recommend substituting StO_2 instead of $ScVO_2$ in septic shock [59–61]. However, the use of VOT increases the accuracy of StO_2 in detecting tissue hypoperfusion by "unmasking pre-existing vasoconstriction in blood vessels" [62].

By inducing occlusion stress, various dynamic variables from VOT can be measured to indicate local metabolic demand and microvascular reactivity. Due to anatomic conditions, both the brachioradialis and the thenar eminence muscles can be easily tested for the vascular occlusion test. These alterations in NIRS-derived dynamic variables are common in septic shock and are associated with poor outcomes. In septic shock, the persistence of the low ascending slope of StO_2 is associated with an adverse outcome [63].

While the value of StO_2 might not be apparent in sepsis, derived parameters obtained using VOT can be perhaps more accurate.

Overall, although the role of NIRS is fully understood so far, it is a compliment for predicting the prognosis of septic patients. Higher quality research on the relationship between $ScvO_2$ and StO_2 and the use of VOT-derived parameters would help to establish management guidelines using NIRS in sepsis.

NIRS can be used in cardiac tamponade as well. It was reported that one of the earliest indications was a sudden fall in $SctO_2$. NIRS may help in early detection and intervention of life-threatening complications following cardiac surgery.

1.4.5.3 Monitoring Cerebral Oxygenation

Monitoring cerebral oxygenation by NIRS is used in major surgeries such as major neurosurgical procedures [64], cardiac surgery during cardiopulmonary bypass [65], cesarean section under spinal epidural anesthesia [66], or carotid endarterectomy to prevent brain injury from hypotension or hypoperfusion. There is a good correlation between NIRS values and transcranial Doppler CD (TCD) and

electroencephalography (EEG) values during ischemia. Whereas the agreement between cerebral oxygenation monitoring by NIRS and invasive brain tissue oxygenation measurement is poor [67]. The regional cerebral oxygen saturation (rSO_2) monitoring via NIRS may be helpful in predicting the prognosis after cardiac arrest [68]. As a noninvasive tool, NIRS is an important complement to multimodal neuromonitoring for the management of acute neurological and neurosurgical conditions, including neurological trauma, subarachnoid hemorrhage, and stroke. It provides a useful noninvasive adjunct to mainstream monitoring in traumatic brain injury. The application with more evidence existed is for the detection of intracranial (space-occupying) hematomas. However, not enough evidence is present to support its use as a surrogate or replacement for any invasive monitoring modality such as ICP, brain tissue oxygen tension, or jugular bulb saturation have not yielded sufficiently consistent results.

The technology has been growing significantly and can be merged with other imaging modalities so that more and more novel methods of data acquisition and analysis are available in clinical practice. Therefore, the utility of NIRS, as a noninvasive neurological monitoring technology, will be enhanced to provide more information for both clinical practice and research.

1.4.5.4 Peripheral Arterial Disease

Peripheral arterial disease (PAD) is the narrowing of peripheral vessels of the body. The changes in muscle metabolism can be quantified by NIRS in patients with PAD.

1.4.6 Summary

NIRS can indicate the status of tissue oxygen utilization, and it can be a valuable supplement to other physiological monitoring modalities [69]. There are some limitations to NIRS. First, NIRS cannot distinguish between arterial and venous blood. In cerebral oximetry, NIRS gets approximately 84% of its contribution from venous blood. Therefore, NIRS can be used to estimate "regional cerebral venous oxygen saturation," also called "venous weighted saturation" [70]. Second, NIRS is susceptible to interferences from the environment, temperature, age, obesity, tissue edema, and vascular tone (the use of vasoactive drugs included) [53]. Third, the heterogeneity in septic shock may prevent local StO2 assessed at a single site from representing the overall microcirculatory function. With the development of biological techniques, NIRS and its extensions, such as the functional NIRS (fNIRS) [71] and the near-infrared photoacoustic imaging platform (NIR PAI) [72], have been received considerable attention in biological or clinical imaging fields. Overall, NIRS is a low-cost, noninvasive monitoring modality and more research is warranted before its routine use in clinical practice.

1.5 Capnography (Dead Space Calculation)

Capnography is the measurement of carbon dioxide (CO_2) in exhaled gas. It provides a noninvasive method to estimate arterial CO_2 by the numeric display of the partial pressure of end-tidal CO_2($P_{ET}CO_2$), as well as a way to calculate airway dead space with its waveform [73].

1.5.1 Capnometry

In clinical practice, infrared absorption spectrometry is commonly used for sampling CO_2 content. Sometimes, mass spectrometry and colorimetric CO_2 sensor are used because of their advantages.

1.5.1.1 Infrared Absorption Spectrometry

The principle of infrared spectroscopy relies on the absorption of infrared light when it passes through a sampling gas. It measures CO_2 quantitatively as its absorption rate is positively correlated with the percentage of CO_2 in the sample. The infrared analysis is quick enough to display a waveform in real-time [74]. Yet, there still are some limitations to this technique. Some anesthesia gas, such as nitrous oxide (N_2O), whose infrared absorption peak is extremely close to carbon dioxide, may cause interference during the measurement. Filters or correction factors should be used to reduce errors.

Mainstream Capnometer

The mainstream capnometer places its sensor directly into the ventilation circuit with the advantages of a faster response, a smaller size and fewer opportunities to malfunction, and also a lower dead space. However, it may cause an obstruction in the airway. Therefore, it is better to use it on patients with intubation.

Sidestream Capnometer

Sidestream capnometer, which differs from mainstream capnometer, withdraw gas out of the breathing circuit for sampling. The gas will be sent to an analyzing module through a narrow tube. Because of the length of the transport tubing, a delay is inevitable. Moreover, moisture and secretions will block the sensor so that the tubing needs to be checked regularly. Besides, calibrating is also needed regularly. Sidestream capnometer can be configured to use in patients with non-intubation.

1.5.1.2 Mass Spectrometry

The mass spectrometry ionizes the gas into ions in order to separate them according to their mass and charge. With this technique, gases will be distinguished precisely by every breath. It will also be able to differentiate N_2O and CO_2. However, considering the high cost and weight, mass spectrometry is not available at the bedside [75].

1.5.1.3 Colorimetric CO_2 Sensor

A colorimetric CO_2 sensor can qualitatively analyze CO_2 in the expired gas. There is a color change of the detector when CO_2 exists. It is widely used to confirm that the endotracheal tube does not enter the esophagus.

1.5.2 Capnography

Capnography displays a continuous waveform of the partial pressure of CO_2 (PCO_2) in the exhaled gas. The content of CO_2 in the air is usually defined as zero.

1.5.2.1 Time-Based Capnography

Time-based capnography takes PCO_2 as *y*-axis and time as *x*-axis. There is a routine change in the capnogram of a healthy person which can be identified as four phases (Fig. 1.4).

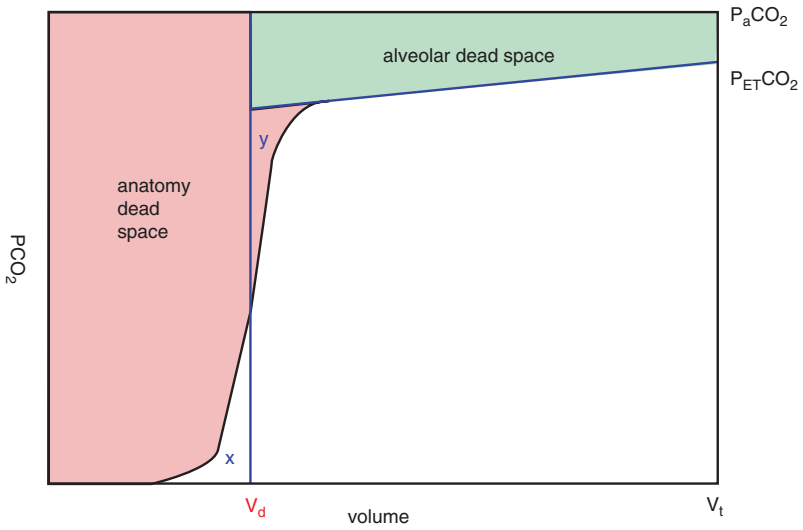

Fig. 1.4 Time-based capnogram. PCO_2, partial pressure of CO_2 in the expired gas; $P_{ET}CO_2$, partial pressure of end-tidal CO_2

In phase I, PCO_2 remains zero. Because at this period inspiration take place and no CO_2 is detected. Then at the beginning of expiration, the analyzed gas comes from anatomical dead space which includes airway and endotracheal tube in mechanically ventilated patients. Therefore, PCO_2 is still zero.

In phase II, there is an upstroke in the graphic, representing a mixture of alveolar gas and air.

In phase III, the waveform becomes almost horizontal, which made this phase also known as an alveolar plateau. But actually, the curve rose gently because of the different V/Q ratio. Those alveoli with lower V/Q lead to a longer emptying time and a continuous ascending of the wave. At the end of phase III, PCO_2 reaches a peak. This highest level of PCO_2 is called end-tidal PCO_2 ($P_{ET}CO_2$).

In phase IV, PCO_2 declines sharply towards zero. Inspiration begins and a new cycle starts.

1.5.2.2 End-Tidal PCO_2 ($P_{ET}CO_2$)

End-tidal PCO_2 ($P_{ET}CO_2$) is commonly used to represent alveoli PCO_2 (P_ACO_2) and further represents arterial CO_2 (P_aCO_2) in clinical practice. A normal $P_{ET}CO_2$ depends on pulmonary blood flow, metabolism, and alveolar ventilation. P_ACO_2 is determined by the ventilation/perfusion ratio (V/Q).

If $V/Q = +\infty$ (no perfusion), then $P_ACO_2 \approx 0$;

If V/Q is normal, then $P_ACO_2 \approx$ arterial CO_2 (P_aCO_2);

If $V/Q \approx 0$ (no ventilation), then $P_ACO_2 \approx$ venous CO_2 (P_VCO_2);

Under normal circumstances, $P_{ET}CO_2$ correlates well with P_aCO_2 at only a difference of 5 mmHg ($P_{a\text{-}ET}CO_2 = 5$ mmHg), which can be used to predict P_aCO_2. Yet in pathological occasions, such as pulmonary hypoperfusion, pulmonary embolism, and cardiac arrest, they stay no longer relative. In fact, anything that leads to an increase of dead space ventilation could enlarge $P_{a\text{-}ET}CO_2$, including excessive PEEP and high-rate low-tidal-volume ventilation.

1.5.3 Clinical Applications—Abnormal Waveform of Time-Based Capnogram

1.5.3.1 Obstructive Lung Disease

Bronchospasm, COPD, asthma, and bronchiolitis in infants are the common causes of obstructive lung disease. The obstruction of airways leads to a reduction in ventilation, but usually normal in pulmonary perfusion. This will slow down the exhaled time and widen the graphic. The slope of phase II flattened, and phase III is increased, because of the delay in CO_2 discharge. The waveform turns into a "shark fin" like shape [76]. By monitoring the gradient of phase III, clinical decisions could be made and the effect of therapy could be observed. In addition, accurate lung injury can also result in such kind of curve change.

1.5.3.2 Cardiac Arrest and CPR (Cardio-Pulmonary Resuscitation)

There is a significant decrease in cardiac output and pulmonary perfusion in cardiac arrest. The waveform shows a decrease in phase III due to insufficient blood flow, making the graphic a lower plateau. The capnogram can be used to monitor the efficiency of CPR. A raise of $P_{ET}CO_2$ lower than 10 mmHg in 20 min CPR is usually associated with poor outcomes [77]. The return of spontaneous circulation appears as a significant increase in PCO_2.

1.5.3.3 Patient-Ventilator Asynchrony

The Patient-ventilator asynchrony is indicated by deflection during the plateau phase. Usually, it suggests ineffective triggering (small incisura) or a spontaneous breathing effort (deep incisura). On either occasion, physicians should be aware of the graphic and make adjustments to the trigger sensitivity.

1.5.4 Volume-Based Capnography

Volume-based capnography takes PCO_2 as *y*-axis and expired volume as *x*-axis. It has a waveform similar to the time-based capnogram. Phase I includes gas from the dead space and tubes. Phase II represents a mixture of alveoli gas and air. Phase III, the alveolar plateau, mainly contains CO_2 from alveoli. And when the CO_2 content goes to a peak value, it is called $P_{ET}CO_2$.

1.5.4.1 Dead Space Calculation

Dead space, also called as physiological dead space, are ventilated areas with no contribution to gas exchange. The dead space is further segmented into anatomy and alveolar dead space. Anatomy dead space refers to the airway between mouth and bronchiole terminals. It is related to the bodyweight of the patient, with approximately 150 mL for a 70 kg person. For the alveoli that did not participate in gas exchange, the total volume of the none efficient alveoli is called alveolar dead space, which is approximately zero in healthy people. Instrumental dead space is also mentioned in critical care units and should be subtracted in the calculation.

Dead space ventilation (V_d) can be calculated through the equation below: (Enghoff modification of the Bohr equation).

$$V_d / V_T = \left(P_aCO_2 - P_ECO_2\right) / \left(P_aCO_2\right)$$

V_T represents tidal volume; P_aCO_2 represents arterial PCO_2; P_ECO_2 represents the mean pressure of CO_2 in expired gas (the value often used in calculations is $P_{ET}CO_2$).

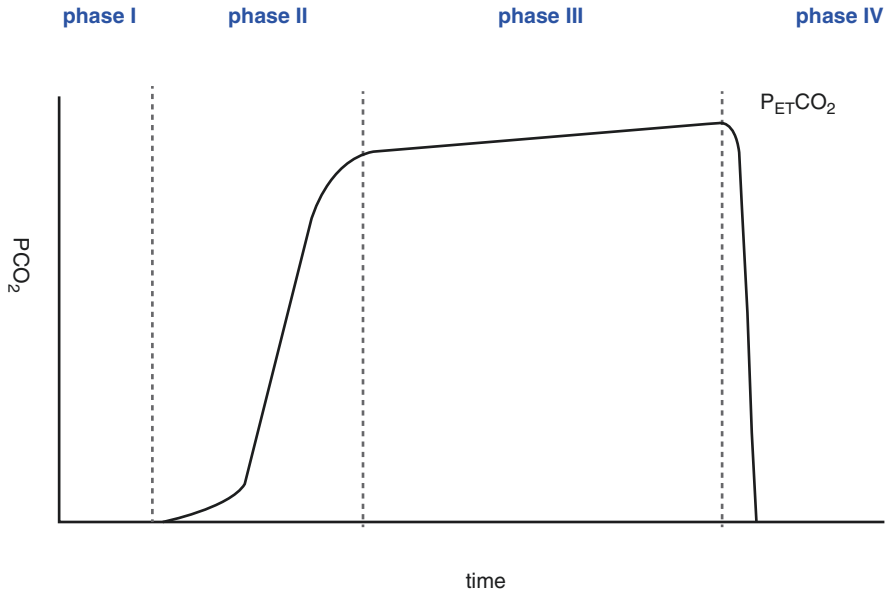

Fig. 1.5 Volume-based capnogram. V_d, volume of anatomy dead space; V_t, tidal volume; $P_{ET}CO_2$, partial pressure of end-tidal CO_2; P_aCO_2, partial pressure of arterial CO_2

Anatomy dead space can be measured through the graphic (Fig. 1.5). A perpendicular line crosses the extension line of an alveolar plateau in order to make area x equals y. The volume from zero to the foot of the perpendicular line is anatomy dead space.

In an ideal condition, if there is no dead space (neither anatomy nor alveolar), the CO_2-volume curve would be like a right angle that goes straightly upward at the zero points then turn right as it reaches P_aCO_2. As a result, the area between the ideal curve and the real curve can be seen as physical dead space (summation of the colored area). Furthermore, if we assume there is no alveolar dead space and no mixture of the alveolar gas and air, the waveform will start with a flat graphic then rise straightly up to P_aCO_2 at the point of V_d (volume of anatomy dead space). That is, the duration when the air of anatomy dead space runs out. The area between the two curves is the alveolar dead space.

1.5.5 Clinical Application

1.5.5.1 Pulmonary Embolism

Pulmonary embolism is related to disproportion V/Q, decrease in gas exchange, and increase of alveolar dead space. Different from obstruction lung disease, the increase of dead space resulted in a flatter phase III because both high V/Q and normal V/Q

lung units are emptied simultaneously. In other words, there is no delay in CO_2 discharge. Volume-based capnography can be used to monitor the response to therapy for pulmonary embolism.

1.5.5.2 PEEP

In critically ill patients, PEEP is commonly used to keep the alveolar open to ensure SpO_2. The CO_2-volume capnogram provides real-time monitoring for clinicians to reduce dead space by adjusting PEEP parameters. It is believed that the PEEP which minimizes the gap between $P_{ET}CO_2$ and P_aCO_2 is the best PEEP [78].

1.6 Transcutaneous Carbon Dioxide Monitor

Transcutaneous CO_2 ($P_{tc}CO_2$) monitoring is used as a noninvasive method to manifest changes in arterial CO_2 pressure (P_aCO_2). Nowadays, it is usually used in combination with an oximetry electrode which can provide both P_aCO_2 and P_aO_2 value simultaneously.

1.6.1 Principle

Transcutaneous monitors detect CO_2 by a slightly warmed up sensor attached to the skin. CO_2 is measured by an electrochemical sensor behind a flat glass membrane permeable to CO_2. The principle of the sensor is based on potentiometric titration. A reference electrode and an indicator electrode (a pH glass electrode) are inserted into the tested solution to form a working battery. The reaction between CO_2 and the electrode causes a change in hydrogen concentration, resulting in an electromotive force change of the battery which can be measured. This is also known as the Stow-Severing electrode.

The sensor is usually heated up to 42 °C to increase dermal capillary blood flow and capillary permeability, which all contribute to the diffusion of CO_2 through the skin. However, monitoring can also be performed at 37 °C with the introduction of a correction factor. This is because the gap between $P_{tc}CO_2$ and P_aCO_2 is widened at a lower temperature. In contrast, the monitoring is more sensitive at 42 °C but presents with a higher risk of being burned.

The fact that the value of $P_{tc}CO_2$ is always bigger than P_aCO_2 is probably because of two factors, heating and skin metabolism. The former may increase partial CO_2 production by approximately 4.5% per degree. The latter, which refers to CO_2 emission of the tissues between capillary and skin surface, may have an influence of 5 mmHg [79]. A series of algorithms are used to achieve the best consistency with the arterial pressure of CO_2.

1.6.2 Applications

Transcutaneous monitoring provides a feasible and convenient way to monitor CO_2, especially during high-frequency oscillatory ventilation (HFOV). In patients receiving HFOV, the linear relation between exhaled CO_2 (end-tidal CO_2, $P_{ET}CO_2$) and arterial CO_2 (P_aCO_2) became unstable, making it unfeasible to estimate P_aCO_2 by $P_{ET}CO_2$, while $P_{tc}CO_2$ remains correlated.

Transcutaneous monitoring is more widely applied in neonatal and pediatric departments due to the thinner squamous epithelium of children [80]. In mechanical ventilation, cyanotic congenital heart disease, and transportation of critically ill children, $P_{tc}CO_2$ shows an acceptable accuracy. In other cases which needs continuous blood gas monitoring (such as bronchoscopies, pulmonary function testing, apnea testing, therapeutic monitor for peripheral vascular disease), $P_{tc}CO_2$ also resulted in a good correlation.

1.6.3 Limitation

The probe requires regular re-membrane and calibration. The membrane must be changed every 2 weeks; however, in some models, the time frame is prolonged to 6 weeks at most. Calibration is essential for the sensor every 12 h. It is usually built in the system by manufacturers when it leaves the factory.

Blood gas analysis is still the gold standard of P_aCO_2. A contrast verification with blood gas analysis is needed before putting the monitor into use. Also, the transcutaneous monitor cannot replace the detection of $P_{ET}CO_2$.

The skin condition may affect its reliability as the sensor is contacted to the skin directly. Monitoring is inaccurate in patients with skin edema or skin thickness. Cleaning is recommended to remove dead skins and oils. And a drop of contact gel before the sensor attachment will as though improve its sensitivity. It is better to place the sensor at an area rich in blood supply, usually the earlobe. The most common commercial form is an earlobe clap.

The burn is another issue that limits the use of transcutaneous monitoring, especially in premature infants. Sensors need to be replaced every 2 h to prevent empyrosis. The alternative solution is putting down the temperature to 37 °C which improves patient tolerance. Monitoring time can be prolonged to 8–12 h at this temperature [81].

References

1. Wagner PD. The physiological basis of pulmonary gas exchange: implications for clinical interpretation of arterial blood gases. Eur Respir J. 2015;45(1):227–43.
2. Aboab J, Louis B, Jonson B, et al. Relation between PaO2/FIO2 ratio and FIO2: a mathematical description. Intensive Care Med. 2006;32(10):1494–7.

3. Hughes JM. Assessing gas exchange. Chron Respir Dis. 2007;4(4):205–14.
4. Feiner JR, Weiskopf RB. Evaluating pulmonary function: an assessment of PaO2/FIO2. Crit Care Med. 2017;45(1):e40–8.
5. Cutts S, Talboys R, Paspula C, et al. Adult respiratory distress syndrome. Ann R Coll Surg Engl. 2017;99(1):12–6.
6. Mellemgaard K. The alveolar-arterial oxygen difference: its size and components in normal man. Acta Physiol Scand. 1966;67(1):10–20.
7. Wong JJ, Loh TF, Testoni D, et al. Epidemiology of pediatric acute respiratory distress syndrome in Singapore: risk factors and predictive respiratory indices for mortality. Front Pediatr. 2014;25(2):78.
8. Floyd J, Wu L, Hay BD, et al. Evaluating the impact of pulse oximetry on childhood pneumonia mortality in resource-poor settings. Nature. 2015;528(7580):S53–9.
9. Cressoni M, Caironi P, Polli F, et al. Anatomical and functional intrapulmonary shunt in acute respiratory distress syndrome. Crit Care Med. 2008;36(3):669–75.
10. Elliott JE, Duke JW, Hawn JA, et al. Increased cardiac output, not pulmonary artery systolic pressure, increases intrapulmonary shunt in healthy humans breathing room air and 40% O2. J Physiol. 2014;592(20):4537–53.
11. Kawamura G, Kitamura T, Homma I, et al. Mechanisms underlying the improvement of arterial oxygenation using positive end-expiratory pressure during surgery under sevoflurane anesthesia and propofol anesthesia: a retrospective clinical study. Masui. 2013;62(6):652–9.
12. Van Meter A, Williams U, Zavala A, et al. Beat to beat: a measured look at the history of pulse oximetry. J Anesth Hist. 2017;3(1):24–6.
13. Jubran A. Pulse oximetry. Crit Care. 2015;19:272.
14. Fine I, Kaminsky A. Possible error in reflection pulse oximeter readings as a result of applied pressure. J Healthcare Eng. 2019;7293813
15. Chan ED, Chan MM, Chan MM. Pulse oximetry: understanding its basic principles facilitates appreciation of its limitations. Respir Med. 2013;107(6):789–99.
16. Pretto JJ, Roebuck T, Beckert L, et al. Clinical use of pulse oximetry: official guidelines from the Thoracic Society of Australia and new Zealand. Respirology. 2014;19(1):38–46.
17. Terrill PI. A review of approaches for analysing obstructive sleep apnoea-related patterns in pulse oximetry data. Respirology. 2019;25:475. https://doi.org/10.1111/resp.13635.
18. Plana MN, Zamora J, Suresh G, et al. Pulse oximetry screening for critical congenital heart defects. Cochrane Database Syst Rev. 2018;3:D11912.
19. Huijgen QC, Effing TW, Hancock KL, et al. Knowledge of pulse oximetry among general practitioners in South Australia. Prim Care Respir J. 2011;20(4):456–8.
20. Kiekkas P, Alimoutsi A, Tseko F, et al. Knowledge of pulse oximetry: comparison among intensive care, anesthesiology and emergency nurses. J Clin Nurs. 2013;22(5–6):828–37.
21. Nitzan M, Romem A, Koppel R. Pulse oximetry: fundamentals and technology update. Med Devices (Auckl). 2014;7:231–9.
22. Hess DR. Pulse oximetry: beyond SpO2. Respir Care. 2016;61(12):1671–80.
23. Tusman G, Bohm SH, Suarez-Sipmann F. Advanced uses of pulse oximetry for monitoring mechanically ventilated patients. Anesth Analg. 2017;124(1):62–71.
24. Marx G, Reinhart K. Venous oximetry. Curr Opin Crit Care. 2006;12(3):263–8.
25. Vincent JL. The pulmonary artery catheter. J Clin Monit Comput. 2012;26(5):341–5.
26. Scheinman MM, Brown MA, Rapaport E. Critical assessment of use of central venous oxygen saturation as a mirror of mixed venous oxygen in severely ill cardiac patients. Circulation. 1969;40:165–72.
27. Shimizu S, Enoki Y, Kohzuki H, et al. Determination of Hufner's factor and inactive hemoglobins in human, canine, and murine blood. Jpn J Physiol. 1986;36(5):1047–51.
28. Bizouarn P, Blanloeil Y, Pinaud M. Comparison between oxygen consumption calculated by Fick's principle using a continuous thermodilution technique and measured by indirect calorimetry. Br J Anaesth. 1995;75(6):719–23.

29. Walton RAL, Hansen BD. Venous oxygen saturation in critical illness. J Vet Emerg Crit Care (San Antonio). 2018;28(5):387–97.
30. Reinhart K, Kuhn HJ, Hartog C, et al. Continuous central venous and pulmonary artery oxygen saturation monitoring in the critically ill. Intensive Care Med. 2004;30(8):1572–8.
31. Van BPA, Van IJ, Boerma EC, Holman ND, et al. No agreement of mixed venous and central venous saturation in sepsis, independent of sepsis origin. Crit Care. 2010;14(6):R219.
32. Kopterides P, Bonovas S, Mavrou I, et al. Venous oxygen saturation and lactate gradient from superior vena cava to pulmonary artery in patients with septic shock. Shock. 2009;31(6):561–7.
33. Reinhart K, Rudolph T, Bredle DL, et al. Comparison of central-venous to mixed-venous oxygen saturation during changes in oxygen supply/demand. Chest. 1989;95:1216–21.
34. Van Beest PA, Van der Schors A, Liefers H, et al. Femoral venous oxygen saturation is no surrogate for central venous oxygen saturation. Crit Care Med. 2012;40(12):3196–201.
35. Rivers E, Nguyen B, Havstad S, et al. Early goal-directed therapy in the treatment of severe sepsis and septic shock. N Engl J Med. 2001;345(19):1368–77.
36. Yealy DM, Kellum JA, Huang DT, et al. A randomized trial of protocol-based care for early septic shock. N Engl J Med. 2014;370(18):1683–93.
37. Jubran A, Mathru M, Dries D, Tobin MJ. Continuous recordings of mixed venous oxygen saturation during weaning from mechanical ventilation and the ramifications thereof. Am J Respir Crit Care Med. 1998;158(6):1763–9.
38. Georgakas I, Boutou AK, Pitsiou G, et al. Central venous oxygen saturation as a predictor of a successful spontaneous breathing trial from mechanical ventilation: a prospective, nested case-control study. Open Respir Med J. 2018;12:11–20.
39. Teixeira C, da Silva NB, Savi A, Vieira SR, Nasi LA, Friedman G, et al. Central venous saturation is a predictor of reintubation in difficult-to-wean patients. Crit Care Med. 2010;38(2):491–6.
40. Lipcsey M, Woinarski NC, Bellomo R. Near infrared spectroscopy (NIRS) of the thenar eminence in anesthesia and intensive care. Ann Intensive Care. 2012;2(1):11.
41. Creteur J. Muscle StO2 in critically ill patients. Curr Opin Crit Care. 2008;14(3):361–6.
42. Mesquida J, Gruartmoner G, Espinal C. Skeletal muscle oxygen saturation (StO2) measured by near-infrared spectroscopy in the critically ill patients. Biomed Res Int. 2013;2013:502194.
43. Santora RJ, Santora RJ, Moore FA. Monitoring trauma and intensive care unit resuscitation with tissue hemoglobin oxygen saturation. Crit Care. 2009;13(Suppl 5):S10.
44. Millikan GA. Experiments on muscle haemoglobin in vivo; the instantaneous measurement of muscle metabolism. Proc R Soc Lond B. 1937;123:218–24.
45. Jobsis FF. Noninvasive, infrared monitoring of cerebral and myocardial oxygen sufficiency and circulatory parameters. Science. 1977;198(4323):1264–7.
46. Ferrari M, Giannini I, Sideri G, et al. Continuous non invasive monitoring of human brain by near infrared spectroscopy. Adv Exp Med Biol. 1985;191:873–82.
47. Ferrari M, Zanette E, Sideri G, et al. Effects of carotid compression, as assessed by near infrared spectroscopy, upon cerebral blood volume and hemoglobin oxygen saturation. J R Soc Med. 1987;80(2):83–7.
48. Boushel R, Langberg H, Olesen J, et al. Monitoring tissue oxygen availability with near infrared spectroscopy (NIRS) in health and disease. Scand J Med Sci Sports. 2001;11(4):213–22.
49. Ward KR, Ivatury RR, Barbee RW, et al. Near infrared spectroscopy for evaluation of the trauma patient: a technology review. Resuscitation. 2006;68:27–44.
50. Mancini DM, Bolinger L, Li H, Kendrick K, Chance B, Wilson JR. Validation of near-infrared spectroscopy in humans. J Appl Physiol (1985). 1994;77:2740–7.
51. Marin T, Moore J. Understanding near-infrared spectroscopy. Adv Neonatal Care. 2011;11:382–8.
52. Mancini DM, Bolinger L, Li H, Kendrick K, Chance B, Wilson JR. Validation of near-infrared spectroscopy in humans. J Appl Physiol (1985). 1994;77:2740–7.
53. Mesquida J, Gruartmoner G, Espinal C. Skeletal muscle oxygen saturation (StO2) measured by near-infrared spectroscopy in the critically ill patients. Biomed Res Int. 2013;2013:502194.

54. Gómez H, Torres A, Polanco P, et al. Use of non-invasive NIRS during a vascular occlusion test to assess dynamic tissue O(2) saturation response. Intensive Care Med. 2008;34:1600–7.
55. Gómez H, Mesquida J, Simon P, et al. Characterization of tissue oxygen saturation and the vascular occlusion test: influence of measurement sites, probe sizes and deflation thresholds. Crit Care. 2009;13(suppl 5):S3.
56. Orbegozo Cortes D, Rahmania L, Irazabal M, et al. Microvascular reactivity is altered early in patients with acute respiratory distress syndrome. Respir Res. 2016;17:59.
57. Poriazi M, Kontogiorgi M, Angelopoulos E, et al. Changes in thenar muscle tissue oxygen saturation assessed by near-infrared spectroscopy during weaning from mechanical ventilation. Minerva Anestesiol. 2014;80:666–75.
58. Kwon Y, Lee SH, Ryoo HC, Patrick H. Noninvasive thenar muscle tissue oxygen saturation as a surrogate of central venous oxygen saturation in patients with severe sepsis: 223-T. Crit Care Med. 2005;33(12):A167.
59. Napoli AM, Machan JT, Forcada A, Corl K, Gardiner F. Tissue oxygenation does not predict central venous oxygenation in emergency department patients with severe sepsis and septic shock. Acad Emerg Med. 2010;17:349–52.
60. Mesquida J, Masip J, Gili G, Artigas A, Baigorri F. Thenar oxygen saturation measured by near infrared spectroscopy as a noninvasive predictor of low central venous oxygen saturation in septic patients. Intensive Care Med. 2009;35:1106–9.
61. Allan C, Philips H, Kemp J, Celinski M, Jonas M. Near infrared spectroscopy (NIRS) and its comparison with traditional parameters of oxygen delivery in septic intensive care patients. Int Care Med. 2009;35(suppl 1):S28.
62. Gómez H, Torres A, Polanco P, et al. Use of non-invasive NIRS during a vascular occlusion test to assess dynamic tissue O(2) saturation response. Intensive Care Med. 2008;34:1600–7.
63. Creteur J, Carollo T, Soldati G, et al. The prognostic value of muscle StO2 in septic patients. Intensive Care Med. 2007;33:1549–56.
64. Messerer M, Daniel RT, Oddo M. Neuromonitoring after major neurosurgical procedures. Minerva Anestesiol. 2012;78:810–22.
65. Brady K, Joshi B, Zweifel C, et al. Real-time continuous monitoring of cerebral blood flow autoregulation using near-infrared spectroscopy in patients undergoing cardiopulmonary bypass. Stroke. 2010;41:1951–6.
66. Sun S, Liu NH, Huang SQ. Role of cerebral oxygenation for prediction of hypotension after spinal anesthesia for caesarean section. J Clin Monit Comput. 2016;30:417–21.
67. Kerz T, Beyer C, Huthmann A, et al. Continuous-wave near-infrared spectroscopy is not related to brain tissue oxygen tension. J Clin Monit Comput. 2016;30:641–7.
68. Storm C, Leithner C, Krannich A, et al. Regional cerebral oxygen saturation after cardiac arrest in 60 patients? A prospective outcome study. Resuscitation. 2014;85:1037–41.
69. Wahr JA, Tremper KK, Samra S, Delpy DT. Near-infrared spectroscopy: theory and applications. J Cardiothorac Vasc Anesth. 1996;10:406–18. https://doi.org/10.1016/S1053-0770(96)80107-8.
70. Edmonds HL, Rodriguez RA, Audenaert SM, Austin EH, Pollock SB, Ganzel BL. The role of neuromonitoring in cardiovascular surgery. J Cardiothorac Vasc Anesth. 1996;10:15–23.
71. Newton E, Butskiy O, Shadgan B, et al. Outcomes of free flap reconstructions with near-infrared spectroscopy (NIRS) monitoring: a systematic review. Microsurgery. 2019;
72. Jung D, Park S, Lee C, et al. Recent progress on near-infrared photoacoustic imaging: imaging modality and organic semiconducting agents. Polymers (Basel). 2019;11(10)
73. Walsh BK, Crotwell DN, Restrepo RD. Capnography/capnometry during mechanical ventilation: 2011. Respir Care. 2011;56(4):503–9.
74. Kerslake I, Kelly F. Uses of capnography in the critical care unit. BJA Education. 2017;17(5):178–83.
75. McSwain SD, Hamel DS. End-tidal and arterial carbon dioxide measurements correlate across all levels of physiologic dead space. Respir Care. 2010;55(3):288–93.
76. Nassar BS, Schmidt GA. Capnography during critical illness. Chest. 2016;149(2):576–85.

77. Levine RL, Wayne MA, Miller CC. End-tidal carbon dioxide and outcome of out-of-hospital cardiac arrest. N Engl J Med. 1997;337(5):301–6.
78. Theerawit P, Sutherasan Y, Ball L, Pelosi P. Respiratory monitoring in adult intensive care unit. Expert Rev Resp Med. 2017;11(6):453–68.
79. Eberhard P. The design, use, and results of transcutaneous carbon dioxide analysis: current and future directions. Anesth Analg. 2007;105(6):S48–52.
80. Chitilian HK, David, & Melo M. Respiratory monitoring. In: Miller's anesthesia. 2014. p. 1541–1579.
81. Restrepo RD, Hirst KR, Wittnebel L, Wettstein R. AARC clinical practice guideline: transcutaneous monitoring of carbon dioxide and oxygen: 2012. Respir Care. 2012;57(11):1955–62.

Chapter 2
Respiratory Mechanics

Jian-Xin Zhou, Yan-Lin Yang, Hong-Liang Li, Guang-Qiang Chen, Xuan He, Xiu-Mei Sun, Ning Zhu, and Yu-Mei Wang

2.1 Pressure and Flow Data Acquisition in Respiratory Mechanics Researches

Accurate measurements of pressure and flow rate are essential in respiratory mechanics researches [1, 2]. Apart from airway pressure displayed on the mechanical ventilator, additional sources of pressure measurements, such as tracheal pressure, gastric pressure, and esophageal pressure, are useful for differentiating the influence of the airway resistance and chest wall elastance on the lung mechanics [3–7]. Flow measurement is fundamental for lung volume evaluation during mechanical ventilation [1, 2, 8]. In this chapter, frequently used techniques and instruments for pressure and flow data acquisition are introduced.

2.1.1 Pressure Acquisition by Pressure Transducer

A pressure transducer is a device that converts pressure into an analog electrical signal. One of the most commonly used in respiratory mechanics is the strain-gauge based transducer, by which the conversion of pressure into an electrical signal is accomplished by the physical deformation of strain gages incorporated in the pressure transducer [9]. This type of transducer measures the pressure relative to atmospheric pressure. For example, peak airway pressure value of 30 cmH_2O at sea-level altitude (atmospheric pressure of 760 cmH_2O) indicates the absolute pressure of 793 cmH_2O.

J.-X. Zhou (✉) · Y.-L. Yang · H.-L. Li · G.-Q. Chen · X. He · X.-M. Sun · N. Zhu
Y.-M. Wang
Department of Critical Care Medicine, Beijing Tiantan Hospital, Capital Medical University, Beijing, China

J. Zhou et al. (eds.), *Respiratory Monitoring in Mechanical Ventilation*,
https://doi.org/10.1007/978-981-15-9770-1_2

The accuracy of pressure measurement by a pressure transducer is dependent on regular calibration. Two parameters have to be considered for calibration, gain and offset [10]. Gain is the slope of calibration curve, while offset indicates the transducer output with zero input. Transducer gain and offset are usually calculated according to transducer specifications. Two kinds of calibration methods can be used for pressure measurements, two-point and one-point calibration. Two-point calibration can be used when transducer specifications are unknown [11]. In case of long-term measurement, such as respiratory mechanics study for several days, transducer gain and offset may drift significantly from their nominal values. In this situation, two-point calibration may be useful to regain transducer specifications. For two-point calibration, a known source of input has to be applied, usually using the water column as a reference and zero (atmospheric pressure) as another source of input.

For a certain pressure transducer, the gain value is usually quite stable with short-term duration, such as several hours, while the offset value is prone to a greater drift. In this situation, one-point calibration with only zeroing the transducer (opening to atmospheric pressure) is employed. One-point calibration is based on the hypothesis that the transducer calibration curve only shifts vertically but the slope remains unchanged. It has been strongly recommended to perform the one-point calibration before starting each epoch of data acquisition.

2.1.2 Flow Acquisition by Fleisch Pneumotachograph

The physical basis of flow measurement is Poiseuille's law of laminar flow. As gas flow through a pipeline with known resistance, the flow rate can be calculated as:

$$\dot{V} = \Delta P \pi r \wedge 4 / 8nl \tag{2.1}$$

where $\dot{V}$ is the gas flow rate, ΔP is the pressure drop along the resistance, r is the radius of the pipeline, n is the gas viscosity, and l is the length of the pipeline.

If the resistance is constant and sufficiently low so as not to impede airflow, and if the gas viscosity is unchanged, the flow rate is directly proportional to the pressure drop along this pipeline [12]. Since Poiseuille's law is applied under conditions of laminar flow, turbulence may result in the overestimation of flow rate. Thus, the accuracy is improved when the turbulent flow is minimized.

The most frequently used airflow measurement is the Fleisch pneumotachograph, which is the gold standard for flow evaluation in respiratory mechanics research [13]. Fleisch pneumotachograph is composed of a large number of brass capillary tubes in a parallel array. This function provides a small fixed resistance to laminar airflow. Two differential pressure transducers are attached to the pressure collecting ports on both the beginning and ending sides of the tube. As gas passes through the tube, pressure drop develops and is measured.

Because the flow rate varies widely in human and animal spontaneous and mechanically ventilated breathings, a single model would not be suitable to provide

optimal measurement in this wide range of flow rates. There are different models of Fleisch pneumotachograph with different inner diameter and length of the capillary tube. The most frequently used models for respiratory mechanics research are type 00 and type 000, with respective inner diameter of 6 and 9 mm and length of 75 mm [13]. The dead space of the pneumotachograph also affects the accuracy of measurement. Studies have shown that in a dead space the instrument of 15 mL is the cutoff value for measurement accuracy. The dead space of type 00 and type 000 Fleisch pneumotachograph is 0.9 and 2.0 mL, respectively.

In order to avoid the condensation of water vapor in the Fleisch pneumotachograph channels, the instrument is incorporated with heating apparatus. The new version of Fleisch pneumotachograph is equipped with on-demanded heating system. Otherwise, Fleisch pneumotachograph may be used with the protection of heated-moisture-exchanger.

According to the equation of Poiseuille's law, the accuracy of measurement by pneumotachograph is affected by several factors including the gas viscosity, temperature, and humidity. Therefore, the Fleisch pneumotachograph should be calibrated before each epoch of measurements using the same source of gas with the same temperature and humidity [14].

Usually, a large syringe (e.g., 1 L) is used to calibrate pneumotachograph with room air. At this time, the effects of temperature and humidity on the measurement should be considered. Gas in the lungs is at body temperature (37 °C) and fully saturated with water vapor. Measured gas through pneumotachograph is approximately at room temperature and partially saturated with water vapor. Thus, for representing the gas volume in the lungs, gas volume measured under ambient temperature and pressure saturated with water vapor (ATPS) or standard temperature and pressure with dry (ATPD) are needed to convert to the volume under body temperature and pressure saturated with water vapor (BTPS). This conversion is based on Charles's law, which states that gas volume decreases as the temperature decreases [15, 16]. Table 2.1 shows the conversion factors for volume calculation from ATPS to STPD and BTPS.

2.2 Esophageal/Gastric Pressure Monitoring

Mechanical ventilation is an important support therapy, that has been widely used in the intensive care unit (ICU). Mechanical ventilation can improve oxygenation and maintain ventilation function by replacing or assisting the activities of respiratory muscles. In addition, mechanical ventilation can also win valuable time for patients to treat other diseases. However, with more and more extensive application of mechanical ventilation, it is found that mechanical ventilation itself will cause damage to patients to a certain extent. In addition to varying degrees of influence on the hemodynamics of the patients, mechanical ventilation may also lead to the aggravation of the original lung injury and even the occurrence of new lung injury, named as ventilator-induced lung injury (VILI) [17]. In recent years, with the

Table 2.1 Conversion factors for volume calculation from ATPS to STPD and BTPS

Temperature (°C)	ATPS (mmHg)	Factor	
		STPD	BTPS
10	9.2	0.952	1.153
11	9.8	0.949	1.148
12	10.5	0.945	1.143
13	11.2	0.940	1.138
14	12.0	0.936	1.133
15	12.8	0.932	1.128
16	13.6	0.928	1.123
17	14.5	0.924	1.118
18	15.5	0.920	1.113
19	16.5	0.916	1.108
20	17.5	0.911	1.102
21	18.7	0.906	1.096
22	19.8	0.902	1.091
23	21.1	0.897	1.085
24	22.4	0.893	1.080
25	23.8	0.888	1.075
26	25.2	0.883	1.069
27	26.7	0.878	1.063
28	28.3	0.874	1.057
29	30.0	0.869	1.051
30	31.8	0.864	1.045
31	33.7	0.859	1.039
32	35.7	0.853	1.032
33	37.7	0.848	1.026
34	39.9	0.843	1.020
35	42.2	0.838	1.014
36	44.6	0.832	1.007
37	47.1	0.826	1.000
38	49.7	0.821	0.994
39	52.4	0.816	0.987
40	55.3	0.810	0.980

ATPS Ambient temperature and pressure, saturated with water vapor, *STPD* Standard temperature and pressure, dry, *BTPS* Body temperature and pressure, saturated with water vapor

pathophysiology of VILI being explored, the concept of lung protective ventilation strategy has been proposed [18]. Lung protective ventilation strategies individually are helpful to reduce VILI by monitoring respiratory mechanics (including pressure and flow) at the bedside. The airway pressure (Paw) at the open of ventilator tubing reflects the pressure gradient over the entire respiratory system (lung and chest wall). In some cases, such as obesity, thoracic, or abdominal disease, the Paw cannot reflect actualpressure gradient over the lung because the higher percentage of Paw is used to overcome the elastance of the chest wall. The monitoring of pleural

pressure (Ppl) or esophageal pressure (Pes) may help to distinguish the pressure gradients acting on the lung and chest wall.

On the other hand, when the patient has spontaneous breathing, the inspiratory muscles and the ventilator both participate in breathing activity during assisting ventilation mode. And the pressure inflating the lung comes from the pressure generated by the ventilator and the patient's inspiratory muscles. Nowadays, the role of patients' breathing efforts during mechanical ventilation is still controversial. Some studies have pointed out that a certain degree of breathing effort can maintain the expansion of the lung tissue in the dependent region and further improve oxygenation and prevent the occurrence of diaphragm disused atrophy [19, 20]. Epidemiological data show that the proportion of clinical application of auxiliary ventilation is gradually increasing, suggesting that doctors pay more and more attention to the role of spontaneous breathing [19]. However, excessive breathing effort also can induce spontaneous lung injury (P-SILI) [21]. And studies found that early using continuous infusion of neuromuscular blockers in severe ARDS patients to remove spontaneous breathing can improve patient survival [22]. Therefore, it is very important to monitor spontaneous breathing efforts and to balance the relationship between mechanical ventilation and spontaneous breathing effort during assisting ventilation. The Monitoring of Pes, intragastric pressure (Pga) and a series of parameters derived from Pes and Pga can be used to quantitatively assess spontaneous breathing efforts. This chapter will briefly introduce Pes and Pga monitoring technology from the aspects of physiological basis, technology points, and potential clinical application.

2.2.1 Physiological Basis

The lungs are located in the thoracic cavity and surrounded by the visceral pleura. The visceral pleura and parietal pleura that is close to the chest wall formed the pleural cavity. The lungs and chest wall are connected through the pleural cavity. As two elastic structures, the lungs and chest wall will deform when pressure is applied and recover the original shape after the pressure is removed. The lung has a tendency to recoil and the chest wall has a reverse trend that prevents the lung from collapsing. When a person is in an upright position during resting, Ppl is a slightly negative value.

Understanding the pressure gradient of different parts of the respiratory system is the basis for learning respiratory mechanics. Figure 2.1 and Table 2.2 show the pressure gradient of different respiratory structures. The pressure gradient over the respiratory system (Prs) is the difference between the alveolar pressure (Palv) and the body surface pressure (Pbs); the pressure gradient over the chest wall (Pcw) is the difference between Ppl and Pbs; the pressure gradient over the lung, named as transpulmonary pressure (PL), is the difference between Palv and Ppl; transdiaphragm Pressure (Pdi) is the difference between abdominal pressure (Pab) and Ppl [23, 24]. When the lungs are at resting condition, the

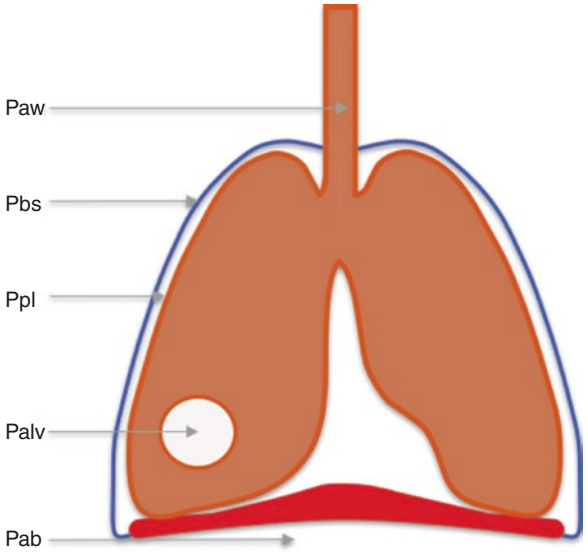

Fig. 2.1 Schematic drawing of pressures for the respiratory system. *Paw* Airway pressure, *Pbs* Body surface pressure, *Ppl* Pleural pressure, *Palv* Alveolar pressure, *Pab* Abdominal pressure

Table 2.2 Pressure gradient of different respiratory structures

Structure	Definition	Formula
Total respiratory system	Trans-Respiratory System Pressure (Prs)	Prs = Palv – Pbs = Paw – Pbs
Chest wall	Trans-Chest Wall Pressure (Pcw)	Pcw = Ppl − Pbs
Lung	Transpulmonary Pressure (PL)	PL = Palv – Ppl = Paw − Ppl
Diaphragm	Transdiaphragm Pressure (Pdi)	Pdi = Pab − Ppl

Palv Alveolar pressure, *Pbs* Body surface pressure, *Paw* Airway pressure, *Ppl* Pleural pressure, *Pab* Abdominal pressure

glottis is open and no airway closure exists, Palv is equal to Paw. In the formula, Paw can be instead of Palv to calculate Prs and PL. Learning the pressure gradient between different respiratory structures under physiological conditions is very important for us to understand the changes in respiratory mechanics in the state of disease. Observing the relationship between PL and Pcw can reflect the pattern of movement between the chest wall and lung during breathing. Pdi provides a way to evaluate diaphragm movement and quantify spontaneous breathing efforts.

During inspiration, the volume of the lungs and chest wall changes with pressure changing. The driving pressure of the respiratory system is generated by the contraction of respiratory muscles during spontaneous breathing, by the ventilator during controlled ventilation and by both during assisting ventilation. The total pressure (Ptot) of the respiratory system includes the sum of the pressure provided by the ventilator (Paw) and the respiratory muscle pressure (Pmus) of the patient. Ptot is used to overcome the elastance and resistance of the respiratory system. The equation of gas motion (2.1) describes the above relationship:

$$\text{Ptot} = \text{Paw} + \text{Pmus} = P_0 + \text{Ers} \times V + \text{Rrs} \times \dot{V} \tag{2.2}$$

P_0 is the Paw at the beginning of inspiration, Ers is the elastance of the respiratory system, Rrs is the airway resistance of the respiratory system, V is the change of volume, and $\dot{V}$ is the flow. When ventilation mode is set in volume control ventilation with a constant flow, the V and $\dot{V}$ are set parameters. According to Eq. (2.1), Ers and Rrs can be calculated by the inspiratory and expiratory occlusion [23]. In addition, Eq. (2.1) can be converted into different breathing patterns and conditions.

In a controlled ventilation mode and patients have no breathing effort, Pmus is zero and Ptot is completely provided by the ventilator. The elastance of the respiratory system can be distinguished as the elastance of the lungs and chest wall. Equation (2.1) can be transformed into Eq. (2.2):

$$\text{Ptot} = \text{Paw} = P_0 + \text{Ers} \times V + \text{Rrs} \times \dot{V} = P_0 + \text{Ecw} \times V + E_{\text{L}} \times V + \text{Rrs} \times \dot{V} \tag{2.3}$$

In Eq. (2.2), Paw, P_0, V, and $\dot{V}$ can be continuously monitored by the ventilator. When the inspiratory occlusion is preformed, the flow is 0 and the resistance is also 0. The remaining variables Ecw and EL represent the change of Pcw and PL in unit of volume, respectively. And measuring Ppl or Pes is the best way to distinguish the portion of Paw acting on lung and chest wall.

Spontaneous breathing effort refers to the process of respiratory movement and energy consumption driven by respiratory muscles. In patients with spontaneous breathing efforts, Pmus becomes a very important part of the Ptot that drives breathing movements. Under normal physiological conditions, the inhalation is an active process and the exhalation is a passive process. Diaphragm is the main inspiratory muscle, which is located between the thoracic cavity and abdominal cavity. When diaphragm contracts, the downward movement of the diaphragmatic dome enlarges the chest cavity and expands the lungs and chest wall. The diaphragm relaxes as exhale, and the lungs and chest walls return to their original state. The forces of all respiratory muscles can be reflected by monitoring Ppl or Pes. The Pdi calculated with Pab or Pga can reflect the force of the diaphragm during breathing.

2.2.2 Esophagus Pressure Estimates Pleural Pressure

Ppl is an important quantitative index for describing the respiratory mechanical characteristics, but it can only be obtained by invasive methods which cannot be widely used in clinical. As an alternative method, Pes is rather noninvasive method that can be real-time monitored at the bedside. In 1950s, Buytendijk firstly found that Pes could estimate Ppl [25]. Later, researchers found that although Pes tends to be more positive than Ppl, the change of the Pes and Ppl were similar [26, 27]. The measurement of Pes, instead of Ppl, can improve our understanding of the mechanical properties of the lungs and chest wall. A series of derived parameters also can

enhance our further understanding of the pathophysiology of respiratory failure and VILI.

It should be noted that when the person is in the upright position, the lower third of the esophagus is very close to the pleural cavity and the Ppl can be passed to the esophagus accurately. At this position, Pes is close to the adjacent Ppl [28]. However, in the supine position, the weight of the mediastinum and abdominal pressure both increase Pes. Some studies have pointed out that the Pes is over Ppl about 5 cmH_2O due to the effects of body position and mediastinum [29]. In addition, the heterogeneity of the gravity gradient in the lungs also influence Pes. Pes may underestimate Ppl in dependent regions and overestimate Ppl in nondependent regions. In addition, factors such as lung and chest wall deformation, pleural effusion, esophageal smooth muscle reactivity, increased abdominal pressure, and characteristics of the esophageal manometers may affect the absolute value of Pes. Although the absolute value of Pes is still controversial, it is generally believed that Pes can represent the average level of Ppl in both animal and human studies and the changes between Pes and Ppl have a good correlation. For making sure Pes to reflect Ppl accurately, the technical aspects of Pes measurement are important. It usually includes the characteristics of the esophageal manometers, placement position, balloon inflating volume, and data interpretation.

2.2.3 Technology

The monitor of Pes mainly depends on placing esophageal manometers. There are mainly three types of esophageal manometer tubes: balloon catheters, fluid-filled catheters, and direct pressure sensors. The most commonly used catheters are balloon catheters. Some esophageal balloon catheters have two balloons that can monitor Pes and Pga at the same time. Some esophageal balloon catheters even have the function of nasal feeding, which can be used as gastric tubes. The Pes can be measured by connecting the end of esophageal balloon catheters to the pressure transductor, such as pressure measuring device, the pressure sensor of the ECG monitor, or the auxiliary pressure port integrated into the ventilator. The accuracy of Pes monitoring can be affected by many factors, including the placement of the balloon catheter, the volume of the balloon, and the data interpretation.

2.2.3.1 Position of Esophageal Balloon Catheter and Balloon Volume

First, insert the esophageal balloon catheter into the stomach through the esophagus by the nose or oral, the balloon is inflated in an approximate air and connected to a pressure transductor. Awake patients can be asked to cooperate with swallowing. Then, judge whether the catheter is in the stomach by Pes waveform. For patients with spontaneous breathing, breathing efforts induce Paw decreasing; meanwhile, the diaphragm contraction induces Pga increasing. For patients without

spontaneous breathing, the Pes appearing "jagged" waveform when pressing the abdomen continuously suggested that the balloon is located in the stomach. For catheters with gastric tubes function, the position can be judged by extracting gastric juice. Then, withdraw the catheter into the esophagus slowly. For patients with spontaneous breathing, it can be seen that the Pes waveform changes from a positive waveform to a negative waveform during inspiration. For patients without spontaneous breathing, the Pes waveform is always a positive waveform. But it can be seen that Pes obviously increases when the balloon passes through the cardia of esophagus accompanying cardiac artifacts increasing, then the Pes gradually decreases when withdrawing balloon continually [30]. The depth of the catheter tip from the nose is about 35–45 cm. During the placement of the catheter, it is necessary to observe the phenomenon of cough or sudden rise in Paw, avoiding inserting into the airway by mistake [31].

The material, compliance, and volume of the balloon will affect the accuracy of Pes monitoring. Nowadays, the materials of balloon are mainly polyethylene and rubber, the former is more commonly used. Because balloon has the characteristic of compliance, an over-inflation balloon will overestimate the pressure around the balloon. Conversely, low inflation volumes cannot conduct the surrounding pressure and underestimate the surrounding pressure. Several in vitro experiments have testified proper balloon volume of commercially available catheters, and the results show that the volume-pressure curve of the balloon is "S" shaped. These studies provide data for the use of different types of catheters [32, 33]. In addition, the esophagus wall is also an elastic tissue and it also can affect Pes. The study found that the volume-pressure of balloon in clinical also showed an "S" shape with an intermediate linear section, which represents the proper filling volume of balloon. The slope of this linear section also reflects the elastance of the esophagus wall that can be used to correct Pes [34, 35]. It should be noted that the balloon should be reinflated after each adjustment of the catheter position.

2.2.3.2 Occlusion Test

In order to ensure the accuracy of Pes, it needs to be testified by the occlusion test (Fig. 2.2). For patients with spontaneous breathing, occlusion tests are a very classic way to judge the position of the catheter [36]. Expiratory occlusion induces the breathing effort of patients that causes the Paw and Pes to decrease. If the ratio of the change of Paw and Pes ($\Delta PES/\Delta Paw$) is between 0.8 and 1.2, the balloon is considered to be in a suitable position, otherwise the location and volume of balloon should be adjusted. The principle of this method is that breathing effort during expiratory occlusion does not change lung volume and transpulmonary pressure, so the changes of Paw and Pes should be consistent. For patients without spontaneous breathing, a positive pressure occlusion test can be performed by compressing chest wall during expiratory occlusion and compare the positive changes in Pes and Paw (Fig. 2.2). The study has shown that the positive pressure occlusion test has a good consistency with traditional occlusion test [37]. Occlusion test has been validated in

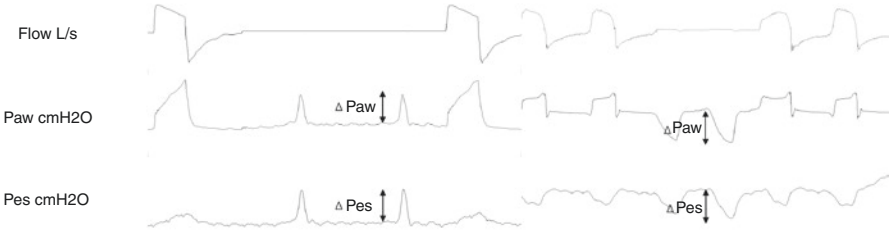

Fig. 2.2 Occlusion test in a spontaneous and a passive patient under mechanical ventilation. Breathing effort during expiratory occlusion does not change lung volume and transpulmonary pressure, so the changes of Paw and Pes should be consistent. During patients with spontaneous breathing (right), the ratio of the change of Paw and Pes (ΔPES/ΔPaw) is between 0.8 and 1.2, the balloon is considered to be in a suitable position and appropriate balloon volume. During patients without spontaneous breathing (left), ΔPES/ΔPaw was obtained by pressing the chest wall. *Paw* Airway pressure, *Pes* Esophageal pressure

different types of patients. The position of the balloon, the volume of the balloon, and the patient's position and lung volume all can affect occlusion test. Before occlusion test, the balloon of the artificial airway should be routinely checked to prevent the air leakage from affecting the occlusion test. In addition to the occlusion test, some catheters have radiopaque markers, and the correct position of the balloon can be judged by a chest X-ray.

2.2.3.3 Other Factors

During Pes monitoring, the amplitude of cardiac artifacts also affects Pes results, which even can up to 4–5 cmH_2O [38]. The study proposed that the use of cardiac cycles to determine the measurement phase of Pes can improve the accuracy of the occlusion test [39]. Adjusting the position of the catheter can lower interference. If the esophageal contraction occurs (the Pes increases significantly and is not related to breath), the measurement of Pes should be stopped until Pes returns to the baseline level. In addition, pay attention to whether the baseline level of Pes is stable. Pes decreasing gradually as time probably suggests balloon leakage, and the esophageal balloon catheter should be replaced.

2.2.4 Application

2.2.4.1 Transpulmonary Pressure during Passive Ventilation

During passive ventilation, the patients do not exist spontaneous breath and all the pressures that drive the respiratory system come from the ventilator. Paw can reflect the mechanics of the respiratory system, but the pressure acting on the lungs is not

identified yet. As Table 2.2 shows, PL is the force that directly expands the lung tissue, which is equal to the difference between Palv and Ppl. Under passive condition, inspiratory and expiratory occlusion (usually 3s) can make the air in airway and alveoli reach balance. At this situation, Paw is considered to be equal to Palv. Ppl can be estimated by Pes. And considering the limitations of Pes monitoring, scholars proposed different mathematical models to improve the accuracy of PL calculation. The three main methods are introduced as follows:

Calculation Method of Transpulmonary Pressure

Direct measurement method: The PL is calculated by the difference between the Paw and the absolute value of Pes during inspiratory and expiratory occlusion, PL = Paw − Pes. Due to the weight of the mediastinal organs and the elastance of the esophagus wall in the supine position, the PL is usually underestimated that may not accurately reflect the conditions of alveoli open and close periodically or the alveoli collapse. Therefore, some scholars estimated the weight of the mediastinum based on the change of Pes in different positions of healthy volunteers [40] and estimated the elastance of esophagus wall based on the change of Pes at different balloon volumes [41]. The study also proposed a simple method to correct Pes by minus 5 cmH_2O directly [42]. But this correction method is suitable for different types of patients remains to be further verified.

Release derived method: The studies suggested that although there were differences in the absolute values of Pes and Ppl, the correlation and consistency of the changes of Pes and Ppl with breath had a good agreement [26, 27]. The release derived method is based on the changes of Paw and Pes under the conditions of mechanical ventilation and atmospheric pressure (ATM). First, measure Paw and Pes during end-inspiratory and expiratory occlusion. Then, the ventilator is disconnected at the end-expiratory occlusion and the Paw and Pes are measured after patients expiring the residual gas in the lungs, finally calculate the PL according to the formula: P_L = (Paw − Paw at ATM) − (Pes − Pes at ATM) [43]. Regardless of the absolute value of Pes, Ppl at the end-expiration is zero during ATM. The advantage of this method is to avoid the influence of mediastinal weight and esophageal wall elastance. The disadvantage is needing to disconnect ventilator, which is possibly harmful for some critically ill patients.

Elastance derived method: This is another method to calculate PL based on pressure changes, proposed by Gattinoni et al. [44]. Under passive ventilation, the Ers and Ecw can be calculated by Paw and Pes obtained from end-inspiratory and end-expiratory occlusion. The Ers is equal to the sum of the EL and Ecw, Ers = EL + Ecw. Using the proportion of EL in the Ers, the PL at end-inspiration can be calculated by the formula: PL = Paw × EL/Ers. This method assumed that the Ers changes linearly during inspiration. The advantage of this method is also to avoid the effect of mediastinal weight; moreover, it does not need disconnecting the ventilator. The disadvantage is that cannot obtain PL at end-expiration.

Some studies compared the agreement of three methods. The PL at end-inspiration calculated by elastance-derived method and release-derived method had a good agreement [45]. Another study measured different lung regions PL in animal models and corpses [46], it found that PL calculated by direct measurement method better reflected PL in the dependent region, which could be used to guide PEEP setting, and PL calculated by elastance-derived method better reflected PL in the non-dependent lung region, which can be used to reduce lung overdistension.

Clinical Application

In controlled ventilation, the purposes of PL are to guide the PEEP setting based on PL at end-expiratory, reduce lung overdistension by limiting PL at end-inspiration and ΔPL and evaluate the patient's recruitability. The main purpose is to lower the risk of VILI and provide evidence for setting mechanical ventilation parameters and other treatments by the above methods.

There is still much controversy about how to select the "optimal PEEP." According to pathophysiology, PL at end-expiration reflects the state of lung tissue at end-expiration, the negative value indicates the possibility of alveolar collapse or atelectasis. In the EPVent study, Talmor titrated PEEP to keep PL at end-expiration calculated by direct measurement method at 0–10 cmH_2O and limit the PL at end-inspiration to less than 25 cmH_2O in ARDS patients. The results showed that the oxygenation and compliance were significantly improved, and the mortality also showed a downward trend, compared to the ARDS network low PEEP table method [44]. However, EPVent-2 study did not yield the same results. This study compared the Pes and ARDS network high PEEP table to guide PEEP setting. The results showed that there was no significant difference in setting PEEP levels between the two groups, meanwhile there were no significant differences in other outcomes [47]. The difference in the responsiveness of PEEP (lung recruitability) may be one of the reasons that resulted in different results of these two studies.

As we all know, recruitment maneuver can open the collapsed alveoli, increase lung volume, and improve oxygenation in patients with ARDS. However, the effect of lung recruitment varies in different patients. That is, not all patients are sensitive to recruitment maneuver, as lung recruitability. Some studies pointed out that patients with lung compliance decreasing are mostly recruitable, while those with chest wall compliance decreasing are mostly unrecruitable [48]. For patients with unrecruitable lung, recruitment maneuver probably induces lung overdistension. Therefore, PL derived from Pes monitoring is essential in assessing the effect and safety of recruitment maneuver.

PEEP can prevent the alveoli opening and closing periodically during breathing and play a role in stabilizing the alveoli. However, PEEP may also cause alveoli overdistension to induce VILI. Compared to airway plateau pressure, PL at end-inspiration is the actual pressure that reflects the state of lung inflation. Grasso believes that setting PEEP based on PL at end-inspiration may be safer and more

effective. The study titrated PEEP to make PL at end-inspiratory be close to 25 cmH_2O in patients with influenza A (H1N1)-associated ARDS and showed that could improve oxygenation and decrease inappropriate use of ECMO [49]. It is currently believed that limiting PL at end-inspiration to below 20–25 cmH_2O can reduce the occurrence of lung overdistension and reduce the risk of VILI [49, 50].

With introducing the concept of driving pressure, it is believed that it may be related to mortality in patients with ARDS. The part of the driving pressure acting on the lung is the transpulmonary driving pressure (ΔPL), that may be the key to affecting patient mortality [51, 52]. Studies suggested that for patients with ARDS, ΔPL less than 10–12 cmH_2O may help reduce the risk of VILI [50]. But these conclusions need further research and verification.

2.2.4.2 Quantitative Assessment of Spontaneous Inspiratory Efforts

Under assisting/supporting ventilation, it is important to assess the patient's spontaneous inspiratory efforts, because the pressure inflating the lung comes from the ventilator and patient's spontaneous inspiratory efforts. Proper spontaneous inspiratory efforts can improve oxygenation and reduce the occurrence of respiratory muscle atrophy that is helpful to wean as soon as possible. Strongly spontaneous inspiratory efforts may lead to P-SILI. Lacking spontaneous inspiratory effort may cause ventilator-induced diaphragmatic dysfunction (VIDD). Clinicians usually judge the extent of spontaneous inspiratory effort by observing the patient's breathing pattern and amplitude. However, patients might already have existed severe respiratory muscle fatigue if the above symptoms appear, and the symptoms and signs cannot quantitatively assess spontaneous inspiratory effort. Besides, the parameters displayed by the ventilator also cannot assess the patient's spontaneous inspiratory effort. A combination of Pes and Pga monitoring can quantitatively assess spontaneous inspiratory efforts, including pressure swings, work of breathing, and pressure time product. These parameters can help to better adjust mechanical ventilation settings and guide weaning, identify patient-ventilator asynchronous and intrinsic PEEP (PEEPi).

Quantitative Signs

Pressure swings. Pressure swings refer to the change of pressure during breathing, which is usually equal to the difference between the pressure at the expiratory flow of zero (Pexp) and the pressure at the inspiratory flow rate of zero (Pinsp). The formula is: $\Delta P = \text{Pexp} - \text{Pinsp}$. The pressure in the formula can be Pes, Pga, and Pdi. During spontaneous breath, Pes decreased and Pga and Pdi increased. The calculation of the pressure swings is very simple and can be monitored in real-time at the bedside. However, the Pes swings do not take into account the effects of time, the elastance of chest wall, and PEEPi. Therefore, it is difficult to assess the energy expenditure of the respiratory muscles.

Work of Breathing (WOB) and Mechanical Power (MP)

When a force is applied to an object, the object moves in the direction of the force, it is considered as working on the object. Working is always accompanied by a change in energy, the international unit is Joule (J). WOB refers to the change of volume caused by pressure during breathing. The formula is: $\mathrm{WOB} = \mathrm{P} \times \mathrm{V} = \int_0^v P dv$. WOB is usually expressed as joule per liter (J/L). Normal values in healthy adults at resting are approximately 0.35–0.7 J/L [53]. The Campbell diagram drawn by dynamic Pes and lung volume divided the WOB into three parts: resistance, elastance, and PEEP (Fig. 2.3). The limitations of WOB mainly include two points: first, WOB cannot reflect changes in isovolumic contraction because WOB is calculated based on the change of volume induced by pressure; Second, WOB does not consider the effect of time. If the time is different but the same pressure causes the same volume change, the energy is also different. The main energy of WOB is mechanical energy in mechanical ventilation. Combining WOB with respiratory rate can obtain mechanical power, also known as mechanical power (MP). MP integrates several parameters of pressure, volume, and time, which can well reflect the energy consumption of respiratory muscles. Studies showed that the increase in MP is related to the occurrence of VILI [54, 55].

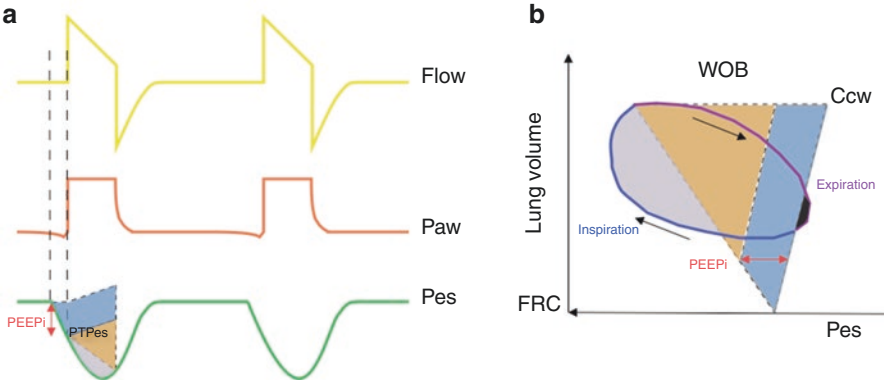

Fig. 2.3 Schematic diagram of WOB and PTPes. (**a**) Shows the pressure and velocity waveforms in pressure support ventilation mode. From top to bottom, flow velocity, airway pressure, and esophageal pressure were shown, respectively. The part between the two dotted lines in (**a**) is the part that overcomes PEEPi. It can be seen that Pes has begun to decline, but the flow velocity has not changed. In the Pes pressure-time curve in (**a**), the colorful area of PTPes includes three parts: overcoming airway resistance (gray), elastic resistance (yellow), and PEEPi (blue). (**b**) Shows the pressure–volume curve based on Pes and lung volume. The area of the color area indicates that the WOB also includes three parts: overcoming airway resistance (gray), elastic resistance (yellow), and PEEPi (blue). In addition, the black area at the end of breath in (**b**) indicates the patient's active expiratory effort. *Paw* Airway pressure, *Pes* Esophageal pressure, *PEEPi* Intrinsic PEEP, *WOB* Work of breathing, *Ccw* Chest wall compliance, *FRC* Functional residual capacity

Pressure Time Product (PTP)

The pressure time product (PTP) refers to the integral of pressure over time. The formula is $Ptp = P \times t = \int_{t}^{t} Pdt$, the unit of PTP is $cmH_2O \times s$, which is usually calculated in a minute, expressed as $cmH_2O \times s/min$. The normal resting state is 60–150 $cmH_2O \times s/min$ [56]. Applying different pressures can reflect different respiratory muscle conditions. PTP calculated by Pes (PTPes) is used to assess overall respiratory muscle activity. PTP calculated by Pdi (PTPdi) is used to reflect the diaphragm muscles. PTP can also be divided into three parts: resistance, elastance, and PEEPi (Fig. 2.3). Compared with WOB, PTP integrates time parameters and has a good correlation with energy consumption in a certain range. In addition, PTP also can calculate changes in muscle during isovolumetric contraction which is suitable to evaluate ineffective spontaneous breathing efforts in patients with asynchronous and PEEPi. PTP also can guide weaning and adjust analgesic and sedative drugs.

Clinical Application

Although there is still controversy about whether to maintain spontaneous inspiratory effort in patients with mechanical ventilation, it is clear that excessive or insufficient spontaneous inspiratory effort will lead to serious related complications and increasing the incidence of adverse outcomes. Excessive or prolonged ventilator support may lead to inadequate spontaneous inspiratory effort and inducing VIDD. The occurrence of VIDD is associated with adverse outcomes such as prolonged ICU stay. A certain degree of diaphragm contractility can prevent atrophy [57, 58]. On the other hand, strong spontaneous inspiratory effort induces the increase in PL swings that may increase stress and induce lung overdistension, even induce asynchrony, leading to P-SILI. In addition, strong spontaneous inspiratory efforts also cause Ppl decreasing and gas in the lungs redistributing, that is, air flows from the nondependent region into the dependent area. Decreased Ppl can also increase Ptm of blood vessel, leading to pulmonary edema. When the inspiratory load is excessive, the activity of the expiratory muscles increases significantly. Abdominal muscle contraction can lead to increasing intra-abdominal pressure and Ppl. High Ppl might cause alveoli collapsing and atelectasis during expiration. Pes/Pga monitoring during mechanical ventilation should be strengthened in clinical practice to assess patient's inspiratory effort.

In recent years, the patient-ventilator asynchrony has caused wide attention. The asynchrony can result in severe hypoxemia in patients, increasing WOB, and even increasing mortality and prolonging ICU stays [59, 60]. From the perspective of pathophysiology, asynchrony may cause an increase in ΔPL and/or an increase in tidal volume during ventilation, which may lead to increasing stress and lung overdistension and further inducing VILI or exacerbating lung injury. The above mechanism may be the root reason for adverse outcomes in patients with asynchrony. Many asynchronies cannot be identified by Paw monitoring alone. Only combining

with the Pes can distinguish types of asynchrony. It is important to know the types of asynchrony to guide clinical treatment.

For example, double trigger and reverse trigger are two kinds of asynchrony in clinic. These two types are very similar according to Paw waveform. It is difficult to distinguish them without other equipment. However, the occurrence mechanism and treatment of them are quite different. They can be distinguished when applying Pes waveforms. The double trigger is caused by strong inspiratory effort and the second breath is triggered again after the first breath completion. In a reverse trigger, the first breath is triggered by ventilator and then it triggers diaphragm contracting which generates the second breath. Although the two types of asynchrony can both lead to an increase in ΔPL and tidal volume, the mechanisms are totally different and treatments are also different. The double trigger might require increasing the depth of analgesia and sedation, while the reverse trigger is exactly the opposite. Therefore, no matter from the perspective of the pathophysiological mechanism of the disease, or guiding clinical treatment, it is very important to monitor Pes for monitoring asynchrony.

Patients with mechanical ventilation all need to wean. Studies found that PTPes in patients who failed in weaning was higher than those who succeed in weaning [61]. The increase in PTPes may be related to the increase of load on the respiratory muscles. Monitoring Pes and Pga might be helpful to identify the reason for weaning failure and guide treatment. For example, if an increase in airway resistance leads to PTPes increasing, the clinician needs to give treatments such as suction and bronchodilators; if an increase in elastance resistance leads to PTPes increasing, the clinician needs to consider the possibility of pulmonary edema. In addition, Pes swings can also guide weaning by assessing inspiratory efforts that are superior to the rapid shallow breathing index [62].

For patients with spontaneous breathing, Pes is the most accurate way to measure PEEPi. The main causes of PEEPi include incomplete expiration or restricted airflow. Patient's inspiratory efforts need to overcome PEEPi before increasing lung volume. PEEPi can lead to asynchrony, fatigue of respiratory muscles, and the increase of WOB, even induce lung overdistension and further affect hemodynamics. Under spontaneous breathing conditions, PEEPi is equal to the change of Pes from the beginning of Pes falling to the beginning of the inspiratory flow. However, it should be noted that when the patient expiratory muscles (abdominal muscles) are active, that is, active expiratory appears, the change of Pes should be subtracted from the change in Pab to reflect the actual PEEPi [63].

2.2.4.3 Assess Heart–Lung Interactions

Cardiopulmonary interaction refers to the effect on the circulatory system when the pressure of the respiratory system changes. The main pressures affecting cardiopulmonary interactions are Ppl and PL. The effect of increased Ppl on the circulatory system is mainly related to tidal ventilation, which produces a preload effect [64]. The effect of increased PL on the circulatory system is mainly related to lung

inflation, which produces an afterload effect. In addition, there are differences in the effects of the Ppl and PL on the circulatory system under different ventilation modes. The Pes monitoring can be used to measure the transmural pressure of the cavity. The transmural pressure of the cavity (Ptm) is equal to the inside pressure minus the surrounding pressure. Ptm represents the pressure of the distending cavity and reflects the state of volume in the cavity.

During mechanical ventilation, especially in high PEEP levels, there might be some limitations to assess right ventricular preload and predict volume responsiveness by right atrial pressure (RAP). Applying high levels of PEEP can induce the increase of Ppl and the increase of RAP after pressure is transmitted to the right atrium. As Ppl increase, the resistance of venous return resistance increases, systemic venous return decreases, and right atrial transmural pressure (RAPtm) decreases. Studies found that pulse variability by Pes correction can better predict volume responsiveness [65]. Conversely, an increase in PL can cause an increase in right ventricular afterload and RAPtm. On the other hand, Ppl can affect left ventricular afterload through left ventricular transmural pressure (LVPtm). Left ventricular afterload is positively correlated with LVPtm and the radius of the left ventricle and negatively correlated with the thickness of the left ventricle. In some cases of heart disease (such as dilated cardiomyopathy), the radius of left ventricular increasing and the thickness of left ventricular decreasing results in a significant increase in left ventricular afterload. During mechanical ventilation, an increase in Pes causes a decrease of LVPtm and left ventricular afterload and an increase of cardiac output. Some studies pointed out that an increase in Ppl can cause a decrease of left ventricular afterload, which can increase left ventricular stroke volume and systolic blood pressure in acute heart failure [66].

The dramatic changes in Ppl during spontaneous breathing effort can be shown as a significant change in pulse amplitude with breathing. During spontaneous breathing efforts, Pes increased significantly from −25 mmHg in the inspiration to 8 mmHg in the expiration that resulted in RAPtm increasing significantly. If a patient's spontaneous breathing effort is too intense due to some diseases, it may cause acute negative pressure pulmonary edema [67]. Its mechanism is related to changes of PL and Ptm of small interstitial blood vessels, which further lead to pulmonary capillary disease and leakage. In addition, a significant decrease in Ppl also leads to increasing systemic venous return, pulmonary circulation pressure, and left ventricular afterload.

2.3 Diaphragm Electromyography (EMG)

The main task of the respiratory muscles is to maintain ventilation and perform non-ventilatory behaviors. As the dominant respiratory muscles, the force generated by the diaphragm can be assessed with transdiaphragmatic pressure (Pdi), which is usually measured with bilateral phrenic nerve stimulation. In normal conditions, the diaphragm generates forces for ventilatory behaviors comprising only 30% of

maximal Pdi, whereas non-ventilatory behaviors (e.g., signs) require forces ~60% of maximal Pdi [68, 69]. Near-maximal forces are only generated during expulsive behaviors (e.g., sneezing, coughing).

On the other hand, neuromotor control of respiratory muscles is reflected in muscle electrical activity, which is recorded with electromyography (EMG). Detected with electrodes, usually, the EMG signals are amplified, filtered, and digitized for data analysis. Robust linear correlation between twitch Pdi and peak diaphragm muscle root mean square (RMS) EMG/suggesting that diaphragm EMG measurements may be used as a surrogate of muscle force generation, permitting assessment of neural respiratory drive continuously in various conditions [70, 71].

In critically ill patients, EMG has proven useful in providing better insight into breathing patterns in the control of breathing. The respiratory impulse originated from the neurons of the brainstem, carried via motor nerves, transmit through neuromuscular junctions, and propagate along the respiratory muscle fiber membranes. Any failure of these sites can result in abnormal EMG signals. Combined with other mechanical function tests or alone, the EMG can access the efficacy of the muscle's contractile function and sometimes, diagnose neuromuscular pathology.

2.3.1 EMG Equipment

Three pathways are established to detect the electrical signal of the diaphragm: transcutaneous, transesophageal, and intramuscular pathway, by placing the sensors on the skin overlying the area of apposition of the diaphragm to the chest wall, swallowed into the esophagus to measure crural diaphragm EMG, or inserted into the diaphragm directly with needle, wire, or hook electrodes. Of these methods, the electrical activity of the heart during contraction inevitably interferes with the electrical signal of the diaphragm measured with a transcutaneous and transesophageal pathway. Due to the characteristics of invasive and discomfort, the intramuscular pathway is impractical to use in critically ill patients.

2.3.2 Surface Electrodes

Not only the diaphragm, but the electrical activity of the accessory muscles could also be monitored with surface electrodes. The advantages of these methods include noninvasive and simple to use. Depending on the researcher's knowledge of anatomy, the electrodes are placed over or as close as possible to the target muscles, and no standards are recommended in terms of the electrode design or positioning. Thereafter, the main drawback of the surface electrodes to monitor diaphragm is the unreliability of the acquired signals, contaminated with the signals from irrelevant

muscles, and variate with the differences of body composition (e.g., subcutaneous fat) [72–74]. It must be pointed out that the surface electrodes measure signals just from the costal diaphragm component.

2.3.3 Esophageal Electrodes

Decades ago, investigators mounted pairs of electrodes outside a catheter and acquire the electrical signals of the crural diaphragm by inserting the catheter into the esophagus [75, 76]. In anatomy, the motor innervation zone (a region with a high density of motor endplates) of the crural diaphragm of adults lies 1–3 cm cephalad to the gastroesophageal junction, and compared with the right, the left side approximately 1 cm cephalad [77]. It is very hard to keep the attachment of the electrodes to the monitored crural diaphragm since the electrode catheter could move up to 8 cm during inspiration [78].

Multipair esophageal electrodes have been developed to optimize the diaphragm-electrode positioning, by mounting a serial of ring electrodes on one catheter, fixed distance with each other. All electrodes signals monitored and paired continuously, and the signals from each paired electrodes caudal and cephalad to the central area of the crural diaphragm will have a similar amplitude and opposite polarity, under the condition of the same distance from the center. The signal-to-noise ratio could be enhanced, and the artifact originating from the diaphragm movement could be reduced by double subtract the signals [79]. Based on the acquired reliable diaphragm EMG signals, in 1999, Sinderby et al. developed a novel ventilatory mode, which provides the proportional pressure support to match the patient's inspiratory effort, known as the neutrally adjusted ventilatory assist (NAVA) [80].

The limitation of the esophageal electrodes includes mini-invasive, discomfort, and relatively expensive of the commercially available catheter. Abnormal esophageal anatomy makes it difficult to place the catheter and increases the risk of complications. Contrary to the surface electrodes, furthermore, the signals only sample the crural portions of the diaphragm, instead of the representation of the whole diaphragm.

2.3.4 Signal Disturbances

The feasibility and reliability of the acquired signals are important for data analysis and interpretation. A good electrical signal should remain stable in frequency and amplitude; however, usually interfered with the power line frequency and movement. The movement of the electrodes and the change of the pressure on the electrode results in large-amplitude, low-frequency artifacts. Since high-pass filters could filter out most of the motion artifacts, loss of low-frequency power from the EMG signal are inevitable. Various originated noises are usually assumed to have constant power density and are estimated with the signal-to-noise ratio.

2.3.5 Cross-talk Signals

Cross-talk signals refer to the signals originating from muscles other than the muscles being investigated. As mentioned above, the amplitude and frequency parameters of the EMG are strongly affected by the cardiac contraction (10 times the power of the diaphragm EMG with a much lower frequency), and it is hard to separate these two components. There are two techniques developed to reduce the electrocardiography (ECG) contamination: the gating technique, which removes a section (0.4 s) of the EMG signal centered on the QRS complex [81] and the double-subtraction technique, which subtracts an ECG template from the diaphragm EMG signal at each occurrence of the ECG waveform [82].

Apart from ECG, both the esophageal peristalsis and abdominal/intercostal muscle activity contribute to the signal contamination of the diaphragm, all of which should be identified and excluded carefully [83, 84].

2.3.6 Application in the ICU

Continuous monitoring of the electrical activity of the diaphragm is very important for critically ill patients. Diaphragm dysfunction is popular in ICU, attributed to the ventilator over- or under-assist, neuromuscular blocking with drugs, and malnutrition, which in turn contribute to the difficult weaning. The diaphragm EMG provides useful information about phrenic nerve and diaphragm function. What is more important, the signals of the diaphragm electrical activity could be used to trigger the ventilator and adjust the level of ventilatory assistance. This novel ventilator mode, specifically, NAVA, has the great advantage of preserving appropriate inspiratory effort during spontaneous breathing [85], improve the patient-ventilator synchrony [86], and facilitate the liberation from ventilator [87].

It is well known that diaphragm active during inspiration and relaxes during expiration. However, it has been demonstrated that contraction of the diaphragm may persist throughout expiration, suggesting a “tonic” activity of the respiratory muscles, especially in healthy premature and full-term newborns, and patients with decreased end-expiratory lung volume (EELV) [88]. When PEEP is applied, the tonic diaphragm activation decreased and the phasic activation increased. This phenomenon could only be detected by the diaphragm EMG, other than other techniques.

2.3.7 Summary

Similar to the electrocardiogram, the electromyography can be used to assess the level of activation of diaphragm fibers and detect the potential neural and neuromuscular pathology. What is more, the electrical activity of the diaphragm could be used

to guide the ventilation proportional to the patient's effort. However, the complexity of data analysis and interpretation combined with the various artifacts limit the application of this technique, which needs to be dealt with in the future.

2.4 Compliance and Resistance

The impedance of respiratory system can be roughly divided into two categories: elastance and inelastic resistance. The former mainly includes the elastic resistance of the lungs and the elastic resistance of the chest wall, which is 2/3 of the main total resistance during breathing. The inelastic resistance includes frictional resistance and inertance, which accounts for about 1/3 of the total resistance when breathing quietly, of which the frictional resistance of the airway is the main.

In respiratory system, the flow of gas is accomplished by the pressure difference, and the respiratory resistance is overcome by driving pressure response. The motion equation of respiratory system is as follows:

$$P = {}^{1}\!/_{C} \times \Delta V + R \times \upsilon + I \times \sigma \tag{2.4}$$

Among them, elastance is often expressed by the reciprocal of compliance (C) and the displacement distance of the respiratory system is expressed by the change of lung volume (ΔV). R represents the airway resistance of the respiratory system, υ represents the gas flow rate, I represents the inertance, and σ represents the acceleration of flow. In general, the inertance of the respiratory system is very small and can be ignored. Formula (2.3) can be simplified to:

$$P = {}^{1}\!/_{C} \times \Delta V + R \times \upsilon \tag{2.5}$$

2.4.1 Elastance and compliance

Elasticity is one of the main characteristics of respiratory system. As to each given lung volume, there is a corresponding elastance for volume maintenance. Arithmetically, the elastance equals to the sum of lung elastance and chest wall elastance.

$$E = E_{\text{lung}} + E_{\text{chest wall}} \tag{2.6}$$

Compliance is the reciprocal of elastic resistance and is a commonly used clinical concept. Respiratory system compliance (Crs) is a measure of elasticity or distensibility, which can be classified into two categories, compliance of the lungs and chest wall. We can mutate the equation based on Eq. (2.5). The normal respiratory compliance is in the range of 50–70 mL/cmH2O.

$$1/C_{\text{rs}} = 1/C_{\text{lung}} + 1/C_{\text{chest wall}} \tag{2.7}$$

2.4.1.1 Lung Compliance (Clung)

Clung is defined as the lung volume change per unit transpulmonary pressure (PL) gradient change. The formula is: $C_{lung} = \Delta V/\Delta P_L$ (L/cmH_2O). Clung was S-shaped on the *P–V* curve (Fig. 2.4). The slope of the middle part is the biggest, that is, the compliance is normal, and the lung has good extensibility. The compliance decreased in the upper part of the S-shaped curve. Collagen fibers play a major role in high volume, which is called the inextensibility of the lung. The incidence of lung injury increased significantly at this stage. In the lower part of the curve, there is a low volume segment with alveolar trapping and a significant decrease in compliance. The elastic resistance of the lung comes from two aspects: the surface tension formed by the interface between the liquid layer and the gas on the alveolar surface, and the elastic retraction force of the elastic fibers of the lung, the former accounts for about 2/3 of the pulmonary elastic resistance, and the latter accounts for about 1/3. On the other hand, the compliance of the lung is variable, and the inspiratory branch and expiratory branch of the *P–V* curve are different, and there is a lag phenomenon (Fig. 2.4). And there is a difference in compliance between quick inhalation and slow inhalation. The variability of Clung may be related to the surface tension of alveoli and the viscosity of lung tissue.

In normal subjects, Clung is referred to be 150 mL/cmH_2O [90]. when it comes to pulmonary fibrosis, alveolar edema, or discontinuation of ventilation, the compliance is decreased due to the interference of lung inflation or partial atelectasis. In addition, reduced compliance is also found in patients with increased pulmonary venous pressure. For patients with pulmonary emphysema, compliance increases as elastic tissue alters. Notably, compliance also increases during acute asthma attack due to unclear mechanisms. Several factors have been reported to affect compliance, including lung volume, posture, pulmonary blood volume, age, bronchial smooth muscle tone, and comorbidities.

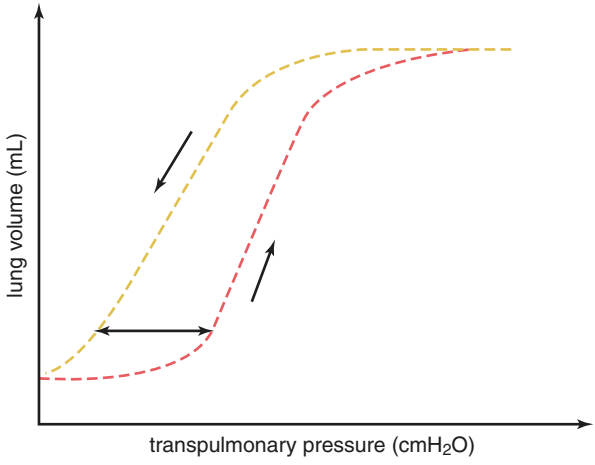

Fig. 2.4 S-shaped *P–V* curve of the lung. The abscissa of the figure is transpulmonary pressure and the ordinate is lung volume. The red dotted line indicates the inhalation process and the yellow dotted line indicates the exhalation process. The two curves do not overlap because of the lag phenomenon. The slope of the curve is Clung

2.4.1.2 Chest Wall Compliance (Ccw)

Ccw is defined as a change in lung volume per unit change in the pressure gradient between the pleural pressure (Ppl) and body surface pressure. The formula is: $C_{cw} = \Delta V/\Delta Ppl$ (L/cmH_2O). Ccw is usually described as milliliters per centimeters of water (mL/cmH_2O) or liter per kilopascal (L/kPa). The reference value of Ccw is approximately 200 mL/cmH_2O [91]. When the lung volume is 67% of the total lung capacity, the chest is in its natural position. When the lung volume is less than 67% of the total lung capacity, the elastic retractive force of the chest is outward, which is the power to inhale and the resistance to exhale. On the contrary, when the lung volume is greater than 67% of the total lung capacity, the elastic retractive force of the chest is inward, which becomes the resistance to inhale and the power to exhale. Increased age, obesity, thoracic scars are clear sources for reducing Ccw. Moreover, researches have shown that posture is an affecting factor of Ccw. Compared to the supine position, Ccw is elevated with the seat position and lessened in the prone subjects.

2.4.1.3 Measurement of Respiratory System Compliance in Mechanical Ventilation

According to the measurement procedures, Respiratory system compliance (Crs) is classified as dynamic respiratory system compliance (Cdyn) or static respiratory system compliance (Cst) in mechanical ventilation. Cdyn is measured throughout the regular process of normal rhythmic breathing and is the tidal volume (VT) divided by the end inspiration airway pressure minus end exhalation airway pressure both at no flow point, while Cst is VT divided by the pressure gradient that plateau pressure (Pplat) subduce positive end-expiratory pressure (PEEP) which is measured after the inspiratory and expiratory hold. The formula of Cdyn and Cst is:

$$C_{dyn} = V_T / \left(P_{end-insp} - P_{end-exp} \right) \tag{2.8}$$

and

$$C_{st} = V_T / \left(P_{plat} - \text{PEEP} \right), \tag{2.9}$$

respectively.

By using an esophageal balloon catheter, a pressure transducer, and a spirometer, Ppl can be measured. By using Ppl, we can calculate PL which is the pressure acting on the lungs. Lung Compliance (Clung) and Ccw can be obtained as lung volume changes dividing by different pressure gradients, respectively.

2.4.2 Resistance

Inelastic impedance includes frictional resistance and inertance. Frictional resistance is the ratio of pressure difference to velocity, and inertance is the ratio of pressure difference to flow acceleration. The frictional resistance of the respiratory

system mainly refers to the friction between the gas molecules and the airway wall when the gas flows through the respiratory tract, also known as airway resistance, which is the most common cause of obstructive pulmonary dysfunction in clinic. The relative displacement of chest and lung tissue will also produce frictional resistance. In addition, the inertance of an object mainly depends on the weight per unit volume (density), the degree of change (displacement), and velocity (acceleration). In general, the inertance of the respiratory system is very small and can be ignored.

2.4.3 Gas Flow and Resistance

2.4.3.1 Laminar Flow

When transferred along a regular, straight, and unbranched tube, laminar flow moves as a series of concentric cylinders, where the peripheral of the cylinder moves relatively slower than the center of the cylinder. As a result, a cone is established in front of the laminar flow. Pressure gradient ΔP and flow rate are calculated as:

$$\Delta P = \text{flow rate} \times \text{resistance}$$

and

$$\text{Flow rate} = \frac{\Delta P \times \pi \times (\text{radius})^4}{8 \times \text{length} \times \text{viscosity}},$$

respectively. Therefore, the resistance is qualified as:

$$\text{Resistance} = \frac{8 \times \text{length} \times \text{viscosity}}{\pi \times (\text{radius})^4} \tag{2.10}$$

2.4.3.2 Turbulent Flow

Turbulent flow occurs in high flow rates, tubular angles, diameter change, or branched tubes, which remains an irregular movement that superposes on the gas movement along the tube. Unlike laminar flow, the front of turbulent flow presents with square rather than cone. As to quantitative calculation, resistance concerning turbulent flow is slightly different from that of laminar flow. That is, the driving pressure of turbulent flow is proportional to the square of the gas flow rate, is proportional to the density of the gas, is theoretically fifth power of the radius, and is independent of the viscosity. When gas flow involves partial or total turbulent flow, the pressure gradient can be calculated as follows, Pressure gradient = k_1(flow) + k_2(flow)^2. The parameter k_1 and k_2 from the equation contain the components of laminar and turbulent flow, respectively. In healthy human subjects,

k_1 and k_2 are summarized to be 0.24 and 0.03. Additionally, the equation can be simplified as:

$$\text{Pressure gradient} = k\left(\text{flow}\right)^n \tag{2.11}$$

In this equation, parameter n indicates the nature of flow (1—pure laminar flow, 2—pure turbulent flow, between 1 and 2—complex). The parameters *K* and *n* in the equation are summarized to be 0.24 and 1.3 in normal human subjects.

2.4.3.3 Reynolds Number

Reynolds number is applied for indicating the nature of gas flow when the progress of gas movement is through a straight tube. Reynolds number can be quantified as follows: linear gas velocity × tube diameter × gas density/gas viscosity. A Reynolds number greater than 4000 indicates that the gas flow is mainly consisted of turbulent flow, whereas less than 2000 indicates laminar flow. A Reynolds number between 2000 and 4000 indicates complex flow that contains both turbulent and laminar flow. Moreover, the Reynolds number is associated with the Entrance length. Entrance length = 0.03 × tube diameter × reynolds number. The entrance length is defined as the distance for establishing laminar flow. As we can conclude from this equation, gas with a low Reynolds number is less resistant and easier to establish laminar flow.

2.4.4 Characteristics of Airway Resistance

Respiratory resistance is consisting of two components, frictional resistance (including airway resistance and tissue resistance) and inertance. Airway resistance is mainly caused by friction. Given the nature of gas flow is much more complex in pulmonary airway than modulation, it is impractical to simply classify the gas flow into laminar or turbulent. As a result of anatomical characteristics, physically, stable laminar flow cannot be established until the last several levels of airway generation. Consequently, excessive turbulent flow potentially creates more frictional resistance through the transduction of gas flow. Tissue resistance is thought to be originated from the lung and chest wall, especially the chest wall, and referred as the viscous force within the tissues. Tissue resistance is rarely related to end-expiratory pressure or tidal volume. It is reported that the tissue resistance owns a 50% weight of total respiratory resistance in anesthetized healthy subjects. In several clinical circumstances, it is important to contemplate the influence of tissue resistance and differentiate the tissue resistance from the total respiratory resistance. Inertance is another component of respiratory resistance. Inertance is difficult to measure and conventionally believed negligible during normal respiration. However, inertance creates significant impedance during high-frequency ventilation.

2.4.5 *Influencing Factors of Airway Resistance*

Physical compression is one of the major factors that affect respiratory resistance. Physical compression can be classified into volume-related and flow-related airway collapse. Volume-related airway collapse occurs in patients with reduced lung volume. Assuming other factors stay constant, airway resistance is reverse proportional to the lung volume when lung volume declines. Expiratory airway collapse causes "valve" effect as well as gas trapping, which increases the airway resistance and leads to an increase in residual volume and functional residual capacity [92]. Flow-related airway collapse occurs specifically in airways beyond the 11th generation for the absence of cartilaginous structures during the maximal forced expiration, where the Ppl remains higher than the atmosphere [93]. As gas flow along the airway, there will be an equal-pressure point, where the Ppl is equal to the atmosphere. Hence, small airways affiliated to the equal-pressure point will be unable to overcome the transmural pressure gradient and develop airway collapse.

Muscular contraction affects the airway diameter through neural pathways, humoral regulations, reflection to stimulations, and inflammatory responses [94, 95]. Neural pathways mainly act through the parasympathetic system and noncholinergic parasympathetic nerves. Acetylcholine on M3 muscarinic receptors causes contraction of bronchial smooth muscle, while vasoactive intestinal peptide produces muscular relaxation by promoting the production of nitric oxide. Sympathetic system plays a deficient role in airway muscular contraction based on existing evidence. Nevertheless, β2-adrenergic receptors are highly sensitive to circulating adrenaline. When it comes to a sympathetic stress response, elevated adrenaline concentration makes great contributions to muscular tone. Stimulations also give rise to muscular contraction. Mechanical stimulation, inhalation of water, cold air, chemical aerosol, or medications are underlying causes of bronchoconstriction. Local cellular secretion is another important mechanism of muscular contraction. Pathogens or allergens activate the secretion of cytokines and amplify the inflammatory response. Among patients with hyperresponsive airway, this mechanism effortlessly generates bronchoconstriction or even bronchospasm.

2.5 Auto-PEEP

In 1982 [96], Pepe and Marini first used the term "auto-PEEP," which was the abbreviation of auto generated positive end-expiratory pressure. Pepe and Marini also described the measurement technique and clinical implications in their study. They found that alveolar pressure could remain positive during the expiratory phase, even the PEEP (positive end-expiratory pressure) was not applied. And they noted that this "auto-PEEP" phenomenon could severely depress cardiac output by increasing intrathoracic pressure. Nowadays, studies in this field have been deeply conducted.

2.5.1 Definition and Terminology

From the Greek word, auto means "self." During the expiratory phase, the respiratory system cannot fully return to relaxed position before the next inspiration initiates. This results in the pressure gradient, which will drive the end-expiratory flow until the sudden stop of inspiratory forces from patient or ventilator. The total end-expiratory alveolar pressure is the sum of the applied PEEP and auto-PEEP.

Auto-PEEP is also termed as PEEPi (intrinsic PEEP) or occult PEEP, which makes confusion of these terms. Auto-PEEP and intrinsic PEEP can be equal when no PEEP is set [97].

Auto-PEEP can be caused by dynamic hyperinflation (DH). The lung volume should return to the relaxation volume at end-expiration in normal conditions, when the patients have airflow obstruction, the lung volume may exceed predicted FRC (functional residual capacity) [98]. Dynamic hyperinflation and air (or gas) trapping (AP) are not always similar, and short expiratory time can produce dynamic hyperinflation without physically trapping gas. For example, in asthma patients without intubation, inspiratory muscles are still working in the early exhalation, and the glottis braking leads to dynamic hyperinflation. On the other hand, gas trapping can be reversed at modest tidal inspiratory pressures in obesity and ARDS (acute respiratory distress syndrome) patients, which have weak inspiratory efforts [97]. So, auto-PEEP can be differentiated into three types: (1) with DH and AP; (2) with DH and without AP; and (3) without DH.

Flow limitation describes the dynamic condition when the flow is limited and cannot be increased anymore, even by increasing alveolar pressure or decreasing airway-opening pressure, which is always related to small airway collapse.

2.5.2 Causes and Determinants

Auto-PEEP can be generated in several pathophysiological and clinical conditions, such as increased airway resistance (including increased equipment expiratory resistance), short expiratory time, long time constant of the respiratory system, high minute volume, tidal expiratory flow limitation, COPD (chronic pulmonary disease), ARF (acute respiratory failure), and obesity.

In fact, expiratory time is a relative concept, and the proportion of expiratory time in the entire respiratory cycle is the key to lead to auto-PEEP. In other words, the time constant of the respiratory system is the key, rather than the seconds of the expiratory time exactly [99].

Dynamic airway collapse is also considered as the intrinsic factor of auto-PEEP [98]. In ventilated COPD patients, the exacerbation of airflow obstruction is caused by dynamic airway collapse and flow limitation.

2.5.3 Effects and Consequences

The effects on respiratory mechanics, gas exchange, and hemodynamics are similar between the intrinsic PEEP (auto-PEEP) and the extrinsic PEEP.

Auto-PEEP is a common cause of dyspnea and patient-ventilator asynchrony (such as noneffective triggering). Studies also show that auto-PEEP is related to VILI (ventilator-induced lung injury), the increase of WOB (work of breathing), and worsen the efficiency of the respiratory muscles.

As for the hemodynamic consequences, the effects of PEEP have been known for more than 60 years. Auto-PEEP can reduce cardiac output by increasing intrathoracic pressure and it can decrease arterial pressure [96]. The dynamic hyperinflation may also cause bradycardia and vasodilation by autonomic reflexes. Auto-PEEP can be a cause of shock and cardiac arrest. Some studies further indicate that it is a common cause of pulseless electrical activity in patients with positive pressure ventilation. During cardiopulmonary resuscitation, auto-PEEP can prevent the return of spontaneous circulation [100].

2.5.4 Detection and Measurement

The auscultation and clinical symptoms can help to suspect the existence of auto-PEEP, the symptoms including (1) the enlargement of chest circumference; (2) lower-effective ventilation; (3) shock, deterioration of cardiovascular function, increased pulmonary artery wedge pressure that cannot be explained with the circulatory system functions; (4) the abrupt increase of the airway peak pressure during volume-preset ventilation and the abrupt decrease of the tidal volume during pressure-preset ventilation, and (5) the decrease of the plateau pressure that cannot be explained with the decrease of respiratory system compliance.

The auto-PEEP can be detected after a EEO (end-expiratory occlusion), with the abrupt increase of the airway pressure. After several seconds of EEO (at least 2–3 s), the stable pressure can be obtained, which is called the total PEEP. Total PEEP is the sum of external PEEP (preset PEEP) and intrinsic PEEP (auto-PEEP).

The intrathoracic pressure changes can be instead of the measurement of esophageal pressure (Pes), which can help to detect auto-PEEP. When the flow still exists during expiratory, the abrupt decrease in Pes indicates that the patient performs an active inspiratory effort. To trigger the ventilator, the inspiratory effort must overcome and counterbalance the auto-PEEP [101]. So in patients with active inspiratory effort, the measurement of auto-PEEP is shown as Fig. 2.5. Auto-PEEP is measured as the negative deflection of esophageal pressure between the start of inspiratory effort and the start of ventilator insufflation (the point of zero flow).

The flow limitation can be detected by manual compression of the abdomen after EEO [99]. The doctor puts his hand on the abdominal wall of the patient, with the

palm on the umbilicus oriented perpendicularly to the axis between the xiphoid process and the pubis. Once the insufflation is finished, the doctor makes firm but gentle compression of the abdomen in an anteroposterior direction throughout the whole expiration. Flow limitation is diagnosed when there is all or part of overlap on the flow-volume loops between the compression and passive expiration. If the compression makes the expiratory flow at any volume be higher than passive conditions, the patient has no flow limitation. This method can increase pleural pressure, so it may be appropriate during the convalescent stage of the disease, considering the safety and validity of the method [102].

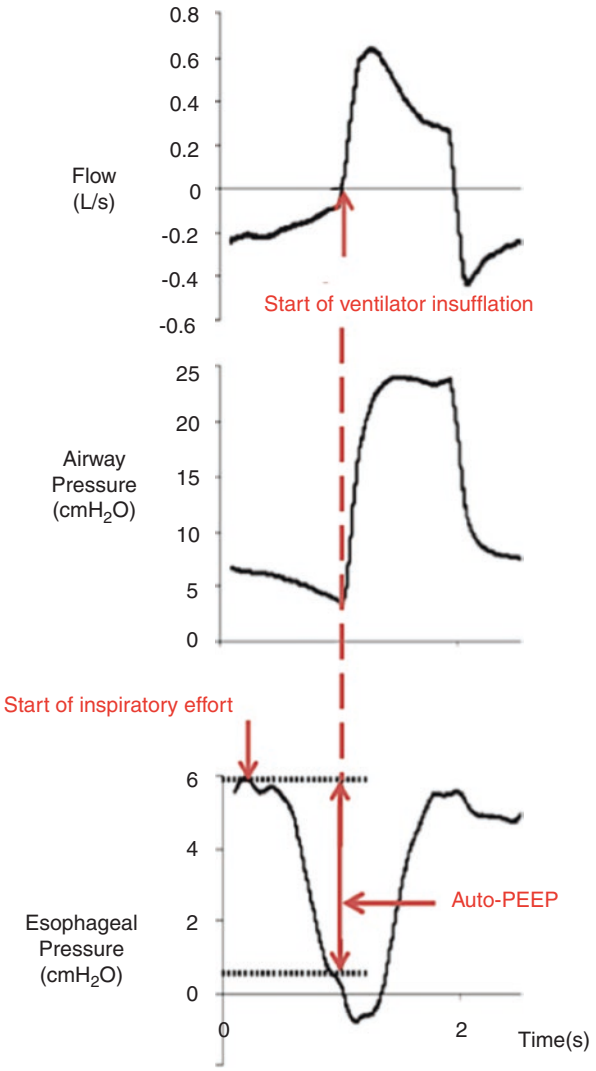

Fig. 2.5 The measurement of auto-PEEP. In patients with active inspiratory effort, auto-PEEP is measured as the negative deflection of esophageal pressure between the start of inspiratory effort and the start of ventilator insufflation (the point of zero flow)

2.5.5 Management and Treatment

Auto-PEEP can be eliminated by several methods including (1) changes of ventilator parameters; (2) reduction of the patient's ventilation requirements; (3) reduction of the expiratory resistance, and (4) use of appropriate external PEEP.

In obstructive patients, the reduction in tidal volume and increase in expiratory time can decrease dynamic hyperinflation. As mentioned before, the proportion of expiratory time in the entire respiratory cycle is the key, so increasing inspiratory flow or reducing breathing frequency could more effectively reduce auto-PEEP.

In 1989, Tobin [103] used the model of the waterfall over a dam to explain the effect of external PEEP (the downstream pressure) on auto-PEEP (the upstream pressure). The downstream pressure is the external PEEP, and the upstream pressure is auto-PEEP. According to this theory, applying external PEEP will unload the burden of the inspiratory muscles and help weaning but it will induce VILI if there is no existence of expiratory flow limitation.

Some studies [99] indicated that flow limitation could be effectively reduced by bronchodilators and the sitting position, and it could be the most effective therapies to reduce auto-PEEP by decreasing airway resistance and time constant of the respiratory system.

2.6 Pressure-Time Curve

2.6.1 Background

Although mechanical ventilation is an important sustaining treatment for patients, especially with acute respiratory disease syndrome, it also can cause ventilator-induced lung injury (VILI) when ventilations result in lung atelectrauma and overdistension. In 2000, the shape of dynamic Pressure–time (*P–t*) curve analysis during constant flow-volume control ventilation was introduced as a noninvasive and real-time method to identify whether lung exists atelectasis and overdistension during ventilation at the bedside [104].

2.6.2 Physiology

Airway pressure-time (Paw-t curve shows the change of airway pressure (Paw) against time, Paw is expressed in cmH_2O and time in second (s) on the ventilator waveform. During volume-controlled ventilation with a constant flow, the volume

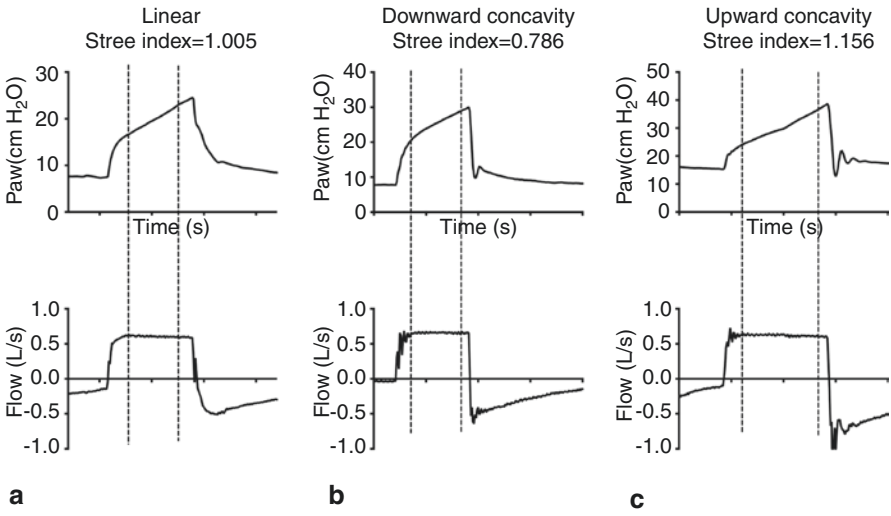

Fig. 2.6 The examples of airway pressure-time (Paw-t) curve. The upper figures show the Paw-t curves and the lower figures show the corresponding flow waveforms. The dotted lines represent the beginning or end of the constant flow. During the constant flow, the Paw-t curve in (**a**) is linear (stress index = 1.005), the Paw-t curve in (**b**) is downward concavity (stress index = 0.786), and the Paw-t curve in (**c**) is upward concavity (stress index = 1.156)

of gas is increased at a constant rate as time, it can be used as a surrogate for a pressure-volume curve to some extent. When assuming airway resistance is constant with inflation, the slope of Paw-t curve reflects the change of respiratory system elastance (as the reciprocal of compliance respiratory system). A linear Paw-t curve represents that the respiratory system elastance remains unchanged throughout tidal inflation (Fig. 2.6a); A downward concavity Paw-t curve represents that respiratory system elastance decreases throughout tidal inflation and suggests existing tidal recruitment, so the positive end-expiratory pressure (PEEP) need to be increased to open collapse lung for avoiding atelectrauma (Fig. 2.6b); An upward concavity Paw-t curve represents that elastance increases because of appearing overdistention with inflation, suggesting that the PEEP, tidal volume, or both need to be decreased (Fig. 2.6c). To qualitatively evaluate the shape of Paw-t curve, the Paw and time can be fitted by the following equation:

$$\text{Paw} = a \times \text{time}^{b} + c$$

where a represents the slope of Paw-t curve as time is equal to 1 s; c is the value of Paw as the time of 0 s; and b is a dimensionless parameter reflecting the shape of the Paw-t curve, which is named stress index (SI). If SI value is between 0.9 and 1.1, the Paw-t curve is linear, SI < 0.9 is downward concavity shape, and SI > 1.1 is upward concavity shape [105].

2.6.3 Measurement

The Method of Calculating SI Manually: First, adjust the ventilation mode to volume-controlled ventilation with a constant flow. To avoid the influence of spontaneous inspiratory efforts, it is better to use neuromuscular blockade or increase sedation level to make Ramsay score of 5. Second, collect Paw and flow. It is recommended to record the Paw and flow for at least 5 breaths in a high sampling frequency with no phase lag; Third, identify the constant flow segment. The constant flow segment is usually identified as the fluctuation is within ±3% of the steady value. Meanwhile, to eliminate the influence of on-flow and off-flow transients, the constant segment should be further narrowed for 50 ms; Forth, The Levenberg–Marquardt algorithm can be used to fit mean Paw and time based on the equation and calculate the SI and R^2 values [105].

Calculations need to be aborted if any following conditions occur: (1) A constant segment is not found because of noise, artifacts, or air leakage; (2) The length of the identified constant segment is less than one-third of the entire inspiratory phase; and (3) R^2 values of the fitting are lower than 0.95 [105].

The Method of Calculating SI by Software: At present, an instrument is mainly used in the field of respiratory monitor, (ICU-Lab KleisTEK, Bari, Italy), can be used to collect Paw and flow in 200 Hz by putting a transducer between the Y-piece of the ventilator circuit and the endotracheal tube, and it also can calculate SI value by automatic procedure (Fig. 2.7). Besides, several types of ventilators can automatically measure SI such as Servo-i or Servo-u (Maquet, Sweden), SV800 (Mindray Co. China), and Luft3 (Leistung, Argentina).

The Method of Calculating SI by Inspection: Besides automatic measurements of SI from ventilators, obtaining SI is still inconvenient in clinical practice because it needs specific software to collect data or rather complex calculations. The previous study introduced a simple method by visually inspecting the ventilator screen waveforms to evaluate SI reliably and accurately [106]. First, clinical physicians need to freeze the ventilator waveform when patients are ventilated in volume control ventilation with a constant flow. Second, identify the midpoint of the constant inspiratory flow waveform and then find the corresponding point on the Paw-t waveform. Third, put a ruler on the ventilator screen and make it pass through the point as the reference of the tangent line for Paw-t waveform. Forth, judge the relationship of this ruler and Paw-t waveform by visually inspecting:

(1) If the Paw-t waveform almost coincides with the ruler, the Paw-t curve is linear, indicating a SI value between 0.9 and 1.1; (2) if the two sides of Paw-t waveform are both deviating downward from the ruler, the Paw-t curve is downward concavity, indicating an SI < 0.9; and (3) if the two sides of the Paw-t waveform are both deviating upward from the ruler, the Paw-t curve is upward concavity, indicating an SI > 1.1 (Fig. 2.8).

Meanwhile, another study also observed the accuracy of direct visual inspection of SI by ventilators' screen [107]. They enrolled 30 patients with ARDS and set

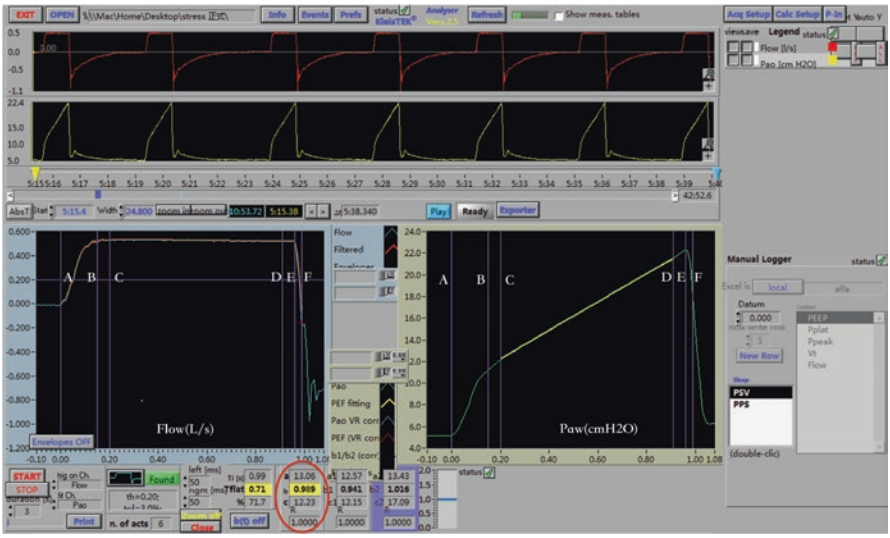

Fig. 2.7 The example of stress index calculated automatically by ICU-Lab. The figure shows the result of automatic calculation of stress index by an instrument that is mainly used in the field of respiratory monitor, ICU-Lab (KleisTEK, Bari, Italy). The red is flow waveform and yellow is pressure waveform in the upper that is selected to calculate stress index. And lower left and lower right are the mean flow-time and pressure-time waveform that are selected to calculate stress index. The line A and F represent the beginning and end of inspiration. The line B and E represent the beginning and end of constant flow. The line C and D represent the true beginning and end of constant segment after the constant flow segment is further narrowed for 50 ms for avoiding the influence of on-flow and off-flow transients. The Paw and time between line C and line D can be fitted by the following equation: Paw = $a \times \text{time}^b + c$, and b value can be shown automatically (0.989 in this figure)

mechanical ventilation in two different inspiratory flow (40 and 60 L/min). The study found that physicians can distinguish three types of SI correctly. Besides, the lower constant flow (as 40 L/min) could improve the sensitivity of visual inspection.

2.6.4 The Specific Pressure–Time Curves

The Sigmoidal Shape of Paw-t Curves: In some situations, the Paw-t curve shows a sigmoidal shape with an initial downward concavity and a final upward concavity, probably because alveolar is opened at the beginning and alveolar exists overdistension at the end as inflation. Under these circumstances, it would be best to divide into two portions and calculate the SI respectively [105]. It was recommended that adjust PEEP to obtain linear in the first portion and set the tidal volume to obtain linear in the second portion (Fig. 2.9).

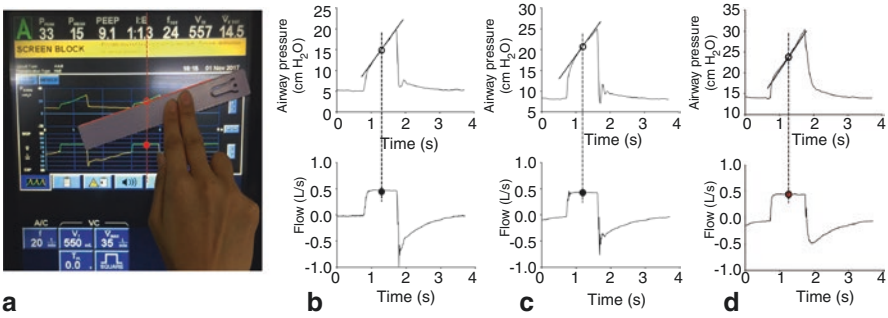

Fig. 2.8 Schematic of the method for visually inspecting the airway pressure-time (Paw-t) waveform and stress index (SI) classification. First, the midpoint on the constant inspiratory flow (red dot) is identified; second, the corresponding point (red dashed line and red circle) on the Paw-t waveform is confirmed; third, a ruler is put on the ventilator screen to mark the tangent line (red solid line) passing through the middle point (**a**). The relationship of this tangent line and the Paw-t waveform is visually inspected and classified into three categories. The Paw-t waveform almost coincident with the tangent line is judged as a linear shape (**b**), indicating an SI value between 0.9 and 1.1. The off-line software measured SI to be 0.98 in this case. When the two sides of the Paw-time waveform both deviate downward from the tangent line, this is categorized as a downward concavity (**c**), indicating an SI 0.9. The off-line software measured SI to be 0.80 in this case. When the two sides of the Paw-time waveform both deviate upward from the tangent line, this is categorized as an upward concavity (**d**), indicating an SI 1.1. The off-line software measured SI to be 1.20 in this case

The Transpulmonary Pressure-Time Curves: When the esophageal pressure (Pes) was measured by an esophageal catheter, the transpulmonary pressure (PL) can be calculated by the equation as PL = Paw − Pes. The PL and time are also described as the following equation:

$$\mathrm{PL} = a \times \mathrm{time}^{b} + c.$$

In fact, the previous studies showed the SI obtained by Paw-t curves could reflect SI of obtained PL-t curve well.

2.6.5 Clinical Application of SI

The measurement of SI monitoring provides a noninvasive, repeatable, and real-time method to monitor respiratory mechanics at the bedside.

In 2000, Ranieri et al. first tested PL-t curves profile in an isolated rat lung injury model [104]. They adjusted tidal volume and PEEP to obtain three types of SI. The study found that set a tidal volume as 6–8 mL/kg and adjust PEEP to keep SI within 0.9–1.1 contributed to reducing VILI and had the lowest histological injury score

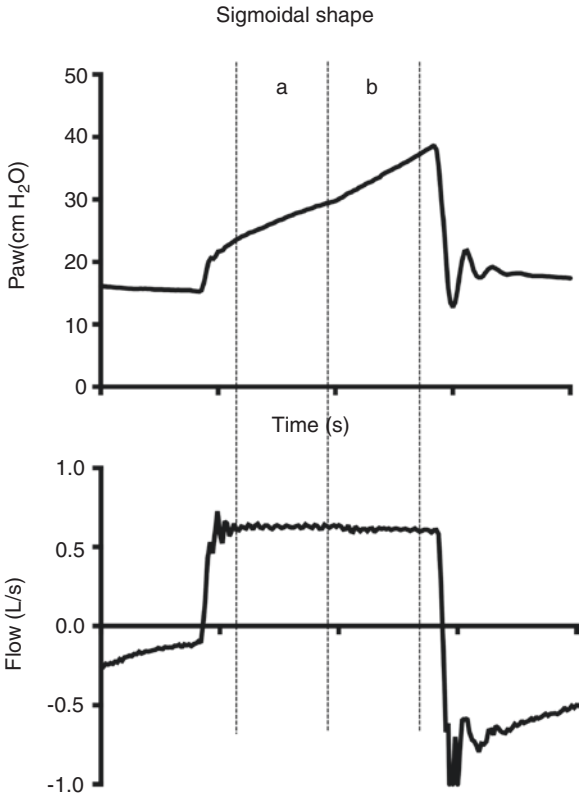

Fig. 2.9 The example of the sigmoidal shape of pressure-time curve. The figure shows the pressure-time (Paw-t) and corresponding flow waveform. This Paw-t curve presents a sigmoidal shape with an initial downward concavity (a) and upward concavity (b)

(Il-6 and MIP-2 levels). And further animal studies also found that the SI could identify tidal recruitment and overdistension accurately compared to CT scan [109–112].

The SI also has been validated in clinical settings [113–117]. Grasso et al. performed a cohort study in 15 ARDS patients, they adjusted PEEP levels randomly according to Blood Institute's ARDS Network (ARDSnet) and SI strategy with other parameters remained consistent [113]. And SI strategy tended to set lower PEEP and had obvious lower biomarkers of lung injury (IL-6, IL-8, and TNF-a) compared to ARDSnet. The further study introduced that combining the values of plateau pressure (>25 cmH_2O) and SI (>1.05) has the highest diagnostic accuracy to identify the overdistension compared to CT scan [115].

But Chiumello et al. compared PEEP levels selected by different methods in patients with different recruitability of the lung, Express, stress index, esophageal pressures, PEEP/FiO_2 table [118]. Besides the PEEP/FiO_2 table, other methods all provided a similar PEEP in the lung with different recruitability. But it seems unreasonable to set high PEEP for low recruitable lung.

2.6.6 The Limitations of SI

First, it just can be used in constant flow ventilation. Meanwhile, deep sedation or paralysis are required to obtain a reliable measure. Second, resistance needs to be assumed constant with inflation. Third, in situations of pleural effusions, high intraabdominal pressure, or heterogeneous lung disease, the ability of SI to identify injurious ventilation needs to be discussed.

2.6.7 Conclusion

In conclusion, a dynamic P-t curve could be used to identify injurious ventilation to some extent, but it is important to pay attention to the theoretical assumptions of applying SI.

2.7 Pressure-Volume Curves

2.7.1 Introduction

The pressure-volume curve (*P–V* curve) is an important index reflecting the mechanical characteristics of the respiratory system. For clinicians, well understanding of the different manifestations of the *P–V* curve under different pathophysiological conditions are helpful to guide the ventilator parameters setting in a clinical scenario and promote the clinical researches.

The *P–V* curve first appeared in the description of acute respiratory distress syndrome (ARDS) in the 1970s [119], since then its role in diagnosis and monitoring has been gradually recognized. However, it was until 1984, when Matamis and colleagues described the relationship between the *P–V* curve and different stages of acute lung injury in adult ARDS patients, that the curve was recognized as a potentially important tool clinically [120]. With further researches on ARDS patients' mechanical ventilator-related lung injury and the effect of ventilator-related strategies on patients' prognosis [121, 122], the *P–V* curve has aroused wide interest among clinicians. By the mid-1990s, *P–V* curves had been widely used in mechanical ventilation to reduce ventilators-associated lung injury. However, with the development of research, there was not enough evidence to prove that protective lung ventilation guided by the *P–V* curve can significantly improve the outcome of patients. Currently, rather than directly used to guide the parameter setting of mechanical ventilation in clinical practice, the *P–V* curve was served to enhance intensivists' understanding of diseases and further clinical diagnosis and treatment.

In this chapter, we will elaborate the clinical applications and recent progress of the *P–V* curve.

2.7.2 Equation of Motion

Before developing the description of applications of the *P–V* curve in clinical practice, it was necessary to briefly understand the equation gas motion of the respiratory system. It is written as follows:

$$\mathrm{PRS} = \mathrm{ERS}\cdot V + \mathrm{RAW}\cdot \dot{V} + \mathrm{PEEPTot}$$

in which PRS is the pressure in the respiratory system, ERS is the resistance in the respiratory system, V was volume, RAW is airway resistance, $\dot{V}$ is airway flow, PEEPTot is the total positive end-expiratory pressure. According to this motion equation, it is no difficult to find that airway pressure of the respiratory system mainly consists of three components in patients without spontaneous breathing during mechanical ventilation. It is no doubt that airway resistance always existed during airflow movement. Therefore, accurate measurement of elastic resistance of the respiratory system, of which reciprocal also called compliance, at static state needs to minimize the influence of airway resistance. Thus, a static *P–V* curve was also named the compliance curve. The comparison of static and dynamic *P–V* curves will be introduced in the following paragraphs.

2.7.3 Static and Dynamic Pressure–Volume Curves

P–V curves can be categorized into dynamic *P–V* curves and static *P–V* curves. The dynamic *P–V* curve is a comprehensive indicator of lung/chest wall compliance and airway resistance. It is much easier to measure, but cannot reflect the overall compliance of the respiratory system accurately due to the interference of airway resistance. The static *P–V* curve is the curve of lung volume and pressure under ideal conditions. Therefore, the static *P–V* curve is more accurate, but also more tedious. In the actual measurement process, it is impossible to interrupt the patient's breathing completely. Thus, it was difficult to achieve an absolute steady state of the respiratory system, and the curve we get is often referred to as the quasi-static *P–V* curve.

At present, in the measurement of the *P–V* curve, the Low Constant-Flow Method is widely used in clinical practice for its simplicity and easy operation, which can minimize the influence of the respiratory airway resistance on measurement results [123, 124]. At the early stage, researchers prefer the dynamic *P–V* curve since not need to disconnect ventilators [125–127]. In 2001, Adams and colleagues [128] investigated the effects of dynamic and static *P–V* curves on different aspects of respiratory mechanics in dogs with oleic-acid-induced lung injury. They measured a quasi-static *P–V* curve using the super-syringe method and compared it with the curves measured with the constant inspiratory flow of 10, 30, and 50 L/min. They found that as the inspiratory flow increased, the curve drifted to the right and the initial volume of all curves is positively correlated with PEEP level during the measurement of the dynamic *P–V* curve. It was not difficult to infer from this study that

when measured with a high flow, the pressure value at the same volume will leave a large pressure change, which is probably caused by airway resistance.

On the contrary, a multicenter study of 28 patients with ALI and ARDS presented a conflicting viewpoint. Stahl et al. [129] detected changes in respiratory mechanics (compliance and recruitment) during dynamic measurements with an incremental PEEP. They suggest that dynamic measurements may be more appropriate for mechanically ventilated patients than the static *P–V* curve. Of course, the application of the dynamic *P–V* curve is still controversial. This chapter will introduce the widely used static *P–V* curve measurement method in detail.

2.7.4 Measurement Techniques and Mathematical models

2.7.4.1 Measurement Techniques

The traditional quasi-static *P–V* curve measurement mainly include the following three methods: super-syringe method, multiple-occlusion method, and low constant-flow method.

Super-syringe Method: The super-syringe method was first introduced in 1975. In the 1980s, it was gradually applied to the description of the different stages of ARDS [120, 121]. Before tracing the curve, the ventilator should be disconnected from the patient and a large syringe of 2–3 L and a manometer should be connected at the end of the endotracheal tube. The pressure value is recorded while pushing the syringe from FRC. Each injection of 100 mL gas is followed by a pause of 2–3 s to allow the pressure in the lungs to reach the quasi-static status to acquire the inspiratory branch of the curve. The pressure–volume value is recorded and repeated until the pressure reaches 40 cmH_2O. At this point, stop the injection and gradually deflate gas in the same way, drawing the curve of the expiratory branch. Taking the pressure as the *X*-axis and the corresponding volume as the *Y*-axis, a quasi-static *P–V* curve is drawn [130].

The virtue of this measurement method is that the quasi-static *P–V* curves of the inspiratory phase and the expiratory phase can be recorded simultaneously. Drawbacks are as follows: (1) additional syringes are required; (2) the ventilator has to be disconnected during measurements; (3) cumbersome and time-consuming operation, which may lead to the risk of hypoxemia; (4) sedation and muscle relaxation are essential; (5) it was not easy to measure curves with different PEEPs; and (6) the continuous gas exchange, gas compressibility, and gas temperature change cannot be controlled in the measurement process. Figure 2.10 shows that the pressure-volume curve is acquired with the low constant-flow method.

Multiple-Occlusion Method: The multiple-occlusion method (also called "ventilator method") was developed in the late 1980s and first described by Levy et al [131]. By periodically interrupting tidal breathing at different lung volumes during volume-controlled mode with a constant flow, different plateau pressures are obtained by blocking at the end of inspiratory and a quasi-static

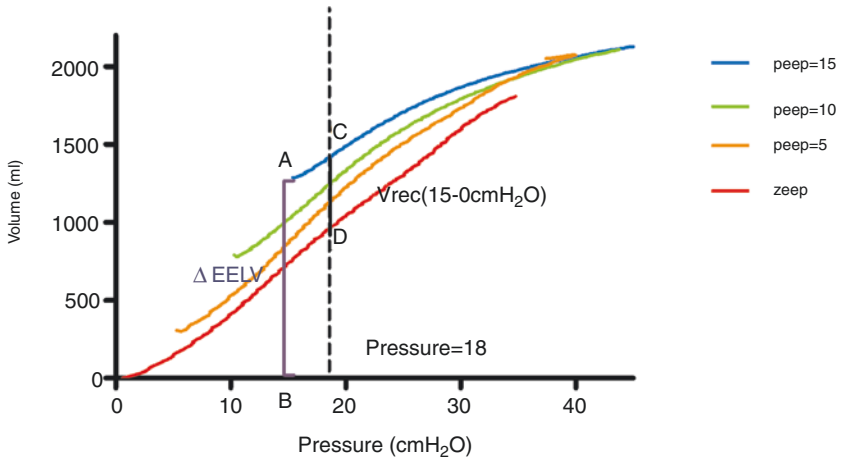

Fig. 2.10 Pressure–volume curve acquired with the low constant-flow method under different levels of PEEP (inspiratory phase). The purple solid line AB means that the difference in the end-expiratory lung volume (ΔEELV) between peep = 15 and zeep. The black solid line CD means that the lung recruited volume (V_{rec}) between peep = 15 and zeep. *PEEP* Positive end-expiratory pressure

P–V curve is constructed, based on the assumption that the lung relaxation volume (or FRC) remains at the same baseline during each measurement. In the early 1990s, this method was gradually applied to the determination of the low inflection point and high inflection point of the *P–V* curve [132, 133] and the effect of different PEEP levels on pulmonary retraction in ARDS patients [134, 135]. Since this method is measured under normal ventilation conditions, it does not need to disconnect the ventilator. At the same time, the volume change caused by oxygen absorption could be negligible since each measurement lasted for 3 s. Compared with the super-syringe method, this method has less hysteresis. Meanwhile, the time consumed for each measurement is about 15 min and its accuracy is poor, which hindered the application of this method in clinical practice [125, 130].

Low Constant-Flow Method: The low constant-flow method was developed by Suratt and coworkers based on the dynamic measurement method [136, 137]. After inflate and deflate the respiratory system with a continuous low flow, a quasi-static *P–V* curve with pressure as the *X*-axis and volume as the *Y*-axis could be drawn. Besides, capacity is calculated by integrating flow rate and time. The most suitable flow rate ranges from 3 to 9 L/min, while higher flow will cause the curve shift to the right significantly [123, 124, 135]. Compared with the super-syringe method, even the flow rate as low as 1.7 L/min might produce a certain drift [130]. Many modern ventilators equipped this function and could be performed quickly at the bedside without extra special equipment. Furthermore, this method does not need to disconnect the ventilator and no need to modify the lung volume before the measurement. However, oxygen absorption still existed in this method.

Mathematical Models: A significant interobserver variability exists in the inflection pressure point interpretation, with a maximum difference of 11 cmH_2O for the same patient [139], although some study also reported good consistency [140]. To avoid these limitations, several mathematical models [141–243] have been proposed. Although the fitting degree of the data models was fine, the results obtained from different data models of the same curve were also different [144].

Most researches used the model described by Venegas and colleagues [141], which was a sigmoid equation, symmetric to the inflection point. Several other models tried to improve the flexibility of the equations, but some of them have not been clinically verified. Therefore, the differences between different models should be taken into account while setting data or comparing the results of different studies based on these models.

2.7.5 Fundamental Concepts of the P–V *Curve*

Characters of the *P–V* Curve: The *P–V* curve is normally measured in an upright, awake, and relaxed subject. The typical shape is generally described as alike sigmoid, consisting of three segments separated by two inflection points [140], and reflecting the balance between the lung and the chest wall. The compliance of the first and third segments is low and nonlinear. The intermediate segment between the upper and lower inflection points is considered linear and is used to calculate "linear" compliance. Changes in the linear compliance of the *P–V* curve usually imply different stages of different diseases.

Hysteresis: The term hysteresis refers to unrecoverable energy or delayed recovery of energy which is applied to a system in physics. Since the lungs are not an ideal elastic system (in which energy changes can be recovered immediately), there is a notable difference between the inspiratory and expiratory branches of the *P–V* curve, which increased with increasing volume and most pronounced when the volume reached FRC [145].

As early as the 1950s, researchers had recognized the surface tension as a factor of hysteresis, which verified by filling the lungs with saline and air separately on the *P–V* curve measurement [145]. Subsequently, researchers found that small volume excursions might have more to do with the intrinsic tissue composition of the lung than alveolar surfactant [146]. Besides, hysteresis increased significantly when the alveolar collapse was caused by pulling the lungs out of the chest wall. In general, in the process of *P–V* curve measurement, recruitment/derecruitment, surfactant, stress relaxation, and gas absorption are the main reasons leading to hysteresis [130].

Supine Posture: When the subject was in the supine position, the measured *P–V* curve of the chest wall shifted to the right and rotated counterclockwise. FRC was reduced by half and respiratory compliance increased in the supine position compared to the supine position, possibly due to differences in abdominal compliance in different positions. Similarly, it is not difficult to understand that when patients have ascites, intraperitoneal bleeding or abdominal hypertension, etc., the abdominal compliance will be reduced, which will affect the respiratory system compliance.

Intrinsic Positive End-expiratory Pressure: Intrinsic positive end-expiratory pressure (PEEPi) is another influential factor in the measurement of the *P–V* curve, mainly represented by the presence of positive alveolar pressure at the end of the expiratory period. PEEPi is mainly caused by shortened expiratory time or slow exhalation due to high airway resistance, resulting in higher alveolar pressure at the end of an exhalation than the endotracheal pressure and incorrect measurement of respiratory compliance. In other words, when PEEPi is present, the pressure difference between the end of exhalation and the end of inhalation is overestimated, leading to an underestimation of respiratory compliance [148]. Besides, PEEPi has been shown to contribute to a portion of re-expanded alveolar hyperventilation. Therefore, it is important to empty the lungs by extending the exhalation time before the *P–V* curve is measured.

Lung Versus Chest Wall: The *P–V* curve of the respiratory system is composed of two main parts: the lung and the chest wall. The chest wall compliance is equal to the change in volume divided by the change in trans-chest pressure measured by the esophageal pressure tube, and the lung compliance is equal to the change in volume divided by the change in transpulmonary pressure. As compliance changes, it is important to recognize the extent to which both are present in different diseases. The relationship between the three is as follows:

$$1/C_{RS} = 1/C_{L} + 1/C_{CW}$$

In which C_{RS} is the compliance of the total respiratory system, C_{L} is the compliance of the lung, and C_{CW} is the compliance of the chest wall. For subjects breathing normally and peacefully, a linear relationship between compliance is usually assumed.

When the volume is lower than the FRC, the chest wall has a greater influence on the overall compliance. In contrast, when the volume is higher than the FRC, the lung contributes more [130]. They play different roles in different diseases. In patients with acute lung injury or ARDS, although chest wall compliance sometimes decreased [149], there are more changes in lung compliance [150].

2.7.6 Clinical Alterations and Applications

2.7.6.1 Clinical Alterations

Acute Respiratory Distress Syndrome: The *P–V* curve is the earliest and most applied to the research of ARDS. In 1967, Ashbaugh and colleagues found that the static compliance of ARDS patients was reduced [130]. Subsequently, it was found that the changes in the *P–V* curve could well reproduce the conditions of ARDS at different stages. These early studies have led to more research outputs on the *P–V* curve to guide the setting of mechanical ventilation parameters and clinical treatment.

ARDS is mainly divided into three stages: acute/early stage, subacute stage, and recovery stage. In the acute/early stages of ARDS, the disease is characterized by

interstitial and alveolar edema and atelectasis [147]. Histologic changes showed a marked LIP and hysteresis on the inspiratory arm of the *P–V* curve, but the reduction in pulmonary compliance was not significant [120, 151]. As the disease progresses to the subacute phase, pulmonary tissue fibrosis and alveolar filling occur, manifested by LIP disappearance and significantly reduced compliance of the inspiratory and expiratory branches. As the patient gradually recovered, the *P–V* curve returned to normal, hysteresis decreased, but the LIP was not easy to see.

Obesity: In sedation, anesthesia and morbidly obese patients, Pelosi et al. found that the FRC of the subjects was significantly reduced [152]. Pelosi and colleagues also found that with the increase of BMI, the lung compliance and chest wall compliance of obese subjects decreased, mainly due to the decrease of lung compliance [153, 154]. Meanwhile, increasing PEEP could improve the decrease in lung compliance [155].

Congestive Heart Failure: In patients with congestive heart failure, the alveoli are filled with fluid, the air-fluid interface is damaged, and the volume of alveolar is reduced. This phenomenon is similar to the early changes in ARDS. Animal experiments have shown that the decreased respiratory compliance in patients with congestive heart failure is much greater than the decrease in gas volume, and it may be that the presence of fluid in small airways leads to increased hysteresis [156]. But it has yet to be confirmed in humans.

Interstitial Lung Distress: Alveolar fibrosis and reduced pulmonary air content are the causes of the decrease in the volume axis of the *P–V* curve of interstitial pulmonary disease. Although the change in the *P–V* curve is due to a decrease in the volume of air contained in the alveoli, it is not equivalent to a decrease in the total volume of the chest. Studies have shown that, due to the uncertainty of tissue and blood volume, the change of the total volume in the chest can be increased, unchanged, or decreased [130]. Therefore, the *P–V* curve is not a sensitive indicator for assessing alveolar fibrosis.

Intraabdominal Hypertension: Since the abdomen is one of the important factors affecting chest wall compliance, the increased abdominal pressure will affect the measurement of the *P–V* curves, such as ascites, intraperitoneal bleeding, pregnancy, intraperitoneal infection, and abdominal surgery. Increased abdominal pressure leads to a downward and rightward shift in the *P–V* curve of the respiratory system [157, 158].

2.7.7 Clinical Applications

Guide to the PEEP Settings: Lemaire et al. first defined the "best PEEP" level proposed by Suter as 2 cmH_2O above the LIP of the inspiratory phase of the *P–V* curve [159, 160]. However, a series of subsequent studies have shown that the "best PEEP" may not be the optimal PEEP for lung recruitment [161–164]. It has

also been suggested that the LIP may represent only the beginning of significant lung recruitment rather than the optimal PEEP setting for lung recruitment [165]. Studies have found that setting PEEP above LIP value 7–9 cmH_2O can further promote lung recruitment, improve oxygenation, and prevent recruitment of the lung [166, 167]. Some studies thought that pulmonary retention occurred throughout the aspirating branch of the *P–V* curve [168, 169]. Although it can significantly improve oxygenation, LIP-based PEEP does not improve the lung injury and long-term outcome of ARDS in animal models or even lead to local hyperventilation [170, 171]. It has also been suggested that perhaps the *P–V* curve of the expiratory phase is more representative of small airway closure and atelectasis, focusing on protective lung ventilation by setting PEEP values in the inspiratory branch. According to the expiratory phase of the *P–V* curve, Takeuchi et al. believed that higher PEEP was needed to prevent derecruitment. However, higher PEEP can lead to lung overventilation and potential risks [164]. The optimal PEEP has been debated for decades, not just by the *P–V* curve, but by integrating multiple indicators and patient-specific differences. As Gattinoni et al. said, the "best PEEP" might not exist [172]. The "best PEEP" should be optimal for oxygenation, hemodynamics, compliance, etc.

Measure the Recruitment Volume: A proper PEEP can help reduce mechanical ventilation-related lung injury while maintaining alveolar collapse [173, 174]. Therefore, ARDS patients with mechanical ventilation need to evaluate lung recruitment and derecruitment. The PEEP related recruitment volume refers to the change of lung volume on the *P–V* curve under the conditions of PEEP and zero end-expiratory pressure (ZEEP) [135, 175]. The change in capacity represents both recruitments for collapsed alveoli and expansion of opened alveoli [176]. Computed tomography (CT) is the accepted golden standard for evaluating alveolar recruitment and derecruitment [177, 178]. Since CT is radioactive and not easy to operate beside the bed, lung ultrasound and the *P–V* curve are often used for bedside monitoring of lung recruitment and guiding PEEP settings [171, 179, 180]. Experimental results show that the retentive volume measured by CT and the *P–V* curve method has a good correlation, but cannot be converted mutually [177].

Monitor the Airway Closure: Airway closure is the obstruction of airflow between the proximal and distal airways and alveoli. Airway closure was thought to be mainly found in patients with obesity, asthma [181–183]. However, in recent years, Chen et al. measured the *P–V* curve of the respiratory system in 30 patients with moderate/severe ARDS with different PEEP levels and found that about 1/4 to 1/3 of patients had airway closure, which was far higher than people's cognition of airway closure and disturbed people's previous understanding of PEEPi and the LIP [181]. Later, Sun et al used the electrical impedance tomography (EIT) to carry out relevant verification. The omission of airway closure might not only affect the wrong calculation of diving pressure but also increases the risk of ventilator-associated lung injury [185]. Figures 2.11 and 2.12 show that the airway opening

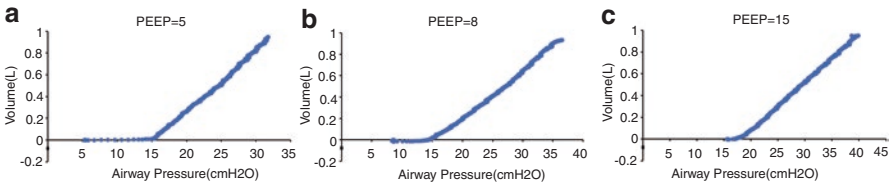

Fig. 2.11 Low-flow inflation pressure-volume curves were obtained from one patient. Curves A, B, and C were obtained at 5, 8, and 15 cmH_2O of positive end-expiratory pressure (PEEP), respectively. The airway opening pressure (AOP) was 15 cmH_2O

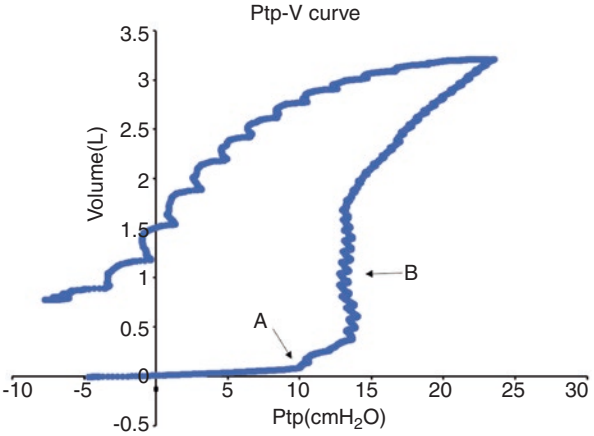

Fig. 2.12 The above data were obtained from another patient with airway closure. This figure reflects changes in transpulmonary pressure (Ptp) and lung volume (*V*). Arrow A indicates that the airway opening pressure (AOP) is about 10 cm. Arrow B indicates a significant increase in lung volume when the transpulmonary pressure is greater than a certain value, which more vividly reflects the phenomenon of airway closure

pressure (AOP) was acquired with the low constant-flow method and the relationship between transpulmonary pressure and lung volume in patients with airway closure.

2.7.8 Summary

For decades, researchers have been deeply understanding and studying the *P–V* curve, which is still used in clinical observation process and clinical research, although rarely used directly alone to guide ventilator setting. We believe that researches on the different pathophysiological conditions of the *P–V* curves could improve clinicians' understanding of diseases, useful for clinical diagnosis and treatment, all of which still remain the vital focuses of interest.

2.8 Flow-Volume Loop

Flow-volume loop provides information on the dynamic characteristics of respiratory system resistance [186, 187]. In this chapter, we will introduce the normal flow-volume loop and distinguishable shapes indicating specific pathophysiological conditions. We will not discuss the spirometry measurements during pulmonary function test, such as forced expiratory volume or forced vital capacity.

2.8.1 Normal Flow-volume Loop

The flow-volume loop is a plot of inspiratory and expiratory flow (on the *Y*-axis) against volume (on the *X*-axis) during the respiration (Fig. 2.13A). It has to be noted that some reports display the expiratory limb in the positive position of the flow-axis, whereas others display expiratory limb in the negative position of the flow-axis. We will use the negative expiratory limb in this chapter.

A normal flow-volume loop starts at both zero flow and volume [188–190]. Flow increases after the beginning of inspiration to reach the peak inspiratory flow (PIF) and then decreases to zero at the end of inspiration. The shape of the inspiratory limb on the flow-volume loop depends on the breathing that is spontaneously active generated or delivered by positive mechanical ventilation with constant or decelerating inspiratory flow pattern. After the starting of expiration, which is always passive even during positive mechanical ventilation, the flow reaches peak expiratory flow (PEF) more rapidly than that for PIF and then decreases to zero in a nearly straight or a convex line.

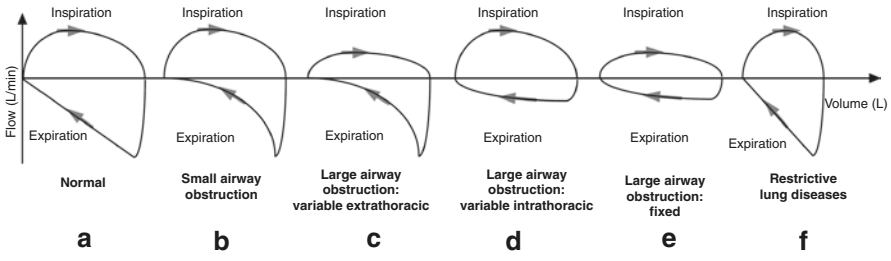

Fig. 2.13 Flow-volume loop during normal and various pathophysiological conditions. (A) normal condition; (B) small airway obstruction; (C) large airway obstruction with variable extrathoracic; (D) large airway obstruction with variable intrathoracic; (E) large airway obstruction with fixed point; and (F) restrictive lung diseases

2.8.2 *Abnormal Flow-Volume Loop During Various Pathophysiological Conditions*

The shape of the flow-volume loop is useful for indicating the type of lung and airway pathophysiology, air trapping, responses to treatments, airway leak and airway secretions, or water in the ventilator circuit.

In patients with obstructive lung diseases, as most common types of chronic obstructive pulmonary disease (COPD) and asthma, the small airways are partially obstructed by certain pathological conditions. The gas in the large airways can be first exhaled without significant resistance followed by the gas in the small airways flows slowly due to obstruction in these areas. The typical change on expiratory limb of flow-volume loop is concaved shape with a relatively normal PEF (Fig. 2.13B) [191].

Flow-volume loop evaluation can also be helpful for the detection of large airway obstruction, with different changes of shape depending on obstruction located at intrathoracic, extrathoracic, or both [192]. In variable extrathoracic obstruction, the obstruction is blown outwards during expiration but suck into the trachea with partial obstruction during inspiration. Thus, the typical change of flow-volume loop is the flattening of the inspiratory limb with a relatively normal expiratory limb (Fig. 2.13C). The pathophysiology of variable intrathoracic obstruction is the opposite of the extrathoracic obstruction. One of the most common reasons for intrathoracic obstruction is intrathoracic located tracheal tumor. The obstruction is sucked outwards during inspiration and pushed into the trachea with partial obstruction during expiration. The typical change of flow-volume loop is the flattening of the expiratory limb with a relatively normal inspiratory limb (Fig. 2.13D). In the fixed large airway obstruction, intrathoracic and extrathoracic obstructions occur simultaneously, with examples of tracheal stenosis due to intubation and circular tracheal tumor. Thus, the inspiratory and expiratory limbs of the flow-volume loop are both flattened (Fig. 2.13E).

In accordance with flow-time tracing showing obstructive abnormality with air trapping (Fig. 2.14a), the flow-volume loop can also detect air trapping with the

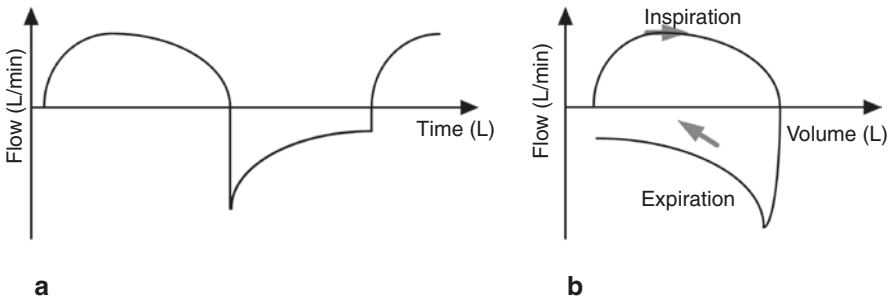

Fig. 2.14 Flow-time curve (**a**) and flow-volume loop (**b**) show obstructive abnormality with air trapping

expiratory limb not reaching zero flow rate at the end of expiration (Fig. 2.14b) [186, 187].

The flow-volume loop can also be used for clinical evaluation of the therapeutic effect [193]. Figure 2.15 schematically shows the flow-volume loops in a mechanically ventilated patient with asthma before and after the administration of bronchodilator. The effect of bronchodilator on resistance is only focused on the expiratory limb of the loop, while no influence on the inspiratory resistance.

The restrictive lung diseases are characterized as a decrease in the total lung volume [194]. The flow-volume loop analysis can suggest restrictive lung diseases despite the inability to accurate diagnosis. Because of the normal airway resistance, the shape of the flow-volume loop remains normal, but the total lung volume decreases as shown on the volume-axis (Fig. 2.13F).

Expiratory flow limitation represents the lack of expiratory flow response to an increase in the driving pressure. It has been shown that expiratory flow limitation is common in mechanically ventilated patients with a variety of pathophysiological conditions, and is associated with adverse clinical outcomes [195, 196]. The determination of expiratory flow limitation relies on the analysis of the flow-volume loop. The negative expiratory pressure (NEP) technique is used to detect expiratory flow limitation [197]. During expiration, a negative pressure (-5 cmH_2O) is applied at the airway opening to increase the transpulmonary driving pressure, and the flow-volume loop is compared with preceding breath without negative expiratory pressure (Fig. 2.16). In patients with expiratory flow limitation, adding negative expiratory pressure will not increase expiratory flow throughout the whole expiratory phase, while this phenomenon will not occur in patients without expiratory flow limitation. The onset of flow limitation is shown by an inflection point on the expiratory limb of the flow-volume loop, by which NEP maneuver also provides a quantified diagnosis of flow limitation as the percentage of exhaled tidal volume where limitation occurs.

Analysis of flow-volume loop can provide information on ventilation circuit (including artificial airway) leak, which is characterized by that expiratory tidal

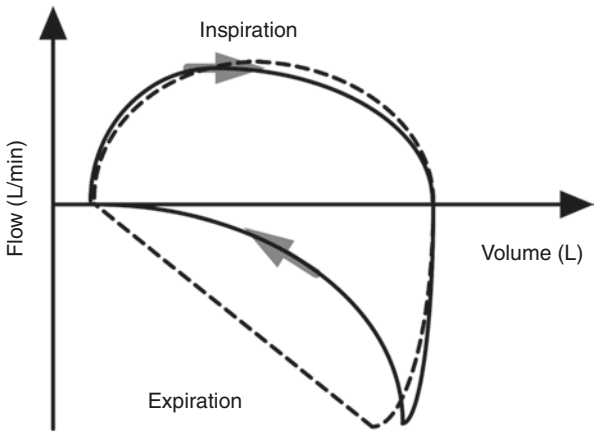

Fig. 2.15 Flow-volume loops in a mechanically ventilated patient with asthma before (solid line) and after the administration of bronchodilator (dashed line)

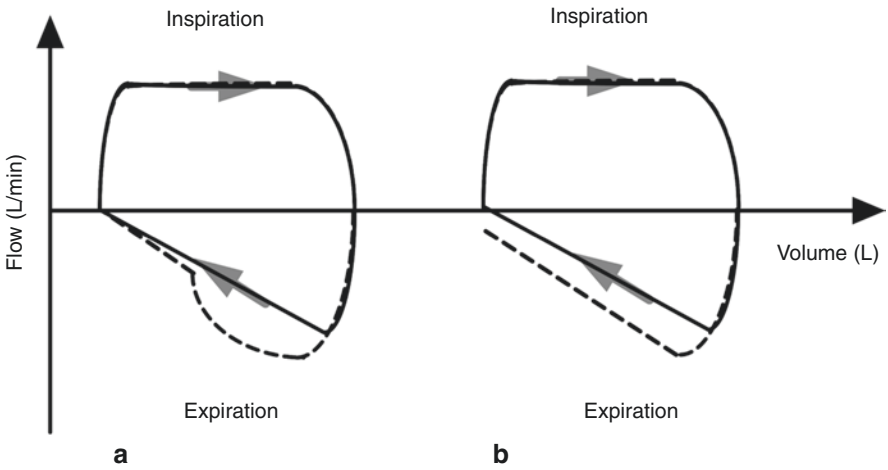

Fig. 2.16 Flow-volume loop in a patient with expiratory flow limitation, a negative pressure is applied at the airway opening during expiration (**a**). Panel **b** shows the flow-volume loop in preceding breath without negative expiratory pressure

volume cannot return to zero value in volume-time tracing and on expiratory limb of the flow-volume loop [198, 199]. Also for monitoring of ventilation circuit, a typical saw-tooth shape on both inspiratory and expiratory limbs of the flow-volume loop represents excessive secretion in the airway or water condense in the ventilator circuit [200].

In conclusion, the flow-volume loop can provide important information on the type of lung and airway abnormalities, expiratory flow limitation and air trapping, responses to treatments, as well as airway and ventilator circuit problems. However, it has to say that the flow-volume loop analysis should be used in combination with the collection of history, and observation of clinical symptoms and signs.

2.9 Transpulmonary Pressure and Driving Pressure

2.9.1 Transpulmonary Pressure

2.9.1.1 Definition

According to equations of motion in respiratory system, when patients have no spontaneous breathing, the peak airway pressure (Ppeak) can be calculated.

$$\text{Ppeak} = \text{Flow} \times \text{Resistance} + \text{VT} / \text{Crs} + \text{PEEP}$$

The resistance means the airflow resistance. VT is the tidal volume, Crs is the respiratory system compliance, and PEEP is the positive end-expiratory pressure.

The plateau pressure (Pplat) is the lowest pressure that is needed to deliver certain volume of air to the lung. Imagine that if the time of gas delivery is infinitely long, the flow is infinitely close to zero, and the platform pressure is not related to the airway resistance.

$$\text{Pplat} = \text{VT} / \text{compliance} + \text{PEEP}$$

When patients have no spontaneous breathing, the platform can reflect the alveolar pressure during inspiration, so the guideline recommends that the platform pressure should be controlled within 30 cmH_2O in passive breathing patients. But when the patient has spontaneous breathing, monitoring of the airway pressure or tidal volume cannot accurately reflect the lung's force (or stress). The essential cause of barotrauma is not the airway pressure, but the alveolar excessive inflation.

Transpulmonary pressure (Ptp) is the pressure spent to overcome the elastic resistance of the alveoli to increase the lung volume, which is calculated as the difference between the airway pressure (Paw) and the pleural pressure (Ppl).

$$\text{Ptp} = \text{Paw} - \text{Ppl}$$

Ptp is the actual force distending the lung during respiration. Instead of airway pressure [201], it could be a better expression of lung distension (alveolar excessive inflation) and as a consequence of the risk of VILI (ventilator-induced lung injury) (Fig. 2.17) [202].

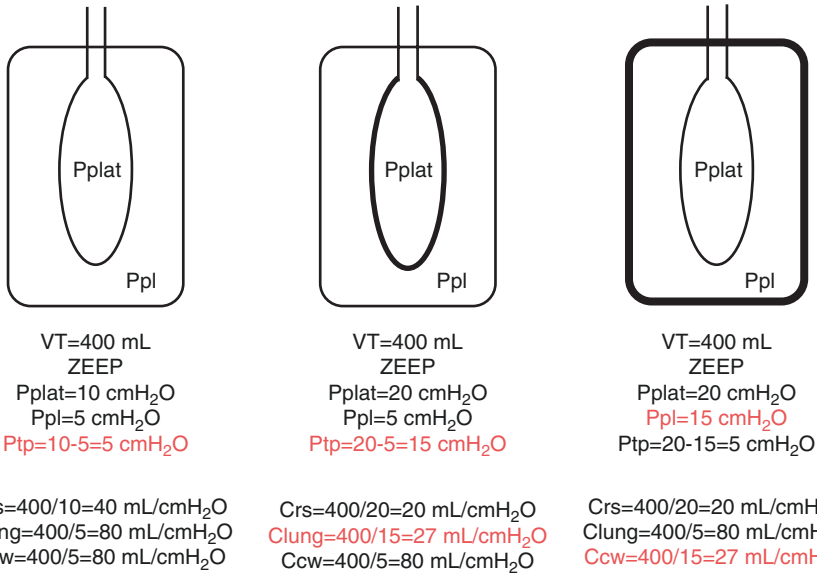

Fig. 2.17 Transpulmonary pressure in different compliance of lung and chest wall. The calculation formula is shown in the figure. The bold part represents low compliance

2.9.2 Measurement

Since it is difficult to measure the pleural pressure (Ppl) directly at the bedside, the esophageal pressure (Pes) is used to reflect the effective Ppl. When the airway occlusion reaches a certain time (usually for 3 s), the airway pressure is balanced with the alveolar pressure, so the airway occlusion pressure is the replacement of the alveolar pressure.

The direct method of the measurement of Ptp is the calculation of the difference in absolute airway and esophageal pressure. However, chest pressure conducts to the lower section of the esophagus and takes through the esophageal wall and the mediastinal organ (especially in supine position). Therefore, using the absolute value of esophageal pressure to calculate Ptp is controversial, and there are many factors that influence the accuracy of esophageal pressure [203].

Between the orthostatic and supine position, the absolute difference value of esophageal pressure can be 3 cmH_2O because of the mediastinal weight [204]. Different filling volume of balloon applied as 0.5 and 1.0 mL can cause the difference of esophageal pressure in 2 cmH_2O [205]. The elastance of the esophageal wall may also affect the accuracy of the esophageal pressure monitoring result [206]. Therefore, a correction of direct reduction by 5 cmH_2O has been applied [207], which need to be further proofed.

Nonetheless, the influence of the absolute esophageal pressure value in different patients is individual, and the measurement of directly derived method may be inaccurate. Therefore, measuring the variation of Ptp may be more accurate.

The early study compared the difference between the measurement of Ppl and Pes, and the result showed that the absolute values were different, but changes in Ppl with Pes during the respiration cycle had good relevance and consistency [208]. Therefore, the correction methods of Ptp measurement are recommended based on the changes of Pes, including the release-derived method and the elastance-derived method [209].

2.9.3 Release-Derived End-Inspiratory Ptp

Ptp is measured as the change in Paw and Pes due to tidal inflation from end-inspiration to atmospheric pressure.

$$\begin{aligned}\text{Ptp} = &\left(\text{Paw at end} - \text{inspiration} - \text{atmospheric pressure}\right)\\ &-\left(\text{Pes at end} - \text{inspiration} - \text{Pes at atmospheric pressure}\right)\end{aligned}$$

2.9.4 Elastance-Derived End-Inspiratory Ptp

Ptp is calculated as the product of the end-inspiratory Paw and the ratio of the lung to respiratory system elastance.

Elastance related to tidal volume. Elastance of the respiratory system (Ers), lung (El), and chest wall (Ecw) during tidal inflation was calculated as the changes in Paw, Ptp, and Pes between end-inspiration and PEEP divided by the inspired tidal volume.

Based on Chiumello's observations, the release-derived method and the elastance-derived method were quite similar, and the release-derived method and direct method were not related. The release- and elastance-derived end-expiratory transpulmonary pressure method was also mentioned [209]. But the results of this part were not given.

The advantage of the release-derived method is that the mediastinal weight and the esophageal wall elasticity basic remain stable, while the disadvantage is that the method needs to disconnect the ventilator from the patient. The advantage of the elastance-derived method is that the method does not need to disconnect the ventilator from the patient, while the disadvantage is that cannot be proofed at end-expiratory.

2.9.5 Application

2.9.5.1 ARDS (Acute Respiratory Distress Syndrome)

Ptp is the key to sustain continuously open of the alveolar at the end of expiratory, and PEEP level can directly influence Ptp [207].

The meaning of Pes monitoring is to: (a) determine the demand of PEEP in ARDS patients, (b) guide the PEEP settings during mechanical ventilation, (c) select the minimum PEEP to keep Ptp between 0 and 10 cmH_2O at the end of expiratory, (d) avoid alveolar and airway collapse during expiratory, (e) minimize the shear stress and barotrauma, (f) improve ventilation and oxygenation, and finally achieve individual settings of PEEP.

2.9.5.2 Obesity and High Abdominal Pressure

Excessive fat can increase elastic resistance of the chest wall and rise up the diaphragm, which can cause obvious increase of the pleural pressure, and leads to alveolar collapse. The mechanical ventilation in obesity treatment, therefore, should be set to a higher level of PEEP, balance the increased pleural pressure or abdominal pressure, and make the Ptp become positive at the end of the expiratory [210].

2.9.5.3 Cardiopulmonary Diseases

Mechanical ventilation strategies guided by Ptp, including the titration of PEEP and the lung recruitment can (1) improve oxygenation and ventilation, (2) avoid barotrauma due to the sudden rise of Ptp, and (3) avoid the influence of circulation and the cardiac output due to inappropriate setting of high PEEP.

2.9.5.4 Driving Pressure

When patients have no spontaneous breathing, driving pressure (ΔP) is calculated as the difference between the plateau pressure (Pplat) and PEEP.

$$\Delta P = \text{Pplat} - \text{PEEP} = \text{VT} / \text{Crs}$$

Actually, ΔP calculated by respiratory system compliance is the driving pressure of airway, which is influenced by the compliance of chest wall and lung function. The decrease of chest wall compliance (caused by high abdominal pressure) leads to overestimate the driving pressure of airway, and cause miscalculations of lung function. So the transpulmonary driving pressure (ΔPtp) can be used by esophageal pressure monitoring.

When patients have no spontaneous breathing [211],

$$\Delta Ptp = \text{VT} / \text{Clung} = \text{Ptp at the end of inspiratory} - \text{Ptp at the end of expiratory}$$
$$= \left(\text{Pplat} - \text{Pes at the end of inspiratory}\right) - \left(\text{PEEP} - \text{Pes at the end of expiratory}\right)$$

The transpulmonary driving pressure and the tidal volume related determine the stress of lung tissue during lung expansion, which determines the possibility of VILI [212, 213]. The study in 2015 [214] showed that ΔP was the most effective risk factor, and the decreases in ΔP owing to changes in ventilator settings were strongly associated with increased survival.

2.10 Occlusion Airway Pressure

Abstract
Occlusion airway pressure (P0.1) has been used in the past four decades to quantify the output of the respiratory drive. P0.1 is a simple, convenient measurement that could be performed in patients with any level of consciousness with or without artifact airway. Potential application of P0.1 is the assessment of patients, which helps to know more about the magnitude of patients' spontaneous inspiratory efforts, and about the state of the muscles, lungs, and chest wall. Although P0.1 has been proposed as a measurement of respiratory output, there are sources of errors and potential pitfalls in it. Interpretation of the data, however, requires a comprehensive understanding of the nature of the P0.1 itself.

2.10.1 Introduction

Respiratory muscles as the effectors perform the function of breath after receiving the motor output from the central controller in the brain. In the meantime, sensors will gather the information on the status of the reparatory system and feed it to the

central controller, which adjusts the impulse of output. Therefore, understanding the respiratory drive may help to analytically differentiate some problems: the failure of respiratory neurogenesis; the abnormality of respiratory muscle; changed respiratory mechanics. In patients with existing lung injury, the respiratory muscles with the command of too high respiratory drive generated regional forces and may lead to injurious effects on a regional level [215]. Goligher et al. [216] found that decreasing thickness of diaphragm was related to abnormally low inspiratory effort; increasing thickness was related to excessive effort, much abnormal respiratory drive is a risk factor for both lung and diaphragmatic injury.

Several measurements have been used to estimate the respiratory drive, which is predominantly evaluated by measuring phrenic nerve activity or through electromyography (EMG). However, these measurements have some limitations, some are invasive or complex technically and some are hard to standardize or can be complicated by cross talk. An alternative validated measurement of the respiratory drive is the airway occlusion pressure, which is the negative airway pressure developed at 0.1 s after the onset of an inspiratory effort against a complete occluded airway. P0.1 is a reliable, measurable, and noninvasive measurement that has been proposed as the indirect indicator of respiratory drive. As a useful index of output, Whitelaw first described P0.1 in 1975 [217], which is unaffected by respiratory system resistance and compliance. Various physiologic or clinical studies have been performed on changes in P0.1 under very different conditions: ARF (acute respiratory failure) [218], COPD (chronic obstructive pulmonary disease) [219], ARDS (Acute Respiratory Distress Syndrome), the weaning period [220], and non-pulmonary diseases [221].

2.10.2 Rational

As one of the basic components of the respiratory control system, respiratory muscles perform the function of breathing after receiving the output from control center and transform into flow (or volume) and pressure. Typically, minute ventilation or tidal volume is an indirect indicator of respiratory output, which depends on the respiratory drive and the respiratory system resistance and compliance. For example, in a given output the higher resistance and (or) lower compliance result from lower ventilation. With the drawback, ventilation cannot be used as a reliable index reflecting changes in the activity of the respiratory center. The same is true for airway pressure, but the influence of respiratory mechanics on which can be eliminated by occlusion maneuver. Grunstein et al. [222] introduced this method, which occluded the anesthetized cat's airway at FRC and measured the amplitude of tracheal pressure generated during subsequent inhalation efforts. During occlusion, the inspiratory muscles contracted nearly isometrically without flow and change in volume (except a small amount due to decompression), the resistance and compliance of the respiratory system do not influence measurement. Therefore, the occlusion pressure is independent of the mechanical properties of the respiratory system [217].

Clearly, for awake patients, when an airway occlusion maneuver is performed, the patient will be aware of airway occlusion and react to the mechanical load through violent reflex or conscious reactions and generate extra pressures, which results in occlusion pressure cannot be used to assess the respiratory drive. Although such influence is very small in anesthetized humans, conscious once is more likely to display obvious reaction to airway occlusion [223]. In order to make airway occlusion pressure an effective indicator to evaluate respiratory center output in the absence of airway occlusion, it is necessary to ensure that airway occlusion maneuver itself might not disturb the neuronal discharge applied to the respiratory muscles. In theory, there is a delay between the increase in airway resistance load and the subject's detection and response to the load, so that the initial increase in airway pressure will be equivalent to the respiratory output when airway load is not increased. In the experiment of Whitelaw et al. [217], they reported the response time of normal subjects to occlusion was never less than 0.15 s; the neuronal discharge during the first part of (<0.1 s) the occluded breath is the same as during unobstructed breathing. In addition, measurement of P0.1 is unaffected by vagal volume-related reflexes [224]. So it was reasonable to take the occlusive pressure generated at 0.1 s after inhalation as the index of respiratory center output.

Respiratory muscles contract and generate negative pressure inside the pleural space firstly, which consequently transmits to the airway, so the negative inspiratory pressure begins earlier in the pleural space than in the airways, particularly in patients with variable levels of intrinsic PEEP (PEEPi) increasing an inspiratory threshold load. In patients with PEEPi, there is a longer delay between the onset of inspiratory effort and the drop in airway pressure during an end-expiratory occlusion than without PEEPi. In fact, the pleural occlusion pressure (which can be measured by esophageal pressure, Pes) generated in the first 100 ms of the inspiratory can be used to infer the respiratory driver better than airway occlusion pressure whether PEEPi exists or not. Unfortunately, the technical aspects of Pes measurement, including the many sources of error and artifact hinder the use in clinical. Furthermore, Daniele Murciano had proved that no differences between the esophageal and tracheal occlusion pressure in patients with COPD, except patients with marked increase in the compliance of the soft aspects of the upper airways and airway flow resistance [225]. In addition, Conti et al. [226] have demonstrated that airway occlusion pressure at 0.1 s in the airway is a reliable surrogate of that in the pleural in patients with variable levels of PEEPi.

Since it is not currently defined or available to quantify the activities of the control center precisely, it is impossible to verify the correlation between respiratory center output measured by any evaluation method and the actual output. Over the past decades, various studies have demonstrated that P0.1 can be used as a reliable indicator to evaluate respiratory center output. Altos MD found a direct relationship between changes in occlusion pressure and ventilatory responses to CO_2 in normal individuals [227]. Close correlations have been observed between changes in phrenic and diaphragm electrical activity and the change in occlusion pressure during a single and over multiple breaths [228–230]. Hussain has reported that P0.1 is generally consistent with changes in the pressure of the diaphragm and is linearly

related to the rate of rise of the electromyography of the diaphragm over a wide range [231]. Marini et al. showed that p0.1 was closely related to the patient's work of breathing, despite the ventilatory assistance [232].

2.10.3 Technical Aspects Relating to the Acquisition of Occlusion Pressures

P0.1 can be measured in the conscious or unconscious patient with or without an endotracheal tube. The standard measurement of P0.1 consists of a pressure transducer and occlusion device both attached to the inspiratory circuit (endotracheal tube, mouthpiece, or fitted facial mask) in sequence. The pressure signals recorded on a high-speed strip chart (at least 25 mm/s) to accurately determine the first 100 ms of inspiration were transferred via an analog-digital converter to a computer for online data sampling and pressure recording [233]. A rudolph-type valve is usually taken as an occlusion device that separates inspiration from expiration, allowing the selective occlusion of inspiration [234, 235]. The valve is closed during the patient's expiration in order to occlude the next inspiration, and it should be reopened quickly after the 100 ms, so that the patient can continue to breathe. Conscious subjects must be unable to anticipate occlusions, which must be done silently and unexpectedly. P0.1 measurement technique has been developed as an integrated function in a standard respirator which can be easily performed through an inspiratory circuit equipped with a demand valve [236, 237], but it is necessary to confirm that the opening delay time of the inhalation demand valve in the ventilator is more than 100 ms, otherwise, the monitoring results are unreliable. It is common to average the values of physiology measurements because of the variability. Takeshi Kera [238] has reported that the minimum number of measurements required for a valid P0.1 was 4. All the P0.1 measurements must be taken under the same conditions [239].

2.10.4 Interpretation of the Data

Before analyzing the clinical implications of P0.1 value, the possible bias that exists under certain specific physiopathologic situations or technologic aspects need to be taken into account. Underestimated or overestimated P0.1 value leads to Faulty results. In healthy subjects, P0.1 varies between 0.5 and 1.5 cmH_2O; In stable patients with COPD, P0.1 is around 3 cmH_2O; in acute respiratory failure due to COPD or ARDS, P0.1 maybe 10 cmH_2O or more [240, 241].

To obtain accurate results, measurement of P0.1 should be performed at relaxed FRC, because the elastic recoil of the respiratory system is zero, and the pressure measured is the net pressure developed by the respiratory muscles under this

condition. An increase in lung volume changes end-expiratory muscle length by shortening inspiratory muscles at the end of expiratory. Because of the length–tension relationship of the muscles, the contractile force of the diaphragm decrease [242–245]. Physiology experiment investigates the effect of lung volume on contraction characteristics of the human diaphragm and reveals that a change in FRC of 500 mL should change transdiaphragmatic pressure generated for a given stimulus by 10% [245]. For example, a reduced P0.1 value with no change in respiratory motor output would be expected with pulmonary hyperinflation and an elevated FRC.

The expiratory muscles are inactive during quiet breathing but are active during hyperventilation and in other conditions in which there is active contraction of the expiratory muscles, therefore, if inspiration starts below equilibrium lung volume, the value of P0.1 recorded can be partly produced by the relaxation of expiratory muscles.

Although P0.1 is widely regarded as an indicator of central drive, clinical value of this technique in respiratory muscle disease has not been proven due to the dependence of P0.1 on respiratory muscle strength is at present unknown. Patients in the intensive care unit often develop significant muscle weakness, occlusion pressure generated by which will underestimate motor output [246], for example normal occlusion pressure implies an abnormally high motor output.

The results of Baydur [247] study demonstrated that in patients with neuromuscular disease, despite muscle weakness P0.1 is not decreased, and in fact, it is markedly increased. In the model of acute respiratory muscle weakness provided by partial curarization of healthy subjects, the slope of P0.1 response to CO_2 is increased even though the ventilatory response is reduced [248]. However, in patients with chronic weakness the ventilatory and P0.1 slopes are both diminished (even though resting P0.1 is normal or increased) [249].

Similarly, patients with muscle incoordination or flail chest will make lower than normal occlusion pressure for the same motor output, even if the muscles are strong.

During occluded respiratory efforts the transmission of changes in alveolar pressure to the mouth depends on the product (=time constant, *T*) of the airway resistance (Raw) and the compliance of the upper (extrathoracic) airways (Cuaw). The magnitude of Cuaw depends on the compliance caused by the compressibility of gas in the extrathoracic airways (including measuring apparatus) and, to a larger extent, on the structural (tissue) compliance of the upper airways (cheeks, base of the oral cavity, etc.). In normal subjects T is small, and hence the values of esophageal and mouth P0.1 should not differ appreciably. In patients with increased Raw and such as COPD patients, however, T may increase sufficiently to cause significant differences between esophageal and mouth occlusion pressures [225]. Therefore, P0.1 measured at the mouth in non-intubated patients can underestimate respiratory drive. Marazzini and coworkers [250] compared the pressures generated at the mouth and in the esophagus during the first 0.1 s of inspiratory efforts against a closed airway in normal subjects and in patients with chronic obstructive pulmonary disease (COPD) during CO_2 rebreathing. They found that normal subjects showed similar responses to CO_2 in terms of both mouth and esophageal pressure, whereas

the patients with COPD exhibited a greater response in P0.1 measured in the esophagus than at the mouth.

On the other hand, in patients with COPD with upper airways bypassed (tracheostomized or intubated) the time constant would be substantially reduced. In that case, a marked reduction in Cuaw will offset even a very high value for Raw, and hence the differences between esophageal and tracheal pressure during occluded respiratory efforts are smaller than those between esophageal and mouth pressure, and the P0.1 is a reliable measure of respiratory neuron efferent activity

2.10.5 Application

In patients under spontaneous assisted ventilation, clinicians should better understand inspiratory efforts of patient. Monitoring of respiratory muscle activity and/or respiratory drive is mandatory. Since P0.1 is a reasonable index of the respiratory drives and can be measured easily at bedside, it should be used much more widely in clinical practice to detect patients at high risk of patient self-inflicted lung injury (P-SILI) [251].

Monitoring P0.1 helps to adjust the ventilator without over or under assistance preventing mechanical ventilation relative complications. Recently, Rittayamai et al. [252] found that inspiratory effort was strongly correlated with P0.1 under pressure control, intermittent mandatory, and synchronized intermittent mandatory ventilation, a cutoff value for P0.1 above 3.5 cmH_2O had a sensitivity of 92% and specificity of 89% in predicting PTPes >200 $cmH_2O \times s \times min^{-1}$, which mean excess patient's inspiratory effort. Pletsch-Assuncao et al. [253] recently reported an optimal threshold of P0.1 $\leq$1.6 cmH_2O to diagnose over assistance defined by WOB <0.3 J/L or >10% ineffective efforts (with a sensitivity of 62% and a specificity of 87%). Alberti A [254] found a level of pressure supportable to generate a condition of near-relaxation in each patient, evidenced by P0.1 values <1.5 cmH_2O and WOB values close to 0 J/L. During pressure support ventilation, P0.1 may be a more sensitive parameter than breathing pattern determines of optimal support level, which is sufficient to maintain moderate diaphragmatic activity without inducing fatigue. Alberti [254] suggests that a pressure level sufficient to maintain P0.1 below 3.5 cmH_2O be set, as suggested by the correlation between P0.1 and WOB. Lotti and colleagues have designed a closed-loop control of P0.1 applied to pressure support ventilation which automatically adjust pressure support ventilation based on a target P0.1 prescribed by the physician.

High auto-PEEP increases the work of breathing needed to trigger the ventilator and increase the number of ineffective triggering. Smith and Marini [255] found that PEEP levels that counterbalance PEEPi reduce the mechanical work of breathing during the machine-assisted ventilatory cycle. However, the optimal peep is difficult to select, Mancebo et al. [256] demonstrated that P0.1 can assess the effect of external PEEP on counterbalancing the auto-PEEP sensitively and especially there was a significant correlation between individual changes in P0.1 and in work

of breathing (WOB) when external PEEP was increased. Moreover, no patient exhibited a decrease in P0.1 and a simultaneous increase in WOB. The decrease in P0.1 was concomitant with a decrease in patients' inspiratory WOB. So, P0.1 can help to titrate PEEP in patient with dynamic hyperinflation.

Some clinically stable patients who meet established weaning criteria fail to wean. The ventilatory center tends to respond to ventilatory distress, increasing its output as ventilatory demands increase which suggests that P0.1 can be different between patient weaning success and failure. P0.1 has been proposed to be a useful predictor for successful ventilator weaning in several studies of small groups of patients. Among a group of 16 patients with COPD, Murciano et al. [257] found that 5 patients who had a persistently high P0.1 (7.1 ± 2.4 cmH_2O) required reintubation and the 11 who showed a decrease in P0.1 (4.7 ± 1.8 cmH_2O) before extubation were successfully weaned. In 11 patients with COPD and 9 with ARF, Herrera et al. [258] found that the mean P0.1 values were high in patients who required mechanical ventilation support and were low in patients who were extubated without complication. They suggested that the P0.1 of 4.2 cmH_2O separated patients who could and could not be successfully weaned. Recently, in a group of 12 patients with COPD, Sassoon et al. [259] found that 5 patients who failed to wean had a higher P0.1 (8.0 ± 0.4 cmH_2O) than the 7 patients whose weaning was successful (4.0 ± 0.5 cmH_2O). They suggested that the P0.1 of 6.0 cmH_2O separated patients who could and could not be successfully weaned.

The accuracy of P0.1 alone as a predictor of the success of weaning is compromised in muscle weakness patients with low P0.1 despite a high ventilatory demand, therefore, was later linked with maximal inspiratory pressure (PIMax), hypercapnic challenge, and f/Vt. The index P0.1/PIMax increases the reliability of P0.1 in detecting the need for mechanical ventilatory support [260].

Montgomery et al. [261] used hypercapnic challenge to study ventilatory reserve. These investigators found a tendency toward greater P0.1 in unsuccessfully weaned patients compared with successfully weaned patients, but the difference was not significant. When breathing a hypercapnic mixture that raised end-tidal PCO_2, approximately 10 mmHg, successfully weaned patients had greater augmentation of P0.1, expressed as the ratio of P0.1 during CO_2, stimulation to P0.1 during baseline, than did those who were unsuccessfully weaned. Ventilation increased more during the hypercapnic challenge in those patients who were successfully weaned, but the overlap of results between the two groups rendered this test inaccurate for predicting weaning success. In Fernandez's study, [262] they found that even when clinical selection is made with great care and a 30-min trial of spontaneous breathing is performed, as many as 18% of patients require reintubation. In this group of life-threatened patients, measuring P0.1 and P0.1*f/Vt on low PSV during the breathing trial is of little help.

Many integrative weaning indexes of discontinuation from mechanical ventilation have been proposed for clinical use, but few provide comparative data with P0.1 optimal threshold values of P0.1 alone or combined with other parameters for weaning are still a matter of debate. We still require more extensive experience with large, well-defined patient groups, uniform techniques and criteria, and an

assessment of the extent to which the prediction of weanability saves lCU costs. Nevertheless, preliminary data certainly suggests some usefulness.

2.10.6 Limitation

Indexes of ventilation control have a wide range of normal values and are easy to be overinterpreted. P0.1, in particular, is difficult to interpret because the theory needed for a detailed physiological interpretation of it is complex and has many pitfalls. P0.1 is a valid index of neural output only at FRC. Breath-to-breath scatter in the data requires averaging of many breaths to obtain precise results and measurement of P0.1 should be performed in the same situation.

2.10.7 Future Perspectives

P0.1 has commonly been used as an index of a neuromuscular ventilatory drive. Measurement of P0.1 is noninvasive, simple, and seems promising to help clinicians to improve their ventilator settings and to determine weaning in the individual patient at the bedside. Although P0.1 is difficult to interpret, exploration of its practical uses will be most useful if based on the study of numerous patients using correlations of the data with clinical situations, or with other mechanics or control measurements.

2.11 Pressure Time Product

During assist ventilation, the work of breathing (WOB) generated by respiratory muscle should remain in a suitable range, avoiding muscle fatigue or weakness. The classic method to measure WOB is Campbell diagram and pressure time product (PTP) [263]

2.11.1 Physiology

2.11.1.1 Inspiratory Muscles

During spontaneous breathing, the diaphragm is the main inspiratory muscles. The diaphragm contraction cause the pleural pressure (Ppl) dropping and abdominal pressure (Pab) rising, the pressure of diaphragm can be evaluated by the difference of Ppl and Pab, called the transdiaphragmatic pressure (Pdi) [264]:

$$\text{Pdi} = \text{Ppl} - \text{Pab}$$

When respiratory load increases, the accessory inspiratory muscles, i.e., sternomastoid, parasternal, scalene, and rib cage muscles also generate contraction, which also induce chest wall expanding and Ppl dropping [265]. The pressure of all inspiratory muscles is called as Pmus. So, Ppl is equal to the sum of the Ppl and the pressure gradient over the chest wall (Pcw):

$$\text{Ppl} = \text{Pmus} + \text{Pcw}$$

In clinical, the esophageal pressure (Pes) is used to estimate the Ppl [266]. So:

$$\text{Pmus} = \text{Pes} - \text{Pcw}$$

The standard method to calculate Pcw needs subjects to stay in passive ventilation and all respiratory muscles are relaxed that usually muscle paralysis. In this condition, Pmus is zero and Pes is equal to Pcw [267]. The Pcw also can be estimated by the ratio of the tidal volume and the theoretical values of the compliance of chest wall (Ccw). According to the pervious study in healthy subjects, the theoretical values of Ccw was equal to 4% of vital capacity. But this method might not be accurate because Ccw can be influenced by some illness [268].

2.11.1.2 Expiratory Muscles

During resting ventilation, expiration is a passive process. The elastic energy restored during inspiratory is consumed in overcoming resistance and persistent forces of inspiratory muscles during expiration. The expiratory muscles, abdominal wall muscles, internal interosseous intercostal, and the triangularis sterni muscles need to contract for increasing Ppl when load of inspiratory muscles increase or expiratory resistance increases [e.g., patients with chronic obstructive pulmonary disease (COPD)] [269].

2.11.2 WOB and Campbell Diagram

According to physics, the work is equal to the product of force and the distance of an object moves when the force is applied on an object. And for the respiratory system, the pressure causes the change of volume. So,

$$\text{WOB} = P \times V = \int_0^V P \times dv$$

where $\int_0^V P \times dv$ represents the integral of the pressure applied and corresponding change of volume. The pressure unit is usually expressed as cmH_2O, volume unit is expressed as L, so work unit is L × cmH_2O. In practice, work unit is normally expressed as in the form of joules (J). 1 J represents the amount of work required to

move 1 L of gas by the pressure of 10 cmH_2O. WOB also could express as joules divided by the corresponding tidal volume per breathing cycle (J/L). The power of breathing is also calculated, expressed as J/min, by multiplying the work per breath cycle by the respiratory rate per minute.

The calculation of WOB in patients with spontaneous breathing is complex and the development of Campbell diagram revaluates this procedure [270]. Meanwhile, it further allows to divide WOB into its elastic (lung and chest wall) and resistive components with the help of esophageal pressure monitoring (Fig. 2.18).

In Campbell diagram, the vertical axis is the change values of Pes and horizontal axis is the change of volume during breathing. Besides, the Pes in passive ventilation also need to be measured to calculate the compliance of lung (CL) and chest wall (Ccw). The slope of Ccw line is the value of Ccw that starts from the functional residual volume (FRC) and corresponding pressure is equal to Pes at FRC in totally passive ventilations. The CL line can be plotted in a similar method. The area (ADCBCA) subtended by Ccw, Pes, and inspired volume represents the

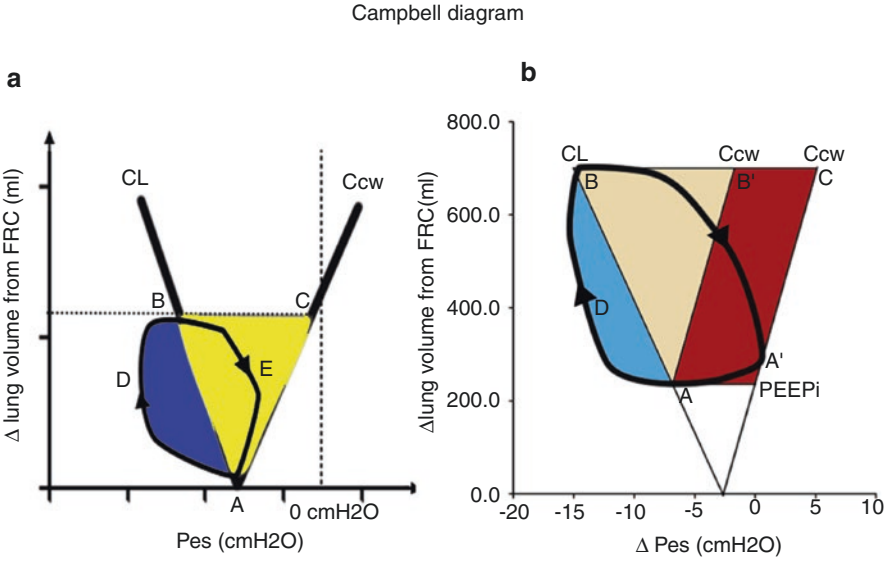

Fig. 2.18 Schematic diagram of the work of breathing (WOB). (**a**) The horizontal axis is the change of volume during breathing and the vertical axis is the change values of Pes. The compliance of lung (CL) line and the compliance of chest wall (Ccw) line start at the volume of functional residual volume (FRC) and corresponding pressure is equal to Pes at FRC in totally passive ventilation (A). The area (ADCBCA) subtended by Ccw, Pes, and inspired volume represents the WOB generated by respiratory muscles, the area (ABCA) represents the WOB against the elastic force of lung and chest wall, and the area (ABDA) represents the WOB against resistance. (**b**) If PEEPi exists, the alveolar pressure remains positive and the lung volume is higher than FRC before inspiration. The second Ccw line needs to be plotted from intrinsic PEEP (PEEPi), the area (ADCBA′A) represents the WOB generated by respiratory muscles, the area (ABB′A) represents the WOB against the elastic force of lung and chest wall, the area (AB′CA′A) represents the WOB against PEEPi, and the area (ABDA) represents the WOB against resistance

WOB generated by Pmus, the area (ABCA) represents the WOB against the elastic force of lung and chest wall, and the area (ABDA) represents the WOB against resistance.

But when PEEPi appears, the alveolar pressure remains positive and the lung volume is higher than FRC at end-expiration. PEEPi can be assessed by the different values of Pes between the beginning of inspiratory and the start of ventilator inflating gas. So, the area (ADCBA′A) represents the WOB generated by Pmus, the area (ABB′A) represents the WOB against the elastic force of lung and chest wall, the area (AB′CA′A) represents the WOB against PEEPi, and the area (ABDA) represents the WOB against resistance. If the Pes-volume loop of expiratory extends the elastic work area, this extended area represents the active expiratory WOB.

It also should be noticed that the PEEPi not only influences expiratory muscles but also influences inspiratory muscles. Inspiratory muscles must contract to generate pressure that is equal to PEEPi at least before lung volume changes. This part of inspiratory efforts is considered as ineffective inspiratory efforts, but without volume changing, Campbell diagram cannot measure this ineffective WOB. In this situation, the PTP might be more suitable to measure muscle WOB [268].

2.11.2.1 Limitations

Firstly, the measurement of WOB needs Pes monitoring and using the absolute of Pes to estimate Ppl still exists debate. Second, the measurement of Ccw is rather complex and often needs muscle paralysis. Third, it does not allow to measure WOB during isometric contractions, such as existing PEEPi. Last, WOB does not consider the effect of duration and frequency of contractions. For example, the different breath might present the same change of volume when the same Pes is applied but could take a long time. The longer breath might require more energy actually.

2.11.2.2 Applications

The measurement of WOB is helpful to optimize and understand the effects of mechanical ventilation. The normal values of WOB in healthy subjects is around 0.5 J/L or 5.0 J/min. But it is still difficult to determine the optimal WOB level for individuals who receive mechanical ventilation. And the previous study also found that the WOB was not an adequate parameter to guide weaning. The WOB had an obvious overlap between subjects weaned successfully and non-successfully [271]. Whether measuring WOB could guide clinical decisions that still need to be explored.

2.11.3 PTP

The PTP is the integral of the pressure and the time of pressure acting.

$$\text{PTP} = P \times t = \int Pdt$$

The pressure is usually expressed in cmH_2O and time unit is second (s). The PTP unit of every breath is $cmH_2O \times s$ and it is also commonly calculated in the period of 1 min (as PTP-min).

With the help of Pes monitoring, the PTP of respiratory muscle (PTPmus) can be calculated. Meanwhile, the Ccw also needs to be measured in passive

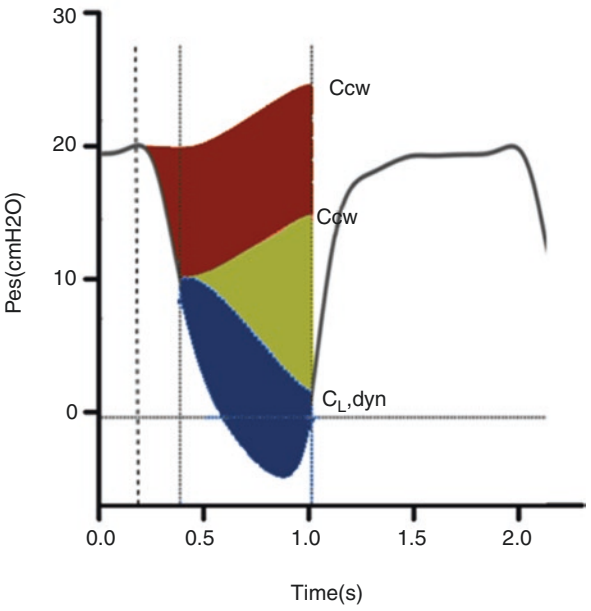

Fig. 2.19 Schematic diagram of pressure time product. The *X* axis is time and the *Y* axis is esophageal pressure (Pes). The pressure time product (PTP) of Pes represents the PTP of respiratory muscle (PTPmus). The first vertical dashed line represents the onset of inspiratory effort (Pes begins decreasing), the second dashed line represents the onset of inspiratory flow generated by ventilator, the difference of Pes between the first and second line is intrinsic PEEP (PEEPi). The third dashed line represents the end of inspiration. The compliance of the chest wall (Ccw) can be measured in passive ventilation or be estimated by using 4% of vital capacity. If PEEPi exists, two Ccw lines need to be plotted from the onset of inspiratory effort and the onset of inspiratory flow, respectively. The PTPmus is equal to the area subtended by the upper Ccw line and Pes curve from the onset of inspiratory effort and the end of inspiratory. Combined with the dynamic lung compliance (CL,dyn), the PTPmus can be classified into three components: effort to overcome PEEPi (red), resistance (gray), and elastic of respiratory system (yellow). PTP of PEEPi is equal to the area subtended by Ccw lines between the onset of inspiratory effort and the onset of inspiratory flow generated by ventilator. PTP of resistance is equal to the area subtended by CL,dyn line and Pes curve. And PTP of elastance is equal to the area subtended by Ccw line and CL line between the onset of inspiratory flow and the end of inspiratory

ventilation or estimated by using 4% of vital capacity (Fig. 2.19). If subjects exist in the PEEPi, two Ccw lines need to be plotted, one starts at the onset of Pes decreasing (starting inspiratory effort) and another starts at the onset of inspiratory flow generated by the ventilator, respectively and both end at the end of inspiration. And Pes in the deference between at the onset of Pes decreasing and inspiratory flow generated by ventilator is the value of PEEPi. And dynamic lung compliance (CL,dyn) starts at the onset of inspiratory flow generated by ventilator and ends at the end of inspiratory. The PTPmus is equal to the area subtended by Ccw line and Pes curve from the onset of inspiratory effort and the end of inspiratory. The PTPmus can be classified into three components, effort to overcome PEEPi, resistance, and elastic of respiratory system. PTP of PEEPi is equal to the area subtended by Ccw lines between the onset of inspiratory effort and the onset of inspiratory flow generated by ventilator. PTP of resistance is equal to the area subtended by CL, dyn line and Pes curve. And PTP of elastance is equal to the area subtended by Ccw line and CL line between the onset of inspiratory flow and the end of inspiratory.

If the gastric pressure (Pga) is monitored simultaneously that can be used to estimate Pab, the transdiaphragmatic pressure (Pdi) also can be measured by the difference of Pga and Pes, as Pdi = Pga − Pes. The PTP of diaphragm (PTPdi) can be calculated to assess the diaphragm effort, that is equal to the area subtended by the baseline value of Pdi at the end-expiratory and Pdi curve from the onset of flow and the end of inspiratory.

2.11.3.1 Limitations

First, the measurement of PTP does not consider the effect of flow and volume. For the subjects with equal PTP, oxygen cost differs with different volumes and flow. Second, it also needs to measure Ccw that requires passive ventilation and muscle paralysis [268].

2.11.3.2 Applications

The normal values of PTP in healthy subjects is around 120 $cmH_2O \times s/min$. And it had a linear relationship with the oxygen cost of breathing with a relatively constant inspiratory flow during ventilation [272]. It was related to lung mechanics, ventilator demands, and PEEPi. It has worthy to assess the patient-ventilator interactions or weaning according to the different components of PTP. But Jubran et al. found the PTP has a quite variable range in patients with COPD or respiratory failure during pressure-assist ventilation [273]. And there still has not an accurate threshold value of PTP to guide ventilation setting and weaning.

2.12 Transdiaphragmatic Pressure

2.12.1 Background

The diaphragm is the major inspiratory muscle. During spontaneous breathing, the contraction of diaphragm can push the abdomen outward and expand the pleural cavity. When pleural pressure is lower than atmospheric pressure, the air can flow into the lung. Diaphragm dysfunction is common in patients with critical illness. Mechanical ventilation, sepsis, drugs, and other diseases are all risk factors for diaphragm dysfunction. The diaphragm weakness can cause respiratory failure and prolong mechanical ventilation that is related to increase length and cost of intensive care unit, even increase morbidity and mortality. Since 1960, the transdiaphragmatic pressure (Pdi) is introduced to describe diaphragm force, which is equal to the difference between abdominal pressure (Pab) and pleural pressure (Ppl) [274].

2.12.2 Measurement

In clinical, the esophageal and gastric pressure (Pes and Pga) can be measured by inserting esophageal balloon catheters into the esophagus and stomach, respectively. The Pes can be used to estimate Ppl and the Pga can estimate Pab [275].

So, Pdi = Pes − Pga

But the absolute value of Pes and Pga are influenced by multiple factors, like mediastinum weight, gastric tone, and the abdominal hydrostatic gradient. So, the maximal inspiratory swings in Pdi (Pdi-max) is mainly used to evaluate diaphragm function [274]. There are several methods to obtain maximal inspiratory effort, as follows:

1. Sniff Maneuver: Patients are encouraged to perform a sharp and short sniff as forceful as possible. The sniffs are repeated until maximal Pdi appears and remains constant (about six sniffs). Every sniff should have at least two stable breath [277].
2. Mueller Maneuver: Patients are encouraged to inspire strongly as airways closed. The nose-clip and mouthpiece can be used to close airways. In subjects with mechanical ventilation, the expiratory occlusion can be used to close airways. It can also be repeated several times and the maximal Pdi swings are chosen (about four maneuvers) [278].
3. Expulsive Maneuver: Patients need to learn how to use their diaphragm-abdomen maximally. First, make our stomach hard as a rock and bear down as for defecation. The patients can hum softly to make sure glottis open and the lung volume is near to functional residual volume [278].
4. Mueller-Expulsive: Patients performed the Expulsive maneuver and Mueller maneuver sequentially [275, 278].

5. Phrenic Nerve Electrical Stimulation: The phrenic nerve of sternomastoid muscle can be stimulated by placing two pairs of percutaneous bipolar electrodes in the neck to induce diaphragm contract as airways closed. And electrodes are connected to a stimulator that provides a constant voltage. The intensity of stimulator can be increased as a step of 10v until Pdi-max appears maximal values. To avoid twitch potent diaphragm strength, subjects should have a rest and quiet breath for 10–20 min before stimulating. The bilateral phrenic nerves need to be stimulated simultaneously to obtain the entire diaphragm contractility. It also can provide information about hemidiaphragm function if only the left or right electrode performs stimulation [279].
6. Phrenic nerve magnetic stimulation: The magnetic stimulation can be performed by a specific instrument, like Magstim 200 (Magstim Co. Ltd, Whitland, Dyfed, Wales, UK) to induce maximal contraction of diaphragm by placing circular coil over the nerve roots of fifth to seventh cervical vertebra as airways closed. We can move coil down and up across the midline of fifth to seventh cervical vertebra until Pdi-max occurs the maximal values [279].

The former four methods all need the cooperation of subjects. The previous studies enrolled 64 normal subjects and compared Pdi-max measured by Sniff and Mueller maneuver methods [277]. The study found that Sniff maneuver was a rather easier and reproducible method to evaluate diaphragm strength. Expulsive and Mueller-Expulsive maneuver are so difficult that is not used frequently in the clinical setting [275]. The electrical and magnetic stimulation are non-volitional methods. But electrical stimulation needs placing electrodes in the right position and is difficultly applied in patients with short neck, trauma, or swelling. To symmetrical stimulation successfully, it needs to repeat stimulating that might induce painless, neck trauma and swelling. So, magnetic stimulation is more comfortable and easily performed comparing to electrical stimulation. But magnetic stimulation can influence diaphragm and muscles in the upper rib cage, while electrical stimulation mainly acts on the diaphragm, so Pdi-max by magnetic stimulation is slightly higher than electrical stimulation [276].

2.12.3 Interpretation

The length and geometry of diaphragm can influence pressure inducing by the diaphragm and lung volume is a major determinant to modify the length and increase the radius of curvature. The different maneuvers can influence the rate of lung volume changing and diaphragm contraction. Besides, absolute values of Pdi-max are related to lung initial volume, size, body position, gender, and history of diseases [275]. So, it has a wide variation among inter-subjects and there is no threshold for assessing diaphragm dysfunction yet. And it also should be remembered that the conditions of measurement should be standardized as comparing Pdi-max of intra-subjects. The normal value of Pdi in healthy adults is approximate 100 cmH_2O [275].

2.12.4 Clinical application

Arguably, Pdi-max can be a gold standard for the assessment of diaphragm contractility. The low values remind patients of existing muscle weakness, but the huge variation in individuals can cause misinterpretation of Pdi-max easily. The previous study found that Pdi-max 0 is a reliable method to diagnose bilateral diaphragm paralysis [280]. However, the previous study also compared Pdi-max measured by phrenic nerve electrical stimulation in patients with weakness ($N = 15$) and healthy subjects ($N = 20$), the results shown that the Pdi-max in only four patients with severe weakness was lower than the lowest values in control patients [281]. Besides, the low values also could be caused by poor technique or effort. A high value is helpful to exclude diaphragm weakness. Besides, the tension-time index of the diaphragm (TTdi) was introduced to assess breath effort. It is the product of the ratio of the average of Pdi (Pdi-mean) and Pdi-max and the ratio of inspiratory time (Ti) and total respiratory cycle time (Ttot) in a normal breath, expressed as TTdi = Pdi-mean/Pdi-max × Ti/Ttot. The normal value for healthy subjects is 0.03 at rest and TTdi exceeding 0.15 probably limited diaphragmatic blood flow and developed diaphragm fatigue [282, 283].

2.12.5 Conclusion

The measurement of Pdi provides a reliable method to evaluate diaphragm function. However, the complexity of monitoring and interpretation restricts clinical practice. Further studies should focus on how to use Pdi to detect diaphragm dysfunction more effectively and easily.

2.13 WOB: The Electrical Activity of Diaphragm-Derived Method

In assisted ventilation modes, the patient's respiratory muscles and the ventilator contribute to the WOB together. The golden standard of measuring the pressure generated by respiratory muscles (Pmusc) is based on Pes measurement; however, it needs the expertise to place the balloon and interpret data correctly. The tight correlation between the intensity of diaphragmatic electromyogram and the transdiaphragmatic pressure (Pdi) has been clearly illustrated [284, 285], and the linear behavior also exists between Pmusc and Eadi. Compared with Pdi monitoring, the electrical activity of the diaphragm (Eadi) is less invasive, and more widely used in clinical practice. There are two Eadi-derived indexes available to assess the patient's inspiratory effort during NAVA mode.

2.13.1 Pmusc/Eadi index

The conception of Pmusc/Eadi index (PEI, also termed as neuromechanical efficiency) has been proposed in 2013 by Bellani et al., which indicates the amount of pressure (in cmH_2O) that the respiratory muscles of the patients are generating for each microvolt of electrical activity [286]. PEI is highly variable among different patients but quite stable within each patient under different conditions of ventilator assistance. PEI could be calculated in three different conditions: during regular tidal ventilation (PEI_{dyn}), during occlusions using the esophageal-derived Pmusc ($PEI_{occl,pes}$), and during occlusions using the airway pressure drop ($PEI_{occl,paw}$).

Since the study has shown that the $PEI_{occl,paw}$ is a good surrogate of PEI_{dyn}, by multiplying with Eadi, continuous estimation of Pmusc could be derived with the following equation [286]:

$$\text{Pmusc}_{\text{Eadi}} = \text{Eadi} \times \text{PEI}_{\text{occl,paw}}$$

The maximal pressure developed during the respiratory cycle (Pmusc), the pressure-time product (PTP_{Eadi}), and inspiratory mechanical work of breathing (WOB_{Eadi}) can be calculated based on the $Pmusc_{Eadi}$, and a good correlation with the standard values derived from the esophageal catheter has been established [286].

2.13.2 Patient-Ventilator Breath Contribution (PVBC) Index

The relative contribution of the patient's effort to the lung distending pressure is hard to differentiate, except special mode such as proportional assist ventilation (PAV+). We have known that the $\Delta Pes/\Delta P_L$ index could measure the relative contribution of inspiratory muscles and ventilator to breathing since it allows the dissociation of the relative contribution of lung distending pressures ($P_L = \Delta Paw - \Delta Pes$) generated by the inspiratory muscles (ΔPes) and the ventilator (ΔPaw). Similar to that, in NAVA mode, it is possible to quantify this variable, by calculating the ratio of tidal volume normalized to neural inspiratory effort in two consecutive breaths with and without ventilator assist respectively, which expressed as follows:

$$\text{PVBC index} = \left(\text{Vt} / \Delta\text{EAdi}\right)_{\text{no-assist}} / \left(\text{Vt} / \Delta\text{EAdi}\right)_{\text{assist}})$$

PVBC could reliably predict the fraction of breathing effort generated by the patient: a PVBC index close to 1 indicates that the patient is generating Vt all by himself, with little contribution from the ventilator, whereas a PVBC index close to zero indicates that the ventilator almost contributes to all of Vt. The relationship between PVBC and $\Delta Pes/\Delta P_L$ is curvilinear but squared PVBC ($PVBC^2$) resulted in a near-perfect linear 1:1 relationship to $\Delta Pes/\Delta P_L$ [287].

2.13.3 Limitations

First, it must be pointed out that Eadi measures the electrical activity generated by the diaphragm only, and is more closely related to the neural drive, while Pmusc, as measured by Pes, includes the pressure generated by all the respiratory muscles (e.g., accessory muscles). Second, the Eadi value is multiplied for the same $PEI_{occl,paw}$ (assuming equal to PEI_{dyn}) value throughout the inspiration, although the PEI_{dyn} does change over time. Third, it is not clear whether this method is applicable in patients with intrinsic PEEP or chronic obstructive pulmonary disease either. Fourth, the diaphragmatic efficiency may influence PEI, e.g., under the over- or under-assistance from the ventilator. Furthermore, reference values for EAdi-derived parameters are not yet known.

2.13.4 Summary

Although very heterogeneous among different patients, the PEI fairly constant within each patient, and PVBC can assess the patient inspiratory effort during assisted ventilation. Since the use of Eadi monitoring is becoming increasingly popular, it is promising to estimate WOB alone, instead of derived from Pes monitoring.

2.14 Mechanical Power

Mechanical ventilation is a major support for respiratory failure, which also can cause ventilation-induced lung injuries (VILI). Actually, VILI is caused by the interaction between what the ventilator delivers to the lung parenchyma and how the lung parenchyma accepts it. With the development of respiratory monitoring and technologies, the understanding of VILI has increased. Two factors should be taken seriously: one is the ventilator and the other one is the condition of the lungs. The ventilator and the lung may interact, which may cause VILI. Firstly, different components of the ventilator load can cause different reaction, including the pressure [288], volume [289], flow (F) [290], and respiratory rate (RR) [291]. Secondly, the response to a given ventilator load depends on the conditions of the lung parenchyma. The lung conditions depend on the amount of edema, which leads to decreased lung dimensions [292], lung inhomogeneity, increased stress risers [293], and cycling collapse and reopen [294]. What is more, perfusion, pH, gas tensions, and temperature are always neglected. In one word, VILI is a comprehensive syndrome.

All the causes are components of a unique physical variable (i.e., the pressure, volume), while the amount of edema is the most common lung-related causes of VILI (i.e., the ARDS severity).

There are so many parameters which can be the ventilator-generated causes of VILI, including pressure, volume, flow, and respiratory rate. However, they are all explored separately. And it is quite clear that the components of energy load, which are expressed per unit of time, include tidal volume, pressure, and flow. This energy load is called mechanical power (MP), which is comprehensive of all the parameters [295].

In the past, MP was calculated according to the classical equation of motion with the addition of PEEP originally [295–297] and has three important components [298]. The first one is respiratory system elastance, which is the energy associated with the tidal volume (VT)/driving pressure (DP). Airway resistance is the second component, which is related to the energy associated with gas movement. The third one equals the energy needed to overcome tension in the fibers due to PEEP, which is PEEP-related energy. All these factors together generate the energy applied to the respiratory system, which, expressed per minute, is the MP. MP can be calculated by pressure-volume curve. The power is defined as the area between the inspiratory limb of the Δ-transpulmonary pressure (x)–volume curve and the volume axis (y) and is measured in joule [296].

Energy was computed on the pressure-volume graph:

$$\text{Energy}\left(\text{N} * \text{m}\right) = \text{Pressure}\left(\text{N} / \text{m2}\right) * \text{Volume}\left(\text{m3}\right)$$

Then convert cmH_2O * mL in Joule (1 L * cmH_2O = 0.000098 J), we can get the MP.

This is the original method using *P–V* curves loops to calculate the MP. Recently, a simpler power equation is suggested. And it shows a good relationship with the original equation, but without the need for *P–V* curves. In 2016, Gattinoni and colleagues proposed this simple model for the quantification of MP at the bedside. They also discussed its possible relevance in setting a "safe" mechanical ventilation [295]. They compared the calculated energy and the measured energy as obtained from the *P–V* curves recorded during tidal ventilation of healthy and ARDS patients at different PEEP levels. Finally, they verified which ventilation variables included in the equation mostly influenced the final ventilation power.

The simple way relies on the equation of motion. They used all the parameters obtained during respiratory monitoring to calculate the MP.

2.14.1 Derivation of Mechanical Power Equation

According to the classical equation of motion [299] (with the addition of PEEP [297]), MP can be obtained.

2.14.1.1 Equation of Motion

Based on the equation of motion, the pressure (P) in the whole respiratory system is calculated as:

$$P = \text{ELrs} * \text{VT} + \text{Raw} * F + \text{PEEP}$$

where ELrs represents respiratory system elastance, VT is tidal volume, Raw is airway resistance, F is flow.

In fact, every component of the equation of motion is one pressure:

$$\text{ELrs} * \Delta V = \text{Pplat} - \text{PEEP}\left(\text{one component of pressure due to the elastic recoil}\right).$$

$$\text{Raw} * F = \text{Ppeak} - \text{Pplat}\left(\text{one component of pressure due to the motion}\right),$$
$$\text{being Raw} = \left(\text{Ppeak} - \text{Pplat}\right) / \text{F}$$

PEEP = Pend-expiration (another component of pressure). It reflects the baseline tension of the lung, which represents the pressure present in the respiratory system when VT and flow are equal to zero.

2.14.1.2 Energy Per Breath

The lung has its resting volume. If we want to increase its volume (ΔV) above its resting volume, an energy needs to be given to the respiratory system. The energy is the product of the absolute value of pressure (P) times the variation of volume (ΔV), i.e., $P * \Delta V$. For this calculation, there is an assumption that the P–V curve of the respiratory system (or of the lung) is linear in the range of volumes considered. As shown in Fig. 2.20, the graphic is composed of a large triangle (AHE), and a parallelogram (Resistive, CEFG) is added on the right.

The left axis of AHE represents the total volume, which include TV and PEEP-induced lung volume (PEEP volume) (the line of AH, ΔV = TV + PEEP volume), while the upper axis represents the plateau pressure (the line of HE). And the slope represents the compliance of the system.

Energy Per Breath Without PEEP (Zero PEEP, ZEEP)

The product of the absolute value of pressure (P) times the variation of volume (ΔV) is called energy, i.e., $P * \Delta V$. Thus, the area of the triangle is the energy applied to compensate the elastic recoil, i.e., Energy = 1/2 * Pplat * ΔV.

Energy Per Breath with PEEP

Applying PEEP, there will be a rest volume. Thus, there will be an energy to reach the PEEP volume (V_{PEEP}), which is equal to 1/2 * PEEP * V_{PEEP} (the tringle of ABC, elastance static). This energy is needed only once as long as PEEP will be maintained. However, during tidal ventilation, this part (ABC) equals zero. Because of PEEP, more energy is needed to inflate the lung over the rest volume (V_{PEEP}). The rest of the large triangle (AHE) represents the elastic energy delivered at each tidal breath, which results from the sum of two components: one is the TV to reach the

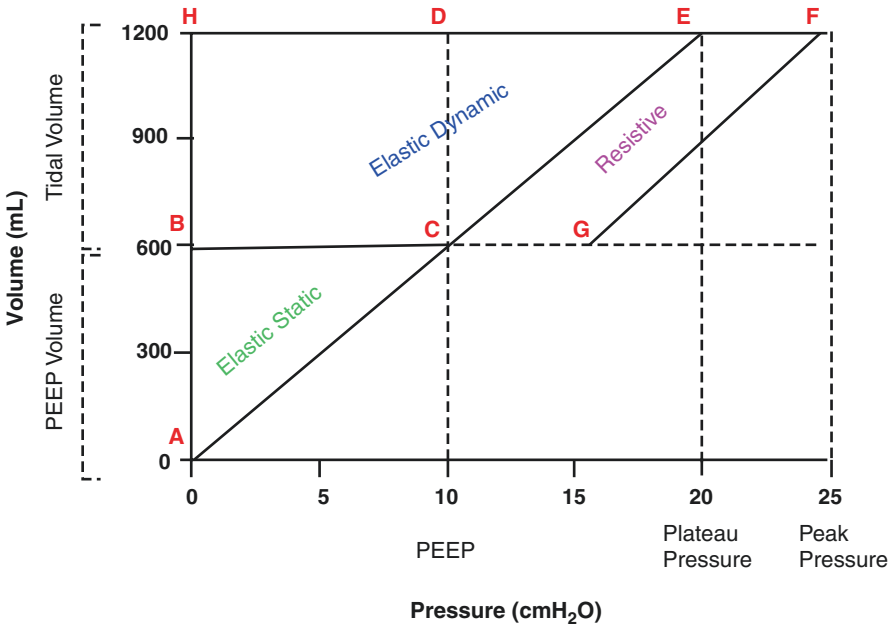

Fig. 2.20 A graphical representation of the power equation. The graphic is composed of a large triangle (AHE), to which a parallelogram (Resistive, CEFG) is added on the right. The left cathetus of the big triangle represents the total volume (i.e. TV + PEEP volume), while the upper cathetus represents the plateau pressure. The slope of the hypotenuse represents the compliance of the system, (in our case 1200 mL/20 cmH_2O = 60 mL/cmH_2O). The area of this large triangle (AHE) is the total elastic energy present at plateau pressure and equals (1200 mL * 30 cmH_2O)/2 * 0.00009 8 = 1764 J. This total elastic energy has two components: the smaller triangle (Elastic Static, ABC), which represents the energy delivered just once when PEEP is applied, and the larger rectangle trapezoid (Elastic Dynamic, BHEC), whose areas represent the elastic energy delivered at each tidal breath. Note that the rectangle trapezoid results from the sum of two components (both azure): a rectangle, whose area is TV * PEEP (third component of the power equation), and a triangle, whose area is TV * ΔPaw * 1/2, equal to ELrs * TV * 1/2 (first component of the power equation). The third component of the power equation is the area described by the Resistive parallelogram (yellow), whose area is equal to (Ppeak − Pplat) * TV

Pplat (the small triangle CDE, VT * (Pplat − PEEP)), the other is the volume displaced from the V_{PEEP} up to the plateau volume (the rectangle BCDH, VT * PEEP).

Energy Per Breath for Gas Motion

Energy per breath for gas motion almost equals to the area of the parallelogram on the right side, in which one side is the (Ppeak − Pplat) and the other side is the VT. This representation is actually a simplification of the reality, since it may change during VCV or PCV mode.

Accordingly, the energy per breath can be computed by multiplying each pressure in the motion equation by the volume variation, as follows:

$$E_{\text{breath}} = \text{VT} * \text{PEEP} + \frac{1}{2}\text{VT} * \left(\text{Pplat} - \text{PEEP}\right) + \text{VT} * \left(\text{Ppeak} - \text{Pplat}\right)$$

Two areas are divided in the second term of the equation, which is equal to VT * (Pplat – PEEP), which approximate the integral of their product. However, the first and the third terms of the equation do not require any correction, as they represent a parallel translation along the axis.

According to the respiratory mechanics and some equations, the Ebreath can be changed.

Premises:

$$\text{Pplat} - \text{PEEP} = \text{VT} * \text{Ers}$$

$$\text{Ppeak} - \text{Pplat} = \text{Raw} * \text{Flow} = \text{Raw} * \frac{\text{VT}}{\text{Tinsp}}$$

$$\text{Tinsp} = \text{Ttotal} * \frac{I:E}{\left(1 + I:E\right)}$$

Thus, we can change the E_{breath} as follows:

$$E_{\text{breath}} = \text{VT} * \text{PEEP} + \text{VT}^2 * \left(\frac{1}{2}\text{Ers} + \text{RR} * \left(\frac{\left(1 + I:E\right)}{60 * \text{I:E}}\right) * \text{Raw}\right)$$

The volumes express in liters and the pressures in cmH_2O, then their product multiplied by 0.098 can be Joules. Then, power per breath will be calculated.

2.14.1.3 Mechanical Power

According to the equation, the MP was expressed as power per minute in J/min will be:

$$\text{MP}_{rs} = 0.098 * \text{RR} * \left\{\text{VT} * \text{PEEP} + \text{VT}^2 * \left(\frac{1}{2}\text{Ers} + \text{RR} * \left(\frac{\left(1 + I:E\right)}{60 * \text{I:E}}\right) * \text{Raw}\right)\right\}$$

where 0.098 represents the conversion factor from L * cmH_2O to J, RR represents respiratory rate, Ers represents the elastance of the respiratory system, I:E represents the ratio of inspiratory and expiratory time, Raw represents the airway resistance, and VT represents the tidal volume. This formula makes it possible to estimate all the effects of changing whatever variable (tidal volume, driving pressure, respiratory rate, resistance) on the MP applied to the respiratory system.

Gattinoni and coworkers calculated the changes of MP as a function of the increase (in 10% steps) of one of its determinants while keeping other components constant. Tidal volume, driving pressure, and inspiratory flow exponentially increased MP by a factor of 2. A 1.4 exponential increase in MP was registered with frequency, while a linear increase was observed with PEEP.

2.14.2 Mechanical Power and VILI

MP may be a predictor of VILI, which is all the parameters of ventilator-related components. According to the motor equation, all the components of VILI are represented in the MP equation [300]:

The product Ers * VT is nothing else than the driving pressure. It is the pressure needed to overcome the elastic forces of the whole respiratory system.

The product Raw * F is the pressure moving the gas inside the respiratory system, and PEEP is the pressure compensating the baseline static stretch of the lung fibers.

A key challenge for the application of MP is that it needs to be adapted to account for the differences of the lung conditions, including lung size, degree of inhomogeneity, and local distribution of stress and strain. In the other words, the same MP may produce different effects in healthy or injured lungs. As the same MP may be safely applied to a normal lung while will be injurious to a diseased lung. Someone will argue that the smaller the lung available for ventilation, the higher the potential harm delivered with the same power amount. Thus, the MP normalized for the lung volume would provide a more accurate indicator of injury potential. For example, the lung of ARDS is "baby lung", which represents the reduction of FRC. This reduction will be associated with a higher normalized power. Severe ARDS (for example, with FRC 500 mL) may generate 58 mJ/min/mL of MP (approximately 20-times applying to a healthy lung with the same setting) [301]. Of course, the association of MP and injury is unknown, further studies should verify to explore that.

In 2016, Cressoni and coworkers performed a study to identify a MP threshold associated with VILI in animal study [296]. Three animals were ventilated with a MP known to be lethal (TV, 38 mL/kg; Pplat, 27 cmH_2O; and RR, 15 breaths/min). Other groups (three piglets each) were ventilated with the same TV per kilogram and PL but at different RR (12, 9, 6, and 3 breaths/min). The authors identified a MP threshold for VILI. Also, they did nine additional experiments at the respiratory rate of 35 breaths/min and MP below (TV 11 mL/kg) and above (TV 22 mL/kg) the threshold. All animals ventilated with a power above 12 J/min developed whole-lung edema while in those ventilated with a lower MP, CT scans showed mostly isolated densities. They found a significant correlation between power, increased lung weight, and lung elastance, along with worsened oxygenation. They demonstrated that 12 J/min may be a meaningful threshold of VILI, and may be a predictor of mortality and survival.

2.14.3 Mechanical Power and Mortality

Apart from the association with VILI, does MP can predict mortality? Or how can it predict mortality?

Recently, a secondary analysis of data investigated the role of MP as a predictor of 90-day survival [302]. The data were from 787 ARDS patients included in two [303, 304] randomized trials. A study was performed to confirm the role of MP, which was very similar to the study of Cressoni. They demonstrated that 12 J/min of MP was a meaningful threshold and was associated with a low probability of survival. Interestingly, they also found that the value of the MP in J/min was very close to that of driving pressure in cmH_2O. Further researches should be performed to confirm if MP can be a significant independent predictor of survival. However, its computation at the bedside should be recommended.

MP was known to be related to the development of VILI. Some investigators performed an analysis of data stored in the databases of the MIMIC–III and EICU. The study examined the association between MP and mortality in critically ill patients receiving mechanical ventilation [305]. This is the first clinical investigation to explore that MP generated by the mechanical ventilator is associated with patient-centered outcomes. They found that higher MP was independently associated with higher ICU mortality, lower ventilator-free days and alive at day 28, and longer stay in ICU and hospital; the impact of MP was consistent and independent of the presence of ARDS.

There was empirical evidence showing that MP could be used to predict risk of mortality in mechanical ventilation patients [305]. However, the smaller the lung available for ventilation, the higher the potential harm delivered with the same power amount. In other words, the effect of MP on VILI was dependent on the lung condition. Recently another second analysis was performed to investigate whether MP normalized to predicted body weight (norMP) was superior to other ventilator variables [306]. One hundred and fifty nine patients' data were included, which were from eight randomized controlled trials conducted by the ARDSNet. Among all the ventilator variables, norMP displayed a significantly higher AUROC value than any other individual variables including MP. What is more, the effect of norMP was dependent on the severity of ARDS. Although norMP had no significant effect on mild ARDS patients with respect to the mortality outcome, norMP was associated with significantly increased risk of worsening of ARDS. MP normalized to predicted body weight was a good ventilator variable in predicting mortality in ARDS patients.

2.14.4 Mechanical Power for PCV

According to Gattinoni, the MP can be calculated using a set of parameters routinely measured during VCV. The calculation of MP according to the equation is based on the assumption that at VCV mode Paw was in a linear rise during

inspiration. However, it is not suitable for calculating MP during pressure-controlled ventilation (PCV) [307]. Because in PCV, Raw cannot be calculated by (Ppeak − Pplat)/Flow and Flow by VT/Tinsp. Further, an increase in VT is always negatively weighted in both original and simplified calculations, then the effect of recruitment is neglected. Zhao et al. [307] illustrated an example of MP calculation during decremental PEEP titration under PCV. They calculated MP with the original and simplified equations. However, there was no tight relationship between these two MP.

Becher and coworkers describe two equations for estimating MP during PCV and assess their validity in patients ventilated with this mode [308]. They retrospectively analyzed PCV data of patients enrolled in two previously published studies [309, 310]. And they excluded datasets with assisted spontaneous breathing and during VCV. They described two equations for estimating MP during PCV. They also assessed the validity in patients ventilated with this mode.

One is that MP during PCV was calculated according to the simplified equation. The simplified equation was based on the assumption of an ideal "square wave" Paw during inspiration:

$$\mathrm{MP_{PCV}} = 0.098 * \mathrm{RR} * \mathrm{VT} * \left(\Delta P_{\mathrm{insp}} + \mathrm{PEEP}\right)$$

where MP represents mechanical power, ΔP_{insp} represents the change in Paw during inspiration, PEEP represents the positive end-expiratory pressure (both cmH_2O), VT represents the tidal volume (l), and RR represents the respiratory rate (1/min), with 0.098 as a correction factor to obtain the result in J/min.

The other one was additionally calculated according to the comprehensive equation taking into account inspiratory pressure rise time (Tslope):

$$\mathrm{MP_{PCV(slope)}} = 0.098 * RR$$
$$* \left[\left(\Delta P_{\mathrm{insp}} + \mathrm{PEEP}\right) * \mathrm{VT} - {\Delta P_{\mathrm{insp}}}^2 * C * \left(0.5 - \frac{R * C}{T_{slope}} + \left(\frac{R * C}{T_{\mathrm{slope}}} \right)^2 * \left(1 - e^{\frac{-T_{\mathrm{slope}}}{R * C}} \right) \right) \right]$$

where C represents the compliance (l/cmH_2O) and R represents the resistance ($cmH_2O/l/s$).

They also calculated MP using *P–V* curve loops, which is defined as MPref. Both $\mathrm{MP_{PCV}}$ (r^2 = 0.981; bias +0.73 J/min; 95% limits of agreement −1.48 to +2.93 J/min) and $\mathrm{MP_{PCV}}$(slope) (r^2 = 0.985; bias +0.03 J/min; 95% −1.91 to +1.98 J/min) were highly correlated to MPref. Disregarding Tslope, the simplified equation allows estimation of MP for PCV with a small bias. However, this equation corrects this bias, and requires knowledge of T_{slope}, *R*, and *C*. If just knowing VT, RR, PEEP, and ΔP_{insp}, the simplified equation may still yield acceptable results for most clinical situations. With the simplified equation, MP for PCV can be calculated at bedside.

2.14.5 Conclusion

Paying attention to mechanical power might help extending focus on VILI. MP will remind doctors not only the TV and DP but also the flows and RR and the most important is their combination. Thus, any reduction in any component of the cyclic mechanical power should lower the risk of VILI. However, the clinical application of MP lacks direct proof. More clinical evidences should be provided. The way to normalize the MP to the lung size and the degree of inhomogeneity may be a suitable way. Further studies are needed to test the meaningful significance of MP. And if the ventilator software can include the power equation, it can overcome the limitation, which is the assumption needed for easier calculation (e.g., linear pressure-volume relationship). Moreover, this may help clinicians to evaluate their choices in terms of MP at the bedside.

References

1. Hess DR. Respiratory mechanics in mechanically ventilated patients. Respir Care. 2014;59:1773–94.
2. Lucangelo U, Bernabe F, Blanch L. Respiratory mechanics derived from signals in the ventilator circuit. Respir Care. 2005;50:55–65; discussion 65-57
3. Akoumianaki E, Maggiore SM, Valenza F, Bellani G, Jubran A, Loring SH, Pelosi P, Talmor D, Grasso S, Chiumello D, Guerin C, Patroniti N, Ranieri VM, Gattinoni L, Nava S, Terragni PP, Pesenti A, Tobin M, Mancebo J, Brochard L. The application of esophageal pressure measurement in patients with respiratory failure. Am J Respir Crit Care Med. 2014;189:520–31.
4. Lethvall S, Sondergaard S, Karason S, Lundin S, Stenqvist O. Dead-space reduction and tracheal pressure measurements using a coaxial inner tube in an endotracheal tube. Intensive Care Med. 2002;28:1042–8.
5. Mauri T, Yoshida T, Bellani G, Goligher EC, Carteaux G, Rittayamai N, Mojoli F, Chiumello D, Piquilloud L, Grasso S, Jubran A, Laghi F, Magder S, Pesenti A, Loring S, Gattinoni L, Talmor D, Blanch L, Amato M, Chen L, Brochard L, Mancebo J, Group PL. Esophageal and transpulmonary pressure in the clinical setting: meaning, usefulness and perspectives. Intensive Care Med. 2016;
6. Sharshar T, Desmarais G, Louis B, Macadou G, Porcher R, Harf A, Raphael JC, Isabey D, Lofaso F. Transdiaphragmatic pressure control of airway pressure support in healthy subjects. Am J Respir Crit Care Med. 2003;168:760–9.
7. Uchiyama A, Yoshida T, Yamanaka H, Fujino Y. Estimation of tracheal pressure and imposed expiratory work of breathing by the endotracheal tube, heat and moisture exchanger, and ventilator during mechanical ventilation. Respir Care. 2013;58:1157–69.
8. Pierce R. Spirometry: an essential clinical measurement. Aust Fam Physician. 2005;34:535–9.
9. Chuang HC, Huang DY, Tien DC, Wu RH, Hsu CH. A respiratory compensating system: design and performance evaluation. J Appl Clin Med Phys. 2014;15:4710.
10. César Cassiolato. Pressure transmitters: sensors, trends, market and applications, Intech Edition 74; 2005
11. Desager KN, Cauberghs M, Van de Woestijne KP. Two-point calibration procedure of the forced oscillation technique. Med Biol Eng Comput. 1997;35:752–6.
12. Graham BL, Steenbruggen I, Miller MR, Barjaktarevic IZ, Cooper BG, Hall GL, Hallstrand TS, Kaminsky DA, McCarthy K, McCormack MC, Oropez CE, Rosenfeld M, Stanojevic

S, Swanney MP, Thompson BR. Standardization of spirometry 2019 update. An official American Thoracic Society and European Respiratory Society Technical Statement. Am J Respir Crit Care Med. 2019;200:e70–88.
13. Sullivan WJ, Peters GM, Enright PL. Pneumotachographs: theory and clinical application. Respir Care. 1984;29:736–49.
14. Cross TJ, Kelley EF, Hardy TA, Isautier JMJ, Johnson BD. The syringe potentiometer: a low-cost device for pneumotachograph calibration. J Appl Physiol (1985). 2019;127:1150–62.
15. Lellouche F, Taille S, Maggiore SM, Qader S, L'Her E, Deye N, Brochard L. Influence of ambient and ventilator output temperatures on performance of heated-wire humidifiers. Am J Respir Crit Care Med. 2004;170:1073–9.
16. Lyazidi A, Thille AW, Carteaux G, Galia F, Brochard L, Richard JC. Bench test evaluation of volume delivered by modern ICU ventilators during volume-controlled ventilation. Intensive Care Med. 2010;36:2074–80.
17. Parker JC, Hernandez LA, Peevy KJ. Mechanisms of ventilator-induced lung injury. Crit Care Med. 1993;21(1):131–43. https://doi.org/10.1097/00003246-199301000-00024.
18. Acute Respiratory Distress Syndrome Network, Brower RG, Matthay MA, Morris A, Schoenfeld D, Thompson BT, Wheeler A. Ventilation with lower tidal volumes as compared with traditional tidal volumes for acute lung injury and the acute respiratory distress syndrome. N Engl J Med. 2000;342(18):1301–8. https://doi.org/10.1056/NEJM200005043421801.
19. Yoshida T, Fujino Y, Amato MBP, Kavanagh BP. Fifty years of research in ARDS. Spontaneous breathing during mechanical ventilation. Risks, mechanisms, and management. Am J Respir Crit Care Med. 2017;195(8):985–92. https://doi.org/10.1164/rccm.201604-0748CP.
20. Goligher EC, Fan E, Herridge MS, Murray A, Vorona S, Brace D, et al. Evolution of diaphragm thickness during mechanical ventilation. Impact of inspiratory effort. Am J Respir Crit Care Med. 2015;192(9):1080–8. https://doi.org/10.1164/rccm.201503-0620OC.
21. Brochard L, Slutsky A, Pesenti A. Mechanical ventilation to minimize progression of lung injury in acute respiratory failure. Am J Respir Crit Care Med. 2017;195(4):438–42. https://doi.org/10.1164/rccm.201605-1081CP.
22. Papazian L, Forel J-M, Gacouin A, Penot-Ragon C, Perrin G, Loundou A, et al. Neuromuscular blockers in early acute respiratory distress syndrome. N Engl J Med. 2010;363(12):1107–16. https://doi.org/10.1056/NEJMoa1005372.
23. Akoumianaki E, Maggiore SM, Valenza F, Bellani G, Jubran A, Loring SH, et al. The application of esophageal pressure measurement in patients with respiratory failure. Am J Respir Crit Care Med. 2014;189(5):520–31. https://doi.org/10.1164/rccm.201312-2193CI.
24. de Vries H, Jonkman A, Shi Z-H, Spoelstra-de Man A, Heunks L. Assessing breathing effort in mechanical ventilation: physiology and clinical implications. Ann Transl Med. 2018;6(19):387. https://doi.org/10.21037/atm.2018.05.53.
25. Buytendijk J. Intraesophageal pressure and lung elasticity [thesis]. Groningen: University of Groningen; 1949.
26. Dornhorst AC, Leathart GL. A method of assessing the mechanical properties of lungs and airpassages. Lancet. 1952;2(6725):109–11. https://doi.org/10.1016/s0140-6736(52)92151-x.
27. Cherniack RM, Farhi LE, Armstrong BW, Proctor DF. A comparison of esophageal and intrapleural pressure in man. J Appl Physiol. 1955;8(2):203–11. https://doi.org/10.1152/jappl.1955.8.2.203.
28. Mojoli F, Torriglia F, Orlando A, Bianchi I, Arisi E, Pozzi M. Technical aspects of bedside respiratory monitoring of transpulmonary pressure. Ann Transl Med. 2018;6(19):377. https://doi.org/10.21037/atm.2018.08.37.
29. Terragni P, Mascia L, Fanelli V, Biondi-Zoccai G, Ranieri VM. Accuracy of esophageal pressure to assess transpulmonary pressure during mechanical ventilation. Intensive Care Med. 2017;43(1):142–3. https://doi.org/10.1007/s00134-016-4589-8.
30. Chen H, Yang Y-L, Xu M, Shi Z-H, He X, Sun X-M, et al. Use of the injection test to indicate the oesophageal balloon position in patients without spontaneous breathing: a clinical feasibility study. J Int Med Res. 2017;45(1):320–31. https://doi.org/10.1177/0300060516679776.

31. Sun X, Zhou J. Esophageal pressure and transpulmonary pressure monitoring. Zhonghua Wei Zhong Bing Ji Jiu Yi Xue. 2018;30(3):280–3. https://doi.org/10.3760/cma.j.issn.2095-4352.2018.03.018.
32. Mojoli F, Chiumello D, Pozzi M, Algieri I, Bianzina S, Luoni S, et al. Esophageal pressure measurements under different conditions of intrathoracic pressure. An in vitro study of second generation balloon catheters. Minerva Anestesiol. 2015;81(8):855–64.
33. Yang Y-L, He X, Sun X-M, Chen H, Shi Z-H, Xu M, et al. Optimal esophageal balloon volume for accurate estimation of pleural pressure at end-expiration and end-inspiration: an in vitro bench experiment. Intensive Care Med Exp. 2017;5(1):35. https://doi.org/10.1186/s40635-017-0148-z.
34. Mojoli F, Iotti GA, Torriglia F, Pozzi M, Volta CA, Bianzina S, et al. In vivo calibration of esophageal pressure in the mechanically ventilated patient makes measurements reliable. Crit Care. 2016;20(1):98–9. https://doi.org/10.1186/s13054-016-1278-5.
35. Sun X-M, Chen G-Q, Huang H-W, He X, Yang Y-L, Shi Z-H, et al. Use of esophageal balloon pressure-volume curve analysis to determine esophageal wall elastance and calibrate raw esophageal pressure: a bench experiment and clinical study. BMC Anesthesiol. 2018;18(1):21–9. https://doi.org/10.1186/s12871-018-0488-6.
36. Baydur A, Behrakis PK, Zin WA, Jaeger M, Milic-Emili J. A simple method for assessing the validity of the esophageal balloon technique. Am Rev Respir Dis. 1982;126(5):788–91. https://doi.org/10.1164/arrd.1982.126.5.788.
37. Chiumello D, Consonni D, Coppola S, Froio S, Crimella F, Colombo A. The occlusion tests and end-expiratory esophageal pressure: measurements and comparison in controlled and assisted ventilation. Ann Intensive Care. 2016;6(1):13–0. https://doi.org/10.1186/s13613-016-0112-1.
38. Higgs BD, Behrakis PK, Bevan DR, Milic-Emili J. Measurement of pleural pressure with esophageal balloon in anesthetized humans. Anesthesiology. 1983;59(4):340–3. https://doi.org/10.1097/00000542-198310000-00012.
39. He X, Sun X-M, Chen G-Q, Yang Y-L, Shi Z-H, Xu M, Zhou J-X. Use of cardiac cycle locating to minimize the influence of cardiac artifacts on esophageal pressure measurement during dynamic occlusion test. Respir Care. 2018;63(2):169–76. https://doi.org/10.4187/respcare.05750.
40. Washko GR, O'Donnell CR, Loring SH. Volume-related and volume-independent effects of posture on esophageal and transpulmonary pressures in healthy subjects. J Appl Physiol. 2006;100(3):753–8. https://doi.org/10.1152/japplphysiol.00697.2005.
41. Talmor D, Sarge T, O'Donnell CR, Ritz R, Malhotra A, Lisbon A, Loring SH. Esophageal and transpulmonary pressures in acute respiratory failure*. Crit Care Med. 2006;34(5):1389–94. https://doi.org/10.1097/01.CCM.0000215515.49001.A2.
42. Talmor D, Sarge T, Malhotra A, O'Donnell CR, Ritz R, Lisbon A, et al. Mechanical ventilation guided by esophageal pressure in acute lung injury. N Engl J Med. 2008;359(20):2095–104. https://doi.org/10.1056/NEJMoa0708638.
43. Chiumello D, Carlesso E, Cadringher P, Caironi P, Valenza F, Polli F, et al. Lung stress and strain during mechanical ventilation for acute respiratory distress syndrome. Am J Respir Crit Care Med. 2008;178(4):346–55. https://doi.org/10.1164/rccm.200710-1589OC.
44. Gattinoni L, Chiumello D, Carlesso E, Valenza F. Bench-to-bedside review: chest wall elastance in acute lung injury/acute respiratory distress syndrome patients. Crit Care. 2004;8(5):350–5.
45. Chiumello D, Cressoni M, Colombo A, Babini G, Brioni M, Crimella F, et al. The assessment of transpulmonary pressure in mechanically ventilated ARDS patients. Intensive Care Med. 2014;40(11):1670–8. https://doi.org/10.1007/s00134-014-3415-4.
46. Yoshida T, Amato MBP, Grieco DL, Chen L, Lima CAS, Roldan R, et al. Esophageal manometry and regional transpulmonary pressure in lung injury. Am J Respir Crit Care Med. 2018;197(8):1018–26. https://doi.org/10.1164/rccm.201709-1806OC.
47. Beitler JR, Sarge T, Banner-Goodspeed VM, Gong MN, Cook D, Novack V, et al. Effect of titrating positive end-expiratory pressure (PEEP) with an esophageal pressure-guided strat-

egy vs an empirical high PEEP-Fio2 strategy on death and days free from mechanical ventilation among patients with acute respiratory distress syndrome: a randomized clinical trial. JAMA. 2019;321(9):846–57. https://doi.org/10.1001/jama.2019.0555.
48. Grasso S, Mascia L, Del Turco M, Malacarne P, Giunta F, Brochard L, et al. Effects of recruiting maneuvers in patients with acute respiratory distress syndrome ventilated with protective ventilatory strategy. Anesthesiology. 2002;96(4):795–802. https://doi.org/10.1097/00000542-200204000-00005.
49. Grasso S, Terragni P, Birocco A, Urbino R, Del Sorbo L, Filippini C, et al. ECMO criteria for influenza A (H1N1)-associated ARDS: role of transpulmonary pressure. Intensive Care Med. 2012;38(3):395–403. https://doi.org/10.1007/s00134-012-2490-7.
50. Mauri T, Yoshida T, Bellani G, Goligher EC, Carteaux G, Rittayamai N, et al. Esophageal and transpulmonary pressure in the clinical setting: meaning, usefulness and perspectives. Intensive Care Med. 2016;42(9):1360–73. https://doi.org/10.1007/s00134-016-4400-x.
51. Loring SH, Malhotra A. Driving pressure and respiratory mechanics in ARDS. N Engl J Med. 2015;372(8):776–7. https://doi.org/10.1056/NEJMe1414218.
52. Baedorf Kassis E, Loring SH, Talmor D. Mortality and pulmonary mechanics in relation to respiratory system and transpulmonary driving pressures in ARDS. Intensive Care Med. 2016;42(8):1206–13. https://doi.org/10.1007/s00134-016-4403-7.
53. Mancebo J, Isabey D, Lorino H, Lofaso F, Lemaire F, Brochard L. Comparative effects of pressure support ventilation and intermittent positive pressure breathing (IPPB) in non-intubated healthy subjects. Eur Respir J. 1995;8(11):1901–9. https://doi.org/10.1183/09031936.95.08111901.
54. Cressoni M, Gotti M, Chiurazzi C, Massari D, Algieri I, Amini M, et al. Mechanical power and development of ventilator-induced lung injury. Anesthesiology. 2016;124(5):1100–8. https://doi.org/10.1097/ALN.0000000000001056.
55. Gattinoni L, Tonetti T, Cressoni M, Cadringher P, Herrmann P, Moerer O, et al. Ventilator-related causes of lung injury: the mechanical power. Intensive Care Med. 2016;42(10):1567–75. https://doi.org/10.1007/s00134-016-4505-2.
56. Brochard L, Martin GS, Blanch L, Pelosi P, Belda FJ, Jubran A, et al. Clinical review: Respiratory monitoring in the ICU - a consensus of 16. Crit Care. 2012;16(2):219–4. https://doi.org/10.1186/cc11146.
57. Ayas NT, McCOOL FD, Gore R, Lieberman SL, Brown R. Prevention of human diaphragm atrophy with short periods of electrical stimulation. Am J Respir Crit Care Med. 1999;159(6):2018–20. https://doi.org/10.1164/ajrccm.159.6.9806147.
58. Goligher EC, Dres M, Fan E, Rubenfeld GD, Scales DC, Herridge MS, et al. Mechanical ventilation-induced diaphragm atrophy strongly impacts clinical outcomes. Am J Respir Crit Care Med. 2018;197(2):204–13. https://doi.org/10.1164/rccm.201703-0536OC.
59. Thille AW, Rodriguez P, Cabello B, Lellouche F, Brochard L. Patient-ventilator asynchrony during assisted mechanical ventilation. Intensive Care Med. 2006;32(10):1515–22. https://doi.org/10.1007/s00134-006-0301-8.
60. Blanch L, Villagra A, Sales B, Montanya J, Lucangelo U, Luján M, et al. Asynchronies during mechanical ventilation are associated with mortality. Intensive Care Med. 2015;41(4):633–41. https://doi.org/10.1007/s00134-015-3692-6.
61. Jubran A, Tobin MJ. Pathophysiologic basis of acute respiratory distress in patients who fail a trial of weaning from mechanical ventilation. Am J Respir Crit Care Med. 1997;155(3):906–15. https://doi.org/10.1164/ajrccm.155.3.9117025.
62. Jubran A, Grant BJB, Laghi F, Parthasarathy S, Tobin MJ. Weaning prediction: esophageal pressure monitoring complements readiness testing. Am J Respir Crit Care Med. 2005;171(11):1252–9. https://doi.org/10.1164/rccm.200503-356OC.
63. Lessard MR, Lofaso F, Brochard L. Expiratory muscle activity increases intrinsic positive end-expiratory pressure independently of dynamic hyperinflation in mechanically ventilated patients. Am J Respir Crit Care Med. 1995;151(2 Pt 1):562–9. https://doi.org/10.1164/ajrccm.151.2.7842221.

64. Repessé X, Vieillard-Baron A, Geri G. Value of measuring esophageal pressure to evaluate heart-lung interactions-applications for invasive hemodynamic monitoring. Ann Transl Med. 2018;6(18):351. https://doi.org/10.21037/atm.2018.05.04.
65. Liu Y, Wei L-Q, Li G-Q, Yu X, Li G-F, Li Y-M. Pulse pressure variation adjusted by respiratory changes in pleural pressure, rather than by tidal volume, reliably predicts fluid responsiveness in patients with acute respiratory distress syndrome. Crit Care Med. 2016;44(2):342–51. https://doi.org/10.1097/CCM.0000000000001371.
66. Pizov R, Ya'ari Y, Perel A. The arterial pressure waveform during acute ventricular failure and synchronized external chest compression. Anesth Analg. 1989;68(2):150–6. https://doi.org/10.1213/00000539-198902000-00015.
67. Bhattacharya M, Kallet RH, Ware LB, Matthay MA. Negative-pressure pulmonary edema. Chest. 2016;150(4):927–33. https://doi.org/10.1016/j.chest.2016.03.043.
68. Khurram OU, Sieck GC, Mantilla CB. Compensatory effects following unilateral diaphragm paralysis. Respir Physiol Neurobiol. 2017;246:39–46.
69. Gill LC, Mantilla CB, Sieck GC. Impact of unilateral denervation on transdiaphragmatic pressure. Respir Physiol Neurobiol. 2015;210:14–21.
70. Beck J, Sinderby C, Lindstrom L, Grassino A. Effects of lung volume on diaphragm EMG signal strength during voluntary contractions. J Appl Physiol (1985). 1998;85(3):1123–34.
71. Bazzy AR, Haddad GG. Diaphragmatic fatigue in unanesthetized adult sheep. J Appl Physiol Respir Environ Exerc Physiol. 1984;57(1):182–90.
72. De Troyer A, Peche R, Yernault JC, Estenne M. Neck muscle activity in patients with severe chronic obstructive pulmonary disease. Am J Respir Crit Care Med. 1994;150(1):41–7.
73. De Troyer A, Estenne M, Ninane V, Van Gansbeke D, Gorini M. Transversus abdominis muscle function in humans. J Appl Physiol (Bethesda, MD 1985). 1990;68(3):1010–6.
74. De Troyer A, Farkas GA. Linkage between parasternals and external intercostals during resting breathing. J Appl Physiol (Bethesda, MD 1985). 1990;69(2):509–16.
75. Petit JM, Milic-Emili G, Delhez L. Role of the diaphragm in breathing in conscious normal man: an electromyographic study. J Appl Physiol. 1960;15:1101–6.
76. Agostoni E, Sant'Ambrogio G, Del Portillo CH. Electromyography of the diaphragm in man and transdiaphragmatic pressure. J Appl Physiol. 1960;15:1093–7.
77. McKenzie DK, Gandevia SC. Phrenic nerve conduction times and twitch pressures of the human diaphragm. J Appl Physiol (Bethesda, MD 1985). 1985;58(5):1496–504.
78. Beck J, Sinderby C, Lindstrom L, Grassino A. Influence of bipolar esophageal electrode positioning on measurements of human crural diaphragm electromyogram. J Appl Physiol (Bethesda, MD 1985). 1996;81(3):1434–49.
79. Sinderby CA, Beck JC, Lindstrom LH, Grassino AE. Enhancement of signal quality in esophageal recordings of diaphragm EMG. J Appl Physiol (Bethesda, MD 1985). 1997;82(4):1370–7.
80. Sinderby C, Navalesi P, Beck J, Skrobik Y, Comtois N, Friberg S, Gottfried SB, Lindstrom L. Neural control of mechanical ventilation in respiratory failure. Nat Med. 1999;5(12):1433–6.
81. Schweitzer TW, Fitzgerald JW, Bowden JA, Lynne-Davies P. Spectral analysis of human inspiratory diaphragmatic electromyograms. J Appl Physiol Respir Environ Exerc Physiol. 1979;46(1):152–65.
82. Bartolo A, Roberts C, Dzwonczyk RR, Goldman E. Analysis of diaphragm EMG signals: comparison of gating vs. subtraction for removal of ECG contamination. J Appl Physiol (Bethesda, MD 1985). 1996;80(6):1898–902.
83. Sinderby C, Lindstrom L, Grassino AE. Automatic assessment of electromyogram quality. J Appl Physiol (Bethesda, MD 1985). 1995;79(5):1803–15.
84. Sinderby C, Friberg S, Comtois N, Grassino A. Chest wall muscle cross talk in canine costal diaphragm electromyogram. J Appl Physiol (Bethesda, MD 1985). 1996;81(5):2312–27.
85. Terzi N, Pelieu I, Guittet L, Ramakers M, Seguin A, Daubin C, Charbonneau P, du Cheyron D, Lofaso F. Neurally adjusted ventilatory assist in patients recovering spontaneous breathing after acute respiratory distress syndrome: physiological evaluation. Crit Care Med. 2010;38(9):1830–7.

86. Sinderby C, Liu S, Colombo D, Camarotta G, Slutsky AS, Navalesi P, Beck J. An automated and standardized neural index to quantify patient-ventilator interaction. Crit Care. 2013;17(5):R239.
87. Roze H, Repusseau B, Perrier V, Germain A, Seramondi R, Dewitte A, Fleureau C, Ouattara A. Neuro-ventilatory efficiency during weaning from mechanical ventilation using neurally adjusted ventilatory assist. Br J Anaesth. 2013;111(6):955–60.
88. Larouche A, Massicotte E, Constantin G, Ducharme-Crevier L, Essouri S, Sinderby C, Beck J, Emeriaud G. Tonic diaphragmatic activity in critically ill children with and without ventilatory support. Pediatr Pulmonol. 2015;50(12):1304–12.
89. Naimark A, Cherniack RM. Compliance of the respiratory system and its components in health and obesity. J Appl Physiol. 1960;15(3):377–82. https://doi.org/10.1152/jappl.1960.15.3.377.
90. Faffe DS, Zin WA. Lung parenchymal mechanics in health and disease. Physiol Rev. 2009;89(3):759–75. https://doi.org/10.1152/physrev.00019.2007.
91. Leith DE, Mead J. Mechanisms determining residual volume of the lungs in normal subjects. J Appl Physiol. 1967;23(2):221–7. https://doi.org/10.1152/jappl.1967.23.2.221.
92. Milic-Emili J, Torchio R, D'Angelo E. Closing volume: a reappraisal (1967-2007). Eur J Appl Physiol. 2007;99(6):567–83. https://doi.org/10.1007/s00421-006-0389-0.
93. Aljuri N, Venegas JG, Freitag L. Viscoelasticity of the trachea and its effects on flow limitation. J Appl Physiol. 2006;100(2):384–9. https://doi.org/10.1152/japplphysiol.00689.2005.
94. Canning BJ, Fischer A. Neural regulation of airway smooth muscle tone. Respir Physiol. 2001;125(1-2):113–27. https://doi.org/10.1016/s0034-5687(00)00208-5.
95. Canning BJ. Reflex regulation of airway smooth muscle tone. J Appl Physiol. 2006;101(3):971–85. https://doi.org/10.1152/japplphysiol.00313.2006.
96. Pepe PE, Marini JJ. Occult positive end-expiratory pressure in mechanically ventilated patients with airflow obstruction: the auto-PEEP effect. Am Rev Respir Dis. 1982 Jul;126(1):166–70.
97. Marini JJ. Dynamic hyperinflation and auto-positive end-expiratory pressure: lessons learned over 30 years. Am J Respir Crit Care Med. 2011;184(7):756–62.
98. Blanch L, Bernabé F, Lucangelo U. Measurement of air trapping, intrinsic positive end-expiratory pressure, and dynamic hyperinflation in mechanically ventilated patients. Respir Care. 2005;50(1):110–23. discussion 123-4
99. Natalini G, Tuzzo D, Rosano A, Testa M, Grazioli M, Pennestrì V, Amodeo G, Marsilia PF, Tinnirello A, Berruto F, Fiorillo M, Filippini M, Peratoner A, Minelli C, Bernardini A, VENTILAB Group. Assessment of factors related to auto-PEEP. Respir Care. 2016;61(2):134–41.
100. Berlin D. Hemodynamic consequences of auto-PEEP. J Intensive Care Med. 2014;29(2):81–6. Epub 2012 May 15
101. Brochard L. Intrinsic (or auto-) positive end-expiratory pressure during spontaneous or assisted ventilation. Intensive Care Med. 2002;28(11):1552–4.
102. Ku SC. It's time to reappraise the impact of auto-PEEP. Respir Care. 2016;61(2):258–9.
103. Tobin MJ, Lodato RF. PEEP, auto-PEEP, and waterfalls. Chest. 1989;96(3):449–51.
104. Ranieri M, Zhang H, Mascia L, Aubin M, Lin CY, Mullen JB, et al. Pressure-time curve predicts minimally injurious ventilatory strategy in an isolated rat lung model. Anesthesiology. 2000;93:1320–8.
105. Terragni P, Bussone G, Mascia L. Dynamic airway pressure-time curve profile (stress index): a systematic review. Minerva Anestesiol. 2016;82(1):58–68.
106. Sun XM, Chen GQ, Chen K, Wang YM, He X, Huang HW, et al. Stress index can be accurately and reliably assessed by visually inspecting ventilator waveforms. Respir Care. 2018;63(9):1094–101.
107. Wongsurakiat P, Yuangtrakul N. Performance and applications of bedside visual inspection of airway pressure-time curve profiles for estimating stress index in patients with acute respiratory distress syndrome. J Clin Monit Comput. 2019;33(2):281–90.

108. De Perrot M, Imai Y, Volgyesi GA, Waddell TK, Liu M, Mullen JB, et al. Effect of ventilator-induced lung injury on the development of reperfusion injury in a rat lung transplant model. J Thorac Cardiovasc Surg. 2002;124(6):1137–44.
109. Gama de Abreu M, Heintz M, Heller A, Szchenyi R, Albrecht DM, Koch T. One-lung ventilation with high tidal volumes and zero positive end-expiratory pressure is injurious in the isolated rabbit lung model. Anesth Analg. 2003;96(1):220–8.
110. Grasso S, Terragni P, Mascia L, Fanelli V, Quintel M, Herrmann P, et al. Airway pressure-time curve profile (stress index) detects tidal recruitment/hyperinflation in experimental acute lung injury. Crit Care Med. 2004;32(4):1018–27.
111. Carvalho AR, Spieth PM, Pelosi P, Vidal Melo MF, Koch T, Jandre FC, et al. Ability of dynamic airway pressure curve profile and elastance for positive end-expiratory pressure titration. Intensive Care Med. 2008;34(12):2291–9.
112. Pan C, Tang R, Xie J, Xu J, Liu S, Yu T, et al. Stress index for positive end-expiratory pressure titration in prone position: a piglet study. Acta Anaesthesiol Scand. 2015;59(9):1170–8.
113. Grasso S, Stripoli T, De Michele M, Bruno F, Moschetta M, Angelelli G, et al. ARDSnet ventilatory protocol and alveolar hyperinflation: role of positive end-expiratory pressure. Am J Respir Crit Care Med. 2007;176(8):761–7.
114. Huang Y, Yang Y, Chen Q, Liu S, Liu L, Pan C, et al. Pulmonary acute respiratory distress syndrome: positive end-expiratory pressure titration needs stress index. J Surg Res. 2013;185(1):347–52.
115. Terragni PP, Filippini C, Slutsky AS, Birocco A, Tenaglia T, Grasso S, et al. Accuracy of plateau pressure and stress index to identify injurious ventilation in patients with acute respiratory distress syndrome. Anesthesiology. 2013;119(4):880–9.
116. Chiumello D, Cressoni M, Carlesso E, Caspani ML, Marino A, Gallazzi E, et al. Bedside selection of positive end-expiratory pressure in mild, moderate, and severe acute respiratory distress syndrome. Crit Care Med. 2014;42(2):252–64.
117. Terragni PP, Rosboch GL, Lisi A, Viale AG, Ranieri VM. How respiratory system mechanics may help in minimising ventilator-induced lung injury in ARDS patients. Eur Respir J Suppl. 2003;42:15s–21s.
118. Chiumello D, Cressoni M, Carlesso E, Caspani ML, Marino A, Gallazzi E, et al. Bedside selection of positive end-expiratory pressure in mild, moderate, and severe acute respiratory distress syndrome. Crit Care Med. 2014;42(2):252–64.
119. Falke KJ, Pontoppidan H, Kumar A, et al. Ventilation with end-expiratory pressure in acute lung disease. J Clin Invest. 1972;51(9):2315–23.
120. Matamis D, Lemaire F, Harf A, et al. Total respiratory pressure-volume curves in the adult respiratory distress syndrome. Chest. 1984;86(1):58–66.
121. Gattinoni L, Pesenti A, Avalli L, et al. Pressure-volume curve of total respiratory system in acute respiratory failure. Computed tomographic scan study. Am Rev Respir Dis. 1987;136(3):730–6.
122. Hickling KG. Ventilatory management of ARDS: can it affect the outcome? Intensive Care Med. 1990;16(4):219–26.
123. Lu Q, Vieira SR, Richecoeur J, et al. A simple automated method for measuring pressure-volume curves during mechanical ventilation. Am J Respir Crit Care Med. 1999;159(1):275–82.
124. Servillo G, Svantesson C, Beydon L, et al. Pressure-volume curves in acute respiratory failure: automated low flow inflation versus occlusion. Am J Respir Crit Care Med. 1997;155(5):1629–36.
125. Ranieri VM, Giuliani R, Fiore T, et al. Volume-pressure curve of the respiratory system predicts effects of PEEP in ARDS: “occlusion” versus “constant flow” technique. Am J Respir Crit Care Med. 1994;149(1):19–27.
126. Lichtwarck-Aschoff M, Kessler V, Sjostrand UH, et al. Static versus dynamic respiratory mechanics for setting the ventilator. Br J Anaesth. 2000;85(4):577–86.
127. Karason S, Sondergaard S, Lundin S, et al. A new method for non-invasive, maneuver-free determination of “static” pressure-volume curves during dynamic/therapeutic mechanical ventilation. Acta Anaesthesiol Scand. 2000;44(5):578–85.

128. Adams AB, Cakar N, Marini JJ. Static and dynamic pressure-volume curves reflect different aspects of respiratory system mechanics in experimental acute respiratory distress syndrome. Respir Care. 2001;46(7):686–93.
129. Stahl CA, Moller K, Schumann S, et al. Dynamic versus static respiratory mechanics in acute lung injury and acute respiratory distress syndrome. Crit Care Med. 2006;34(8):2090–8.
130. Harris RS. Pressure-volume curves of the respiratory system. Respir Care. 2005;50(1):78–98; discussion -9
131. Levy P, Similowski T, Corbeil C, et al. A method for studying the static volume-pressure curves of the respiratory system during mechanical ventilation. J Crit Care. 1989;4:83–9.
132. Roupie E, Dambrosio M, Servillo G, et al. Titration of tidal volume and induced hypercapnia in acute respiratory distress syndrome. Am J Respir Crit Care Med. 1995;152(1):121–8.
133. Amato MB, Barbas CS, Medeiros DM, et al. Effect of a protective-ventilation strategy on mortality in the acute respiratory distress syndrome. N Engl J Med. 1998;338(6):347–54.
134. Broseghini C, Brandolese R, Poggi R, et al. Respiratory resistance and intrinsic positive end-expiratory pressure (PEEPi) in patients with the adult respiratory distress syndrome (ARDS). Eur Respir J. 1988;1(8):726–31.
135. Ranieri VM, Mascia L, Fiore T, et al. Cardiorespiratory effects of positive end-expiratory pressure during progressive tidal volume reduction (permissive hypercapnia) in patients with acute respiratory distress syndrome. Anesthesiology. 1995;83(4):710–20.
136. Suratt PM, Owens DH, Kilgore WT, et al. A pulse method of measuring respiratory system compliance. J Appl Physiol Respir Environ Exerc Physiol. 1980;49(6):1116–21.
137. Suratt PM, Owens D. A pulse method of measuring respiratory system compliance in ventilated patients. Chest. 1981;80(1):34–8.
138. Mankikian B, Lemaire F, Benito S, et al. A new device for measurement of pulmonary pressure-volume curves in patients on mechanical ventilation. Crit Care Med. 1983;11(11):897–901.
139. Harris RS, Hess DR, Venegas JG. An objective analysis of the pressure-volume curve in the acute respiratory distress syndrome. Am J Respir Crit Care Med. 2000;161(2 Pt 1):432–9.
140. Mehta S, Stewart TE, Macdonald R, et al. Temporal change, reproducibility, and interobserver variability in pressure-volume curves in adults with acute lung injury and acute respiratory distress syndrome. Crit Care Med. 2003;31(8):2118–25.
141. Venegas JG, Harris RS, Simon BA. A comprehensive equation for the pulmonary pressure-volume curve. J Appl Physiol (1985). 1998;84(1):389–95.
142. Henzler D, Orfao S, Rossaint R, et al. Modification of a sigmoidal equation for the pulmonary pressure-volume curve for asymmetric data. J Appl Physiol (Bethesda, MD 1985). 2003;95(5):2183–4; author reply 4
143. Ravdin PM, Havlin KA, Marshall MV, et al. A phase I clinical and pharmacokinetic trial of hepsulfam. Cancer Res. 1991;51(23 Pt 1):6268–72.
144. Albaiceta GM, Garcia E, Taboada F. Comparative study of four sigmoid models of pressure-volume curve in acute lung injury. Biomed Eng Online. 2007;6(7)
145. Mead J, Whittenberger JL, Radford EP. Surface tension as a factor in pulmonary volume-pressure hysteresis. J Appl Physiol. 1957;10(2):191–6.
146. Bachofen H, Hildebrandt J. Area analysis of pressure-volume hysteresis in mammalian lungs. J Appl Physiol. 1971;30(4):493–7.
147. Ware LB, Matthay MA. The acute respiratory distress syndrome. N Engl J Med. 2000;342(18):1334–49.
148. Rossi A, Gottfried SB, Zocchi L, et al. Measurement of static compliance of the total respiratory system in patients with acute respiratory failure during mechanical ventilation. The effect of intrinsic positive end-expiratory pressure. Am Rev Respir Dis. 1985;131(5):672–7.
149. Pelosi P, Cereda M, Foti G, et al. Alterations of lung and chest wall mechanics in patients with acute lung injury: effects of positive end-expiratory pressure. Am J Respir Crit Care Med. 1995;152(2):531–7.
150. Polese G, Rossi A, Appendini L, et al. Partitioning of respiratory mechanics in mechanically ventilated patients. J Appl Physiol (1985). 1991;71(6):2425–33.

151. Holzapfel L, Robert D, Perrin F, et al. Static pressure-volume curves and effect of positive end-expiratory pressure on gas exchange in adult respiratory distress syndrome. Crit Care Med. 1983;11(8):591–7.
152. Pelosi P, Croci M, Ravagnan I, et al. Respiratory system mechanics in sedated, paralyzed, morbidly obese patients. J Appl Physiol (1985). 1997;82(3):811–8.
153. Pelosi P, Croci M, Ravagnan I, et al. The effects of body mass on lung volumes, respiratory mechanics, and gas exchange during general anesthesia. Anesth Analg. 1998;87(3):654–60.
154. Pelosi P, Croci M, Ravagnan I, et al. Total respiratory system, lung, and chest wall mechanics in sedated-paralyzed postoperative morbidly obese patients. Chest. 1996;109(1):144–51.
155. Pelosi P, Ravagnan I, Giurati G, et al. Positive end-expiratory pressure improves respiratory function in obese but not in normal subjects during anesthesia and paralysis. Anesthesiology. 1999;91(5):1221–31.
156. Cook CD, Mead J, Schreiner GL, et al. Pulmonary mechanics during induced pulmonary edema in anesthetized dogs. J Appl Physiol. 1959;14(2):177–86.
157. Ranieri VM, Brienza N, Santostasi S, et al. Impairment of lung and chest wall mechanics in patients with acute respiratory distress syndrome: role of abdominal distension. Am J Respir Crit Care Med. 1997;156(4 Pt 1):1082–91.
158. Mutoh T, Lamm WJ, Embree LJ, et al. Abdominal distension alters regional pleural pressures and chest wall mechanics in pigs in vivo. J Appl Physiol (1985). 1991;70(6):2611–8.
159. Lemaire F, Simoneau G, Harf A, Rivara D, Teisseire B, Atlan G, Rapin M. Static pulmonary pressure-volume (P-V) curve, positive end-expiratory pressure (PEEP) ventilation and gas exchange in acute respiratory failure (ARF). Am Rev Respir Dis. 1979;119:328.
160. Suter PM, Fairley B, Isenberg MD. Optimum end-expiratory airway pressure in patients with acute pulmonary failure. N Engl J Med. 1975;292(6):284–9.
161. Jonson B, Richard JC, Straus C, et al. Pressure-volume curves and compliance in acute lung injury: evidence of recruitment above the lower inflection point. Am J Respir Crit Care Med. 1999;159(4 Pt 1):1172–8.
162. Mergoni M, Volpi A, Bricchi C, et al. Lower inflection point and recruitment with PEEP in ventilated patients with acute respiratory failure. J Appl Physiol (1985). 2001;91(1):441–50.
163. Medoff BD, Harris RS, Kesselman H, et al. Use of recruitment maneuvers and high-positive end-expiratory pressure in a patient with acute respiratory distress syndrome. Crit Care Med. 2000;28(4):1210–6.
164. Albaiceta GM, Luyando LH, Parra D, et al. Inspiratory vs. expiratory pressure-volume curves to set end-expiratory pressure in acute lung injury. Intensive Care Med. 2005;31(10):1370–8.
165. Gattinoni L, Pelosi P, Suter PM, et al. Acute respiratory distress syndrome caused by pulmonary and extrapulmonary disease. Different syndromes? Am J Respir Crit Care Med. 1998;158(1):3–11.
166. Albaiceta GM, Piacentini E, Villagra A, et al. Application of continuous positive airway pressure to trace static pressure-volume curves of the respiratory system. Crit Care Med. 2003;31(10):2514–9.
167. Lee WL, Stewart TE, Macdonald R, et al. Safety of pressure-volume curve measurement in acute lung injury and ARDS using a syringe technique. Chest. 2002;121(5):1595–601.
168. Dall'ava-Santucci J, Armaganidis A, Brunet F, et al. Causes of error of respiratory pressure-volume curves in paralyzed subjects. J Appl Physiol (1985). 1988;64(1):42–9.
169. Gattinoni L, Mascheroni D, Basilico E, et al. Volume/pressure curve of the total respiratory system in paralyzed patients: artifacts and correction factors. Intensive Care Med. 1987;13(1):19–25.
170. Brower RG, Lanken PN, Macintyre N, et al. Higher versus lower positive end-expiratory pressures in patients with the acute respiratory distress syndrome. N Engl J Med. 2004;351(4):327–36.
171. Takeuchi M, Goddon S, Dolhnikoff M, et al. Set positive end-expiratory pressure during protective ventilation affects lung injury. Anesthesiology. 2002;97(3):682–92.
172. Gattinoni L, Carlesso E, Cressoni M. Selecting the 'right' positive end-expiratory pressure level. Curr Opin Crit Care. 2015;21(1):50–7.

173. Barbas CS, De Matos GF, Pincelli MP, et al. Mechanical ventilation in acute respiratory failure: recruitment and high positive end-expiratory pressure are necessary. Curr Opin Crit Care. 2005;11(1):18–28.
174. Caironi P, Cressoni M, Chiumello D, et al. Lung opening and closing during ventilation of acute respiratory distress syndrome. Am J Respir Crit Care Med. 2010;181(6):578–86.
175. Ranieri VM, Eissa NT, Corbeil C, et al. Effects of positive end-expiratory pressure on alveolar recruitment and gas exchange in patients with the adult respiratory distress syndrome. Am Rev Respir Dis. 1991;144(3 Pt 1):544–51.
176. Carney DE, Bredenberg CE, Schiller HJ, et al. The mechanism of lung volume change during mechanical ventilation. Am J Respir Crit Care Med. 1999;160(5):1697–702.
177. Lu Q, Constantin JM, Nieszkowska A, et al. Measurement of alveolar derecruitment in patients with acute lung injury: computerized tomography versus pressure-volume curve. Crit Care. 2006;10(3):R95.
178. Nieszkowska A, Lu Q, Vieira S, et al. Incidence and regional distribution of lung overinflation during mechanical ventilation with positive end-expiratory pressure. Crit Care Med. 2004;32(7):1496–503.
179. Rode B, Vucic M, Siranovic M, et al. Positive end-expiratory pressure lung recruitment: comparison between lower inflection point and ultrasound assessment. Wien Klin Wochenschr. 2012;124(23-24):842–7.
180. Caramez MP, Kacmarek RM, Helmy M, et al. A comparison of methods to identify open-lung PEEP. Intensive Care Med. 2009;35(4):740–7.
181. Loring SH, Behazin N, Novero A, et al. Respiratory mechanical effects of surgical pneumoperitoneum in humans. J Appl Physiol (1985). 2014;117(9):1074–9.
182. Behazin N, Jones SB, Cohen RI, et al. Respiratory restriction and elevated pleural and esophageal pressures in morbid obesity. J Appl Physiol (1985). 2010;108(1):212–8.
183. Leatherman JW, Ravenscraft SA. Low measured auto-positive end-expiratory pressure during mechanical ventilation of patients with severe asthma: hidden auto-positive end-expiratory pressure. Crit Care Med. 1996;24(3):541–6.
184. Chen L, Del Sorbo L, Grieco DL, et al. Airway closure in acute respiratory distress syndrome: an underestimated and misinterpreted phenomenon. Am J Respir Crit Care Med. 2018;197(1):132–6.
185. Sun XM, Chen GQ, Zhou YM, et al. Airway closure could be confirmed by electrical impedance tomography. Am J Respir Crit Care Med. 2018;197(1):138–41.
186. Lucangelo U, Bernabe F, Blanch L. Respiratory mechanics derived from signals in the ventilator circuit. Respir Care. 2005;50:55–65. discussion 65-57
187. Hess DR. Respiratory mechanics in mechanically ventilated patients. Respir Care. 2014;59:1773–94.
188. Guntupalli KK, Bandi V, Sirgi C, et al. Usefulness of flow volume loops in emergency center and ICU settings. Chest. 1997;111:481.
189. Graham BL, Steenbruggen I, Miller MR, Barjaktarevic IZ, Cooper BG, Hall GL, Hallstrand TS, Kaminsky DA, McCarthy K, McCormack MC, Oropez CE, Rosenfeld M, Stanojevic S, Swanney MP, Thompson BR. Standardization of spirometry 2019 update. An official American Thoracic Society and European Respiratory Society Technical Statement. Am J Respir Crit Care Med. 2019;200:e70–88.
190. Masekela R, Gray D, Verwey C, Halkas A, Jeena PM. Paediatric spirometry guideline of the South African Thoracic Society: Part 1. S Afr Med J. 2013;103:1036–41.
191. Couriel JM, Hibbert M, Olinsky A. Assessment of proximal airway obstruction in children by analysis of flow-volume loops. Br J Dis Chest. 1984;78:36–45.
192. Aboussouan LS, Stoller JK. Diagnosis and management of upper airway obstruction. Clin Chest Med. 1994;15:35.
193. Reddy R, Cook T, Tenholder MF. Bronchodilatation and the inspiratory flow volume curve. Chest. 1996;110:1226–8.

194. Orton C, Ward S, Jordan S, et al. Flow-volume loop: window to a smooth diagnosis? Thorax. 2015;70:302–4.
195. Shin HH, Sears MR, Hancox RJ. Prevalence and correlates of a 'knee' pattern on the maximal expiratory flow-volume loop in young adults. Respirology. 2014;19:1052.
196. Koutsoukou A, Pecchiari M. Expiratory flow-limitation in mechanically ventilated patients: a risk for ventilator-induced lung injury? World J Crit Care Med. 2019;8:1–8.
197. Valta P, Corbeil C, Lavoie A, Campodonico R, Koulouris N, Chasse M, Braidy J, Milic-Emili J. Detection of expiratory flow limitation during mechanical ventilation. Am J Respir Crit Care Med. 1994;150:1311–7.
198. Carron M, Freo U, Ori C. Usefulness of spirometry in air leak evaluation during laparoscopic surgery in an obese patient with laryngeal mask airway SupremeTM. Br J Anaesth. 2010;105:387–9.
199. Robinson RJ. The use of side-stream spirometry to assess air leak during and after lung volume reduction surgery. Anesthesiology. 1999;91:571–3.
200. Zamel N. Flow volume curve: the "saw-tooth" sign. Eur J Respir Dis. 1986;69:73.
201. Gattinoni L, Chiumello D, Carlesso E, et al. Bench-to-bedside review: chest wall elastance in acute lung injury/acute respiratory distress syndrome patients. Crit Care. 2004;8:350–5.
202. Cherniak RM, Farhi LE, Armstrong BW, et al. A comparison of esophageal and intrapleural pressure in man. J Appl Physiol. 1955;8:203–11.
203. Hedenstierna G. Esophageal pressure: benefit and limitations. Minerva Anestesiol. 2012;78:959–66.
204. Washko GR, O'Donnell CR, Loring SH. Volume-related and volume-independent effects of posture on esophageal and transpulmonary pressures in healthy subjects. J Appl Physiol (1985). 2006;100(3):753–8.
205. Talmor D, Sarge T, O'Donnell CR, et al. Esophageal and transpulmonary pressures in acute respiratory failure. Crit Care Med. 2006;34(5):1389–94.
206. Mojoli F, Iotti GA, Torriglia F, et al. In vivo calibration of esophageal pressure in the mechanically ventilated patient makes measurements reliable. Crit Care. 2016;20:98.
207. Talmor D, Sarge T, Malhotra A, et al. Mechanical ventilation guided by esophageal pressure in acute lung injury. N Engl J Med. 2008;359(20):2095–104.
208. Cherniack RM, Farhi LE, Armstrong BW, et al. A comparison of esophageal and intrapleural pressure in man. J Appl Physiol. 1955;8(2):203–11.
209. Chiumello D, Cressoni M, Colombo A, Babini G, Brioni M, Crimella F, et al. The assessment of transpulmonary pressure in mechanically ventilated ARDS patients. Intensive Care Med. 2014;40:1670–8.
210. Hibbea K, Rice M, Malhotra A. Obesity and ARDSI J 1. Chest. 2012;142(3):785–90.
211. Cortes-Puentes GA, et al. Impact of chest wall modifications and lung injury on the correspondence between airway and transpulmonary driving pressures. Crit Care Med. 2015;43(8):e287–95.
212. Marini JJ. Dynamic hyperinflation and auto-positive end-expiratory pressure: lessons learned over 30 years. Am J Respir Crit Care Med. 2011;184(7):756–62.
213. Silva PL, Moraes L, Santos RS, et al. Recruitment maneuvers modulate epithelial and endothelial cell response according to acute lung injury etiology. Crit Care Med. 2013;41(10):e256–65.
214. Amato MB, Meade MO, Slutsky AS, Brochard L, Costa EL, Schoenfeld DA, Stewart TE, Briel M, Talmor D, Mercat A, et al. Driving pressure and survival in the acute respiratory distress syndrome. N Engl J Med. 2015;372:747–55.
215. Brochard L, Slutsky A, Pesenti A. Mechanical ventilation to minimize progression of lung injury in acute respiratory failure. Am J Respir Crit Care Med. 2016;195(4):438.
216. Goligher EC, Dres M, Fan E, et al. Mechanical ventilation-induced diaphragm atrophy strongly impacts clinical outcomes. Am J Respir Crit Care Med. 2018;197(2):204.
217. Whitelaw WA, Derenne JP, Milic-Emili J. Occlusion pressure as a measure of respiratory center output cm conscious man. Respir Physiol. 1975;23(2):181–99.

218. Milic-Emili J. Recent advances in clinical assessment of control of breathing. Lung. 1982;160(1):1–17.
219. Aubier M, Murciano D, Fournier M, et al. Central respiratory drive in acute respiratory failure of patients with chronic obstructive pulmonary disease. Am Rev Respir Dis. 1980;122(2):191–9.
220. Gallagher CG, Hof VI, Younes M. Effect of inspiratory muscle fatigue on breathing pattern. J Appl Physiol. 1985;59(4):1152–8.
221. Hussain SNA, Pardy RL, Dempsey JA. Mechanical impedance as determinant of inspiratory neural drive during exercise in humans. J Appl Physiol. 1985;59(2):365–75.
222. Grunstein MM, Younes M, Milic J. Control of tidal volume and respiratory frequency in anesthetized cats. J Appl Physiol. 1973;35(4):463.
223. Whitelaw WA, Derenne JP, Milic-Emili J. Occlusion pressure as a measure of respiratory center output cm conscious man. Respir Physiol. 1975;23(2):181–99.
224. Euler CV, Herrero F, Ira W. Control mechanisms determining rate and depth of respiratory movements. Respir Physiol. 1970;10(1):93–108.
225. Murciano D, Aubier M, Bussi S, et al. Comparison of esophageal, tracheal, and mouth occlusion pressure in patients with chronic obstructive pulmonary disease during acute respiratory failure. Am Rev Respir Dis. 1982;126(5):837–41.
226. Conti G, Cinnella G, Barboni E, et al. Estimation of occlusion pressure during assisted ventilation in patients with intrinsic PEEP. Am J Respir Crit Care Med. 1996;154(4 Pt 1):907–12.
227. Altose MD, Kelsen SG, Stanley NN, et al. Effects of hypercapnia on mouth pressure during airway occlusion in conscious man. J Appl Physiol. 1976;40(3):338.
228. Kelsen SG, Altose MD, Stanley NN, et al. Effect of hypoxia on the pressure developed by inspiratory muscles during airway occlusion. J Appl Physiol. 1976;40(3):372–8.
229. Eldridge FL. Relationship between respiratory nerve and muscle activity and muscle force output. J Appl Physiol. 1975;39(4):567–74.
230. Evanich MJ, Lourenco RV. Relation between phrenic nerve activity and intratracheal and intrapleural pressures. Fed Proc. 1974;33:419.
231. Hussain SNA, Pardy RL, Dempsey JA. Mechanical impedance as determinant of inspiratory neural drive during exercise in humans. J Appl Physiol. 1985;59(2):365–75.
232. Marini JJ, Rodriguez RM, Lamb V. The inspiratory workload of patient-initiated mechanical ventilation. Am Rev Respir Dis. 1986;134(5):902–9.
233. Milic-Emili J, Whitelaw W, Grassino A. Measurement and testing of respiratory drive. In: Hornbein T, editor. Regulation of breathing. New York, NY: Dekker; 1981. p. 675–743.
234. Conti G, Antonelli M, Arzano S, et al. Equipment review: measurement of occlusion pressures in critically ill patients. Crit Care. 1998:1(3).
235. Fernández R, Blanch L, Artigas A. Respiratory center activity during mechanical ventilation. J Crit Care. 1991;6(2):102–11.
236. Kuhlen R, Hausmann S, Pappert D, Slama K, Rossaint R, Falke K. A new method for P0.1 measurement using standard respiratory equipment. Intensive Care Med. 1995;21:554–60.
237. Subirana M, Irrazabal C, Bak E, Jara F, Mancebo J. Evaluacion de la medida de la presion de occlusion incorporada en los ventiladores Evita. Med Intensiva. 1997;21:305–10.
238. Kera T, Aihara A, Inomata T. Reliability of airway occlusion pressure as an index of respiratory motor output. Respir Care. 2012;58(5):845–9.
239. Fujii Y, Tanaka H, Toyooka H, et al. Airway occlusion pressure is an indicator of respiratory depression with isoflurane. J Anesth. 1994;8(3):253–5.
240. Anonymous. ATS/ERS statement on respiratory muscle testing. Am J Respir Crit Care Med. 2002;166(4):518–624.
241. Telias I, Damiani F, Brochard L. The airway occlusion pressure (P0.1) to monitor respiratory drive during mechanical ventilation: increasing awareness of a not-so-new problem. Intensive Care Med. 2018;44(9):1–4.
242. Cook CD, Mead J, Orzalesi MM. Static volume-pressure characteristics of the respiratory system during maximal efforts. J Appl Physiol. 1964;19(5):1016–22.
243. Evanich MJ, Franco MJ, Lourenço RV. Force output of the diaphragm as a function of phrenic nerve firing rate and lung volume. J Appl Physiol. 1973;35(2):208–12.

244. Pengelly LD, alderson A, Milic-Emili J. Mechanics of the diaphragm. J Appl Physiol. 1971;30:796.
245. Smith J, Bellemare F. Effect of lung volume on in vivo contraction characteristics of human diaphragm. J Appl Physiol. 1987;62(5):1893–900.
246. Whitelaw WA, Derenne JP. Airway occlusion pressure. J Appl Physiol (1985). 1993;74:1475–83.
247. Baydur A. Respiratory muscle strength and control of ventilation in patients with neuromuscular disease. Chest. 1991;99(2):330–8.
248. Holle RHO, Schoene RB, Pavlin EJ. Effect of respiratory muscle weakness on P0.1 induced by partial curarization. J Appl Physiol Respir Environ Exerc Physiol. 1984;57(4):1150–7.
249. Gibson GJ, Gilmartin JJ, Veale D, Walls TJ, Serisier DE. Respiratory muscle function in neuromuscular disease. In: Jones NL, Killian KJ, editors. Breathlessness. Hamilton, Canada: CME; 1992. p. 66–71.
250. Marazzini L, Cavestri R, Gori D, et al. Diffference between mouth and esophageal occlusion pressure during CO2 rebreathing in chronic obstructive pulmonary disease. Am Rev Respir Dis. 1978;118(6):1027–33.
251. Gattinoni L. Ventilation-induced lung injury exists in spontaneously breathing patients with acute respiratory failure: We are not sure. Intensive Care Med. 2017;43(2):256–8.
252. Rittayamai N, Beloncle F, Goligher EC, et al. Effect of inspiratory synchronization during pressure-controlled ventilation on lung distension and inspiratory effort. Ann Intensive Care. 2017;7(1):100.
253. Pletsch-Assuncao R, Caleffi Pereira M, Ferreira JG, et al. Accuracy of invasive and noninvasive parameters for diagnosing ventilatory overassistance during pressure support ventilation. Crit Care Med. 2017;1
254. Alberti A, Gallo F, Fongaro A, et al. P0.1 is a useful parameter in setting the level of pressure support ventilation. Intensive Care Med. 1995;21(7):547–53.
255. Smith TC, Marini JJ. Impact of PEEP on lung mechanics and work of breathing in severe airflow obstruction. J Appl Physiol. 1988;65(4):1488–99.
256. Mancebo J, Albaladejo P, Touchard D, et al. Airway occlusion pressure to titrate positive end-expiratory pressure in patients with dynamic hyperinflation. Anesthesiology. 2000;93(1):81–90.
257. Murciano D, Aubier M, Lecocguic Y, Kerbiriou P, Pariente R. Tracheal occlusion Tracheal occlusion pressure as an index of respiratory muscle fatigue during acute respiratory failure of COPD patients (abstract). Am Rev Respir Dis. 1984;129:A34.
258. Herrera M, Blasco J, Venegas J, et al. Mouth occlusion pressure (P0.1) in acute respiratory failure. Intensive Care Med. 1985;11(3):134–9.
259. Sassoon CSH, Te TT, Mahutte CK, et al. Airway occlusion pressure. An important indicator for successful weaning in patients with chronic obstructive pulmonary disease. Am Rev Respir Dis. 1987;135(1):107–13.
260. Fernández R, Cabrera J, Calaf N, et al. P0.1/PIMax: an index for assessing respiratory capacity in acute respiratory failure. Intensive Care Med. 1990;16(3):175–9.
261. Montgomery AB, Holle RHO, Neagley SR, et al. Prediction of successful ventilator weaning using airway occlusion pressure and hypercapnic challenge. Chest. 1987;91(4):496–9.
262. Fernandez R, Raurich JM, Mut T, et al. Extubation failure: diagnostic value of occlusion pressure (P0.1) and P0.1-derived parameters. Intensive Care Med. 2004;30(2):234–40.
263. American Thoracic Society/European Respiratory Society. ATS/ERS Statement on respiratory muscle testing. Am J Respir Crit Care Med. 2002;166:518–624.
264. Laporta D, Grassino A. Assessment of transdiaphragmatic pressure in humans. J Appl Physiol. 1985;58:1469–76.
265. Grimby G, Goldman M, Mead J. Respiratory muscle action inferred from rib cage and abdominal V-P partitioning. J Appl Physiol. 1976;41:739–51.
266. Mauri T, Yoshida T, Bellani G, et al. Esophageal and transpulmonary pressure in the clinical setting: meaning, usefulness and perspectives. Intensive Care Med. 2016;42(9):1360–73.
267. Tobin MJ. Principles and practise of intensive care monitoring. 1st ed. New York: McGraw-Hill Companies; 1997.

268. De Vries H, Jonkman A, Shi Z-H, Spoelstra-de Man A, Heunks L. Assessing breathing effort in mechanical ventilation: physiology and clinical implications. Ann Transl Med. 2018;6(19):387.
269. Ninane V, Rypens F, Yernault JC, et al. Abdominal muscle use during breathing in patients with chronic airflow obstruction. Am Rev Respir Dis. 1992;146:16–21.
270. Campbell EJM. The respiratory muscles and the mechanics of breathing. Chicago, IL: Year Book Publishers; 1958.
271. Levy MM, Miyasaki A, Langston D. Work of breathing as a weaning parameter in mechanically ventilated patients. Chest. 1995;108(4):1018–20.
272. Collett PW, Perry C, Engel LA. Pressure-time product, flow, and oxygen cost of resistive breathing in humans. J Appl Physiol. 1985;58(4):1263–72.
273. Jubran A, Graaff WBVD, Tobin MJ. Variability of patient-ventilator interaction with pressure support ventilation in patients with chronic obstructive pulmonary disease. Am J Respir Crit Care Med. 1995;152(1):129–36.
274. Brochard L. Transdiaphragmatic pressure. In: Benito S, Net A, editors. Pulmonary function in mechanically ventilated patients. Update in intensive care and emergency medicine, vol. 13. Berlin, Heidelberg: Springer; 1991.
275. Benditt JO. Esophageal and gastric pressure measurements. Respir Care. 2005;50(1):68–75.
276. Syabbalo N. Assessment of respiratory muscle function and strength. Postgrad Med J. 1998;74(870):208–15.
277. Miller JM, Moxham J, Green M. The maximal sniff in the assessment of diaphragm function in man. Clin Sci (Lond). 1985;69(1):91–6.
278. Laporta D, Grassino A. Assessment of transdiaphragmatic pressure in humans. J Appl Physiol. 1985;58(5):1469–76.
279. Wragg S, Aquilina R, Moran J, et al. Comparison of cervical magnetic stimulation and bilateral percutaneous electrical stimulation of the phrenic nerves in normal subjects. Eur Respir J. 1994;7(10):1788–92.
280. Tobin MJ. Essentials of critical care medicine, vol. 232. New York: Churchill Livingstone; 1989.
281. Mier A, Brophy C, Moxham J, Green M. Twitch pressures in the assessment of diaphragm weakness. Thorax. 1989;44(12):990–6.
282. Bellemare F, Wight D, Lavigne CM, Grassino A. Effect of tension and timing of contraction on the blood flow of the diaphragm. J Appl Physiol Respir Environ Exerc Physiol. 1983;54(6):1597–606.
283. Bellemare F, Grassino A. Effect of pressure and timing of contraction on human diaphragm fatigue. J Appl Physiol Respir Environ Exerc Physiol. 1982;53(5):1190–5.
284. Beck J, Sinderby C, Lindstrom L, Grassino A. Effects of lung volume on diaphragm EMG signal strength during voluntary contractions. J Appl Physiol (Bethesda, MD 1985). 1998;85(3):1123–34.
285. Beck J, Sinderby C, Lindstrom L, Grassino A. Crural diaphragm activation during dynamic contractions at various inspiratory flow rates. J Appl Physiol (Bethesda, MD 1985). 1998;85(2):451–8.
286. Bellani G, Mauri T, Coppadoro A, Grasselli G, Patroniti N, Spadaro S, Sala V, Foti G, Pesenti A. Estimation of patient's inspiratory effort from the electrical activity of the diaphragm. Crit Care Med. 2013;41(6):1483–91.
287. Grasselli G, Beck J, Mirabella L, Pesenti A, Slutsky AS, Sinderby C. Assessment of patient-ventilator breath contribution during neurally adjusted ventilatory assist. Intensive Care Med. 2012;38(7):1224–32.
288. Kumar A, Pontoppidan H, Falke KJ, et al. Pulmonary barotrauma during mechanical ventilation. Crit Care Med. 1973;1(4):181–6.
289. Dreyfuss D, Soler P, Basset G, et al. High inflation pressure pulmonary edema. Respective effects of high airway pressure, high tidal volume, and positive end-expiratory pressure. Am Rev Respir Dis. 1988;137(5):1159–64.

290. Protti A, Maraffi T, Milesi M, et al. Role of Strain Rate in the Pathogenesis of Ventilator-Induced Lung Edema. Crit Care Med. 2016;44(9):e838–45.
291. Hotchkiss JR Jr, Blanch L, Murias G, et al. Effects of decreased respiratory frequency on ventilator-induced lung injury. Am J Respir Crit Care Med. 2000;161(2 Pt 1):463–8.
292. Gattinoni L, Pesenti A, Avalli L, et al. Pressure-volume curve of total respiratory system in acute respiratory failure. Computed tomographic scan study. Am Rev Respir Dis. 1987;136(3):730–6.
293. Cressoni M, Cadringher P, Chiurazzi C, et al. Lung inhomogeneity in patients with acute respiratory distress syndrome. Am J Respir Crit Care Med. 2014;189(2):149–58.
294. Gattinoni L, Pelosi P, Crotti S, et al. Effects of positive end-expiratory pressure on regional distribution of tidal volume and recruitment in adult respiratory distress syndrome. Am J Respir Crit Care Med. 1995;151(6):1807–14.
295. Gattinoni L, Tonetti T, Cressoni M, et al. Ventilator-related causes of lung injury: the mechanical power. Intensive Care Med. 2016;42(10):1567–75.
296. Cressoni M, Gotti M, Chiurazzi C, et al. Mechanical power and development of ventilator-induced lung injury. Anesthesiology. 2016;124(5):1100–8.
297. Marini JJ, Crooke PS 3rd. A general mathematical model for respiratory dynamics relevant to the clinical setting. Am Rev Respir Dis. 1993;147(1):14–24.
298. Marini JJ, Gattinoni L. Energetics and the root mechanical cause for ventilator-induced lung injury. Anesthesiology. 2018;128(6):1062–4.
299. Otis AB, Fenn WO, Rahn H. Mechanics of breathing in man. J Appl Physiol. 1950;2(11):592–607.
300. Tonetti T, Vasques F, Rapetti F, et al. Driving pressure and mechanical power: new targets for VILI prevention. Ann Transl Med. 2017;5(14):286.
301. Gattinoni L, Tonetti T, Quintel M. Intensive care medicine in 2050: ventilator-induced lung injury. Intensive Care Med. 2018;44(1):76–8.
302. Guérin C, Papazian L, Reignier J, et al. Effect of driving pressure on mortality in ARDS patients during lung protective mechanical ventilation in two randomized controlled trials. Crit Care. 2016;20(1):384.
303. Papazian L, Forel JM, Gacouin A, et al. Neuromuscular blockers in early acute respiratory distress syndrome. N Engl J Med. 2010;363(12):1107–16.
304. Guérin C, Reignier J, Richard JC, et al. Prone positioning in severe acute respiratory distress syndrome. N Engl J Med. 2013;368(23):2159–68.
305. Serpa Neto A, Deliberato RO, Johnson AEW, et al. Mechanical power of ventilation is associated with mortality in critically ill patients: an analysis of patients in two observational cohorts. Intensive Care Med. 2018;44(11):1914–22.
306. Zhang Z, Zheng B, Liu N, et al. Mechanical power normalized to predicted body weight as a predictor of mortality in patients with acute respiratory distress syndrome. Intensive Care Med. 2019;45:856–64.
307. Zhao Z, Frerichs I, He H, et al. The calculation of mechanical power is not suitable for intra-patient monitoring under pressure-controlled ventilation. Intensive Care Med. 2019;45(5):749–50.
308. Becher T, van der Staay M, Schädler D, et al. Calculation of mechanical power for pressure-controlled ventilation. Intensive Care Med. 2019;45:1321–3.
309. Pulletz S, Adler A, Kott M, et al. Regional lung opening and closing pressures in patients with acute lung injury. J Crit Care. 2012;27(3):323.e11–8.
310. Becher TH, Bui S, Zick G, et al. Assessment of respiratory system compliance with electrical impedance tomography using a positive end-expiratory pressure wave maneuver during pressure support ventilation: a pilot clinical study. Crit Care. 2014;18(6):679.

Chapter 3
Lung Imaging

Jing-Ran Chen, Quang-Qiang Chen, Jian-Xin Zhou, and Yi-Min Zhou

3.1 X-Ray

3.1.1 Quotation

Chest X-ray radiography is a common auxiliary means in the diagnosis and treatment of critical care. It can provide information about the course of the disease and cardiopulmonary status. And in the critical care unit, patients often need a variety of life-supporting catheters, X-rays can help clinicians determine the location of these catheters and whether there are other complications during the placement of the catheters. Routine chest X-rays can help doctors determine if treatments are effective and manage potential complications.

Since the X-ray is such an important thing, how do we confirm its quality?Rubinowitz AN et al. summarized a series of judgment processes [1]. The first step is to assess the quality of the image technically, then clinicians should focus on the location of patients' catheters such as stomach tube, tracheal cannula, and all other support devices. The next step is to assess the patient's condition. Clinicians should systematically evaluate patients' cardiopulmonary status, size of heart border, look for the effusion of the lung and pleural. Then, clinicians should not forget to compare the current X-ray image with the prior studies and evaluate whether the patient is recovering or getting worse.

J.-R. Chen · Q.-Q. Chen · J.-X. Zhou (✉) · Y.-M. Zhou
Department of Critical Care Medicine, Beijing Tiantan Hospital, Capital Medical University, Beijing, China

J. Zhou et al. (eds.), *Respiratory Monitoring in Mechanical Ventilation*,
https://doi.org/10.1007/978-981-15-9770-1_3

3.1.2 Applications

3.1.2.1 Monitoring and Support Devices

Endotracheal and Tracheostomy Tubes

Endotracheal intubation is common in patients requiring short periods of mechanical ventilation. Improper placement of the endotracheal tube is very common. The location of endotracheal intubation can be simply determined by auscultation to determine whether the respiratory tone of the left and right lung is symmetrical. However, for patients in the critical care unit, the lung is often damaged, so the stethoscope method may not provide accurate information. So, clinicians always choose bedside X-ray to evaluate the endotracheal tube's location. With the patient's head in a neutral position, the proper position of the endotracheal tube is its tip should be located 3–5 cm above the carina [2]. Too deep or too shallow placement of the tube can lead to bad results. Endotracheal tube insertion into the right main bronchus is common because the right main bronchus is thicker and straighter. Deep insertion may lead to hyperventilation of the lung on this side or even lead to pneumothorax, and may lead to contralateral atelectasis. Shallow endotracheal intubation may increase the risk of catheter prolapse or laryngeal injury. Another poorly positioned catheter is that the catheter strays into the esophagus, which, if not detected in time, will lead to excessive accumulation of gas in the gastrointestinal tract, and even lead to gastrointestinal perforation.

The tracheostomy tube is used in patients undergoing prolonged mechanical ventilation. The best position for a tracheostomy tube should be to align its tip with approximately the T3 level. Figure 3.1 shows the right main bronchus intubation.

Enteric Tubes

Gastric tubes are often used for drainage and nutritional feeding. For feeding use, the catheter tip should reach at least to the gastric antrum to reduce the risk of aspiration. Radiology is important for detecting abnormal catheter locations and preventing potentially fatal complications. The catheter may be coiled in the pharynx or esophagus, with a high risk of aspiration. Occasionally, a catheter may cause perforation of the pharynx and pharyngeal capsule. Figure 3.2 shows this situation.

Venous Catheters

Central venous catheters are commonly used for fluid rehydration, parenteral nutrition, or CVP monitoring. To reduce the risk of thrombosis, the central venous catheter tip should be located inside the superior vena cava and outside the venous flap [3]. When the catheter is too deep, it can enter the right atrium, increasing the risk of arrhythmias and heart perforations.

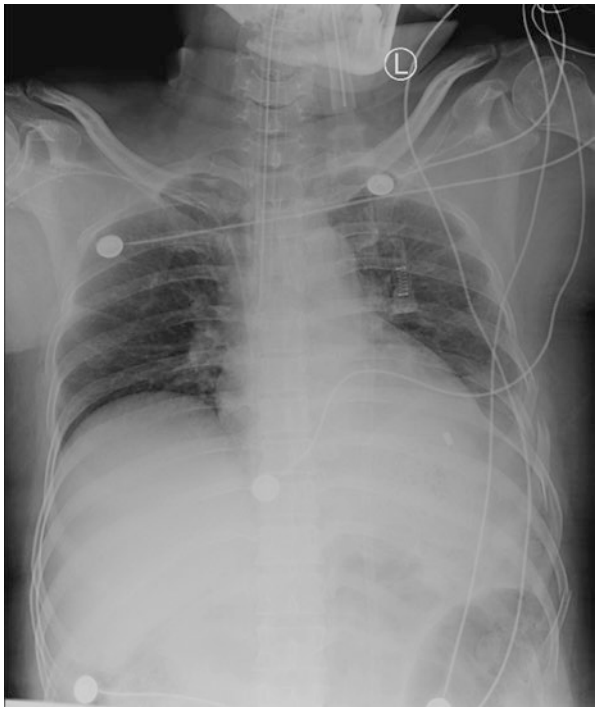

Fig. 3.1 Right main bronchus intubation. This patient's chest radiograph demonstrates the endotracheal tube tip in the right main bronchus

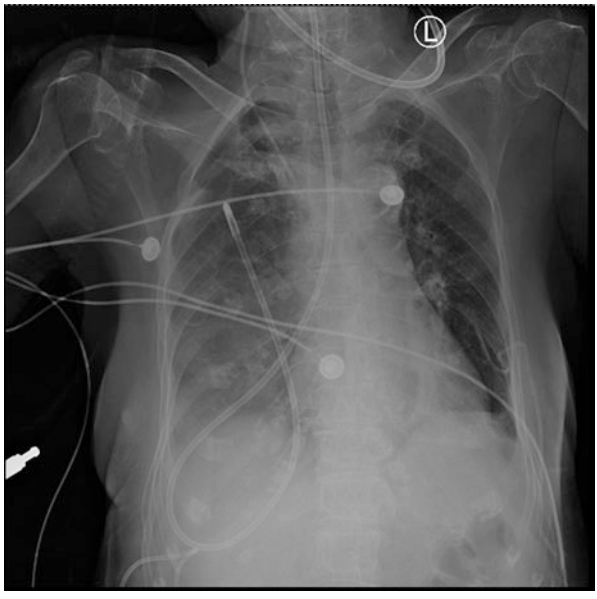

Fig. 3.2 A gastric tube was accidentally inserted into the right lung. The chest radiograph demonstrates an aberrant enteric tube terminating in the right upper lobe

Sometimes a catheter goes into an artery, which is often seen in the subclavian artery or common carotid artery. Bright red blood ejections from the catheter are usually observed when the catheter is inserted into the artery, but this may not be evident in ICU patients with heart failure or hypotension, so X-ray examination is still needed to confirm its position. Subclavian venipuncture is of particular concern because it may result in hemothorax, pneumothorax, or chylothorax.

3.1.2.2 Pulmonary Parenchymal Abnormalities

Atelectasis

Atelectasis, or a decrease in the volume of air in the lungs, is the most common cause of chest X-ray opacity in ICU patients [2]. The most common atelectasis is in the lower-left lobe, followed by the lower right lobe and the upper right lobe [4].

The X-ray manifestations of atelectasis can be classified into direct X-ray signs and indirect X-ray signs. Direct signs include reduced lung transparency in the atelectasis part, an increase in the density of uniformity. In the convalescence period or with bronchiectasis, X-ray may appear uneven density of the cystic transparent area.

Lobular atelectasis is generally in the shape of obtuse and triangular, with broad and pure surfaces facing the costal diaphragmatic pleural surfaces, and the tips pointing to the hilum of the lungs, while the indirect X-ray signs of atelectasis show lateral displacement of the interlobar fissure to atelectasis. As the lung volume shrinks, the bronchi in the lesion area converge with the vascular texture, while the compensatory expansion in the adjacent lung causes the vascular texture to be sparse and shift to the atelectatic pulmonary arch. Clinicians may also see hilum shadow shifting to atelectasis, the hilum shadow shrinks and disappears, and is separated from the dense shadow of atelectasis. Mediastinal, heart, and trachea are shifted to the affected side, especially when the whole lung was atelectasis. However, the more sensitive and accurate diagnosis of atelectasis is CT. Figure 3.3 shows an image of atelectasis.

Pneumonia

ICU patients have a higher incidence of pneumonia due to long-term invasive respiratory support and complex conditions. The X-ray manifestation of pneumonia has a certain relationship with the pathogenic bacteria of infection. It may be performed as a multi-focused, focal consolidation on chest radiographs. Pneumonia may be difficult to distinguish from other causes of lung opacity, such as atelectasis, aspiration pneumonia, and pulmonary edema. Figure 3.4 shows an example of bacterial pneumonia.

Fig. 3.3 Atelectasis. The chest radiograph shows the central space-occupying lesion of the right lung and the right upper lobe obstructs atelectasis

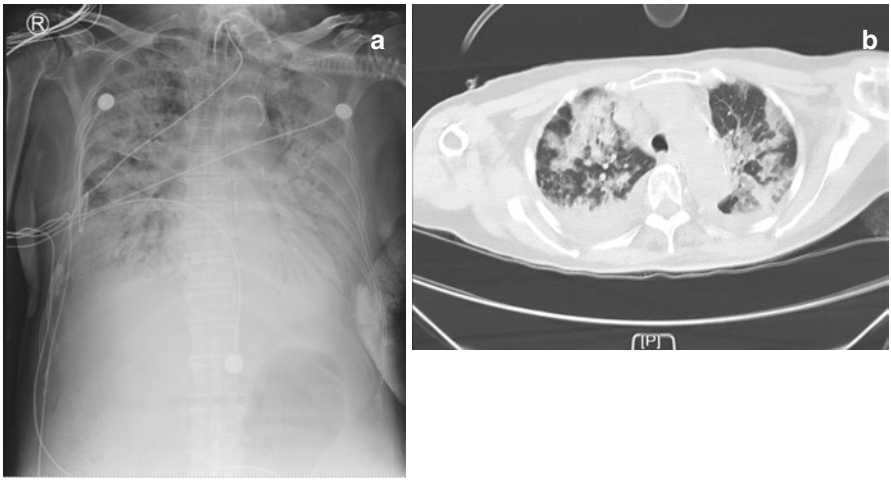

Fig. 3.4 Pneumonia. Panels (**a**) and (**b**) show X-ray and CT images of pneumonia, respectively. The radiograph demonstrates bilateral lung inflammation with partial consolidation

Pneumothorax

Pneumothorax can result from underlying lung disease, inappropriate respiratory support levels, and medical procedures. Most of the pneumothorax radiographs have clear pneumothorax lines, that is, the boundary line between atrophic lung tissue and the gas in the pleural cavity, showing an outward convex line shadow, the pneumothorax line is a transparent area without lung texture, and the line is

compressed lung tissue. Mediastinal and cardiac migration to the healthy side can be seen in a large amount of pneumothorax. The gas-liquid level can be seen with pleural effusion (Fig. 3.5). For patients in the ICU, chest radiographs in the supine position are often performed. Such patients often do not show the traditional pneumothorax images in chest X-ray, but deep sulcus may be observed [5]. In the supine position, as the pneumothorax increases in volume, the intrapleural air accumulates from the anteromedial region to the laterocaudal region (Fig. 3.6). Hence, the

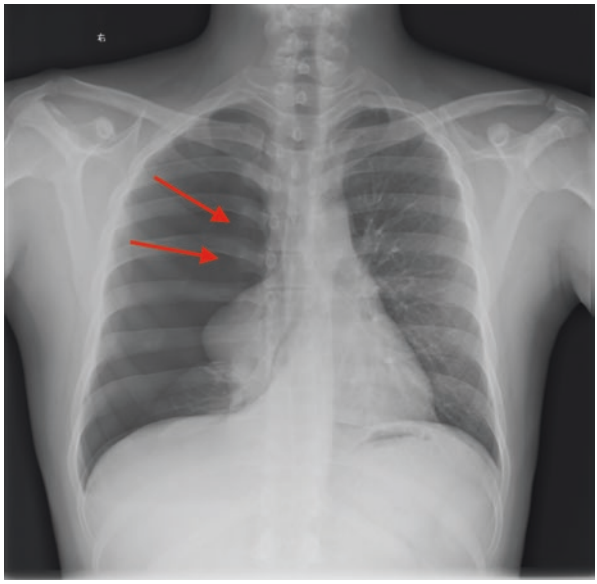

Fig. 3.5 Pneumothorax. Upright chest radiograph showing a right apical pneumothorax. A thin line of visceral pleura is visible (arrows). The right lung is about 95% compressed

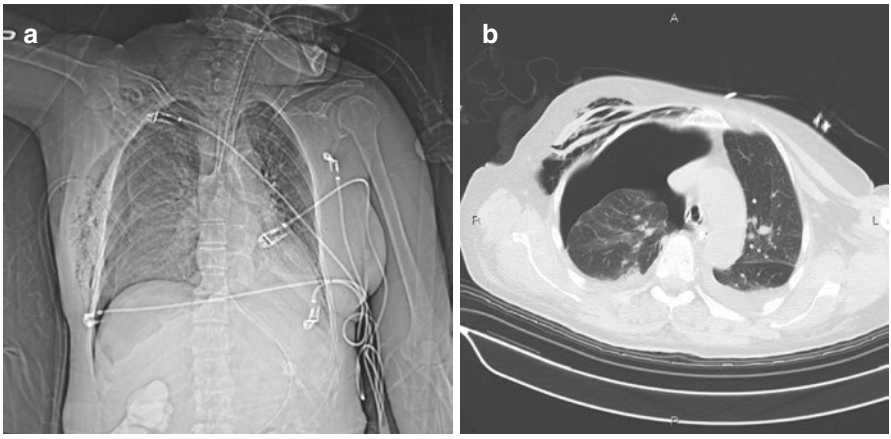

Fig. 3.6 Pneumothorax. Panel (**a**) shows "Deep sulcus sign", which can be seen in supine patients. It demonstrates lucent deep lateral costophrenic sulcus and lucency of the right lower hemithorax. Panel (**b**) shows the CT scan taken on the same day which confirmed the presence of pneumothorax in the right thorax

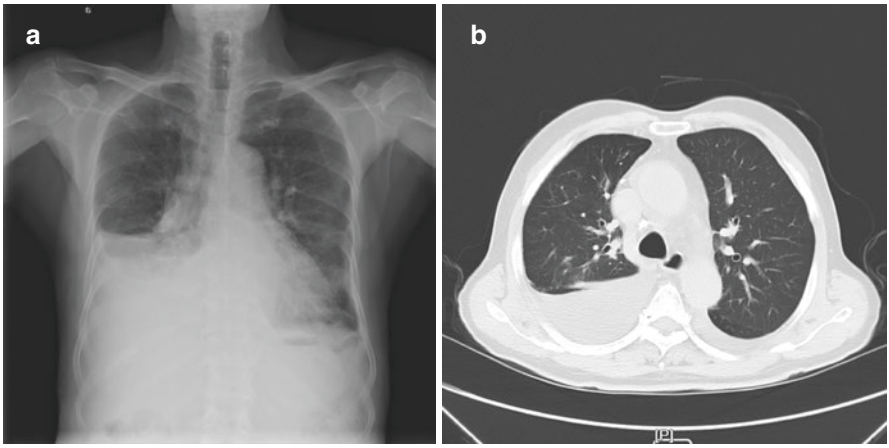

Fig. 3.7 Layering pleural fluid. Panels (**a**) and (**b**) show X-ray and CT images of pleural fluid, respectively. (**a**) Shows blunting of the right costophrenic angles. (**b**) CT image in the same patient confirms right pleural effusions

so-called deep sulcus sign is performed as a deep and lucent costophrenic angle which extends more inferiorly than usual. But so far, the golden standard for the diagnosis of occult pneumothroax is still the CT scan.

Pleural Fluid

Pleural effusion is common in ICU patients. The presence of pleural effusion in sitting or standing chest radiographs is indicated by the appearance of a blunt costophrenic angle. However, chest radiographs in the supine position are not sensitive to the diagnosis of pleural effusion and may present only as hazy opacification pulmonary images. CT examination can not only confirm the presence of pleural effusion but also reveal the pulmonary, mediastinal, and pleural conditions, suggesting the etiology of pleural effusion. Figure 3.7 shows the image of layering pleural fluid under X-ray.

3.2 Lung and Diaphragm Ultrasound

3.2.1 Introduction

Ultrasound is a noninvasive technology and has been employed for the bedside assessment of the lung reliably. As a versatile imaging technique, ultrasound provides insights into the presence of lung consolidation, pleural effusion, or interstitial-alveolar syndrome, especially, it allows the possibility of gaining regional

information. In recent years, ultrasound has played a crucial role in bedside assessment of the critically ill among imaging techniques. In 1942, a neuroscientist Karl Dussik first introduced the use of an ultrasound machine as a medical diagnostic tool [6] and André Dénier first described the diagnostic application of ultrasound [7]. More importantly, in 1989, the Fraçois Jardins intensive care team introduced the application of lung ultrasound in emergency care. Since 1991, point-of-care ultrasound (POCUS) has been used by intensive care physicians for the diagnosis of intensive care medicine. In recent years, the International Consensus Conference on lung ultrasound has standardized nomenclature, technique, and indications to use lung ultrasound in critical care practice [8]. Ultrasound evaluation of diaphragm function and structure is accurate, safe, and noninvasive. Bedside ultrasound was used to evaluate the diaphragm function by measuring the diaphragm activity, diaphragm thickness, and the change rate of diaphragm thickness. It was used to identify the diaphragm dysfunction and the loss of diaphragm function.

3.2.2 Lung Ultrasound

3.2.2.1 Selection of Lung Ultrasound Probe

Conventional examination modes are divided into B-mode and M-mode. B-mode ultrasound is a mode in which a linear or convex probe scans an anatomical plane and then converts it into a two-dimensional image. M-mode ultrasound is a mode to record the reciprocating motion of a structure toward or away from the probe. Different probes have their own characteristics. Generally, high-frequency probes have weak penetration capacity, but high resolution. On the contrary, low-frequency probes have strong penetration capacity, but low resolution. Firstly, according to the patient's body shape and chest wall thickness, low-frequency probes (convex array or phased probe, frequency 1–5 MHz) which can detect a certain depth are usually selected; secondly, high-resolution high-frequency probes (linear array probe, frequency 5–10 MHz) can be selected for pleural lesions or pneumothorax according to the location of the lesions. For obese patients, low-frequency probe is recommended to detect pleural lesions.

3.2.2.2 Operational Skills

Ultrasound examination of the lung does not require a high level of ultrasound section, which can be scanned vertically or parallel to the coastal space. Generally, each side of the chest wall is divided into three parts [9, 10] by the front axillary line and the rear axillary line. Each part is further divided into upper and lower parts, that is, each side of the chest is divided into six areas, a total of 12 bilateral areas, corresponding to different parts of the lungs. Lung ultrasound should be performed by left-right contrast, and all intercostal spaces in each region should be examined in sequence. The probe should be perpendicular to the thorax and slide along the

longitudinal and transverse direction. When the probe is placed in a sagittal position and the angle is adjusted perpendicular to the long axis of the rib space, the marker points generally point to the head side and slip from the head to the foot in the vertical rib space. Most of the pleura can be observed, but the ribs will cover it. Transversely, the probe is placed horizontally along the long axis of the intercostal space, with the marker point facing the sternum and sliding along the long axis of the intercostal space. The whole pleura of the intercostal space can be observed, but it is limited to the pleura of the intercostal space.

3.2.2.3 Image Interpretation

Understanding lung ultrasound images requires familiarity with basic lung ultrasound signs. Because ultrasound cannot penetrate the air, the lungs are the main air-containing organs, combined with the obstructive effect of thoracic bone structure, so the lung has been regarded as the forbidden area of ultrasound examination. However, the lung is an organ of liquid and gas blending. Any lung lesion is accompanied by the change of liquid–gas ratio, and the detection of liquid by ultrasound is sensitive, the change of gas and liquid in the alveoli and interstitium of damaged lungs will produce some ultrasound images and artifacts, which make it possible for lung ultrasound. With the decrease of the ratio of gas to liquid in the lung, the lung lesions, or changes from normal gasified lung tissue to mild interstitial edema, severe interstitial edema and alveolar edema, or from focal to diffuse, eventually develop into consolidation, and even pleural effusion and pneumothorax.

3.2.2.4 Bat Sign

Bat sign is one of the most important signs in lung ultrasound. When the probe is placed vertically in the intercostal space, the bat sign can be seen (Fig. 3.8). The images depict upper and lower adjacent ribs, rib echo ultrasound, and pleural lines, which correspond to the lung surface.

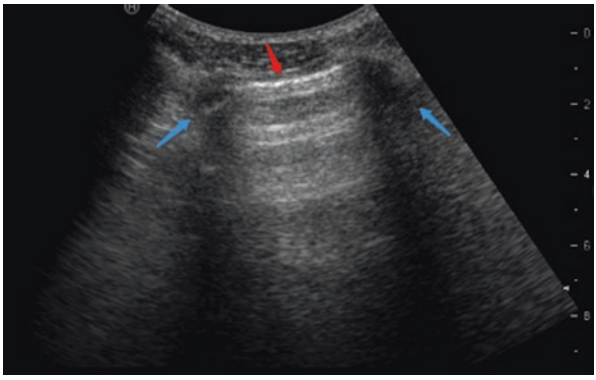

Fig. 3.8 Lung ultrasound sign. Red arrow shows hyperechoic pleura line with adjacent ribs on both sides (blue arrow)

3.2.2.5 Lung Glide Sign

The pleural line moves synchronously with respiratory motion and appears in normal lung tissue. The extent of lung glide reached its maximum in the lower part of the lung, when the lung was descending toward the abdomen. Under B-mode ultrasound, visceral and parietal pleura slipped relatively. and under M-mode ultrasound, hyperechoic pleura line moved to and fro with respiratory motion. Lung glide sign is not obvious in the condition of lung hyperinflation and emphysema. The disappearance of lung glide sign can be seen in pneumonia, atelectasis, pneumothorax, weak breathing, apnea, pleural adhesion, airway obstruction, or one-lung ventilation.

3.2.2.6 A-Line

The high echo artifacts parallel to the pleural line under B-mode ultrasound are called line A (Fig. 3.9). Normal subpleural air-filled lung tissue or intrapleural air because of pneumothorax prevents ultrasonic penetration. The strong reflex of chest wall soft tissue and air-filled lung surface forms line A, which is several times deeper than the distance between skin and pleural line. When subpleural gas is evenly distributed, line A can appear, such as normal lung tissue and pneumothorax. When subpleural gas is unevenly distributed, line A will blur or disappear, such as pulmonary interstitial lesions and alveolar lesions.

3.2.2.7 B-Line

The hyperechoic vertical line from the pleural line to the distal end is line B (Fig. 3.10). Because of the increase of fluid volume in lung tissue, ultrasound produces strong reverberation at the interface between air and water. Normally, the thickness of subpleural interlobular septum is about 0.10–0.15 mm, mostly less than

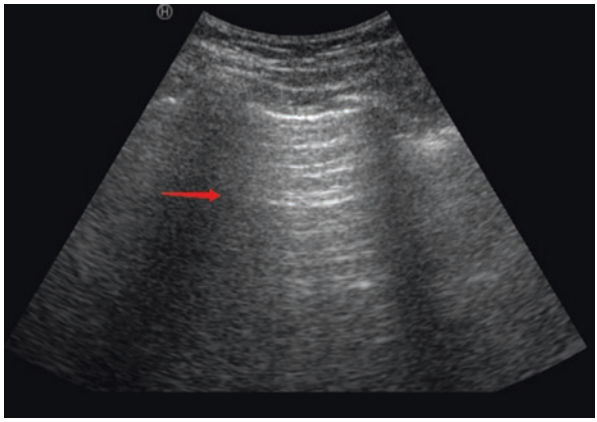

Fig. 3.9 Lung ultrasound sign. The arrow shows a hyperechoic A-line parallel to the pleura line

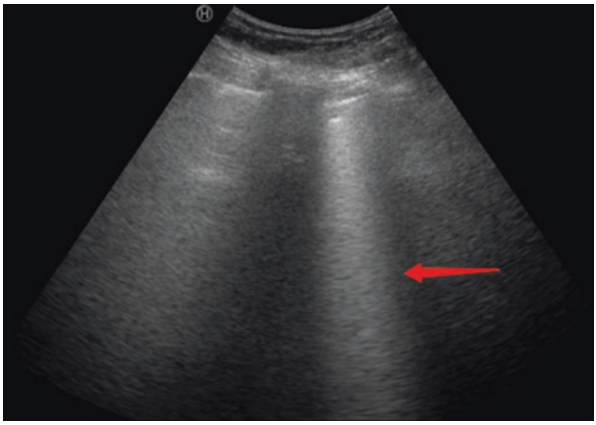

Fig. 3.10 Lung ultrasound sign. The arrow shows that the hyperechoic vertical line from the pleura line to the far end is line B

the resolution of ultrasound (about 1 mm). Therefore, under normal circumstances, most of them are surrounded by strong echoes of alveolar gases and cannot be displayed. There should be less than two B-lines in each intercostal space.

3.2.2.8 Signs of Interstitial Syndrome

Alveolar interstitial syndrome is defined as the presence of three or more adjacent B-lines in a coastal space, which may be limited or diffuse. Linear and convex probes can measure the average distance between B-lines. B-line interval is about 7 mm, suggesting interlobular septal thickening, interstitial pulmonary edema, or lesion; Multiple B-lines with spacing less than 3 mm indicate alveolar pulmonary edema or lesion. The more severe pulmonary edema presents as diffuse B-line. Line B has seven characteristics: comet tail sign; from a pleural line; high echo; laser sample; no attenuation, direct to the edge of the screen; erase line A; and move with the lung sliding.

3.2.2.9 Tissue-Like Sign

Pulmonary tissue has no echo or liver tissue-like echo, and there are irregular boundaries with different depths (Fig. 3.11). The occurrence of lung consolidation suggests that the density of lung tissue changes in this area. Similar to line B, there may be an increase in extravascular lung water or a significant decrease in lung ventilation in this area.

3.2.2.10 Debris Sign

Short-line, debris-like, strong echo spots appear at the junction of consolidated and air-filled alveoli, which are called debris signs (Fig. 3.11). Ultrasound images of lung consolidation are varied at different stages, if the gas in the consolidated lung

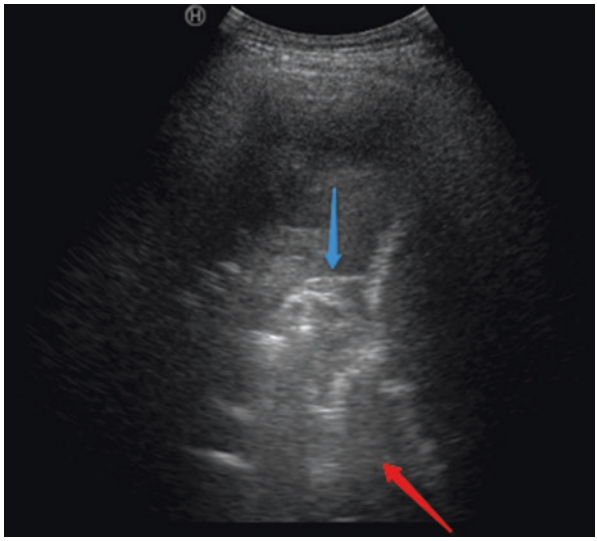

Fig. 3.11 Lung ultrasound sign. The lung consolidation (red arrow) is shown in the figure, and the alveoli are filled with liquid, showing tissue like change; the air-filled bronchi (blue arrow) can be seen, with heterogeneous light/dark echo, and debris like shape

tissue is not fully absorbed, ultrasound shows high echo when it meets gas. In particular, inflammatory lung consolidation occurs in the stage of severe insufficient ventilation and incomplete absorption of air in the lung tissue, ultrasound images can show inhomogeneous bright/dark echoes, similar to debris, so it is called debris sign.

3.2.2.11 Bronchial Inflation Sign

Bronchial inflation sign is a heterogeneous, tissue-like (similar to liver echoes) ultrasound image with a punctate or linear hyperechoic sign. It is also an ultrasound sign in the process of pulmonary consolidation. The reason for this is that the air in the bronchus, which is inside consolidated lung tissue, is not fully absorbed; ultrasound produces a bright echo when it meets gas (Fig. 3.11). According to the dynamic changes of bronchial gas with respiratory motion, there are static bronchial inflation signs and dynamic bronchial inflation signs. Dynamic bronchial inflation sign can rule out the diagnosis of obstructive atelectasis. A small sample study found that dynamic bronchial inflation sign was more common in inflammatory lung consolidation and static bronchial sign was more common in atelectasis. For some inflammatory lung consolidation, bronchial fluid filling signs can also be seen.

3.2.2.12 Pulmonary Pulsation

Pulmonary pulsation is an early and dynamic diagnostic sign of complete atelectasis. Under normal conditions, the slippage of two pleura layers hinders the vibration of pleural line caused by cardiac activity observed by M-mode ultrasound. When the

main bronchial obstruction or one-lung ventilation leads to complete atelectasis, visceral and parietal pleura slide disappears. Under these conditions, pleural line vibration caused by heart beating can be recorded by M-mode ultrasound. The disappearance of lung glide sign under B-mode ultrasound and the pulsation of pleural line with the beating of heart under M-mode ultrasound is called pulmonary pulsation.

3.2.2.13 Stratospheric Sign (Bar Code Sign)

In M-mode imaging, the normal appearance of the lungs is similar to that of the beach. The extrapleural structure presents as a horizontal line parallel to the probe surface, similar to the sea. The lung parenchyma moves with the respiratory cycle and presents a grainy image, similar to the sand on the coast (Fig. 3.12a). In pneumothorax, the pleura is separated from the parietal layer and the visceral layer due to the air contained in the pleural cavity. In M-mode imaging, the absence of parenchymal movement beneath the pleura will produce multiple horizontal parallel lines, replacing the sandy appearance of the coastal marker. This kind of image is similar to bar code or stratosphere, so it is called stratosphere (bar code) sign (Fig. 3.12b).

3.2.2.14 Pulmonary Point

The pulmonary point is a special ultrasound sign in the diagnosis of pneumothorax. In the same image, one side of the lung tissue has the phenomenon of lung sliding and pulsation, while the other side does not exist. This critical point is called a

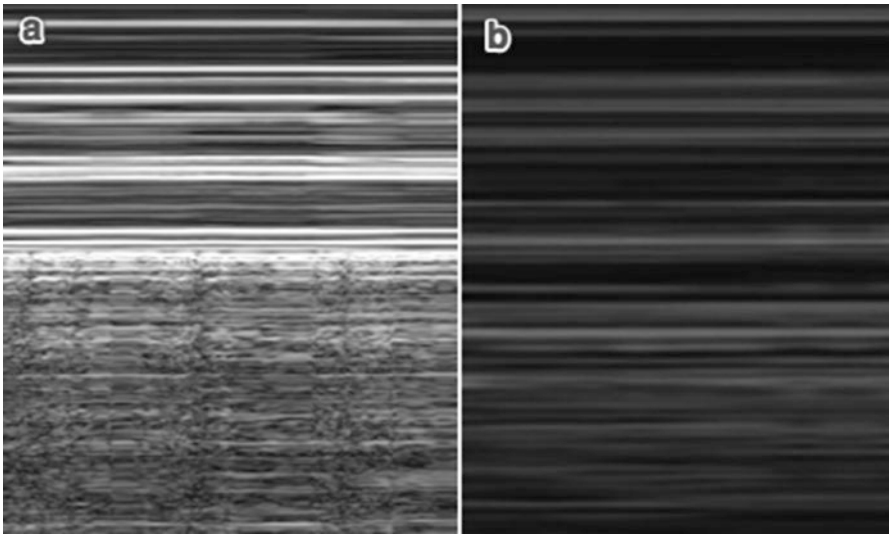

Fig. 3.12 Lung ultrasound sign. Panel (**a**) is beach sign in normal lung; (**b**) is Stratospheric sign in pneumothorax

pulmonary point. This phenomenon is a specific manifestation of pneumothorax. Under B-mode ultrasound, B-line disappeared, A-line and lung glide disappeared, while under M-mode ultrasound, the critical point of ultrasound sign replacing coastal sign was lung point. The principle is that when pneumothorax occurs, ultrasound detects the boundary of lung tissue compressed by gas. Ultrasound detects the side of pneumothorax, showing that lung glide disappears, and the side of normal lung tissue, showing that lung glide exists. But not all pneumothorax has pulmonary point, when the scope of pneumothorax is large or the examination is incomplete, it may not be able to find the pulmonary point, and pulmonary bullae can also be shown as pulmonary point.

3.2.2.15 Quadrilateral Sign/Sinusoidal Sign

Under B-mode, the quadrilateral anechoic zone in the thoracic cavity was found, with four boundary areas being the upper and lower ribs in the intercostal space where the probe was located, and the visceral and parietal pleura. The anechoic zone was pleural effusion (Fig. 3.13). Under M-mode ultrasound, sinusoidal curves can be seen, indicating the regular displacement between the visceral pleura moving with pulmonary expansion and contraction and the relatively fixed pleura line. This phenomenon often occurs at the costophrenic angles of the base of the lung.

3.2.2.16 Curtain Sign

During examination at the base of lung, images of the diaphragm, liver/spleen, or spine disappear as the lung expands during inspiration and appear as the lung volume decreases during expiration. This phenomenon occurs under normal ventilation; when there is pleural effusion or consolidation of pulmonary tissue, the phenomenon weakens or disappears.

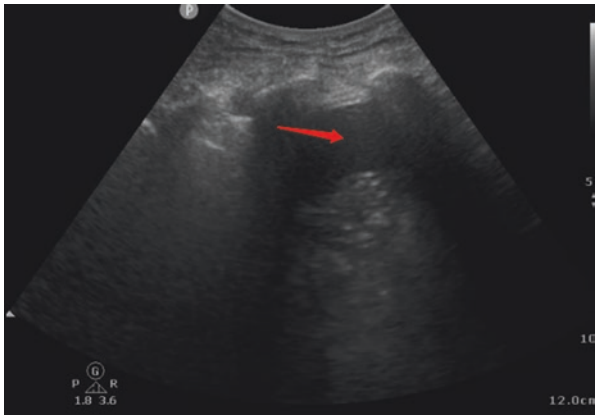

Fig. 3.13 Lung ultrasound sign. The non echo area of the quadrangle shown by the arrow is surrounded by the pleura line of the parietal layer, the upper and lower ribs, and the pleura line of the visceral layer

3.2.3 Application of Lung Ultrasound

Ultrasound is a fast, noninvasive, and real-time imaging method. Lung ultrasound has been gradually improved and standardized. It plays an important role in the diagnosis, treatment, and judgment of disease changes.

3.2.4 Diagnostic Value of Pulmonary Ultrasound in Respiratory Diseases

Several guidelines suggest that procedure guidance and diagnostic assessment by ultrasound can provide bedside information quickly [8, 11–13].

POCUS for diagnostic assessment is of extensive use in intensive care units [14]. POCUS in the emergency department alongside standard diagnostic tests is superior to standard diagnostic tests alone for establishing a correct diagnosis within 4 h [15].

3.2.4.1 Community-Acquired Pneumonia (CAP) and Ventilator-Associated Pneumonia (VAP)

According to the type of pneumonia, the imaging manifestations are different. Ultrasound signs of pneumonia are heterogeneous B-line; pleural abnormalities, mostly small pulmonary consolidation under pleura; debris sign; or bronchial inflation sign. Inflammatory consolidation manifests differently in different stages. Gas is not fully absorbed in the lung tissues of the lesions, which can be manifested as debris sign, accompanied by bronchial inflation sign, mostly dynamic bronchial inflation sign, or can be manifested as liver-like pulmonary tissue when the gas is fully absorbed. The application of lung ultrasound in screening or diagnosing of CAP or VAP has attracted much attention. 70–97% of CAP patients can see lung consolidation accompanied by bronchial inflation sign [16–18]. Consolidation has 93% sensitivity and 98% specificity in the diagnosis of CAP [17]. However, for ICU patients, pulmonary consolidation and bronchial inflation sign can also occur in patients without pneumonia, which is related to long-term bedridden, controlled ventilation, and systemic inflammatory response. It seems that pulmonary ultrasound has limited value in the diagnosis of VAP. However, some scholars regard linear or tree-like dynamic bronchial images as one of the signs of VAP diagnosis, and can easily calculate the clinical ultrasound score at the bedside for early VAP diagnosis. It may even be better than the traditional clinical pulmonary infection score (CPIS) [19].

3.2.4.2 Pulmonary Edema

B-line is the most important ultrasound sign of pulmonary edema. It may be related to alveolar or interstitial exudation. According to the distribution and shape of B-line, it can be divided into homogeneous B-line, heterogeneous B-line, and

converged B-line. The B-line distribution of pulmonary edema due to elevated hydrostatic pressure was more homogeneous, and there was no change of pleural line, and pleural sliding was not affected [20]. The distribution of B-line in osmotic pulmonary edema shows that the non-dependent area is lighter, the dependent area is heavier, and even the signs of pulmonary consolidation appear. In addition, because of the high viscosity of the exudated fluid, the pleural sliding sign usually weakens or even disappears. Pulmonary edema due to elevated hydrostatic pressure is usually secondary to cardiac insufficiency and volume overload. Cardiac echocardiography can show a significant decrease in systolic function and an increase in the diameter of inferior vena cava. Osmotic pulmonary edema is usually secondary to severe infections and other factors, with normal cardiac function or enhanced systolic function without volume overload.

3.2.4.3 ARDS

The pulmonary lesions of ARDS are heterogeneous. Qualitative imaging evaluation of pulmonary exudative lesions and consolidation by lung ultrasound can assist the diagnosis of ARDS [21–23]. The international consensus on lung ultrasound also suggests the diagnosis of ARDS if there are the following signs: (1) inhomogeneous B-line; (2) abnormal pleural line signs; (3) subpleural consolidation of anterior chest wall; (4) normal pulmonary parenchyma; and (5) weakening or disappearing of pulmonary glide sign [8]. The Berlin definition of ARDS [24] suggests a rapid differential diagnosis of pulmonary edema for suspected ARDS patients without risk factors by echocardiography. Therefore, combined cardiopulmonary ultrasound is helpful for real-time diagnosis of ARDS at bedsides, and can differentiate pulmonary edema, atelectasis, pleural effusion, chronic heart failure, pulmonary interstitial fibrosis, and other pulmonary conditions leading to hypoxemia.

3.2.4.4 Atelectasis

Atelectasis can be divided into compressive atelectasis and absorptive atelectasis. The former is usually caused by a large amount of pleural effusion, with sharp and smooth edges, moderate echo, and jellyfish-like shape with the beating of heart and movement of breath, the compressive atelectasis can be reduced or even disappeared after puncture and drainage. The latter is caused by airway obstruction, such as secretions or tumors. Lung ultrasound shows alveolar consolidation and homogeneous hypoechoic structures resembling liver-like structures. Compared with pneumonia, absorbable atelectasis has no dynamic bronchial inflation sign. Bronchial inflation sign is static (initial stage) or nonexistent (total air is reabsorbed in small airways). If bronchial inflation sign is dynamic, obstructive atelectasis can be excluded [25]. Sometimes bronchial fluids can be found, which suggests that secretions or fluids fill the airway.

3.2.4.5 Pleural Effusion

Ultrasound can directly identify pleural effusion and consolidation [26].

Compared with bedside chest radiographs, ultrasound for detecting pleural effusion showed higher accuracy (93% vs. 47%) [8]. Pleural effusion manifests as an echo-free area in dependent region [27, 28].

The appearance of pleural effusion under ultrasound can indicate the nature of the fluid. Pleural effusion can be characterized by anechoic, complex non-encapsulated, complex encapsulated, or homogeneous echo [29]. Generally, complex pleural effusion suggests exudation, whereas anechoic effusion may be transudate. However, transudate can also be manifested as complex non-encapsulated effusion [29]. This is because the transudate is not only water, but also has different components (such as cells, proteins, and fats). Transudate can also behave as an echo-free liquid. Homogeneous echo effusion is a manifestation of hemorrhage or empyema. In some cases, ultrasound images can help to judge the nature of the effusion. For example, thickened pleural or pulmonary consolidation with bronchial inflation sign (suggesting the site of infection) usually indicates exudate. Diffuse pulmonary congestion (B-line) indicates transudate because of heart failure. In supine position, in transverse scanning, the pleural space at the bottom of the lung is 5 cm or larger, which can predict 500 mL or more pleural effusion. The linear relationship between them was also determined. The pleural space per centimeter corresponded to 200 mL effusion [30, 31]. The application of ultrasound in chest puncture can reduce the number of pneumothorax cases and improve operation efficiency, even for more experienced operators [32].

3.2.4.6 Pneumothorax

The sensitivity, accuracy, and negative predictive value of lung ultrasound in the diagnosis of pneumothorax are much higher than those of chest X-ray and are close to those of CT [24], especially for traumatic patients [33, 34]. When diagnosing pneumothorax by lung ultrasound, we need to recognize the pleural sliding sign, pulmonary pulsation sign, B-line, consolidation, and pulmonary point. Pneumothorax can be diagnosed when the pleural slip sign disappears, the stratospheric sign and the pulmonary point are found by pulmonary ultrasound. If the pulmonary point appears below the midaxillary line, it indicates that at least 30% of the pulmonary parenchyma collapses [35].

Although the specificity with the signs described above for diagnosis of pneumothorax is almost 100%, in most cases, it is difficult to determine the pulmonary point because of the different degrees of pulmonary compression and sometimes focal pneumothorax in severe patients. Therefore, when pneumothorax is suspected in clinical practice, one by one lung tissue should be examined, if pleural sliding sign, pulmonary pulsation sign, B-line, consolidation, and pleural effusion can be found, the presence of pneumothorax in the examination site can be excluded.

3.2.4.7 Pulmonary Embolism

Studies have shown that combined cardiopulmonary and vascular ultrasonography can diagnose pulmonary embolism more accurately [13, 36]. Other studies have shown that the specificity and sensitivity of combined cardiac, pulmonary, and vascular ultrasound in the diagnosis of pulmonary embolism are significantly higher than that of single cardiac, pulmonary, or vascular ultrasound, which can significantly improve the diagnosis of suspected pulmonary embolism and reduce the examination rate of CT pulmonary angiography [37, 38]. Because pulmonary embolism mainly affects the oxygenation of patients by affecting the ratio of ventilation to blood flow, there is usually no obvious lung lesion in patients. Ultrasound signs of pulmonary embolism are mainly line A, sometimes wedge consolidation caused by pulmonary infarction, but rarely accompanied by line B or large areas of pulmonary consolidation. In addition, the presence of deep venous thrombosis in lower extremities can be determined by ultrasound screening of lower extremity vessels thus providing indirect evidence for the diagnosis of pulmonary embolism.

3.2.5 Differential Value of Pulmonary Ultrasound in Etiology of Respiratory Diseases

The bedside lung ultrasound in emergency (BLUE) protocol provides a simple method to analyze and diagnose diseases, using the characteristics of lung ultrasound. This diagnostic scheme can diagnose five common causes of respiratory failure in 90.5% of cases of acute respiratory failure [39]. Traditional medical examination methods include medical history and physical examination. The combination of electrocardiogram and echocardiography with BLUE improves the diagnostic accuracy. The first objective of the BLUE program is to quickly diagnose and treat dyspnea symptoms. The second goal is to reduce the use of computed tomography and X-ray avoiding radiation hazards to special patients such as pregnant women [40, 41]. At the same time, the program allows accurate diagnosis of acute respiratory distress in resource-poor clinics.

The BLUE protocol standardized the examination sites of the chest, including the upper blue spot, the lower blue spot, the posterior alveolar, and/or pleural syndrome (PLAPS) points on the left and right sides.

First, looking for lung glide sign. If the lung glide sign exists and there is a clear line A, it is called A-profile. Next venous system examination needs to be done. The specificity of diagnosing pulmonary embolism with lower extremity venous thrombosis was 99%. So before other lung areas are examined, veins need to be analyzed. Posterolateral alveolar pleural syndrome (PLAPS) includes posterior chest wall lung consolidations and pleural effusions. PLAPS can be seen for many reasons, and veins need to be prioritized before PLAPS can be found. It has important clinical significance to find lower extremity venous thrombosis after finding A-profile. If no lower extremity venous thrombosis is found, then look for PLAPS at the PLAPS

examination area. If PLAPS exists, it is called A-no-V-PLAPS image, suggesting pneumonia. Without PLAPS, it is called nude profile (bare image features) (all items are normal), suggesting COPD or asthma. The A′ profile is defined by the presence of A-lines without lung sliding. This profile is seen in pneumothorax. A′ profile requires finding the pulmonary point. If there is a pulmonary point, it strongly suggests pneumothorax. The diagnosis of hemodynamic pulmonary edema is preferred when B features are found. B′ profile (anterior lung B-line without lung sliding), A/B profile (A-line in one hemithorax and the B-line in another hemithorax), and C profile (consolidation of the anterior chest wall) strongly suggest pneumonia. 86% of ARDS patients had one of four pneumonia images.

3.2.6 Monitoring and Guiding Therapeutic Value of Pulmonary Ultrasound

3.2.6.1 Ventilation Score

Since the number and type of ultrasound artifacts (A-line and B-line) seen in the intercostal space of lung ultrasound vary with the loss of pulmonary ventilation function [42], lung collapse or re-expansion can be assessed by tracking the changes in lung ultrasound. In vitro [43] studies have shown that progressive homogeneous ventilation loss determines the transition from A-line to B-line, and the number of B-line gradually increases and fuses. Tissue-like features are present when ventilation is completely lost. Lung ultrasound score (LUS) [44] is a useful tool to quantify the degree of pulmonary ventilation reduction and to compare the degree of improvement of pulmonary ventilation before and after treatment. It realizes the transformation from ultrasound image vectorization to numerical value. According to the axillary front line and the axillary posterior line, the chest wall of the patients was divided into three zones: anterior, lateral, and posterior. The three zones were divided into upper and lower zones, respectively. Thus, one side of the chest wall of the patients was divided into six zones and twelve zones on both sides. Lung ultrasound was performed in each area and scored according to the following criteria: normal pulmonary ventilation (0 points): the presence of lung sliding and horizontal A-lines or no more than two B-lines; moderate pulmonary ventilation reduction (1 point): the presence of multiple uniformly or unevenly segregated B-lines; severe pulmonary ventilation reduction (2 points): multiple rib spaces with combined B-lines; and pulmonary consolidation (3 points): The lungs show tissue-like echoes accompanied by dynamic or static bronchial inflation signs. According to the above criteria, the total score of 12 regions ranges from 0 to 36. Dynamic assessment of LUS can accurately reflect the changes of pulmonary ventilation before and after the implementation of any treatment measures that may affect pulmonary ventilation function thus guiding the next decision-making. Several studies have shown that the clinical value of pulmonary ultrasound in assessing the degree of pulmonary inflation is in good agreement with chest CT. In patients with ARDS, regional

pulmonary ultrasound scores were closely related to tissue density assessed by computed tomography, and the gradual increase in scores from 0 to 3 was significantly related to the increase in density [45].

3.2.6.2 Monitoring the Effectiveness of Antimicrobial Therapy

Lung ultrasound can also be used to evaluate the efficacy of pulmonary infection and can assist in adjusting and stopping antibiotic therapy. The LUS can be calculated by observing regional changes before and after treatment aimed at improving pulmonary ventilation. It has been successfully applied to evaluate antibiotic-induced alveolar reaeration in VAP [46].

3.2.6.3 Monitoring the Extravascular Lung Water (EVLW)

The ultrasound manifestations of EVLW has increased B-line. For acute alveolar or interstitial exudation, increased diffuse B-line can be observed by lung ultrasound. At present, lung ultrasound score can be used for clinical monitoring of EVLW. Baldi et al. [47] evaluated EVLW with B-line score, B-line score correlated well with quantitative CT. The overall LUS was directly correlated with EVLW assessed by pulmonary thermodilution [48], and with the overall lung tissue density assessed by quantitative CT [45]. Increased LUS is an early warning of harmful side effects of fluid resuscitation in sepsis patients, transthoracic lung ultrasound may serve as a safeguard against excessive fluid loading [49]. The LUS is independently related to the 28-day mortality, as well as the APACHE II score and lactate level, in intensive care unit shock patients. A higher elevated LUS on admission is associated with a worse outcome [50].

3.2.6.4 Monitoring Lung Recruitment

Lung reaeration after lung recruitment maneuvers can be monitored by direct and real-time visualization [51]. Bouhemad et al. [52] used LUS to measure the reaeration of PEEP 0–15 cm H_2O in 40 patients with ARDS undergoing mechanical ventilation. The level of pulmonary alveoli (or collapse) was found to be positively correlated with the pressure-volume curve (*P–V* curve). Therefore, ultrasound can assess the potential of lung recruitment, and dynamically monitor and guide the parameter setting of mechanical ventilation. Lung recruitment combined with appropriate PEEP may improve oxygenation and some physiological indexes in ARDS patients, but not in all ARDS patients. The setting of PEEP according to the recruitability of lung can more effectively reopen the collapsed alveoli and reduce the side effects caused by PEEP. Lung ultrasound can synthetically judge the recruitability from the homogeneity, severity, airway patency (dynamic bronchial gas phase), and the presence or absence of tidal recruitment in the examination area. In

the course of recruitment, the response of the lung to different recruitment maneuvers and recruitment time can be assessed by qualitative or semi-quantitative ultrasound scores, and the causes of non-recruitment can be comprehensively analyzed and better treatment strategies can be found [53]. It can also detect the possible barotrauma caused by lung recruitment in time and adjust the treatment in time. It should be noted that pulmonary ultrasound could not detect lung hyperinflation.

3.2.6.5 Prone Position

Ultrasound is helpful in evaluating and managing prone position therapy. Pulmonary tissue in gravity-dependent area of ARDS patients in supine position is not easy to reopen due to the influence of gravity, abdominal pressure, and chest motion amplitude. It has been proved that prone position can improve the degree of pulmonary tissue expansion in gravity-dependent areas either alone or in combination with recruitment maneuver thus improve oxygenation and reduce mortality [54].

In the prone position of ARDS patients, ultrasound can assess the lesions or homogeneity of the lungs, and evaluate the lung recruitment in gravity-dependent areas (PLAPS point and posterior blue point in supine position). The degree of dorsal lung recruitment assessed by lung ultrasound after 3 h in prone position was correlated with clinical positive reaction [55]. Therefore, the effectiveness of prone position can be predicted by semi-quantitative ultrasound score, which also can help to determine the time and frequency of prone position.

3.2.6.6 Weaning

When mechanical ventilation is disconnected, it will cause significant changes in pulmonary ventilation volume. Ultrasound changes of pulmonary ventilation can predict the success or failure of extubation in patients who successfully passed the 1 h spontaneous breathing test (SBT). There was no significant change in overall pulmonary ventilation during the spontaneous breathing test in patients who succeeded in extubation. However, in patients with post-extubation distress, pulmonary ventilation decreased during the SBT [56].

3.2.7 Diaphragm Ultrasound

The diaphragm is an important respiratory muscle. In spontaneous breathing, diaphragm plays an important role in generating tidal volume [57]. Many factors in ICU such as phrenic nerve injury after abdominal or cardiac surgery, neuromuscular disease, mechanical ventilation, sepsis can lead to diaphragm dysfunction, and thus increase the risk of weaning failure and prolong the time of mechanical ventilation [58]. There are some methods of examining diaphragm function, including

electromyography, transdiaphragmatic pressure, X-ray, magnetic resonance imaging, and so on. Most of them are invasive or radioactive examination. Bedside, ultrasound has the advantages of noninvasive, real-time, and highly repeatable. It can not only observe the shape of diaphragm, but also evaluate the function of diaphragm. It has been widely used in clinical diagnosis and treatment of critical care patients.

3.2.8 Measurement

There was no significant difference in the thickness and the change of thickness between the left and right diaphragms. Compared with the left diaphragms, ultrasound could measure the mobility of the right diaphragms more intuitively, and the repeatability of the measurement of the right diaphragms was higher than the left one [59]. Therefore, the liver is often used as an acoustic window to measure the thickness and movement of the right hemidiaphragm. However, when it is suspected that the patient has unilateral diaphragm injury, it is necessary to evaluate the bilateral diaphragm function. For example, in patients undergoing heart surgery, the phrenic nerve injury may cause complete paralysis in half of the diaphragm, while the other part of the diaphragm is not affected, which usually does not cause dysfunction of the whole diaphragm. Therefore, it is necessary to evaluate the function of the two diaphragms separately [60].

3.2.9 Diaphragm Thickness and Change Rate of Diaphragm Thickness

Diaphragmatic thickness refers to the distance between the pleura and peritoneum of the diaphragms at the thoracic involution. When inhaled, the diaphragm contracted and its thickness increased. The change rate of diaphragmatic thickness refers to the change degree of diaphragmatic thickness during respiration, which reflects the contractility of diaphragm [61]. Change rate of diaphragmatic thickness = (maximum end inspiratory diaphragmatic thickness—end expiratory diaphragmatic thickness)/end expiratory diaphragmatic thickness × 100% [62, 63]. In normal conditions, when the lung volume increases from functional residual volume to total lung capacity, the average thickness of diaphragm increases by 54% (range: 42% ~ 78%) [64, 65].

For B-mode ultrasound measurement, select a high-frequency ultrasound probe with a frequency of 7.5 MHz or more, and place it between the axillary front line and the axillary midline between the eighth and tenth intercostals, that is, the junction of the diaphragm and the chest wall. The direction of the probe is perpendicular to the chest wall. Two parallel hyperechoic layers can be seen at a distance of 1.5–3 cm from the skin. The hyperechoic layer near the skin is the pleura layer and

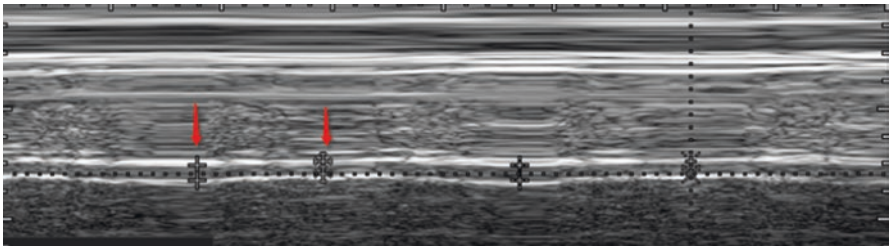

Fig. 3.14 Diaphragmatic thickness measurements. Diaphragmatic ultrasound can measure the thickness at end of inspiratory (left arrow) and at end of expiratory (right arrow), and calculate the change rate of diaphragmatic thickness

the peritoneal layer at a distance. The area with low echo between the two is the diaphragm [66]. The thickness of diaphragm is the distance between pleura and peritoneum. Using ink to mark the skin to locate the diaphragm can improve the repeatability of measurements. The position of M-mode ultrasound measurement is the same as B-mode. The measurement line was selected after the diaphragm was located by a two-dimensional ultrasound. M-mode ultrasound showed that the thickness of diaphragm changed with the change of respiratory cycle along the measurement line (Fig. 3.14). The measurement of diaphragmatic thickness in more than two respiratory cycles with M-mode ultrasound can improve the repeatability of measurement. The accuracy and repeatability of measurement of diaphragmatic thickness and thickness fraction by ultrasonography have been confirmed [61, 64, 67, 68].

3.2.10 Diaphragm Excursion

Diaphragm excursion refers to the displacement between the inspiratory and expiratory ends of the diaphragm. During the measurement, 3–5 MHz probe is selected, and the patient takes a half-lying position (the head of the bed is raised by 30°–45°). The excursion of different parts of the diaphragm is not exactly the same during the breathing process. The excursion of the middle and rear parts is greater than that of the front part. The measurement of the excursion of the diaphragm is mainly to measure the rear part [69]. Since the amplitude of each breath is different in patients with spontaneous breath, it is necessary to avoid recording very deep or very shallow breath as the evaluation result. It is necessary to measure five respiratory cycles and take their average value as the evaluation result [70].

M-mode ultrasound can continuously record the time-position relationship of the diaphragm on the sampling line and quantify the movement amplitude of the diaphragm. The ultrasound probe was placed at the lower edge of the lower rib between the axillary front line and the clavicular midline to make the ultrasound beam perpendicular to the posterior part of the diaphragm. M-mode ultrasound could show

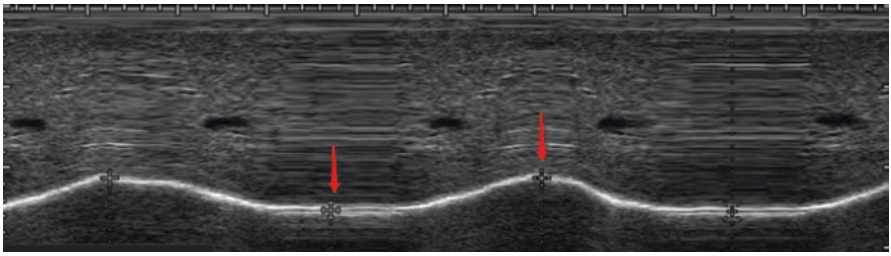

Fig. 3.15 Diaphragmatic excursion measurements. Arrows indicate the beginning (left arrow) and the end of the diaphragmatic contraction (right arrow). The distance between the arrows indicate an excursion (displacement)

the excursion of the diaphragm along the sampling line with the breath. When inhaled, the diaphragm moves down close to the probe, and the M-mode ultrasonic track is upward; when exhaled, the diaphragm moves up far away from the probe, and the M-mode ultrasonic track is downward. Phrenic excursion is the vertical distance from baseline to the highest point of the curve (Fig. 3.15). Research shows that the phrenic mobility of healthy volunteers is about 1.0 cm for men and 0.9 cm for women [59, 71].

3.2.11 Contraction Velocity of Diaphragm

M-ultrasound can show the contraction velocity, inspiratory time, and respiratory cycle time of diaphragm (diaphragm contraction velocity = diaphragm mobility/inspiratory time). Diaphragm contraction velocity was related to the muscle strength of diaphragm. Diaphragm contraction velocity was (1.3 ± 0.4) cm/s when the healthy people were breathing peacefully [71].

3.2.12 Application

3.2.12.1 Weaning

The matching of respiratory demand and respiratory muscle strength is the key to the success of weaning. Therefore, diaphragm function is closely related to the success of weaning. Diaphragmatic thickness is helpful to predict the success of weaning, diaphragmatic mobility, and shallow fast breathing index have similar value in predicting the results of weaning [72–74]. Dinino et al. [73] reported that the sensitivity and specificity for predicting the success of weaning were 88% and 71%, respectively, when change rate of diaphragmatic thickness was more than 30%. The results of Ferrari et al. [74] showed that the sensitivity and specificity of the change

rate of diaphragmatic thickness >36% were 82% and 88%, respectively. More studies have reported that the sensitivity and specificity of predicting the results of weaning are better than those of shallow fast respiratory index and maximum inspiratory pressure when the average diaphragm mobility is 1.1 cm. Farghaly et al. [75] found that the diaphragmatic mobility was 16 mm in the successful group and 9.8 mm in the failure group ($P < 0.0001$). The sensitivity and specificity of the successful withdrawal were 87.5% and 71.2%, respectively. At present, most of the studies on diaphragm mobility and change rate of diaphragmatic thickness are observational studies, and a few are case-control studies. Up to now, there is no further randomized controlled trial to determine the time of withdrawal according to diaphragm mobility and change rate of diaphragmatic thickness. Whether it can reduce the failure rate of extubation still needs to be confirmed by further studies [76].

3.2.13 Differentiation Between Phrenic Atrophy and Phrenic Paralysis

The main manifestations of phrenic atrophy on M-mode ultrasound are the decrease of diaphragm thickness and motion amplitude [77]. The main manifestation of phrenic paralysis is the contradictory movement of the diaphragm, which can occur in one or both sides of the diaphragm. On M-mode ultrasound, it shows the movement track opposite to the normal diaphragm [78]. Ultrasound can directly observe the thickness, thickening and movement track of bilateral diaphragm to determine whether the diaphragm function is abnormal and the type, so as to provide more useful and reliable information for clinical judgment of the causes of respiratory insufficiency in patients [79, 80].

3.2.14 Monitoring Work of Diaphragm

The change rate of diaphragm thickness during mechanical ventilation can reflect the work of diaphragm. Umbrello et al. found that transdiaphragmatic pressure and esophageal pressure were only significantly related to the change rate of diaphragm thickness, but not to diaphragm mobility. Therefore, ultrasonic measurement of the change rate of diaphragm thickness in patients with mechanical ventilation can accurately reflect the work of diaphragm. Monitoring the work of diaphragm can guide the setting of ventilator parameters. Monitoring the thickness of diaphragm by ultrasound, titrating the support level of ventilator parameters, keeping the patient's inspiratory effort at a normal level, can prevent the change of diaphragm shape during mechanical ventilation. Therefore, monitoring the work of diaphragm by ultrasound can guide clinicians to adjust ventilator parameters.

3.2.15 Evaluation of Synchronization

Simultaneous monitoring of diaphragmatic mobility and airway pressure-time curve of patients under M-mode of ultrasound can evaluate synchronization. This method can help to find out whether there is ineffective trigger in patients, calculate the trigger delay time, and guide clinicians to adjust ventilator parameters and treatment plans. M-mode ultrasound provides a mirror image for the change of esophageal pressure waveform. When inhaled, the esophageal pressure drops, the waveform rises, when exhaled, the esophageal pressure rises, and the waveform declines. Ultrasound can provide the whole process of the beginning and end of inspiration in real-time thus avoiding invasive esophageal pressure monitoring [81]. Therefore, the real-time waveform of diaphragm M-mode ultrasound and mechanical ventilation airway pressure can find the time when the patient triggered the ventilator, and evaluate the synchronization, but further clinical research is needed.

3.3 Electrical Impedance Tomography

3.3.1 Overview

As a clinically available and noninvasive technique, electrical impedance tomography (EIT) has been widely used by clinicians. It can provide dynamic tidal images of gas distribution at the patient's bedside.

3.3.2 Principle of EIT Imaging

In short, the principle of EIT imaging is based on the difference in pulmonary tissue's electrical resistance at different phases of respiration. An increased volume of gas in lung tissue increases electrical resistance, while an increased volume of blood or fluid will decrease electrical resistance. While executing EIT, a belt with multiple electrodes is placed around the patient's chest wall. The number of electrodes varies from 8–32 according to various versions and brands of EIT. Each pair of electrodes emitting very small electrical currents alternately, and the rest electrodes read the voltage generated by the current flowing through the chest.

Until a cycle is accomplished, all data needs to build a raw EIT image is acquired, which is called the frame. The EIT ventilation image at this moment can then be displayed according to different imaging methods. Currently, the commonly used imaging technique is based on the change value of the immediate frame and baseline frame, and image frames are usually called relative images. Through these algorithms, a real-time continuous moving image is shown on the screen, enabling clinicians to evaluate patients' ventilation distribution at the bedside and can also obtain more information through off-line analysis software. The reliability of EIT has been

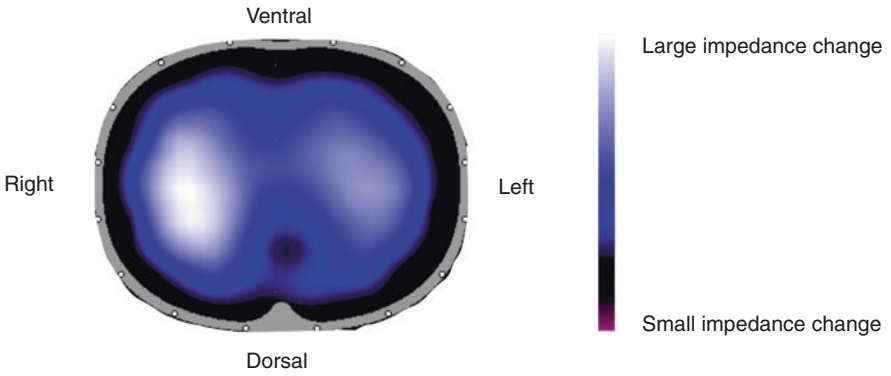

Fig. 3.16 The functional image by EIT. The color scale in the figure indicates different ventilation situation. Darker color shows less ventilated area (small impedance change), lighter colors are the opposite. EIT image is similar to a CT image, which means the anterior side is on the top of the image while the left and the right side is enantiomorphic

confirmed by various common methods, such as CT scan, positron emission tomography, single-photon-emission computed tomography, and pneumotachograph.

The image of EIT is similar to a CT image, which means the anterior side is on the top of the image while the left and the right side is enantiomorphic [82]. The imaging diagram of EIT is shown in Fig. 3.16.

3.3.3 Method of Application

3.3.3.1 How to Place the Belt

The electrode belt should tenderly be placed around the patients' chest. Although the location of the electrode plane impacts the examinations, there has no consensus on the standard electrode belt position for pulmonary EIT monitoring. In a general way, researchers place the belt at 4–5 intercostal space. We do not recommend to place the belt lower than the sixth intercostal space because the diaphragm may periodically enter the measurement plane [83]. The suitable position of the belt is shown in Fig. 3.17.

3.3.4 Data Directly Obtained on the EIT Instrument

3.3.4.1 Regions of Interest (ROI)

EIT is able to observe pulmonary ventilation in different regions. Regions of interest (ROI) mean different regions obtained by various partition methods. EIT can divide ROI vertically or quadrantally by identifying regions with gas ventilation automatically. Clinicians can also customize the ROI according to ventilation conditions and

Fig. 3.17 The suitable position of EIT belt. Commonly, the belt is recommended to be placed between fifth and sixth intercostal space with the green electrode on the right side of the patient

needs. Commonly the chest is vertically divided into four parts from top to bottom averagely, among which ROI 1 and ROI 2 represent a non-dependent area while ROI 3 and ROI 4 represent the dependent area. When dividing as quadrants, usually default ROI 1 as the upper left, ROI 2 as the upper right, ROI 3 as the lower left, and ROI as 4 the lower right quadrant. Figure 3.18 shows two common ways of ROI set.

3.3.4.2 Functional Image

The functional image represents tidal changes in impedance by a time-series, namely the image observed on the EIT screen that gradually changes with respiration. With gas been inhaled into the lung, the impedance of the lung increases, the lung area on the screen expands. While during the expiration phase the impedance decreases, the lung area gradually darkens and disappears. Through the change of vertical or quadrant ROI, prothorax and dorsal, left and right lung distribution of ventilation can be observed. The functional image of EIT correlates well with CT scan and can evaluate the ventilation heterogeneity conveniently.

3.3.4.3 EIT Plethysmogram

EIT plethysmogram is a curve of pulmonary impedance changes accumulated by each breath over a period according to ROI division, containing global and regional data. The change of end-expiratory lung impedance monitored by EIT correlates

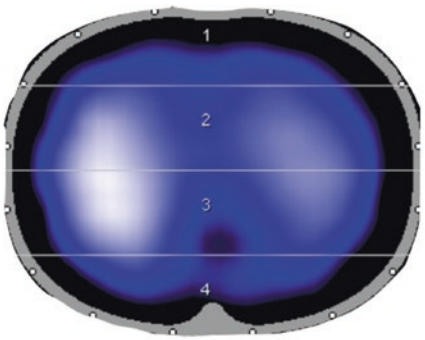

Region of interest : 4 layers	
1	8%
2	42%
3	41%
4	9%

a

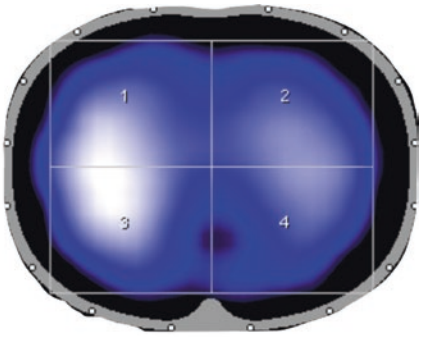

Region of interest : quadrants	
1	27%
2	21%
3	28%
4	20%

b

Fig. 3.18 Regions of interest (ROI). Here a normal EIT image is shown, researchers are able to choose different ROI according to their needs. Gas distribution at each region is expressed as a percentage of global tidal impedance variation

well with the change of end-expiratory lung volume monitored through the nitrogen-washout maneuver. Through the EIT plethysmogram, the trend of volume change can be estimated [84].

3.3.4.4 Basic Definitions in EIT Measurement

For ease of understanding, the following table lists some common concepts when applying EIT (Table 3.1) [85].

3.3.5 Clinical Application

3.3.5.1 Evaluating Ventilation Heterogeneity

The ventilation status of the lung can be observed directly through the EIT screen. Usually, clinicians divide the lung into the non-dependent area and dependent area as we recommended previously. Under normal circumstances, the gas distribution ratio of these two regions is close to 1:1, while during ARDS or patients with diaphragm paralysis the ratio may increase, with gas accumulation more in the upper

Table 3.1 Common concepts of EIT

Name	Definition
Baseline	Baseline (also called reference), is a reference value to determine electrical impedance variations in time difference EIT. Different choice of baseline has a big impact on impedance calculating and data interpretation.
Center of Ventilation (CoV)	Is used to quantify the distribution of ventilation in relation to vertical or quadrantal ROI division and expressed as percentage. CoV is 50% means there is an equal distribution of gas, in the previous condition, CoV less than 50% means a shift distribution towards dependent area.
Change in end-expiratory lung impedance (ΔEELI)	The difference in end-expiratory EIT values between two points of time.
Global inhomogeneity index (GI index)	Means the overall degree of spatial heterogeneity of ventilation.
Pixel	The smallest element in an EIT image and is also the smallest unit in an EIT calculation
Regional ventilation delay (RVD)	RVD quantifies the degree of delay caused by atelectatic area, it measures the delay in the local impedance reaching a particular impedance value, usually up to 40% of the maximum impedance value during a slow inflation maneuver
Tidal impedance variation (TIV)	TIV represents the total impedance change in a breath, the difference between the maximum at the end of inspiration and the minimum at the end of expiration

part, due to the change of respiratory system. Traditionally, clinicians adjust the respirator parameter according to the entirety pulmonary condition and respiratory mechanics—improving the collapse of alveoli by means of recruitment maneuver and elevate the PEEP level. However, this method does not reveal the opposite pathology in different parts of the lung, which is that by keeping some of the alveoli open, you may have overinflated another part of the lung. While with EIT, people can identify ventilation differences among different parts of the lung and achieve regional parameters such as regional compliance so that clinical decisions could be adjusted.

3.3.5.2 Estimation of Lung Collapse and Overdistension

In 2009, costa et al. proposed the method of using EIT to monitor overextension and collapse of the lung to calculate the optimal peep [84]. They divide the lung into multiple pixels, cooperating decremental PEEP titration after maximally recruiting, and calculate every pixel's compliance in each PEEP level through formula 1. They search for the best compliance of a certain pixel that appears at a certain PEEP level. They believe that before the best compliance occurs, the alveoli represented by that pixel are overinflated, and after that, the alveoli tend to collapse. In each PEEP level, they calculate the percent of overextension in each pixel(Overextention $_{\text{pixel}}$%) and the percent of collapse in each pixel(Collapse$_{\text{pixel}}$%). They use data acquires before the best compliance appears through formula 2 to calculate Overextention$_{\text{pixel}}$% and

use data acquires after the best compliance appears through formula 3 to calculate $\text{Collapse}_{\text{pixel}}\%$ by the same token. The percent of collapse is set to zero if the best compliance has not been achieved and the percent of overextension is set to zero after the best compliance has already been achieved.

After a weighted average of all pixels' $\text{Collapse}_{\text{pixel}}\%$ and $\text{Overextention}_{\text{pixel}}\%$ in a certain PEEP, through a special algorithm of EIT, they can finally achieve the cumulated percentage of collapse and overextension for the entire lung in a certain PEEP level. Then, according to the various percentage of collapse and overdistension corresponding to different PEEP, the curve of collapse and overdistension with PEEP can be obtained. The collapse of the lung achieved by this kind of PEEP trial following a recruitment maneuver correlates well with the CT method. This idea is also carried on some EIT machines, enabling clinicians to use EIT to calculate the collapse of the lung right after the PEEP trial and choose optimal PEEP conveniently. But people should bear in mind that PEEP which minimizes alveolar overextension and collapse does not necessarily correspond to peep which maximizes overall lung compliance.

$$\text{Compliance}_{\text{pixel}} = \text{Local impedence variations} / \left(\text{Pplat} - \text{PEEP}\right)$$

$$\text{Collapse}_{\text{pixel}}\% = \left(\text{Best Compliance}_{\text{pixel}} - \text{Current Compliance}_{\text{pixel}}\right) * 100 / \text{Best Compliance}_{\text{pixel}}$$

$$\text{Overextention}_{\text{pixel}}\% = \left(\text{Best Conpliance}_{\text{pixel}} - \text{Current Compliance}_{\text{pixel}}\right) * 100 / \text{Best Compliance}_{\text{pixel}}$$

3.3.5.3 Pendelluft

Traditionally, scholars generally think spontaneous breathing should be encouraged in patients receiving mechanical ventilation, because, on the one hand, it can remain the diaphragmatic muscle's activity to prevent diaphragmatic disuse and paralysis, on the other hand, keep spontaneous breathing can improve regional ventilation, typically the dependent lung region, help reduce respiratory mechanics parameter and maintain hemodynamic stability. However, in patients with ARDS or a strong contraction of the diaphragm, keeping spontaneous breathing may cause the pendelluft phenomenon. This means at the beginning of inspiration, dependent lung region inflates while non-dependent lung region deflates with no change in tidal volume. In other words, the gas is inspired by non-dependent area to dependent area. This phenomenon was detected and reported by Yoshida through EIT [86]. Pendelluft may cause local atelectrauma in non-dependent area and local volutrauma in dependent area, both of that will worsen lung injury. This phenomenon may concern with the injury lung has less behave of fluid-like behavior and distending pressure conduct unevenly through the pulmonary surface. And right because of the uneven conduction of transpulmonary pressure on the pulmonary surface, the

esophageal pressure cannot represent the entire lung condition. Furthermore, this regional and transitory phenomenon cannot be observed by traditional respiratory mechanics monitoring indicators, while EIT can help clinicians identify such ventilation heterogeneity.

3.3.5.4 Pulmonary Perfusion

One of the important objectives of mechanical ventilation is to ensure adequate gas exchange. In addition, to ensure adequate ventilation of the lung, it is also important to ensure adequate pulmonary perfusion. In the article above, we mainly introduced the monitoring and application of EIT in ventilation. In fact, in recent years, the research of using EIT for bedside pulmonary perfusion monitoring has gradually become a hotspot. Both ventilation and blood flow can lead to impedance change which eventually affects EIT monitoring results. This property makes it possible to monitor perfusion by EIT. At present, it is mainly assessed by the "first-pass kinetics" method. The method uses the high conductivity of hypertonic saline as an intravascular contrast agent to help distinguish between pulmonary ventilation and blood flow. Applying this method requires a quick and uniform infusion of 20 mL hypertonic saline through the central venous catheter after a brief pause in inspiration, then the blood signal and ventilation signal will be separated by electrocardiography gating or by algorithms based on the principal component analysis. This method has been confirmed to have a good correlation with electron beam CT, which illustrates EIT is able to detect changes in pulmonary blood flow over time [87].

3.3.6 Other Interesting Clinical Applications

Since 2006, clinicians have found that EIT can detect the presence of pneumothorax. In 2017, Morais et al. reported the incidence of pneumothorax on an ARDS patient during recruitment maneuver in detail, which happened to be recorded by EIT [88]. Pneumothorax shows a sudden increase in brightness in the EIT image, and the increase in ventilation is not proportional to the increase in PEEP. Such reports confirm that the EIT is useful in monitoring patients with the need to perform pressure-injury risk procedures.

Chen et al. put forward the airway closure could be underestimated and overlooked. PEEP levels might be set inappropriately because of this phenomenon [89]. Sun et al. published a case report pointing out that using EIT could confirm airway closure. They evaluated global and regional *P–V* curves, EIT ventilation maps, and plethysmograph waveforms during low-flow inflation, finding that there is a nearly identical infection point on the initial part of both global and regional *P–V* curves,

meaning that no gas enters the lung at the beginning of the inspiration even in the relatively well-ventilated non-dependent area, which means complete airway closure [90].

3.3.7 Advantage of EIT Comparing with CT

Compared to conventional CT, EIT provides bedside, noninvasive, radiation-free, and real-time monitoring, which also provides local information. Applying EIT to ICU patients can avoid the risks associated with transporting patients and may become a more cost-effective option. It is worth noting however that the data provided by the EIT may be relative rather than absolute. Therefore, although EIT is a promising monitoring method, researchers should carefully interpret the data and compare them with the golden standard to maximize the benefits to patients.

3.4 Positron Emission Tomography

3.4.1 Introduction

Positron emission tomography (PET) is a functional image technique of nuclear medicine, which detects and measures the gamma rays generated in vivo, then locates and calculates the concentration of radioactive tracer in regions of interest. After analyzing and reconstructing by computer, PET can display the spatial and temporal distribution of the radioactive tracer in the body that will contribute to diagnosing and treatment of diseases, neoplastic disorders in particular [91, 92].

Brownell and Sweet [93] introduced a method to locate the brain tumors with positron emitters in 1953, which was considered as the first successful attempt to apply annihilation radiation in medical imaging. David Kuhl and Roy Edwards had put forward the concept of emission and transmission tomography in the late 1950s. Based on their work, several inchoate tomographic instruments were designed and constructed at the University of Pennsylvania [93]. Michel M.Ter-Pogossian and his colleagues improved tomographic imaging techniques in 1975 [94, 95], they built a system that can detect the “electronic” collimation of annihilation photons by connecting a hexagonal array of receptors to coincidence circuits and then confirmed that the system has a better performance in contrast and resolution than scintillation cameras testing by computer simulation and animal experiment.

After more than half a century of development, PET is widely used in oncology, neuroimaging, cardiology, infectious diseases, pharmacokinetics, musculoskeletal imaging, and small animal imaging. In this section, we will introduce the simple principles and basic concepts of PET and focus on the application and prospect of PET in respiratory function monitoring.

3.4.2 Conception

3.4.2.1 Positron Emission and Gamma Rays

Elements that are constituted by protons (with positive charge), neutrons (with no charge), and electrons (with negative charge) can be represented as ${}^{A}_{Z}X$. Z named as atomic number means the number of protons in element X which also equals the number of electrons as long as the nuclei are stable. A was called as atomic mass number in this expression which means the number of protons (Z) plus the number of neutrons. The same element has the same atomic number. In other words, for a given element, the number of protons is then determined. In that case, Z can be omitted when X represents a certain element. But a certain element can have different forms that also be called isotopes since the atomic mass number are different.

Proton-rich radio nuclei are unstable and need a nuclear change to stabilize itself. It only has two ways to achieve this progress. One is positron (β+) decay and another way is electron capture. Positron (β+) decay is the process of rearrangement of the nucleus. This transformation reduces a proton and generates a neutron and positive electron (positron) and ejects a neutrino. The positron travels a short distance, interacts with the negative electrons of the surrounding material, loses its mass, and releases two photons moving in opposite directions with equal energy (511 keV) (Fig. 3.19).

The essence of gamma rays, generated by gamma decay is a stream of photons. After the occurrence of α decay, β decay, or electron capture, the daughter nucleus is still in an unstable excited state. Then it releases excess energy in the form of gamma photons to reach a stable state. Photons generated from annihilation radiation after the positron decay mentioned above is a kind of gamma rays [96].

Although the principle of PET scan is to use positron decay for imaging, positrons exist for a very short time and have very weak penetration, so they cannot be detected directly. The gamma rays produced by positron annihilation after positron decay can travel through the body and can be detected in PET scan.

3.4.2.2 Radioactive Tracer

Molecule contained radioactive isotope is called radioactive tracer. Because nuclide reactions are more active than chemical reactions, using radioactive tracer to trace atom or molecule is more sensitive, which means the concentration of radioactive tracer can be very low when using in vivo. Substance labeled by isotope do not change its chemical characteristics and biological function thus radioactive tracer absorbing, distribution, metabolism, and excretion within organisms can uncover the function of certain organs. At present, the sources of medical radionuclides are mainly in three aspects: nuclear reactor, cyclotron, and radionuclide generator. The commonly used radioactive tracer in PET scan is labeled by 11C, 13N, 15O, or 18F (chemical characteristics are similar to H). Those radionuclides are produced from

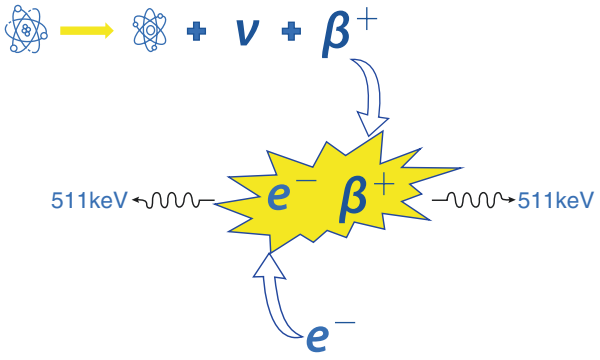

Fig. 3.19 A schematic illustration of positron (β+) decay and annihilation of a positron and an electron. Two photons were produced and moving in opposite directions with equal energy (511 keV)

cyclotron and constitute molecules such as 11CO, 11C methyl albumin, 13N-N2gas, 13N-N2-saline, H215O, C15O, [18F]-fluorodeoxyglucose [97]. Tracer composed of a few other nuclides such as 68Ga-transferrin, 9-(4-[18F]-fluoro-3-hydroxymethylbutyl), and so on are used in PET scan as well to assess pulmonary transcapillary escape rate, gene expression, or other special features.

3.4.3 Applications

Although pulmonary function monitoring is not the primary application field of PET, PET has made some significant contributions in helping to understand respiratory physiology and lung injury mechanism. We will introduce several aspects of the application of PET in lung function monitoring, including ventilation, perfusion, lung vascular permeability, lung water concentration, lung inflammation in ALI and ARDS, enzyme activity, and pulmonary gene expression. At the end of this section, we summarize some limitations of the clinical application of PET.

3.4.3.1 Ventilation and Perfusion

The distribution coefficient (λwater/air) of nitrogen is 0.015 at 37 °C which means the solubility of nitrogen is very low. When saline containing 13N-N2, injected intravenously, reaches the pulmonary capillaries, nearly all 13N-N2 is converted into a gaseous state and diffuses into the alveoli. Rhodes [98, 99] and his colleagues took advantage of this peculiarity and induced a method using 13N-N2 in saline intravenously at a constant rate to measure regional ventilation-perfusion ratio in 1989, and they calculated that mean ventilation–perfusion ratio of healthy human subjects in the left lung and right lung is 0.8 and 0.76, respectively. This method was modified by Mijailovich [100], Musch [101], and their coworkers. They infused a bolus of saline contains 13N-N2 gas intravenously within 3–5 s and then implemented 30–60 s apnea to make sure radioactive gas was trapped in the lung. After

breathing is resumed, radioactive gas was washed out as time goes on. When the tracer was injected into the body, continuous PET scanning was performed to obtain the solubility-time curve of radioactive substances in different regions of the lung. When 13N-N2 saline arrived at the lung capillary which located in regions perfused but having no aeration (shunt region), it cannot release 13N2. 13N-N2 saline will flow away with blood thus the tracer activity will get to an early peak and decline gradually to a plateau during the apnea period. Radioactive tracer cannot arrive at lung region which is not perfused since there is no blood flow. If the perfusion of the region of interest is impaired, the tracer activity will decrease during the period of apnea compared with normal perfusion regions. In some situations, for example, air trapping occurring in asthma or chronic obstructive pulmonary disease, 13N-N2 dissolve in saline change into gas stage when it arrives at the lung capillary during apnea, but on account of no or poor gas exchange, 13N-N2 in gas stage was retained in lung and tracer activity decrease slower than normal gas exchange lung region during the washout period. Investigator proposed a mathematical model to determine the distributions of pulmonary perfusion, ventilation, and shunt and verify the model is accurate in normal animals and acute lung injure animals [102, 103]. Musch and coworkers [101] found that both perfusion and ventilation tend to distribute to dependent regions either in supine position or in prone position in healthy humans with PET scan and 13N-N2 saline bolus technique. Using PET scan and 13N-N2 saline bolus injection technique, they also identified redistribution of perfusion toward collapse regions which may be the reason for the worsening of oxygenation that occurred with sustained inflation or high PEEP [104, 105].

However, with the infusion of 13N-N2, it is not feasible to quantify the ventilation regions poorly perfused thus methods ground on analyzing the kinetics of inhaled tracer are put forward. An inhaled 13N-N2 PET scan was used to measure regional alveolar volume and ventilation in experimental acute lung injury animals to explain the pathophysiology progress of ventilator-induced lung injury [106]. Regional specific volume change (sVol), defined as the ratio of regional tidal volume and regional end-expiratory (EE) gas volume, is another important variable in the mechanism of ventilator-induced injury. sVol associated with tidal volume and lung strain can provide information on the estimation of elastance and ventilation regionally. Tyler J.Wellman and colleagues used 13N-N2 inhaled and washout technique and respiratory-gated PET to assess regional lung expansion [107].

Intravenous injection or inhalation of 13N-N2 can be used to assess regional ventilation, perfusion, shunt, and gas trapping, but, since the need for on-site cyclotrons to produce 13N2, the application of those methods is limited. 68Gallium generated at the PET facility needs no on-site cyclotrons and can be chelated to numerous functional molecules for imaging in PET scan. Hnatowich DJ, Chesler DA, and their group first used 68Gallium in lung image to gain lung perfusion tomography by injecting radioactive albumin microspheres in dogs [108, 109]. It has been proved that PET scan with 68Ga labeled tracer has higher-resolution and more capacity in regional quantitation of lung function compared with conventional ventilation-perfusion ratio imaging (SPECT/CT) in diagnosing patients with suspected pulmonary embolism [110]. In the evaluation of airways disease, PET scan with Galli-gas provides more information in ventilation distribution and has better

performance in differentiating ventilation heterogeneity compared with SPECT with Techne-gas, and this method is expected to be applied in small airways disease [111]. Another study using PET scan with 68Ga labeled albumin aggregates gain an insight into the pathogenesis of ARDS in experimental rats [112]. Investigator has shown that perfusion of regions affected by acid aspiration was increased within 10 min as a result of hyperemic responses and was decreased, as early as 2 h, explained by hypoxic pulmonary vasoconstriction or direct compression of vessels by exudate.

Schuster and coworkers found that the fraction of pulmonary blood flow (PBF) to dependent regions increased while the PaO_2/FiO_2 ratio decreased by measuring regional pulmonary perfusion with H215O in acute lung injury (ALI) patients [113]. Their group also found that the main mechanism of perfusion redistribution to aerated regions rather than flooded alveoli was hypoxic pulmonary vasoconstriction [114].

In summary, with the help of PET scan, a physician can measure global and regional ventilation, perfusion, and ventilation–perfusion ratio, that may make contribution to identifying the presence of pulmonary embolism, assess lung function before radiotherapy, predict lung function after pneumonectomy, evacuate the severity of chronic obstructive pulmonary disease (COPD) and asthma, and understand the mechanism of ALI, VILI, and ARDS.

3.4.3.2 Lung Vascular Permeability and Lung Water Concentration

In 1987, Mark A. Mintun [115] and coworker proved that PET was useful in evaluating vascular permeability changes in acute lung injury experimental animals and patients. They calculated a new index, pulmonary transcapillary escape rate (PTCER), which describes the movement of 68Gallium transferrin from pulmonary vascular to extravascular in dogs repeatedly, and found that there was no significant change of the new index. They also tested it in healthy human volunteers and patients with acute respiratory distress syndrome (ARDS) and showed that the difference of PTCER in normal volunteers and patients with ARDS was similar in an animal model. PET methods can be a substitute for protein flux measurements for evaluating pulmonary vascular permeability accurately. Lung water concentration (LWC) can be assessed accurately and reproducibly by PET with 15O labeled water in supine dog, Velazquez.M [116] and coworkers found an excellent linear correlation between regional LWC measured gravimetrically and regional LWC measured by PET ($r = 0.92$).

3.4.3.3 Lung Inflammation in ALI and ARDS

PET imaging is used in the assessment of inflammation of acute lung injury and acute respiratory distress syndrome as a result of the development of tracer related to the inflammatory response. 2-[18F]fluoro-2-deoxy-D-glucose ([18F]FDG), the most common radioactive tracer applied in PET imaging of

lung inflammation, is transported into cells and transformed into FDG-6-phosphate. The FDG-6-phosphate is trapped in cells temporarily which cannot be metabolized further. PET imaging finished before radioactive tracer is extruded from the cell and filtered by the glomerulus, excreted in the urine eventually. [18F]-FDG is initially used in diagnosing and staging of neoplastic disease, recently it has been used in evaluating lung inflammation. In 2004, Heather A. Jacene [117] and coworkers reported a case of increased [18F]-FDG uptake in pulmonary with acute respiratory distress syndrome patients. They assumed that inflammatory cells involved with the pathogenesis of ARDS utilized glucose at a high rate compared with normal tissue cells, which may explain the phenomenon of increased pulmonary [18F]-FDG uptake they observed. It was proved that the rate of [18F]-FDG uptake was associated with the state of neutrophil activation which made PET scan with [18F]-FDG a useful tool to understand neutrophil kinetics in the pathophysiological process of ALI. Delphine L. Chen [118] observed a similar phenomenon in ALI dogs. They also came up with a method to estimate the rate of [18F]-FDG uptake in the lungs during ALI which was testified by comparing tracer activity derived by PET and blood time-activity data as the gold standard. With those work as the cornerstone, [18F]-FDG PTE imaging can be applied in the following clinical scenarios. If critically ill patients have an increased [18F]-FDG activity in the lungs, the differential diagnosis should include ARDS, this may help to screen ARDS patients early. In another aspect, PET scan with [18F]-FDG is used in quantifying the anti-inflammatory therapies response and assessing the efficacy of novel anti-inflammatory drugs. It also can help to understand the mechanism of ARDS and instruct ventilator parameter settings. It provides visualized evidence that regions with normal aeration on CT scan also affect by lung inflammation. Moreover, the higher plateau pressure (often above 27 cmH_2O) and larger dynamic strain it is, the worse inflammation occurred. These results suggest that for ARDS patients, the tidal volume setting should be relatively small, so as to avoid barotrauma and reduce the inflammatory response [119, 120].

3.4.3.4 Enzyme Activity

Vascular remodeling is one of the most important mechanisms of primary pulmonary hypertension (PPH). The expression of factors, such as angiotensin-converting enzyme (ACE), which may promote vascular remodeling is increased in the region of active remodeling. Many studies have found that the expression of ACE increases in patients with PPH or pulmonary hypertension experimental animals. PET imaging with [18F]-fluoro-captopril has been developed to evaluate lung ACE expression in experimental animals and humans. This method also is used in evaluating the efficacy of ACEI in the treatment of PPH which can attenuate pulmonary hypertension and slow down vascular remodeling [121].

3.4.3.5 Pulmonary Gene Expression

PET reporter gene (PRG) imaging is based on the principle of introducing reporter genes into specific tissues with the help of modern molecular biology methods, the products of which trap radioactive tracers, also called PET reporter probe (PRP), then the PET instrumentation detect the signal generated by PRP, located where the reporter genes express. Herpes simplex virus (HSV) type I thymidine kinase (mHSV1-tk) is one of the most common PET reporter genes used in lungs, and 9-(4-[18F]-fluoro-3-hydroxymethylbutyl) guanine ([18F]FHBG) is used as the PRP. With this technique, it is possible to monitor the effect of transgene therapy in the lungs.

3.4.4 Limitation of Clinical Application of PET

All methods mentioned above share the same inherent limitations of PET. First of all, PET scan requires sophisticated and bulky instruments, as well as extremely high radiation protection requirements, which is almost impossible to be carried out bedside. PET is not suitable for critically ill patients who are difficult to go out for examination. Secondly, because of the complex preparation process of most radioactive tracer, the cost of PET scan is still very high. Many technologies are still in the research stage and cannot be extended to clinical practice. Third, PET scan has a low anatomical resolution, and it often requires CT or MRI scan synchronously to locate lesions accurately.

3.4.5 Perspectives

With the development of molecular imaging, PET scan is playing an increasingly important role in this field. With the help of molecular imaging with PET, the understanding of the imaging changes of diseases has developed from the organ or tissue level to the cellular or molecular level. Therefore, it is expected that diagnosis can be made at the beginning of the disease before it reaches an irreversible state, subsequently gaining an opportunity for the treatment of diseases. Another development of PET scan is equipment upgrading and algorithm optimization of image reconstruction. At present, most PET devices are hybrid and multimodal, which also can perform CT or MRI imaging. In future, the hybridization PET scan will have further development in developing devices with closer functional integration, higher signal quality, and faster imaging speed.

3.5 Magnetic Resonance Imaging

3.5.1 Introduction

Magnetic resonance imaging (MRI) is a form of tomography that used magnetic resonance (MR) to extract electromagnetic signals from the body and reconstruct information about the body. Like PET and SPECT, MRI is also a form of emission tomography, signals of which used for imaging come directly from the object itself with no need for radioactive isotopes, that makes MRI safer. A radio-frequency pulse of a certain frequency was applied to the body in a static magnetic field, then hydrogen protons in the body were stimulated as a result of magnetic resonance. After the pulse is stopped, the proton generates an MR signal in the relaxation process. Image is generated through MR signal reception, spatial coding, and image reconstruction.

3.5.2 Brief History

Flelix Bloch from Stanford University and Edward Purcell from Harvard University independently discovered the phenomenon of magnetic resonance in 1946; hence, they shared the Nobel Prize in physics in 1950. Shortly after the discovery of MR, scientists discovered that hydrogen atoms in water molecules can generate MR, which could be used to obtain information about the distribution of water molecules in the human body and thus accurately map the internal structure of the human body. Based on this theory, scientists succeeded in distinguishing cancer cells from normal tissue in mice by measuring the relaxation time of the MR. In 1972, Paul Lauterbur developed a set of spatial coding methods for MR signals, which could reconstruct the image of the human body. After that, MRI technology became more and more mature and applied in a wide range, becoming a routine medical detection method.

3.5.3 Image-Forming Principle

Nucleons with odd numbers of protons or neutrons, such as 1H, 19FT, and 31P, have an intrinsic property: spin. Normally, the arrangement of nuclear spin axes is irregular, but when placed in an external magnetic field, the spatial orientation of nuclear spin makes a transition from disorder to order. The magnetization vector of the spin system increases gradually, and when the system reaches equilibrium, the magnetization reaches a stable value. If the nuclear spin system is affected by external factors such as a certain frequency of radio-frequency pulse can cause a resonance effect. After the radio-frequency pulse stops, the excited nucleus of the spin system

cannot maintain this state and will revert to the original arrangement state in the magnetic field. At the same time, it will release weak energy which will convert into a radio signal. The signal is detected and analyzed to obtain the image of nuclear distribution in motion. The process by which the nuclei return from an excited state to an equilibrium arrangement is called relaxation. The time it takes is called relaxation time. There are two kinds of relaxation time, T1 and T2. T1 is the spin-lattice or longitudinal relaxation time and T2 is the spin-spin or transverse relaxation time [122].

The most commonly used nucleus for MRI is the hydrogen proton, because it has the strongest signal and widely present in human tissues. There are many factors which include proton density, length of relaxation time, the flow of blood and cerebrospinal fluid, paramagnetic substance, and protein can affect MRI imaging. Another characteristic of MRI is that flowing liquid does not produce a signal called flowing void effect. This makes it possible to separate the pipe network in the body, such as blood vessels and the biliary tract, from the soft tissue.

3.5.4 Classification of MRI

MRI can be divided into plain scan and enhanced scan according to whether the contrast agent is used or not. Plain scan means scanning without contrast agent and enhanced scan use contrast agent in scanning. By injecting an MRI contrast agent, the resonance time of tissues under an external magnetic field can be shortened, the difference of contrast signals can be increased, and the clarity of imaging can be improved. Depending on the purpose of examination, MRI can be divided into Magnetic Resonance Angiography (MRA), Magnetic Resonance Cholangiopancreatography (MRCP), Magnetic Resonance Urography (MRU), Magnetic Resonance Myelography (MRM), and so on.

3.5.5 Contrast Agent of MRI

MRI contrast agents can be divided into longitudinal relaxation contrast agent (T1 preparations) and transverse relaxation contrast agent (T2 preparations). T1 preparations use paramagnetic metal ions to directly affect hydrogen ions in water molecules to shorten T1 thus enhancing the signal and making the image brighter; T2 preparations are used to shorten T2 by interfering with the inhomogeneity of the external local magnetic environment thus weakening the signal and darkening the image. According to the magnetic composition, MRI contrast agents can be divided into three categories: paramagnetism, ferromagnetism, and superparamagnetism. The most commonly used paramagnetic contrast agents in clinical practice are Gadolinium contrast agents.

3.5.6 Application

MRI is widely used for the diagnosis of various diseases especially in the brain, spinal cord, large blood vessels of the heart, joint bones, soft tissue, and pelvic cavity, due to its features of non-radiation, high resolution of soft tissue, and flowing void effect. However, due to the characteristics of MRI scanning technology and the characteristics of the lung itself, the application of MRI in lung diseases is not as usual as others. One of the reasons is that the time required for MRI scanning is relatively long. As a result of the respiratory movement, imaging is often unsatisfactory when there is no suitable contrast agent. Scanning under the condition of breath-holding methods requires well cooperation of the patients, which is more impossible in critically ill patients. Another reason for limiting the clinical application of pulmonary MRI is that the proton density in lung tissues is only one-fifth of that in other solid organs, which is not enough to generate sufficient signals to achieve a satisfactory resolution. However, due to the development of contrast agents and the improvement of imaging speed, MRI is expected to be a radiation-free alternative to CT.

3.5.7 Structural Image

In the field of pulmonary structure imaging by MRI, pulmonary angiography is expected to be widely used. In earlier studies, pulmonary angiography was mainly performed by injecting Gadolinium-enhanced contrast agents to obtain images with satisfactory spatial resolution. However, in recent years, due to increasing concerns about the safety of Gadolinium-enhanced contrast agents, researchers hope to investigate a technology that can perform pulmonary angiography without the need for contrast agents. MRI's unique flowing void effect makes it possible. Balanced steady-state free precession (SSFP) has been considered as a preferent pulse sequence strategy for a long time in pulmonary angiography. Based on SSFP, Bieri [123] and his coworkers proposed ultrafast SSFP pulse sequences, making 3D-MRI pulmonary angiography without contrast agents possible. Bieri reports a case that the reconstructed image has almost no artifact or degradation caused by balanced SSFP. Morphological lung imaging with high spatial resolution and high contrast-to-noise ratio can be obtained using this method mentioned before, which allows visualization of lung parenchyma and airspaces even in inspiration. Another pulse sequence used to acquire a high quality of lung MR image is ultrashort echo-time (UTE) technology. With the assistance of imaging navigator system or respiratory bellows signal to synchronize 3D image acquisition with the respiratory cycle, the UTE acquisition can generate 3D images of the lung in whole with unprecedented spatial resolution and signal-to-noise ratio. Johnson KM [124] and his coworkers used UTE acquisition to obtain images of airway walls, lobar fissures, and other structural features in free-breathing volunteers and patients, which is not exemplary

seen in normal lung MRI. MRI is also used in assessing diaphragmatic motion during inspiration and expiration with satisfied spatial and temporal resolution. MRI has been proved to be a useful method to assess diaphragm movement in COPD patients, and it may play a role in evacuating diaphragm dysfunction in patients undergoing mechanical ventilation. With these advances in pulmonary structural MRI, it is possible to reveal the mechanism ventilator-associated lung injury and changes in pulmonary structures during disease progression in patients with ARDS, which will contribute to the early diagnosis, stratification, and individualized treatment of ARDS patients.

3.5.8 Functional Image

MRI is an effective tool to study pulmonary functions, of which ventilation and perfusion are the two research hotspots. Previous studies have shown that pulmonary ventilation and perfusion are distributed by gravity gradients in healthy individuals. In pathological conditions, lung ventilation and perfusion are redistributed as a result of regulatory mechanisms to compensate for impaired lung function, meet the body's need for oxygen, and eliminate more carbon dioxide produced by metabolism. Measurement of pulmonary ventilation and perfusion, both global and local, is helpful to have a better understanding of the development of pulmonary diseases and therapeutic reactivity.

The first ventilation MRI was performed in 1994 [125], which was implemented by using hyperpolarized 129Xe. 129Xe is gradually replaced by 3He since the latter is easier to polarize. Oxygen-enhanced MRI is another technique used to visualize pulmonary ventilation. It has been confirmed that pulmonary ventilation assesses by hyperpolarized gas MRI is feasible and reliable [126]. The extent of pulmonary ventilation measured by hyperpolarized gas MRI has a good correlation with the measurement results of spirometry. In patients with asthma or COPD, hyperpolarized gas MRI can be used to detect airway obstruction with sensitivity and specificity no less than that of high-resolution CT, which may potentially apply in ARDS patients in the future. High temporal resolution images can be obtained by MRI scanning with gated image acquisition technology, which can show the distribution of ventilation dynamically during continuous breathing, which will make it possible to assess the severity and range of air trapping directly. Thus, dynamic ventilation MRI is going to play an increasingly important role in various obstructive lung diseases since it is quantitative and is no need to expose to radiation.

Unlike 3He, 129Xe is not only existed in the pulmonary gas spaces but also can spread across the blood-gas barrier which makes evaluation of gas exchange quantitatively possible. Hyperpolarized gas MRI with 129Xe can provide information about gas exchange parameters which includes alveolar surface area, septal thickness, and vascular transit time [127]. Hyperpolarized gas MRI is also potentially applied in guiding the mechanical ventilation parameter setting. McGee KP [128] and his coworkers compared the parenchymal elasticity in normal and edematous,

ventilator-injured lung by magnetic resonance elastography (MRE). Their results showed that lung elasticity in animals with regional lung injury decreased compared with normal animals, and in the presence of alveolar flooding, there was no correlation between airway pressure and pressure of the lung parenchyma. Therefore, they cautioned that, unlike conventional pressure-volume approaches, MRE evaluates lung function on the topographical distribution of injury rather than considering the lung as a whole. Maurizio Cereda [129] and his group used 3He MRI as a tool to assess the effect of PEEP on alveolar recruitment and atelectasis-induced hyperinflation in rats ongoing mechanical ventilation and their studies concluded that measuring regional respiratory gas diffusivity by hyperpolarized gas contrast MRI was a potential method to optimize the effects of parameters settings during mechanical ventilation. An animal study [130] reported in 2016 demonstrated that MRI could detect tiny areas of ventilator-induced injury earlier than significant lung injury occurs, which makes MRI a possible research tool to observe the occurrence and development of VILI and the therapeutic effect of protective mechanical ventilation on ALI in real-time. This further understanding of the pathophysiological mechanism during lung injury has attracted attention to the heterogeneity of lung injury and individual variation in response to treatment, leading to the trend of individualized treatment in clinical mechanical ventilation.

Another important aspect of lung function is perfusion. There are two main MR techniques, one of which is a contrast-enhanced MR perfusion image, another is arterial spin labeling (ASL), to assessed pulmonary perfusion. The contrast-enhanced MR perfusion image is performed as follows. A gadolinium-based paramagnetic contrast agent is injected into vein and then a gradient-echo pulse sequence is initiated. The collected signals are integrated and calculated to provide qualitative and quantitative parameters about pulmonary perfusions, such as transit time, volume, and flow of lung blood. However, as mentioned above, non-contrast-enhanced MR perfusion image gradually replaced contrast-enhanced MR perfusion image due to increasing concerns about the safety of contrast agents and the desire for noninvasive examination in a partial patient such as children. With the improvement of MR technologies, limitations of non-contrast-enhanced MR perfusion image such as long acquisition times and artifacts due to motion have been overcome. ASL uses MR-tagged water in blood excited by an inversion pulse as an endogenous contrast agent to generate sensitivity of lung blood flow. Pulmonary perfusion MRI was mainly used in diagnosis and stratification of pulmonary embolism, COPD, asthma, pulmonary cystic fibrosis, and malignant tumor. Researchers integrate pulmonary ventilation and perfusion into a comprehensive index known as ventilation–perfusion (V/Q) ratio since ventilation-perfusion mismatch is a common pathophysiological cause of refractory hypoxemia. There are three main MRI techniques used to measure global and regional ventilation–perfusion ratio: ASL-FAIRER, oxygen-enhanced MRI, and fast gradient-echo with multiple short TE. However, compared with CT and PET, few studies have been reported to evaluate the pulmonary ventilation–perfusion ratio in critically ill patients who needs mechanical ventilation, possibly because the MRI-compatible ventilator is not widely used in clinical practice.

3.5.9 Perspective

With the development of MRI equipment and techniques, newer signal acquisition systems permitting fewer measurements are required to reconstruct entire 3D images, leading to an improved image examinations since MRI is convenient and less invasive. Thanks to the promotion of the MRI-compatible ventilator, it is reasonable to believe that MRI plays an important role in visualizing and quantifying the pulmonary structural and functional changes in patients with mechanical ventilation. According to a clinical review [131], it is inferred that MRI can detect the morphological and pathophysiological patterns (such as "ground-glass opacification" or "consolidation" found by CT) in ARDS patients. Hybrid imaging would be another area in which MRI may play an important role in the future. Inspired by the successful combination of PET and CT, the combination of PET and MRI is an attractive challenge [132]. The high soft-tissue contrast MRI can make up for the low spatial resolution of PET and PET/MRI can reduce exposure to ionizing radiation compared with PET/CT, those advantage of PET/MRI may be useful in assessing structural or functional changes of the lung in mechanically ventilated patients.

References

1. Rubinowitz AN, Siegel MD, Tocino I. Thoracic imaging in the ICU. Crit Care Clin. 2007;23(3):539–73.
2. Bentz MR, Primack SL. Intensive care unit imaging. Clin Chest Med. 2015;36(2):219–34.
3. Cadman A, Lawrance JA, Fitzsimmons L, et al. To clot or not to clot? That is the question in central venous catheters. Clin Radiol. 2004;59(9):349–55.
4. Sheuland J, Hireleman M, Hoang K, et al. Lobar collapse in the surgical intensive care unit. Br J Radiol. 1983;56(668):531–4.
5. Liu SY, Tsai IT, Yang PJ. Pneumothorax and deep sulcus sign. QJM. 2016;109(9):621–2.
6. Dussik KT. On the possibility of using ultrasound waves as a diagnostic aid. Neurol Psychiat. 1942;174:153–68.
7. Dénier A. Les ultrasons, leur application au diagnostic. Presse Méd. 1946;22:307–8.
8. Volpicelli G, Elbarbary M, Blaivas M, et al. International evidence-based recommendations for point-of-care lung ultrasound. Intensive Care Med. 2012;38(4):577–91.
9. Lichtenstein D, Lascols N, Mezière G, et al. Ultrasound diagnosis of alveolar consolidation in the critically ill. Intensive Care Med. 2004;30(2):276–81.
10. Volpicelli G, Mussa A, Garofalo G, et al. Bedside lung ultrasound in the assessment of alveolar-interstitial syndrome. Am J Emerg Med. 2006;24(6):689–96.
11. Bouzat P, Francony G, Declety P, et al. Transcranial Doppler to screen on admission patients with mild to moderate traumatic brain injury. Neurosurgery. 2011;68(6):1603–10.
12. Troianos CA, Hartman GS, Glas KE, et al. Guidelines for performing ultrasound guided vascular cannulation: recommendations of the American Society of Echocardiography and the Society of Cardiovascular Anesthesiologists. J Am Soc Echocardiogr. 2011;24(12):1291–318.
13. Laursen CB, Sloth E, Lambrechtsen J, et al. Focused sonography of the heart, lungs, and deep veins identifies missed life-threatening conditions in admitted patients with acute respiratory symptoms. Chest. 2013;144(6):1868–75.

14. Zieleskiewicz L, Muller L, Lakhal K, et al. Point-of-care ultrasound in intensive care units: assessment of 1073 procedures in a multicentric, prospective, observational study. Intensive Care Med. 2015;41(9):1638–47.
15. Laursen CB, Sloth E, Lassen AT, et al. Point-of-care ultrasonography in patients admitted with respiratory symptoms: a single-blind, randomised controlled trial. Lancet Respir Med. 2014;2(8):638–46.
16. Testa A, Soldati G, Copetti R, et al. Early recognition of the 2009 pandemic influenza A (H1N1) pneumonia by chest ultrasound. Crit Care. 2012;16(1)
17. Gehmacher O, Mathis G, Kopf A, et al. Ultrasound imaging of pneumonia. Ultrasound Med Biol. 1995;21(9):1119–22.
18. Reissig A, Kroegel C. Sonographic diagnosis and follow-up of pneumonia:a prospective study. Respiration. 2007;74(5):537–47.
19. Mongodi S, Via G, Girard M, et al. Lung ultrasound for early diagnosis of ventilator-associated pneumonia. Chest. 2016;149(4):969–80.
20. Al Deeb M, Barbic S, Featherstone R, et al. Point-of-care ultrasonography for the diagnosis of acute cardiogenic pulmonary edema in patients presenting with acute dyspnea: a systematic review and meta-analysis. Acad Emerg Med. 2014;21(8):843–52.
21. Arbelot C, Ferrari F, Bouhemad B, et al. Lung ultrasound in acute respiratory distress syndrome and acute lung injury. Curr Opin Crit Care. 2008;14(1):70–4.
22. Corradi F, Brusasco C, Pelosi P. Chest ultrasound in acute respiratory distress syndrome. Curr Opin Crit Care. 2014;20(1):98–103.
23. Bass CM, Sajed DR, Adedipe AA, West TE. Pulmonary ultrasound and pulse oximetry versus chest radiography and arterial blood gas analysis for the diagnosis of acute respiratory distress syndrome: a pilot study. Crit Care. 2015;19(1):282.
24. Ranieri VM, Rubenfeld GD, Thompson BT, et al. Acute respiratory distress syndrome: the Berlin definition. JAMA. 2012;307(23):2526–33.
25. Lichtenstein D, Meziere G, Seitz J. The dynamic air bronchogram. A lung ultrasound sign of alveolar consolidation ruling out atelectasis. Chest. 2009;135(6):1421–5.
26. Yu CJ, Yang PC, Wu HD, et al. Ultrasound study in unilateral hemithorax opacification. Image comparison with computed tomography. Am Rev Respir Dis. 1993;147(2):430–4.
27. Yu CJ, Yang PC, Chang DB, Luh KT. Diagnostic and therapeutic use of chest sonography: value in critically ill patients. Am J Roentgenol. 1992;159(4):695–701.
28. Lichtenstein D, Hulot JS, Rabiller A, et al. Feasibility and safety of ultrasound-aided thoracentesis in mechanically ventilated patients. Intensive Care Med. 1999;25(9):955–8.
29. Lomas DJ, Padley SG, Flower CD. The sonographic appearances of pleural fluid. Br J Radiol. 1993;66(787):619–24.
30. Vignon P, Chastagner C, Berkane V, et al. Quantitative assessment of pleural effusion in critically ill patients by means of ultrasonography. Crit Care Med. 2005;33:1757–63.
31. Balik M, Plasil P, Waldauf P, et al. Ultrasound estimation of volume of pleural fluid in mechanically ventilated patients. Intensive Care Med. 2006;32(2):318.
32. Perazzo A, Gatto P, Barlascini C, et al. Can ultrasound guidance reduce the risk of pneumothorax following thoracentesis? J Bras Pneumol. 2014;40(1):6–12.
33. Blaivas M, Lyon M, Duggal S. A prospective comparison of supine chest radiography and bedside ultrasound for the diagnosis of traumatic pneumothorax. Acad Emerg Med. 2005;12(9):844–9.
34. Soldati G, Testa A, Sher S, et al. Occult traumatic pneumothorax: diagnostic accuracy of lung ultrasonography in the emergency department. Chest. 2008;133(1):204–11.
35. Volpicelli G, Boero E, Sverzellati N, et al. Semi-quantification of pneumothorax volume by lung ultrasound. Intensive Care Med. 2014;40:1460–7.
36. Taylor RA, Davis J, Liu R, et al. Point-of-care focused cardiac ultrasound for prediction of?Pulmonary embolism adverse outcomes. J Emerg Med. 2013;45(3):392–9.
37. Dunn A. In suspected PE with Wells score>4 or positive D-dimer, multiorgan ultrasonography had 90% sensitivity for PE. Ann Intern Med. 2014;161(8):JC12–3.

38. Nazerian P, Vanni S, Volpicelli G, et al. Accuracy of point-of-care multiorgan ultrasonography for the diagnosis of pulmonary embolism. Chest. 2014;145(5):950–7.
39. Lichtenstein DA, Mezière GA. Relevance of lung ultrasound in the diagnosis of acute respiratory failure. Chest. 2008;134(1):117–25.
40. Kimura BJ, Yogo N, O'Connell CW, et al. Cardiopulmonary limited ultrasound examination for "quick-look" bedside application. Am J Cardiol. 2011;108(4):586–90.
41. Breitkreutz R, Price S, Steiger HV, et al. Focused echocardiographic evaluation in life support and peri-resuscitation of emergency patients: a prospective trial. Resuscitation. 2010;81(11):1527–33.
42. Lichtenstein D, Mézière G, Biderman P, et al. The comet tail artifact. An ultrasound sign of alveolar-interstitial syndrome. Am J Respir Crit Care Med. 1997;156(5):1640–6.
43. Soldati G, Inchingolo R, Smargiassi A, et al. Ex vivo lung sonography: morphologic-ultrasound relationship. Ultrasound Med Biol. 2012;38(7):1169–79.
44. Bouhemad B, Brisson H, Le-Guen M, et al. Bedside ultrasound assessment of positive end-expiratory pressure-induced lung recruitment. Am J Respir Crit Care Med. 2011;183(3):341–7.
45. Chiumello D, Mongodi S, Algieri I, et al. Assessment of lung aeration and recruitment by CT scan and ultrasound in ARDS patients. Crit Care Med. 2018;46(11):1761–8.
46. Bouhemad B, Liu ZH, Arbelot C, et al. Ultrasound assessment of antibiotic-induced pulmonary reaeration in ventilator-associated pneumonia. Critical Care Med. 2010;38(1):84–92.
47. Baldi G, Gargani L, Abramo A, et al. Lung water assessment by lung ultrasonography in intensive care: a pilot study. Intensive Care Med. 2013;39(1):74–84.
48. Zhao Z, Jiang L, Xi X, et al. Prognostic value of extravascular lung water assessed with lung ultrasound score by chest sonography in patients with acute respiratory distress syndrome. BMC Pulm Med. 2015;15:98.
49. Caltabeloti F, Monsel A, Arbelot C, et al. Early fluid loading in acute respiratory distress syndrome with septic shock deteriorates lung aeration without impairing arterial oxygenation: a lung ultrasound observational study. Crit Care. 2014;18(3):R91.
50. Yin W, Zou T, Qin Y, et al. Poor lung ultrasound score in shock patients admitted to the ICU is associated with worse outcome. BMC Pulm Med. 2019;19(1):1.
51. Tusman G, Acosta CM, Costantini M. Ultrasonography for the assessment of lung recruitment maneuvers. Crit Ultrasound J. 2016;8(1):8.
52. Bouhemad B, Rouby JJ. Bedside ultrasound assessment of positive end expiratory pressure–induced lung recruitment. Am J Respir Crit Care Med. 2012;185(4):457–8.
53. Du J, Tan J, Yu K, et al. Lung recruitment maneuvers using direct ultrasound guidance: a case study. Respir Care. 2014;60(5)
54. Mancebo J, Fernández R, Blanch L, et al. A multicenter trial of prolonged prone ventilation in severe acute respiratory distress syndrome. Am J Respir Crit Care Med. 2006;173(11):1233–9.
55. Wang XT, Ding X, Zhang HM, et al. Lung ultrasound can be used to predict the potential of prone positioning and assess prognosis in patients with acute respiratory distress syndrome. Crit Care. 2016;20(1):385.
56. Soummer A, Perbet S, Brisson H, et al. Ultrasound assessment of lung aeration loss during a successful weaning trial predicts postextubation distress. Crit Care Med. 2012;40(7):2064–72.
57. Umbrello M, Formenti P. Ultrasonographic assessment of diaphragm function in critically ill subjects. Respir Care. 2016;61(4):542–55.
58. Demoule A, Jung B, Prodanovic H, et al. Diaphragm dysfunction on admission to the intensive care unit. Prevalence, risk factors, and prognostic impact—a prospective study. Am J Respir Crit Care Med. 2013;188(2):213–9.
59. Boussuges A, Gole Y, Blanc P. Diaphragmatic motion studied by M-mode ultrasonography. Chest. 2009;135(2):391–400.
60. Mayo P, Volpicelli G, Lerolle N, et al. Ultrasonography evaluation during the weaning process: the heart, the diaphragm, the pleura and the lung. Intensive Care Med. 2016;42(7):1107–17.
61. Goligher EC, Laghi F, Detsky ME, et al. Measuring diaphragm thickness with ultrasound in mechanically ventilated patients: feasibility, reproducibility and validity. Intensive Care Med. 2015;41(4):642–9.

62. Gottesman E, Mccool FD. Ultrasound evaluation of the paralyzed diaphragm. Am J Respir Crit Care Med. 1997;55(5):1570–4.
63. Summerhill EM, El-Sameed YA, Glidden TJ, et al. Monitoring recovery from diaphragm paralysis with ultrasound. Chest. 2008;133(3):737–43.
64. David C, Benditt JO, Scott E, et al. Diaphragm thickening during inspiration. J Appl Physiol. 1997;83(1):291–6.
65. Ueki J, De Bruin PF, Pride NB. In vivo assessment of diaphragm contraction by ultrasound in normal subjects. Thorax. 1995;50(11):1157–61.
66. Ayoub J, Cohendy R, Dauzat M, et al. Non-invasive quantification of diaphragm kinetics using m-mode sonography. Can J Anaesth. 1997;44(7):739–44.
67. Wait JL, Nahormek PA, Yost WT, et al. Diaphragmatic thickness-lung volume relationship in vivo. J Appl Physiol. 1989;67(4):1560–8.
68. Umbrello M, Formenti P, Longhi D, et al. Diaphragm ultrasound as indicator of respiratory effort in critically ill patients undergoing assisted mechanical ventilation: a pilot clinical study. Crit Care. 2015;19(1):161.
69. Harris RS, Giovannetti M, Kim BK. Normal ventilatory movement of the right hemidiaphragm studied by ultrasonography and pneumotachography. Radiology. 1983;146(1):141–4.
70. Zambon M, Greco M, Bocchino S, et al. Assessment of diaphragmatic dysfunction in the critically ill patient with ultrasound: a systematic review. Intensive Care Med. 2017;43(1):29–38.
71. Cardenas LZ, Santana PV, Caruso P, et al. Diaphragmatic ultrasound correlates with inspiratory muscle strength and pulmonary function in healthy subjects. Ultrasound Med Biol. 2018;44(4):786–93.
72. Kim WY, Suh HJ, Hong SB, et al. Diaphragm dysfunction assessed by ultrasonography: influence on weaning from mechanical ventilation. Crit Care Med. 2011;39(12):2627–30.
73. Dinino E, Gartman EJ, Sethi JM, et al. Diaphragm ultrasound as a predictor of successful extubation from mechanical ventilation. Thorax. 2014;69(5):431–5.
74. Ferrari G, De Filippi G, Elia F, et al. Diaphragm ultrasound as a new index of discontinuation from mechanical ventilation. Crit Ultrasound J. 2014;6(1):8.
75. Farghaly S, Hasan AA. Diaphragm ultrasound as a new method to predict extubation outcome in mechanically ventilated patients. Aust Crit Care. 2016;30(1):37–43.
76. Sferrazza Papa GF, Pellegrino GM, Di Marco F, et al. A review of the ultrasound assessment of diaphragmatic function in clinical practice. Respiration. 2016;91(15):403–11.
77. Boussuges A, Gole Y, Blanc P. Diaphragmatic motion studied by m—mode uhrasonography: methods, reproducibility and normal values. Chest. 2009;135(2):391–400.
78. Lloyd T, Tang YM, Benson MD, et al. Diaphragmatic paralysis:the use of M mode ultrasound for diagnosis in adults. Spinal Cord. 2006;44(8):505–8.
79. Ayoub J, Cohendy R, Prioux J, et al. Diaphragm movement before and after cholecystectomy: a sonographic study. Anesth Analg. 2001;92(3):755–61.
80. Kim SH, Na S, Choi JS, et al. An evaluation of diaphragmatic movement by M-mode sonography as a predictor of pulmonary dysfunction after upper abdominal surgery. Anesth Analg. 2010;110(5):1349–54.
81. Matamis D, Soilemezi E, Tsagourias M, et al. Sonographic evaluation of the diaphragm in critically ill patients. Technique and clinical applications. Intensive Care Med. 2013;39(5):801–10.
82. Beatriz L, Cecilia H, Ana A. Electrical impedance tomography. Ann Transl Med. 2018;6(2):26.
83. Bachmann MC, Morais C, Bugedo G, et al. Electrical impedance tomography in acute respiratory distress syndrome. Crit Care. 2018;22(1):263.
84. Frerichs I. Electrical impedance tomography (EIT) in applications related to lung and ventilation: a review of experimental and clinical activities. Physiol Meas. 2000;21(2):R1–21.
85. Shono A, Kotani T. Clinical implication of monitoring regional ventilation using electrical impedance tomography. J Intensive Care. 2019;7:4.
86. Yoshida T, Torsani V, Gomes S, et al. Spontaneous effort causes occult pendelluft during mechanical ventilation. Am J Respir Crit Care Med. 2013;188(12):1420–7.

87. Frerichs I, Hinz J, Herrmann P, et al. Regional lung perfusion as determined by electrical impedance tomography in comparison with electron beam CT imaging. IEEE Trans Med Imaging. 2002;21(6):646–52.
88. Morais C, De S, Filho J, et al. Monitoring of pneumothorax appearance with electrical impedance tomography during recruitment maneuvers. Am J Respir Crit Care Med. 2017;195(8):1070–3.
89. Chen L, Del Sorbo L, Luca Grieco D, et al. Airway closure in acute respiratory distress syndrome: an underestimated and misinterpreted phenomenon. Am J Respir Crit Care Med. 2018;197:132–6.
90. Sun XM, Chen GQ, Zhou YM, et al. Airway closure could be confirmed by electrical impedance tomography. Am J Respir Crit Care Med. 2018;197:138–41.
91. Hillner BE, et al. Impact of 18F-FDG PET used after initial treatment of cancer: comparison of the National Oncologic PET registry 2006 and 2009 cohorts. J Nucl Med. 2012;53(5):831–7.
92. Johnson GB, et al. Future of thoracic PET scanning. Chest. 2015;147(1):25–30.
93. Brownell GL, Sweet WH. Localization of brain tumors with positron emitters. Nucleonics. 1953;11(11):40–5.
94. Koukourakis G, et al. Overview of positron emission tomography chemistry: clinical and technical considerations and combination with computed tomography. J BUON. 2009;14(4):575–80.
95. Ter-Pogossian MM, et al. A positron-emission transaxial tomograph for nuclear imaging (PETT). Radiology. 1975;114(1):89–98.
96. Phelps ME, et al. Application of annihilation coincidence detection to transaxial reconstruction tomography. J Nucl Med. 1975;16(3):210–24.
97. Khalil MM. Basic science of PET imaging. Heidelberg: Springer; 2017.
98. Harris RS, Schuster DP. Visualizing lung function with positron emission tomography. J Appl Physiol. 2007;102(1):448–58.
99. Rhodes CG, et al. Quantification of regional V/Q ratios in humans by use of PET. I. Theory. J Appl Physiol (1985). 1989;66(4):1896–904.
100. Rhodes CG, et al. Quantification of regional V/Q ratios in humans by use of PET. II. Procedure and normal values. J Appl Physiol. 1989;66(4):1905–13.
101. Mijailovich SM, Treppo S, Venegas JG. Effects of lung motion and tracer kinetics corrections on PET imaging of pulmonary function. J Appl Physiol (1985). 1997;82(4):1154–62.
102. Musch G, et al. Topographical distribution of pulmonary perfusion and ventilation, assessed by PET in supine and prone humans. J Appl Physiol (1985). 2002;93(5):1841–51.
103. Galletti GG, Venegas JG. Tracer kinetic model of regional pulmonary function using positron emission tomography. J Appl Physiol (1985). 2002;93(3):1104–14.
104. O'Neill K, et al. Modeling kinetics of infused 13NN-saline in acute lung injury. J Appl Physiol (1985). 2003;95(6):2471–84.
105. Musch G, et al. Mechanism by which a sustained inflation can worsen oxygenation in acute lung injury. Anesthesiology. 2004;100(2):323–30.
106. Musch G, et al. Relation between shunt, aeration, and perfusion in experimental acute lung injury. Am J Respir Crit Care Med. 2008;177(3):292–300.
107. Richard JC, et al. Quantitative assessment of regional alveolar ventilation and gas volume using 13N-N2 washout and PET. J Nucl Med. 2005;46(8):1375–83.
108. Wellman TJ, et al. Measurement of regional specific lung volume change using respiratory-gated PET of inhaled 13N-nitrogen. J Nucl Med. 2010;51(4):646–53.
109. Chesler DA, et al. Three-dimensional reconstruction of lung perfusion image with positron detection. J Nucl Med. 1975;16(1):80–2.
110. Hnatowich DJ. Labeling of tin-soaked albumin microspheres with 68Ga. J Nucl Med. 1976;17(1):57–60.
111. Hofman MS, et al. 68Ga PET/CT ventilation-perfusion imaging for pulmonary embolism: a pilot study with comparison to conventional scintigraphy. J Nucl Med. 2011;52(10):1513–9.

112. Borges JB, et al. Ventilation distribution studies comparing Technegas and "Gallgas" using 68GaCl3 as the label. J Nucl Med. 2011;52(2):206–9.
113. Richter T, et al. Reduced pulmonary blood flow in regions of injury 2 hours after acid aspiration in rats. BMC Anesthesiol. 2015;15:36.
114. Schuster DP, et al. Regional pulmonary perfusion in patients with acute pulmonary edema. J Nucl Med. 2002;43(7):863–70.
115. Velazquez M, Schuster DP. Perfusion redistribution after alveolar flooding: vasoconstriction vs. vascular compression. J Appl Physiol (1985). 1991;70(2):600–7.
116. Mintun MA, et al. Measurements of pulmonary vascular permeability with PET and gallium-68 transferrin. J Nucl Med. 1987;28(11):1704–16.
117. Velazquez M, et al. Regional lung water measurements with PET: accuracy, reproducibility, and linearity. J Nucl Med. 1991;32(4):719–25.
118. Jacene HA, Cohade C, Wahl RL. F-18 FDG PET/CT in acute respiratory distress syndrome: a case report. Clin Nucl Med. 2004;29(12):786–8.
119. Chen DL, Schuster DP. Positron emission tomography with [18F]fluorodeoxyglucose to evaluate neutrophil kinetics during acute lung injury. Am J Physiol Lung Cell Mol Physiol. 2004;286(4):L834–40.
120. Bellani G, et al. Lungs of patients with acute respiratory distress syndrome show diffuse inflammation in normally aerated regions: a [18F]-fluoro-2-deoxy-D-glucose PET/CT study. Crit Care Med. 2009;37(7):2216–22.
121. Bellani G, et al. Lung regional metabolic activity and gas volume changes induced by tidal ventilation in patients with acute lung injury. Am J Respir Crit Care Med. 2011;183(9):1193–9.
122. Chrysikopoulos, H.S., Clinical MR imaging and physics. 2009.
123. Bieri O. Ultra-fast steady state free precession and its application to in vivo 1 H morphological and functional lung imaging at 1.5 tesla. Magn Reson Med. 2013;70(3):657–63.
124. Johnson KM, et al. Optimized 3D ultrashort echo time pulmonary MRI. Magn Reson Med. 2013;70(5):1241–50.
125. Albert MS, et al. Biological magnetic resonance imaging using laser-polarized 129Xe. Nature. 1994;370(6486):199–201.
126. MacFall JR, et al. Human lung air spaces: potential for MR imaging with hyperpolarized he-3. Radiology. 1996;200(2):553–8.
127. Matsuoka S, et al. Functional MR imaging of the lung. Magn Reson Imaging Clin N Am. 2008;16(2):275–89. ix
128. McGee KP, et al. Magnetic resonance assessment of parenchymal elasticity in normal and edematous, ventilator-injured lung. J Appl Physiol (1985). 2012;113(4):666–76.
129. Cereda M, et al. Quantitative imaging of alveolar recruitment with hyperpolarized gas MRI during mechanical ventilation. J Appl Physiol. 2011;110(2):499–511.
130. Kuethe DO, et al. Magnetic resonance imaging provides sensitive in vivo assessment of experimental ventilator-induced lung injury. Am J Physiol Lung Cell Mol Physiol. 2016;311(2):L208–18.
131. Chiumello D, et al. Clinical review: lung imaging in acute respiratory distress syndrome patients--an update. Crit Care. 2013;17(6):243.
132. Nensa F, et al. Clinical applications of PET/MRI: current status and future perspectives. Diagn Interv Radiol. 2014;20:438–47.

Chapter 4
Lung Volume Measurement

Jian-Fang Zhou and Jian-Xin Zhou

4.1 Definition of Lung Volumes

Static lung volumes are commonly described as volumes or capacities. Volumes are not subdivided and include tidal volume (V_t), inspiratory reserve volume (IRV), expiratory reserve volume (ERV), and residual volume (RV). However, capacities consist of at least two lung volumes and include total lung capacity (TLC), vital capacity (VC), functional residual capacity (FRC), and inspiratory capacity (IC) (Fig. 4.1). Definition of lung volumes are described in Table 4.1.

4.1.1 Plethysmography

Plethysmography is a mature technique for the determination of lung function, especially FRC and TLC.

Sixty years ago, Dubois et al. used somatic plethysmography to measure lung volumes [1]. Since then, the technology has been improved continuously. Besides the classical whole-body plethysmography, new kinds of plethysmography have been developed, such as optoelectronic plethysmography (OEP), respiratory inductance plethysmography (RIP), and dual band respiratory inductance plethysmography, most of which are mainly used in animal experiment. We will focus on the whole-body plethysmography and OEP in this section.

J.-F. Zhou · J.-X. Zhou (✉)
Department of Critical Care Medicine, Beijing Tiantan Hospital, Capital Medical University, Beijing, China

J. Zhou et al. (eds.), *Respiratory Monitoring in Mechanical Ventilation*,
https://doi.org/10.1007/978-981-15-9770-1_4

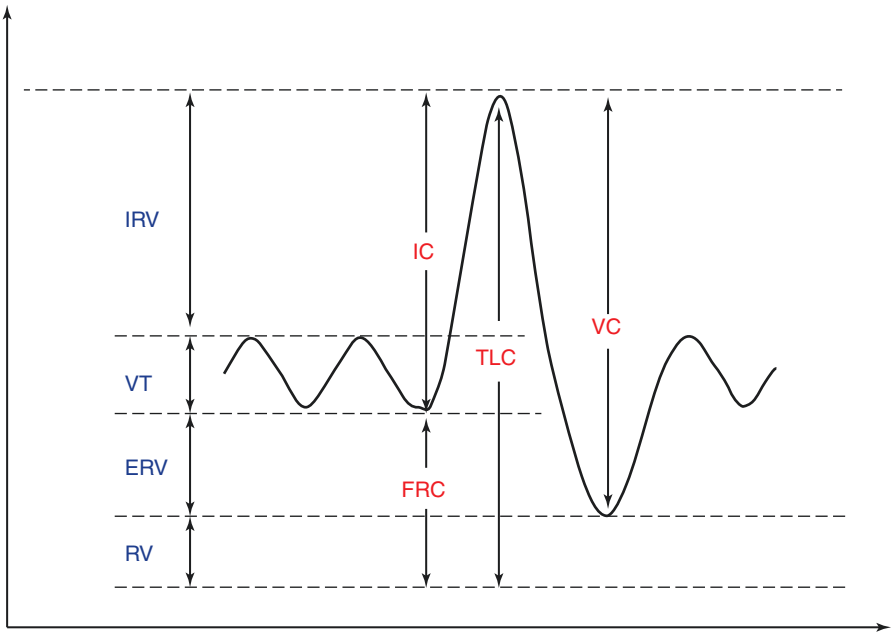

Fig. 4.1 Lung volumes and capacities. *IRV* Inspiratory reserve volume, V_t Tidal volume, *ERV* Expiratory reserve volume, *RV* Residual volume, *IC* Inspiratory capacity, *FRC* Functional residual capacity, *TLC* Total lung capacity, *VC* Vital capacity

4.1.2 Body Plethysmography

4.1.2.1 Principle and Measuring Methods of Whole-Body Plethysmography

The basic physical principle of the whole-body plethysmography is Boyle-Mariotte's Law, which states that the volume of a perfect gas varied inversely with its pressure at a constant temperature and can be expressed as the following equation:

$$PV = K$$

where K is a constant, P is pressure, and V is volume.

For the purpose of measuring lung volumes, as the temperature of lungs in a short time is constant, this law can be interpreted as that: for a fixed mass of gas in a closed compartment, the relative changes in volume of the compartment are always inversely proportional to changes in pressure, and can be expressed as the following equation:

$$P_iV_i = P_fV_f$$

where P_i, V_i is the initial pressure and volume, and P_i, V_i is the final pressure and volume.

Table 4.1 Definition of lung volumes

Tidal volume (V_T)	the volume of air inhaled and exhaled into the lungs in a normal resting breathing.
Inspiratory reserve volume (IRV)	The maximal volume of air that can be inhaled after a normal inspiration.
Expiratory reserve volume (ERV)	The maximal volume of air that can be exhaled after a normal expiration, also the volume of air exhaled from FRC to point of maximal exhalation (RV), so ERV equals FRC minus RV.
Residual volume (RV)	The volume of air still remaining in the lungs after the most forcible expiration.
Total lung capacity (TLC)	The volume of air contained in the lungs at the end of a maximal inspiration and equals IC plus FRC, also equals VC plus RV.
Vital capacity (VC)	The maximum amount of air exhaled from the lungs after a maximum inspiration. It is equal to the sum of IRV, V_T, and ERV.
Functional residual capacity (FRC)	The volume of air present in the lungs at the end of a tidal volume breath, and is the sum of ERV and RV.
Inspiratory capacity (IC)	The maximum volume of air that can be inspired after reaching the end of a normal, quiet expiration. It is the sum of V_T and the IRV.
Forced vital capacity (FVC)	The amount of air can be forcibly exhaled out of the lungs after taking a breath to fill the lungs as much as possible.
Forced expiratory volume in 1 s (FEV1)	The volume of air that can forcibly be blown out in the first 1 s, after full inspiration.
End-expiratory lung volume (EELV)	The volume of air present in the lungs at the end of a tidal volume expiration in mechanical ventilation patients. If PEEP (positive end-expiratory pressure) or CPAP (continuous positive airway pressure) is unused, EELV might be close to the FRC.

If absolute changes of volume are known and the initial and final pressure can be measured, the initial volume of the closed compartment can be calculated.

Thus, if we think a lung as a closed compartment, it is possible to measure the volume of lungs as long as the final volume is known and both the initial and final pressure in alveolar can be measured. The initial volume (unknown) of lungs times the initial pressure is equal to the final volume times the final pressure. Based on this principle, the fumined as follows:

$$\mathrm{FRC} = Kv\frac{\Delta V_{\mathrm{box}}}{\Delta P_{\mathrm{mouth}}}, Kv \approx P\,\mathrm{Baromeric}$$

where ΔV_{box} is the change of volume in the box of body plethysmography when the subject breath normally, and $\Delta P_{\mathrm{mouth}}$ is the change of pressure at the mouth.

Prior to the measurement, the flow and volume should be calibrated using a syringe with calibrated volume [2]. The cabin pressure and mouth pressure should also be calibrated according to the instruction of the manufacturer.

When measuring lung volumes by a body plethysmograph, the test subject should enter into a sealed chamber and hold a mouthpiece in the mouth [3].

Commonly, the lung function test starts with resting normal breath. The pressure at the mouth and in the chamber are measured simultaneously. The mouthpiece will be closed at the end of a normal expiration. Then the patient is instructed to inhale. Inhalation starts from the end-expiration lung volume. As the inspiratory muscles contract, the thoracic and lungs expand, and volumes of thoracic and lungs increase at the same time. As the organs in the thorax are incompressible, the increase of volumes in thorax and lung would be equal. As the volume changes, the decrease of pressure would follow Boyle-Mariotte's law because the instrument is sealed.

If the airway resistance is close to zero, an infinite airflow would quickly enter the lungs without any pressure gradient, and the pressure of the lungs and chamber will increase instantly. Conversely, if the airway is occluded during the inspiratory exercise, the alveolar pressure might decrease greatly, but no airflow enters the lungs.

Actually, there is resistance in the airway and the resistance is finite. Therefore, only when the pressure gradient between the lungs and the chamber overcomes the resistance of the airways, the flow will start to enter into lungs. In other words, the movement of airflow lags behind changes in lung volume. The airflow lag caused by the slight pressure difference in the breathing cycle is called "shift volume," which is much smaller than tidal volume. Shift volume is dynamic and exists in both inhalation and exhalation processes. It is generated by the dynamic pressure change within the lungs and represents the amount of gas that needs to be compressed or decompressed in order to drive the airflow during inspiration or expiration.

During inspiration, this shift volume leads to a pressure drop in the lung, resulting in the flowing of air into lungs, and the opposite is true during expiration. The degree of this pressure drop is related to airway resistance, and airflow can only be generated by overcoming airway resistance. The shift volume represents the volume defect in lungs and the box. As the box is sealed and the walls are very stable, change in lung volume should be equal but opposite to change in the free volume of the box. The free volume of the box can be calculated as follows:

$$Volume_{free} = Volume_{box} - Volume_{body}$$

where $\text{Volume}_{\text{free}}$ is the free volume of the box; $\text{Volume}_{\text{box}}$ is the volume of the box; and $\text{Volume}_{\text{body}}$ is the body volume estimated from the body weight.

As the $\text{Volume}_{\text{free}}$ is computed, the shift volume can be derived from the pressure change according to Boyle-Mariotte's law. Thereby, airway resistance can be evaluated.

Due to the effect of the inspiratory muscles, the volume of the chest cavity increases with the increase of air in lungs. The muscles will maintain their tension for a short period of time. At the end of inspiration, pressure equilibration is reached and the shift volume is reduced to zero. The inspired volume measured at the mouth equals the increase in lung volume, and both represent inspiratory tidal volume (V_{Tin}). Exhalation is reversed but similar to inhalation. With the relaxation of the

respiratory muscles, the lung volumes decrease due to the chest and lung elastic recoil. The expiratory movement continues until the recoil forces of lung and chest wall become equal, and the pressures of alveolar and the box reach equilibrium. At the end of expiration, airflow and shift volume return to zero. Both the expired volume and the volume reduction of lungs can be measured and represent expiratory tidal volume (V_{Tex}).

Other lung volume parameters can be measured by the shutter maneuver. After opening of the shutter, the subject can be instructed to inhale maximally after a normal inspiration, and the IVC can be measured. A similar way can be used to measure the ERV. Then RV and TLC can be computed. Combined with spirometry, a prolonged forced expiration can be performed to measure the forced expiratory volume in 1 s (FEV1) and the forced vital capacity (FVC). Airway resistance can also be measured by spirometry. In this way, information about lung mechanics can be obtained (Fig. 4.1).

4.1.2.2 Clinical Application

Body plethysmographs can measure a variety of respiratory parameters, reflecting lung function and structure. It can provide information on characteristics such as RV and TLC, airway resistance and intrathoracic gas volume (ITGV) 3,4, which is helpful for the differential diagnosis of obstructive airway diseases and restrictive diseases (Table 4.2). Body plethysmography can measure a variety of respiratory parameters reflecting functional and structural aspects of the respiratory system. It can provide information on RV, TLC, and other characteristics, such as airway resistance and intrathoracic gas volume (ITGV) [4, 5], which are helpful for differential diagnosis of obstructive airway diseases and restrictive diseases [3] (Table 4.2). For patients with severe obstructive disease and air-trapping, body plethysmography is particularly appropriate as it is the only technique for FRC measurement including air trapped within the lungs at the distal end of closed airways.

Body plethysmography is the gold standard of TLC and FRC. However, it is irremovable and needs the cooperation of patients, and it is unsafe and impracticable to place a patient undergo mechanical ventilation into a sealed chamber. Therefore, it is not suitable for most of the critically ill patients.

Table 4.2 Differential diagnosis of obstructive airway diseases and restrictive diseases by lung function test

	Raw	RV	TLC	FRC
Obstructive airway diseases	Elevated	Normal or elevated	Normal	Normal or elevated
Restrictive diseases	Normal	Reduced or normal	Reduced	Reduced

4.1.3 Optoelectronic Plethysmography (OEP)

4.1.3.1 Principle of OEP

OEP uses a three-dimensional motion capture system to measure the changes of the chest wall (both absolute values and their variations) during breathing by modeling the surface of the chest and abdomen. OEP uses infrared imaging to assess respiratory kinematics by placing a number of markers on the subject's chest and abdomen surface (Fig. 4.2) and tracking the three-dimensional coordinates of those markers [6–9].

For the standing position, an 89-marker protocol is usually used [9, 10]. According to Aliverti et al. [11] and Romei et al. [12], for subjects in supine

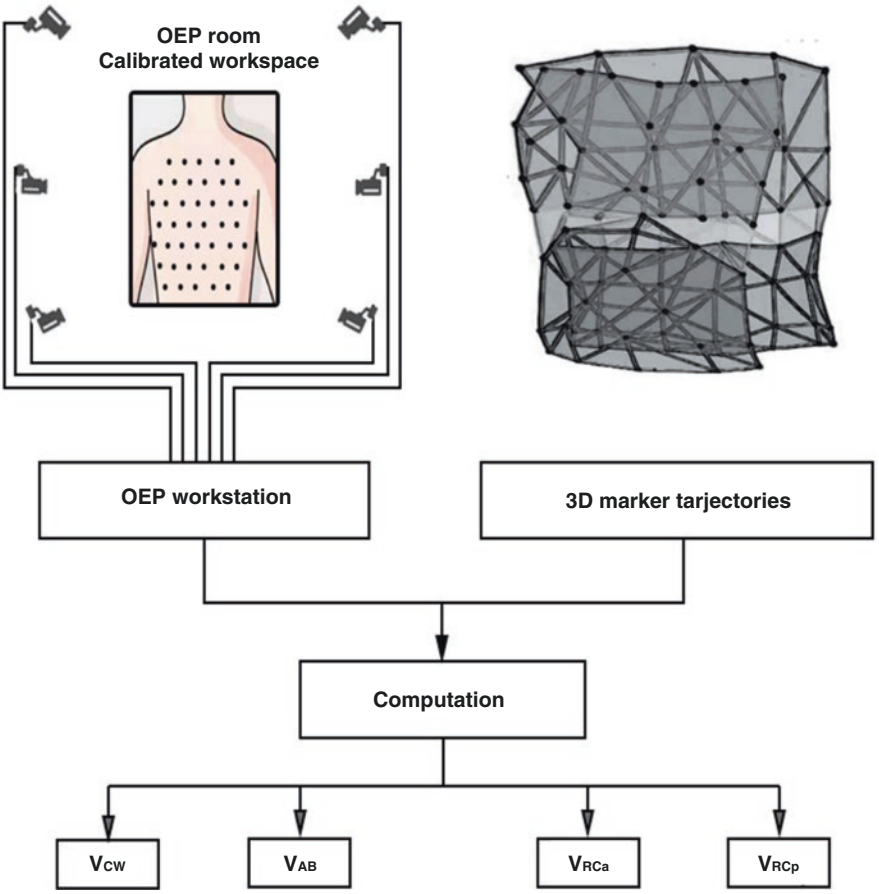

Fig. 4.2 Schematic of OEP working principle; 3D human chest wall reconstructed starting from 3D markers. V_{CW}, V_{RCp}, V_{RCa}, and V_{AB} refer to the volume of pulmonary rib cage, the abdominal rib cage, and the abdomen, respectively. The V_{CW} is the sum of RCp and RCa volumes

position or prone position, such as patients in intensive care unit (ICU), a 52-marker protocol can be used. Four to eight infrared (IR) cameras are used to capture and track the movement of markers that can reflect infrared light. A dedicated workstation is used to synchronize the input and output information to and from cameras. The specialized software in the workstation will compute the three-dimensional trajectories of makers by integrating the information collected from each camera. Then, a geometrical model is applied to measure lung volumes. In this model, every three markers form a triangle and one triangle is defined as a closed surface. The software will calculate the volume contained in each surface. Therefore, we can obtain volume variations of the entire chest wall and its different compartments by using OEP.

4.1.3.2 Calibration

The equipment of OEP should be calibrated before using. First, the 3D position (x, y, and z axes) of a calibration tool need to be calibrated. Each camera should recognize all three axes, otherwise the camera's position needs to be readjusted until it can cover three axes. Then the y-axis to the plane where the subject is located should be measured by moving the wand. At the same time, it is necessary to ensure that cameras can detect the wand as it moves in the range of motion. If the wand cannot be detected, the technician should adjust the speed and movement of cameras [13].

4.1.3.3 Volume Measurements

As shown in Fig. 4.2, the thoracoabdominal lung volume can be divided into three different parts: pulmonary rib cage (RCp), abdominal rib cage (RCa), and the abdomen (AB). RCp begins at the clavicles and jugular notch and ends at the xiphoid; the range of RCa is from the xiphisternum to the lower costal margin; AB ranges from the lower costal margin to the bilateral anterior superior iliac crests. Abdominal volume change refers to the volume change caused by abdominal wall movement, and is the result of the combined action of the diaphragm and expiratory abdominal muscles. This model is the most suitable for studying chest wall kinematics in most conditions, including rest and exercise. It takes into consideration the differences of pressures acting on the RCp and RCa during inspiration. The diaphragm acts directly only on RCa, while other inspiratory muscles mainly act on RCp other than RCa [14]. Lung volumes can be divided into right and left lung volumes.

As described in detail in previous studies [6, 15, 16], lung volumes are calculated by summing the changes of the triangulated surface areas. The following volume variables can be measured by OEP: end-expiratory volume of chest wall (Veecw), pulmonary rib cage (Veercp), abdominal rib cage (Veerca), and abdomen (Veeab); end-inspiratory volume of chest wall (Veicw), pulmonary rib cage (Veircp),

abdominal rib cage (Veirca), and abdomen (Veiab). Tidal volumes of chest wall (V_{cw}), pulmonary rib cage (V_{RCp}), abdominal rib cage (V_{RCa}), and abdomen (V_{AB}) can be assessed by calculating differences of end-inspiratory volumes and end-expiratory volumes. The percentages of volumes of each part to the entire chest volume can also be calculated.

4.1.3.4 Clinical Application

OEP can be used to measure changes in lung volumes in a different status, such as exercising and resting. OEP has also been validated for measuring lung volumes of infants and patients with chronic obstructive pulmonary disease [11, 17, 18]. It is particularly suitable for critically ill patients as the measuring process is noninvasive and does not need the cooperation of patients, and it has also been validated on patients in the prone and supine positions. For mechanically ventilated patients, OPE can assess volume changes of each compartment of the chest wall precisely and can assess action and control of different respiratory muscle groups. Combined with pressure variables, chest wall dynamics can also be assessed.

4.2 Spirometry

A spirometer is an instrument that can measure the volume of air inhaled and exhaled by the lungs. Spirometry is the most commonly used pulmonary function test and is useful in the diagnosis and differential diagnosis of respiratory diseases. Spirometry uses a pneumotachograph to measure volumes, flow rate of air, and frequency of the ventilatory cycle simply and noninvasively [19].

The earliest spirometer appeared in nineteenth century [20, 21]. In 1813, Kentish invented his “Pulmometer,” which had a graduated bell jar in water, with an outlet at the top controlled by a tap. He was the first to try to study ventilatory volumes in disease, and he used his Pulmometer to measure the ventilatory volumes of his three “bronchitis chronica.” He found that the ventilatory volumes of the patients were much lower than those expected, and thought that ventilatory volumes were affected by “mechanical obstruction” and “inflamed state of the bronchiae (*sic*), causing spasmodic action” [21]. An English physician named John Hutchinson invented a spirometer, and he recorded the vital capacities of over 4000 subjects. He found that the vital capacity had a linear relationship with height. Since then, a number of papers described different machines to measure ventilation. Gad (1879) and Regnard (1879) were regarded as the first ones to use spirometers with graphic records [21]. In the twentieth century, more elaborate closed-circuit machines were invented and used to measure lung volumes [21]. In 1959, Wright B.M. and McKerrow C.B. introduced the peak flow meter, which was much cheaper, lighter, and easier for use and could give rapid information in the ward or in the home of patient [21].

4.2.1 Measuring Method

With the improvement of technologies, many spirometers designed for use in primary care do not require daily calibration. However, equipment maintenance, accuracy, and precision checks are still essential for quality spirometry. The international standards state that the volume accuracy and airtightness of the spirometer should be checked at least once a day with a 3 L calibrated syringe, and the measurement errors of volumes should be within acceptable ranges [22]. At the same time, the accuracy of the syringe volume must be guaranteed. The environment of storage and use of the syringe should be with the same temperature and humidity of the test site. The linearity of flow should be checked weekly and that of volume should be checked quarterly. The accuracy of the time scale of the mechanical recorder should be checked with a stopwatch at least quarterly. If a large number of subjects are tested within a day, or the ambient temperature of the test site is changing, the accuracy of the spirometer should be checked more frequently than daily. Volume-type spirometers must be checked for airtightness every day [23].

The most important lung volumes that can be measured by spirometry are FVC and FEV1. When measuring those lung volumes, patients are usually in a sitting position with nares occluded by nose clips or hands to prevent leakage of air through the nasal passages. The technician needs to instruct and encourage the patient to perform the breathing maneuvers. First, ask the patient to inhale deeply. Then, a mouthpiece should be put into the mouth of the patient immediately and be held tightly with lips. Exhalation should be performed with as much force as possible, and make sure there is no air leakage during maximal forced exhalation. For subjects older than 10 years, exhalation should last at least 6 s and until no more air can be expelled from the lungs while maintaining an upright posture. For patients with airways obstruction or older age, exhalation times often require>6 s. However, exhalation times does not need to exceed 15 s. The patient is allowed to rest for a few seconds and the breathing maneuvers need to be repeated until three acceptable maneuvers are obtained [24]. Usually, at least three maneuvers are performed, but if one or more of the maneuvers do not meet the requirement, more attempts should be performed. However, the number of attempts should be not more than eight, which is generally a practical upper limit for most subjects [25, 26]. Multiple prolonged exhalations within a short time may lead to different uncomfortable symptoms, such as light-headedness, syncope, fatigue, and so on. If a patient feels dizzy, the test should be stopped, otherwise syncope might occur due to decreased venous return caused by increased intrathoracic pressure. In order to guarantee the accuracy of lung volumes measured by spirometers, the most important task is to instruct the subject to inhale and exhale rapidly and completely. The waveforms and data should be assessed for reliability and accuracy before analysis. Even if the instrument is accurate, the results obtained by spirometers might be misleading for clinical diagnosis and treatment if the patient did not breath with maximum strength. During measurement, a cough, hesitation, or hold of breath may affect the measured values of FEV1 and FVC [24]. Leakage at the mouth or near or obstruction of the

mouthpiece may also influence the accuracy of measured values. Patients with neuromuscular disease may need assistance from technicians or family members to keep the airtightness of the mouth.

A spirometer can also be used to measure VC and IC. However, the spirometer must meet the requirements for measuring FVC and can be capable of accumulating volume for at least 30 s. When measuring VC, the subject should be instructed and demonstrated how to breathe appropriately in the VC maneuver. The subject should wear a nose clip and be in a seated position. The subject needs to inhale completely from the full expiration position (RV) to assess the IVC or exhale completely from the full inspiration position (TLC) to assess the EVC. If significant differences between IVC and EVC are detected, there might be airways obstruction [27]. Subjects should be relaxed except at the end of the inspiration and expiration. During the test process, the subject exhales completely to RV, then inhales to TLC, and finally exhales to RV again. When measuring IC, subjects should also be relaxed and breathe regularly for several times until the end-expiratory lung volume is stable. Then the subjects should inhale deeply to TLC without hesitation. At least three acceptable maneuvers should be performed and selected for the measurement of VC and IC.

4.2.2 Clinical Application

Spirometers can be used to diagnose certain types of respiratory diseases, such as asthma, bronchitis, emphysema, and so on. Spirometry can measure FEV1 and FVC, which is widely accepted and used as a clinical tool for diagnosing and differential diagnosing of obstructive, restrictive, or mixed ventilatory dysfunction [28–30]. FEV1 can also be used to evaluate the efficacy of treatments and to monitor the severity of respiratory diseases, especially asthma and chronic obstructive pulmonary disease (COPD).

The flow-volume loop (Fig. 4.3) is a plot of the changes in flow rate (on the *Y*-axis) and volume (on the *X*-axis) of the air during the performance of maximally forced inspiratory and expiratory maneuvers, and it is helpful for differential diagnosis of respiratory diseases, such as upper airway obstruction [31–34], dynamic hyperinflation [35], neuromuscular diseases [36], et al.

For patients with mechanical ventilation, side-stream spirometers can be used to measure flow continuously and lung volumes can also be evaluated by the area under velocity-time curve [37]. Spirometers can also be used to measure PEEP-induced recruitment volumes (PEEP-volumes) at the bedside. When measuring the PEEP-volume, a long expiration hold maneuver should be performed and zero end-expiratory pressure (ZEEP) is required, where FRC is assumed to be reached. If FRC is the same at different levels of PEEP, the difference in end-expiratory lung volumes (EELV) ($\Delta EELV = EELV_{\text{high PEEP}} - EELV_{\text{low PEEP}}$) should theoretically be close to the difference in ΔPEEP-volume ($\text{PEEP volume}_{\text{high PEEP}} - \text{PEEP volume}_{\text{low PEEP}}$).

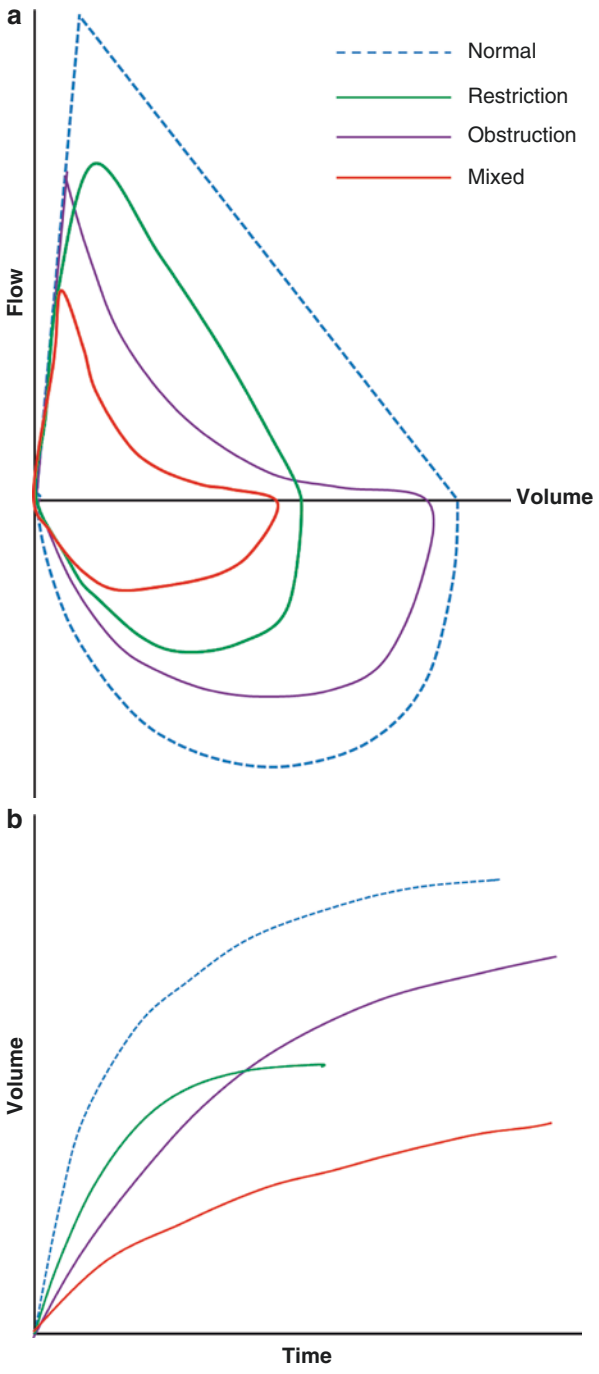

Fig. 4.3 Flow-volume curves of normal, obstruction, restriction, and mixed respiration dysfunction

There are some limitations to spirometry. First, using a fixed FEV1/FVC ratio to define airflow limitation has been criticized as it might result in underdiagnosis in younger subjects and overdiagnosis in elderly subjects. Furthermore, the measurement of lung volumes by spirometers is highly dependent on effort and cooperation of the subject [38].

4.3 Washout/Washin Technique

Washin/washout technique has been applied to measure static lung volumes, and the technique analyzes the concentration changes of a gas with low solubility, such as nitrogen during washin/washout maneuvers.

4.3.1 Washout/Washin technique

Washout/washin technique can be used to measure static lung volumes by inhaling a gas with low blood solubility and continuously measuring and analyzing the concentration of the gas.

Nitrogen washout/washin maneuvers (or Fowler's method) are the most commonly used methods in clinical practice. Nitrogen has low solubility in blood and tissues, low exchange rate in the alveoli, and cannot be absorbed and metabolized by the human body. Thus, it is suitable as a tracer to measure lung volumes, such as dead space volume, functional residual capacity (FRC), or end-expiratory lung volume (EELV), and some other parameters related to airways occlusion, and this method is not directly affected by changes in body metabolism during the measurement process.

4.3.2 Principle

The nitrogen washout/washin technique is based on the law of conservation of mass. There are two types of nitrogen washout/washin techniques, which are single-breath nitrogen test and multiple-breath nitrogen test. Both tests require similar equipment and can estimate FRC/EELV. However, the multiple-breath test might be more accurate in measuring absolute lung volumes.

4.3.3 Single-breath Nitrogen Test

When measuring lung volumes using single-breath nitrogen test, the first step is to increase the fraction of inhaled oxygen (FiO_2) to 1.0, and the patient is directly connected to a spirometer. Ask the subject to take a normal breath of 100% oxygen after

a normal exhalation (at this time the lung volume is FRC or EELV). Then, the subject exhales from V_t. The concentration of N_2, oxygen, and carbon dioxide in exhaled gas are continuously monitored, as well as the gas flow rate.

Resident nitrogen is exhaled out of the lungs progressively. At the beginning, as the subject exhales the pure oxygen that has been inhaled previously but stays in the dead space and is not involved in alveolar exchange, the concentration of nitrogen is initially zero. As the gas in the alveoli exhales and mixes with the gas in the dead space, the nitrogen concentration increases gradually and finally equals to that in the alveoli (C1) [39]. We can obtain the total amount of exhaled gas at any point in time by calculating the area under the flow-time curve. Knowing the total amount of exhaled gas and nitrogen concentration, we can calculate the total amount of exhaled nitrogen (MN). According to the law of conservation of mass, FRC (or EELV) can be calculated by the following equation:

$$M_N = C1 \times \mathrm{FRC}$$

$$\mathrm{FRC} = \frac{M_N}{C1}$$

4.3.4 Multiple-Breath Nitrogen Washout/Washin (MBNW) Test

MBNW method is commonly used for lung function tests in patients with spontaneous breath or mechanical ventilation. Similar to single-breath nitrogen test, at the beginning of MBNW test, FiO_2 is adjusted from the baseline to 1.0. After a normal exhalation (at this time, the amount of gas in the lung is FRC or EELV), the patient is directly connected to a spirometer, and the gas flow rate during breathing is continuously monitored. The concentration of nitrogen is measured from the beginning (C1) to the end of the test. Because there may be nitrogen flushing out of human tissue or signal noise affecting the measurement results, the test can be completed when the nitrogen concentration in the exhaled gas reaches 3% of the baseline [40]. The total amount of exhaled nitrogen (MN) can be calculated according to the total amount of exhaled gas and the real-time concentration of nitrogen. At the beginning and end of the experiment, the amount of N_2 is the same, which is just the amount of N_2 in the FRC. Since there is no material leakage in the system, during the test, the amount of nitrogen remains unchanged (concentration × volume = amount), and the FRC is calculated by the same way of single-breath nitrogen test.

If the patient is initially connected to the spirometer at other lung volumes (such as TLC or RV), the corresponding lung volumes might be measured by the same method. PEEP-induced lung volume changes (referred to as PEEP-volume) can also be assessed simply at the bedside by using passive spirometry. EELV at different PEEP levels can be measured, and the difference in EELV (that is, $\Delta\mathrm{EELV} = \mathrm{EELV}_{\text{high PEEP}} - \mathrm{EELV}_{\text{low PEEP}}$) can be calculated. The patient exhales to zero end-expiratory pressure (ZEEP) for a long time until FRC is assumed to be reached, and the PEEP-volume at different PEEP can be obtained, as well as the difference in PEEP volume

(ΔPEEP volume = PEEP-volume high PEEP − PEEP-volume low PEEP). If the ΔEELV is similar to ΔPEEP volume, we can assume that the FRC has not been modified by the PEEP changes and vice versa.

4.3.5 Modified Nitrogen Washout/Washin Method

Under certain conditions, such as high FiO_2 or high PEEP, the nitrogen washout/washin method might be restricted. Modified nitrogen washout/washin technology can be used to measure FRC or EELV in this situation [41] as this method can be used with a step of small change in FiO_2, and there is no need to interrupt mechanical ventilation. Traditional MBNW methods measure the total amount of nitrogen washed out from the lungs. However, the modified technique estimates the changes of alveolar nitrogen concentration and the variation of tidal volume during washout [42].

The measurement is based on two assumptions: (1) The heterogeneity of the alveolar gas distribution is constant during the measurement process, and the total FRC/EELV does not change until the alveolar gas composition reaches a new equilibrium after changing the FiO_2 [43]; (2) During the measurement, the body's cell metabolism and gas exchange between the pulmonary capillaries and the alveoli are stable.

At the beginning of measurement, the FiO_2 at the ventilator should be changed. In order to measure FRC accurately, the fraction of FiO_2 generally needs to be changed by at least 20% [44, 45]. The air exhaled from the lung consists mainly of O_2, carbon dioxide (CO_2), and N_2. The fraction of nitrogen can be measured with a mass spectrometer technique or calculated as the residual of O_2 and carbon dioxide (CO_2) [40, 45, 46] if the fraction of O_2 and CO_2 are measured continuously during a change in FiO_2, which can be expressed by the following equation [42]:

$$F_i N_2 = 1 - F_i O_2$$

$$F_E N_2 = 1 - F_E O_2 - F_E CO_2$$

(where FiN_2 and FiO_2 are the fraction of nitrogen and oxygen in the inspiratory air, and $F_E N_2$, $F_E O_2$, and $F_E CO_2$ are fraction of N_2, O_2, and CO_2 during the expiration, respectively.)

During measurement, with each additional breath of alveolar ventilation at the increased level of FiO_2, residual nitrogen in the lungs (FiN_2) is diluted and washed out gradually, and the amount of nitrogen remaining in the lung reduces correspondingly. When the nitrogen concentration difference between the washin and washout gas is less than the threshold value set by the manufacturer, the measurement can be terminated and the instrument can calculate the average value of the washin and washout data automatically.

Washout can be completed in 3–4 min in normal subjects. However, for patients with severe obstructive airway disease, the measurement procedure might take more than 15 min, and in this situation the safety of the patient must be guaranteed during the measurement process.

Respiratory gas flow is measured continuously. Gas viscosity is also monitored to correct the measured flow signal [47]. Through the integration of the flow-time curve, the real-time tidal volumes can be calculated. Tidal volume multiplied by the nitrogen concentration is the total amount of nitrogen washed out during exhalation [48]. In order to ensure the accuracy of the calculation, the synchronization of gas flow and concentration measurement should be guaranteed before calculation [40].

The initial volume of nitrogen ($V_{ini}N_2$) in the alveolar is determined by the fraction of nitrogen ($F_{ini}N_2$ and FRC or EELV), and can be expressed as the following equation:

$$V_{\text{ini}}\text{N}_2 = F_{\text{ini}}\text{N}_2 \times \text{FRC}$$

As the FiO_2 is changed and the nitrogen washed out from the lungs, the nitrogen volume in the alveolar changes correspondingly, and the final volume of nitrogen in lungs ($V_{end}N_2$) after the equilibrium time are determined by the final fraction of nitrogen ($F_{end}N_2$) and FRC (or EELV):

$$V_{\text{end}}\text{N}_2 = F_{\text{end}}\text{N}_2 \times \text{FRC}$$

The following equation can be derived if the FRC (or EELV) is constant during the measurement procedure:

$$V_{\text{ini}}\text{N}_2 - V_{\text{end}}\text{N}_2 = \left(F_{\text{ini}}\text{N}_2 - F_{\text{end}}\text{N}_2\right) \times \text{FRC}$$

The fraction of N_2 can be measured directly or calculated by the inverse relationship of changes in fraction of nitrogen and FiO_2:

$$F_{\text{ini}}\text{N}_2 - F_{\text{end}}\text{N}_2 = F_i\text{O}_{2(\text{end})} - F_i\text{O}_{2(\text{ini})}$$

($F_{ini}N_2$ = initial inspiratory N_2 concentration; $F_{end}N_2$ = final N_2 concentration)

The FRC (EELV) can be calculated as follows:

$$\text{FRC} = \frac{\Delta\text{N}_2}{F_{\text{ini}}\text{N}_2 - F_{\text{end}}\text{N}_2} = \Delta\text{N}_2\left(\text{mL}\right) / \Delta Fi\text{O}_2$$

Before calculating the total volume change of nitrogen in alveolar after the change of FiO_2, we can first calculate the breath-by-breath changes of nitrogen. If the inhaled gas is not pure oxygen, inhaled nitrogen should be subtracted when calculating volume change of nitrogen:

$$V_{\text{T}}\text{N}_2 = \left(\text{FiN}_2 \times V_{\text{TAI}}\right) - \left(F_{\text{ET}}\text{N}_2 \times V_{\text{TAE}}\right)$$

(V_TN_2 = breath-by-breath N_2 exchange; FiN_2 = the inspiration N_2 fraction; VTAI = inspiratory alveolar tidal volume; VTAE = expiratory alveolar tidal volume;)

The total change of nitrogen is the sum of each breath changes:

$$\Delta N_2 = \sum V_T N_2$$

The expiratory alveolar tidal volume (VTAE) can be calculated according to Bohr's formula [49].

$$V_{TAE} = V_{CO2} / F_{ETCO2}$$

($FETCO_2$ = end-tidal carbon dioxide fraction; V_{CO2} = Volume of carbon dioxide)

$$V_{AI} = \left(V_I - V_E\right) + V_{AE}$$

(V_{AI} = inspiratory alveolar tidal volume; V_I = inspiratory tidal volume; V_E = expiratory tidal volume)

As the total nitrogen volume change is known, FRC or EELV can be calculated using the above equation.

4.3.6 Clinical Application

In acute lung injury (ALI) and acute respiratory distress syndrome (ARDS), functional residual capacity (FRC) is markedly decreased due to various factors [50]. Measuring FRC (or end-expiratory lung volume [EELV] when PEEP is applied) might help to assess the volume of open and collapsed alveoli, adjust ventilation strategies, and judge their effects [46, 50]. Recently, nitrogen washout/washin technique [41, 43] has been made available in ICU ventilators, allowing bedside EELV measurement. Under certain conditions, such as high FiO_2 or high PEEP, the limitations of nitrogen washout/washin techniques for EELV measurement have not been fully investigated [51].

4.4 Computed Tomography (CT)

CT used in early studies to acquire lung images was a one-of-a-kind scanner developed at the Mayo Clinic (Rochester, MN), which was named as dynamic spatial reconstructor [52, 53]. This scanner could acquire lung volume images in 1/60th of a second. During each static inflation of lungs images were acquired, and ventilation of the region of interest was estimated by assessing regional density changes [54, 55]. Because early CT scanners took as long as 2–5 s to acquire data needed to reconstruct a single slice of the lung, it was hardly used to assess lung

function in the clinical practice and was mainly used for imaging anatomic features. With the development of electron beam CT (EBCT), namely Ultrafast or Cine CT, it has become possible to evaluate both ventilation [56] and perfusion [57] by CT. However, EBCT is currently mainly used for research and is not applied to the clinical arena. In the late 1990s, a new class of CT scanners appeared, called multidetector CT (MDCT) scanners. These MDCT scanners can acquire 64 slices in a single rotation, and one rotation takes only 0.3 s. To obtain lung volumetric images, the subjects only need to hold their breath for 5 s at most. The volume of gas and tissue in the lungs can be assessed by quantitative analysis of CT scan images.

4.4.1 Measuring Lung Volumes by CT

The basic principle of CT is that the X-ray hits the CT detector depends on tissue absorption. X-ray beam transmitted through the body tissue will be captured by the detectors and be converted into visible light, electrical signals, and digital signals in turn. Then, digital signals will be inputted into a computer for processing. In the process of image formation, the body slices will be divided into several cuboids with the same volume, which is called voxel. The attenuation of X-ray can be measured in each voxel or volume element and form a digital matrix. The numbers of voxels depend on the pixel area and thickness of the section and will be converted into different pixels, which are expressed as small squares with different gray levels ranging from black to white. The pixel area depends on the matrix size applied. X-rays pass through the human body, and the attenuation of X-rays has a linear relationship with the physical density (such as radiodensity) of human organs and tissues, which are formed by different composition and with different absorption coefficients. Non-contrast CT images can be obtained by converting attenuation coefficients into gray images.

Lungs volume can be calculated according to the number of voxels present in a specified region. The Hounsfield unit scale (HU) or CT number is a quantitative scale to describe radiodensity. The attenuation of X-ray through air and water is infinitely small. The radiodensity of distilled water is considered to be 0 HU, the radiodensity of bone is +1000, and the radiodensity of air is −1000 HU. The CT number of lung tissue is −500 CT and blood is 20–40 HU. The CT number can reflect density, and the composition of air and tissue ("tissue" includes alveolar edema, interstitial water, blood, and the lung structure) [58] in a given voxel can be estimated according to its CT number and its volume. The CT value of any material can be calculated by the following formula:

$$CT_{\mathrm{m}} = 1000 \times \frac{\mu_{\mathrm{m}} - \mu_{\mathrm{w}}}{\mu_{\mathrm{w}} - \mu_{\mathrm{a}}}$$

where μ_w, μ_a, and μ_m are the attenuation values of water, air, and the material being measured, respectively.

According to this equation, we can calculate the gas/water ratio and gas volume of the given voxel based on CT numbers. For a lung region of interest, if we know the total number of voxels, the total volume, the volume of gas, and the volume of tissue can be computed using the following equations:

$$\text{Volume of the voxel} = \left(\text{size of the pixel}\right)^2 \times \text{section thickness}$$

$$\text{Total volume} = \text{number of voxels} \times \text{volume of the voxel}$$

If the CT number of the region of interest is below 0:

$$\text{Volume of gas} = \left(-\frac{\text{CT}}{1000}\right) \times \text{total volume}$$

$$\text{Volume of tissue} = \left(1 + \frac{\text{CT}}{1000}\right) \times \text{total volume}$$

If the CT number of the region of interest is above 0:

$$\text{Volume of gas} = 0$$

$$\text{Volume of tissue} = \text{number of voxels} \times \text{volume of the voxel}$$

As the volumes of gas and tissue are obtained, the fraction of gas can be calculated:

$$\text{Fraction of gas} = \frac{\text{Volume of gas}}{\text{total volume}}$$

Therefore, both the tidal volume and its distribution of a CT section can be calculated [59]. Then the volume of gas and tissue of the whole lung can be calculated by summing the volumes of all regions of lungs. The volume of both lungs at end-expiration is FRC.

Non-contrast-enhanced CT can be used to measure the ventilation status of different zones and to detect physiological and pathophysiological phenomena in healthy and obstructive lung disease, such as gravity dependence, tissue destruction, and collateral ventilation [60, 61]. The volume of lung tissue is fixed and the volume of gas varies with breathing. During inspiration, air enters into lungs while parenchymal tissue expands and becomes less dense. Intrapulmonary blood volume decreases during inspiration and is affected by heartbeat. In order to rule out the effect of heartbeats on blood volume when lung volumes are measured, a breath-holding method can be used. As the breath-holding time can be significantly longer than heartbeat interval, a constant blood volume can be maintained by averaging over time. In healthy controls, there are large changes in CT density between inspiration and expiration images and indicate normal lung function [62]. If little or no

change in CT density between images of inspiration and expiration, there might be ventilation defects.

The air might be unevenly distributed in different lung regions. Even if the difference between CT numbers of two regions is below 100 HU, CT multivolume imaging can also be detected [60]. Lung zones with a CT number between −900 and −500 HU are considered as normal aerated, those lower than −900 HU are considered as overdistention, those between −500 and −100 HU are considered as poorly aerated, and those between −100 and + 100 HU are considered as nonaerated [58, 63, 64]. Decreased density at FRC indicates air trapping and airways-related impairments, such as bronchiectasis, thickened airways, and mucus plugging, which might result in incomplete exhalation. In contrast, increased density at TLC with consolidations and ground glass opacities suggests that these areas are not properly aerated.

If a PEEP is used and lung recruitment occurs, the volumes of nonaerated lung tissues at a PEEP level of 0 cmH_2O and at a given PEEP can be measured and the difference between the two can be calculated, and that is "PEEP-induced alveolar recruitment." PEEP-induced alveolar recruitment may transform a nonaerated lung area into a hypoventilated area or a hypoventilated area into a normally aerated area. If the gas volume of a normally aerated area increases as the applying of PEEP, there might be PEEP-induced alveolar distension.

4.4.2 Clinical Application

Recently, Computed Tomography (CT) technique [60, 61, 65] has been used to evaluate regional ventilation by assessing changes of the regional intensity between breath-hold images acquired at different lung volumes. CT can also be used to assess ventilation heterogeneities related to gravitational effects and ventilation defects caused by emphysema and asthma [60, 61, 66]. Non-contrast CT imaging might be an alternative to current ventilation-imaging techniques, such as nuclear imaging, xenon-enhanced CT, and hyperpolarized-MRI, as it is much cheaper and easier for ordinary clinical practice [67, 68].

For patients with ARDS, CT can be used to guide the recruitment maneuvers [59] and to calculate the volume of PEEP-induced alveolar recruitment [69]. Although debates still exist, quantitative CT-scan analysis has been considered as a "gold standard" to assess PEEP-induced recruitment.

4.4.3 Limitations

It should be noted that there are several limitations of measuring lung volumes by CT scan: (1) the risk of transport; (2) the radiation exposure; and (3) the time required for quantitative analysis.

4.5 EIT

Electrical impedance tomography (EIT) is a noninvasive and radiation-free clinical monitoring technology that can provide dynamic images of gas distribution in the lungs during breathing at the bedside. EIT was invented over 30 years ago [70]. However, it has been commercially available only in recent 10 years. It has developed rapidly in recent years and is now widely used in clinical research and clinical work.

4.5.1 Principle of EIT

Biological tissue is composed of specific compositions (e.g., lipids, water, electrolytes). If an alternating electric current is applied exogenously, those compositions will respond to the electric current distinctively, which are generally referred to as "bioimpedance." EIT image reconstruction is based on the measurement of changes in lung tissue impedance with breathing by injecting small currents and measuring voltages. During inspiration, the resistivity increases with lung inflation and correlates closely with the amount of air inhaled into the lungs. When the subject takes a deep breath, the resistivity might increase more than twice as many [71]. However, the increase of blood or fluid volume or disruption of cellular barriers raise the conductivity and lowers the impedance.

EIT examinations require a dedicated chest belt with electrodes placed around the patient's chest circumference. Some EIT devices use 16-electrodes belt, and others may use belts with more or fewer number of electrodes. The position of electrodes may affect the findings [72–75]. They are usually placed at the fifth to sixth intercostal level [76] (Please refer to Sect. 3.3 of Chap. 3 for details), and should not be placed lower than the sixth intercostal space so as to avoid the influence of diaphragm on the measurement as the diaphragm may rise and fall with the cycling of breath and enter the measurement plane of EIT [73].

During an EIT examination, very small currents are delivered through pairs of electrodes, while other electrodes measure the resulting voltages. The pairs of injection currents are alternated in turn, and one image can be produced using all voltages measured by electrodes at the end of one full cycle according to specific reconstruction algorithms. A set of EIT data obtained in a cycle is usually referred to as an image frame and is generated by comparison with the data of the reference period at the baseline. The number of frames (or original images) acquired per second corresponds to the EIT scan rate. After reconstruction using an improved finite element mesh, the image is projected into an array of 32 × 32 pixels, where each pixel represents the change in resistance at the corresponding location compared to the foundation during a certain period of time. Therefore, image frames are often referred to as relative images. EIT monitors these impedance changes in real-time

and dynamic images can be obtained, which are projected on the screen and are helpful for understanding ventilation status and air distribution in the lungs.

4.5.2 Measuring TIV by EIT

EIT cannot measure the absolute lung volumes. However, it can measure the changes in impedance, which represent changes of lung volumes in the entire lungs and a given region of interest (ROI), and generate functional EIT images proportional to the local tidal volume (V_t) [77–79]. There is a linear relationship between Δimpedance and Δvolume.

After the EIT signals are properly filtered, the electrical impedances at the end of inspiration and the end of expiration can be measured. Tidal impedance variation (TIV) represents impedance change generated by inspired gas during a tidal breath, and can be calculated as follows:

$$\text{TIV} = \text{Impedance}_{\max} - \text{Impedance}_{\min}$$

TIV is a basic parameter, and other various EIT measures are derived from it. Global TIV is the sum of impedance changes of all pixels across the whole images and represents the changes in the amount of air in both lungs during breathing. Global TIV closely correlates with tidal volume estimated by CT [80–83].

Lungs can be divided into several horizontal layers or quadrants. Regional ventilation of a ROI can be represented by regional TIV and can be calculated by summing the impedance changes in the pixels within the selected ROI.

4.5.3 Measuring Lung Recruitment by EIT

EIT can be used to evaluate PEEP-induced pulmonary dysplasia. First, the end-expiratory electrical impedance at higher PEEP conditions and the electrical impedance at lower PEEP conditions can be measured. The difference between the two is the electrical impedance change caused by high PEEP, which represents its end-respiratory lung volume Changes [84–86]. Using the same method, PEEP-induced lung dilatation with different ROIs can also be calculated.

EIT can be used to evaluate PEEP-induced lung recruitment. The electrical impedance of the chest at the end of expiration with a higher PEEP can be measured, as well as that with ZEEP. The difference in electrical impedance with the higher PEEP and ZEEP can be measured by EIT ($\Delta\text{EELV}_{\text{EIT}}$). The difference in electrical impedance with the lower PEEP and ZEEP can also be measured in the same way. Then lung recruitment (RECR_{EIT}) caused by the higher PEEP can be calculated using the following equation:

$$\text{RECR}_{EIT} = \Delta\text{EELV}_{\text{EIT}} - \Delta\text{EELV}_{\text{Crs}} = \Delta\text{EELV}_{\text{EIT}} - \left(\text{PEEP}_{\text{Low}}\text{Crs} \times \Delta\text{PEEP}\right)$$

($\Delta EELV_{Crs}$ is the change in end-expiratory lung inflation predicted from the respiratory system compliance measured at $PEEP_{Low}$)

The $\Delta EELV_{EIT}$ of different regions can also be measured by the same method using regional end-expiratory impedance changes, tidal volumes, and tidal impedance variations, especially the ECR_{EIT} of non-dependent and dependent lung regions.

4.5.4 Overdistension and Atelectasis/Collapse (ODCL)

During PEEP titration, the regional lung area that might have overdistension and/or collapse (ODCL) can be assessed by monitoring regional compliance at the pixel level. Keeping the driving pressure constant, with the decrease of PEEP, the pixel level compliance in a given region might peak at a certain PEEP level, and the PEEP is the best one for this region. Both increasing and decreasing PEEP will lead to reduction of regional compliance, and result in hyperventilation and alveolar collapse, respectively. Taking the collapsed area as an example, the compliance change of each pixel at a given PEEP level compared with its best PEEP can be calculated according to the following formula:

$$\text{Collpase}_{\text{pixel}}(\%) = \frac{\left(\text{Best Compliance}_{\text{pixel}} - \text{Current Compliance}_{\text{pixel}}\right) \times 100}{\text{Best Compliance}_{\text{pixel}}}$$

Thereafter, the accumulated collapse for the entire lung at each PEEP step is calculated as a weighted average summed up for all collapsed pixels, where the weighting factor is the best pixel compliance estimated by applying the formula [84]:

$$\text{Cumulated Collpase}(\%) = \frac{\sum_{i=1}^{\text{Valid pixels}} (\text{Collapse}_{\text{pixel}}(\%) \times \text{Best Compliance}_{\text{pixel}}}{\sum_{i=1}^{\text{Valid pixels}} \text{Best Compliance}_{\text{pixel}}}$$

(valid pixels, numbers of pixels included for analysis)

The cumulated overdistension can be calculated in the same way. Regional values of tidal hyperinflation can also be obtained by the same formulas considering only the pixels included in $ROI_{non\text{-}dep}$ and ROI_{dep}.

The compliance of different regions might not be the same at a certain PEEP level. Some lung areas might be normally aerated and some areas might have ODCL. At each PEEP level, by labeling those affected pixels showing reduced compliance in the EIT image at each PEEP level, it is possible to display the images of areas with possible ODCL on the screen. EIT users can identify the inconsistency of spatial distribution and asynchrony in time of ventilation among different lung regions by watching the screen at the patient's bedside. In addition, quantitative evaluation is possible by calculating and accumulating the reduction in pixel compliance from the highest value. The theoretical PEEP level with the least

ODCL, that is, the ideal PEEP level, can be identified by performing a PEEP titration trial.

4.5.5 Measurement of Global Inhomogeneity Index (GI index) by EIT

EIT can be used to evaluate the heterogeneity of ventilation distribution, and two EIT measures are used to quantify the ventilation heterogeneity, which are intratidal ventilation heterogeneity (ITV_{Het}) and global inhomogeneity (GI) index. Lungs can be divided into eight equal-volume parts, and ITV_{Het} is the average value of $Vt_{non\text{-}dep}/Vt_{dep}$ ratios during inspiration [84], where $Vt_{non\text{-}dep}$ is the tidal volume in non-gravity-dependent areas and Vt_{dep} is the tidal volume in gravity-dependent areas.

The GI index reflects the spatial distribution and dispersion of tidal breath and can be used to evaluate the heterogeneity of ventilation distribution. It is calculated as the sum of the differences in impedance changes between each pixel and the median value of all pixels within predefined lung regions, divided by the sum of the impedance values of each pixel:

$$\mathrm{GI} = \frac{\sum_{x,y\in \mathrm{lung}} \left| DI_{x,y} - \mathrm{Median}\left(DI_{\mathrm{lung}}\right) \right|}{\sum_{x,y\in \mathrm{lung}} DI_{x,y}}$$

(DI = value of the impedance variation, x, y = the pixel in the identified lung area, $DI_{\mathrm{lung}} = DI$ of all pixels in the predefined lung)

It can be seen that the GI index refers to variance in impedance of each pixel as compared with the entire EIT image. The distribution of gas in the lung is affected by many factors, such as inflammatory response, changes in lung function, or adjustment of ventilator parameters. Therefore, the GI index will also change with the physiological status of the lungs. A smaller GI index indicates more homogeneous ventilation, while a larger GI index indicates more inhomogeneity among different lung regions. With the increase of PEEP, GI might change parabolically. The smallest GI value would be obtained with the best dynamic compliance of the whole lung at a certain PEEP level, which might be the optimal PEEP level. Therefore, monitoring GI by EIT can be helpful to identify the optimal PEEP levels.

4.5.6 EIT Measures for Analyzing Temporal Distribution of Ventilation

Regional ventilation delay (RVD) is an indicator for assessing the homogeneity of aeration of lung regions [85, 86]. When atelectasis is present, there may be a delay in the distribution of inspired gas in the lungs. This temporal delay of certain ROIs

can be detected by real-time EIT images at the bedside. RVD shows the temporal heterogeneity occurring in inspiration by monitoring the relationship between impedance change and the ventilation time course in each pixel. The delay time is estimated between the beginning of the inspiration until the regional impedance reaches a target impedance change value in comparison with the global image by mathematical analysis of the regional impedance-time curves. The target impedance change value is usually set to 40% of the maximum impedance value measured during slow flow ventilation. Regional ventilation delay inhomogeneity (RVDI) is defined as the standard deviation of RVD in all pixels and can be calculated by the following formula:

$$\mathrm{RVD}_i = \frac{\Delta t_{\mathrm{RVD}}}{t_{\max} - t_{\min}} \times 100\%$$

where Δt_{RVD} is the time from the global start of inspiration until the regional impedance change reaching a certain percentage of its maximum value, $t_{\max} - t_{\min}$ is the inflation time, and i refers to each pixel.

A smaller RVDI indicates a more homogeneous distribution. RVD usually occurs in the dorsal regions and might change with decreased or increased PEEP levels. Monitoring RVDI could be useful to estimate the amount of periodical recruitment and collapse during breathing that should be minimized in injured lungs to avoid ventilator-induced lung injury (VALI).

4.5.7 Clinical Application

EIT can monitor the ventilation status of lungs in real-time at the bedside without radiation and is helpful for adjusting the ventilator parameters [87, 88]. For patients with ARDS, EIT can evaluate end-expiratory lung inflation, alveolar collapse and recruitment, entire and regional lung aeration and homogeneity of ventilation at the bedside continuously, and can be used for PEEP titration to determine the optimal PEEP setting with the best alveolar recruitment and minimal overdistention [79, 89, 90].

4.5.8 Limitations

1. EIT cannot measure the absolute value of lung volume.
2. Large chest wounds, multiple chest tubes, nonconductive bandages, or conductive wire sutures may preclude or affect the measurements.

References

1. Dubois AB, Botelho SY, Bedell GN, Marshall R, Comroe JH Jr. A rapid plethysmographic method for measuring thoracic gas volume: a comparison with a nitrogen washout method for measuring functional residual capacity in normal subjects. J Clin Invest. 1956;35(3):322–6.
2. Vilozni D, Efrati O, Hakim F, Adler A, Livnat G, Bentur L. FRC measurements using body plethysmography in young children. Pediatr Pulmonol. 2009;44(9):885–91.
3. Criee CP, Sorichter S, Smith HJ, Kardos P, Merget R, Heise D, Berdel D, Kohler D, Magnussen H, Marek W, et al. Body plethysmography—its principles and clinical use. Respir Med. 2011;105(7):959–71.
4. Stocks J, Godfrey S, Beardsmore C, Bar-Yishay E, Castile R. Plethysmographic measurements of lung volume and airway resistance. ERS/ATS Task Force on Standards for Infant Respiratory Function Testing. European Respiratory Society/American Thoracic Society. Eur Respir J. 2001;17(2):302–12.
5. Zysman-Colman Z, Lands LC. Whole body plethysmography: practical considerations. Paediatr Respir Rev. 2016;19:39–41.
6. Cala SJ, Kenyon CM, Ferrigno G, Carnevali P, Aliverti A, Pedotti A, Macklem PT, Rochester DF. Chest wall and lung volume estimation by optical reflectance motion analysis. J Appl Physiol. 1996;81(6):2680–9.
7. Kenyon CM, Cala SJ, Yan S, Aliverti A, Scano G, Duranti R, Pedotti A, Macklem PT. Rib cage mechanics during quiet breathing and exercise in humans. J Appl Physiol. 1997;83(4):1242–55.
8. Aliverti A, Cala SJ, Duranti R, Ferrigno G, Kenyon CM, Pedotti A, Scano G, Sliwinski P, Macklem PT, Yan S. Human respiratory muscle actions and control during exercise. J Appl Physiol. 1997;83(4):1256–69.
9. Massaroni C, Carraro E, Vianello A, Miccinilli S, Morrone M, Levai IK, Schena E, Saccomandi P, Sterzi S, Dickinson JW, et al. Optoelectronic plethysmography in clinical practice and research: a review. Respiration. 2017;93(5):339–54.
10. Lanini B, Bianchi R, Binazzi B, Romagnoli I, Pala F, Gigliotti F, Scano G. Chest wall kinematics during cough in healthy subjects. Acta Physiol (Oxford, England). 2007;190(4):351–8.
11. Aliverti A, Dellaca R, Pelosi P, Chiumello D, Gatihnoni L, Pedoti A. Compartmental analysis of breathing in the supine and prone positions by optoelectronic plethysmography. Ann Biomed Eng. 2001;29(1):60–70.
12. Romei M, Mauro AL, D'Angelo MG, Turconi AC, Bresolin N, Pedotti A, Aliverti A. Effects of gender and posture on thoraco-abdominal kinematics during quiet breathing in healthy adults. Respir Physiol Neurobiol. 2010;172(3):184–91.
13. Ferrigno G, Pedotti A. ELITE: a digital dedicated hardware system for movement analysis via real-time TV signal processing. IEEE Trans Biomed Eng. 1985;32(11):943–50.
14. Konno K, Mead J. Measurement of the separate volume changes of rib cage and abdomen during breathing. J Appl Physiol. 1967;22(3):407–22.
15. Aliverti A, Dellaca R, Pedotti A. Optoelectronic plethysmography: a new tool in respiratory medicine. Recenti Prog Med. 2001;92(11):644–7.
16. Borghese NA, Ferrigno G. An algorithm for 3-D automatic movement detection by means of standard TV cameras. IEEE Trans Biomed Eng. 1990;37(12):1221–5.
17. Dellaca RL, Ventura ML, Zannin E, Natile M, Pedotti A, Tagliabue P. Measurement of total and compartmental lung volume changes in newborns by optoelectronic plethysmography. Pediatr Res. 2010;67(1):11–6.
18. Vogiatzis I, Georgiadou O, Golemati S, Aliverti A, Kosmas E, Kastanakis E, Geladas N, Koutsoukou A, Nanas S, Zakynthinos S, et al. Patterns of dynamic hyperinflation during exercise and recovery in patients with severe chronic obstructive pulmonary disease. Thorax. 2005;60(9):723–9.
19. Ferguson GT, Enright PL, Buist AS, Higgins MW. Office spirometry for lung health assessment in adults: a consensus statement from the National Lung Health Education Program. Chest. 2000;117(4):1146–61.

20. Valentinuzzi ME, Johnston R. Spirometry: a historical gallery up to 1905. IEEE Pulse. 2014;5(1):73–6.
21. Spriggs EA. The history of spirometry. Br J Dis Chest. 1978;72(3):165–80.
22. Miller MR, Hankinson J, Brusasco V, Burgos F, Casaburi R, Coates A, Crapo R, Enright P, van der Grinten CP, Gustafsson P, et al. Standardisation of spirometry. Eur Respir J. 2005;26(2):319–38.
23. Townsend MC. The effects of leaks in spirometers on measurements of pulmonary function. The implications for epidemiologic studies. J Occup Med. 1984;26(11):835–41.
24. Standardization of Spirometry. Update. American Thoracic Society. Am J Respir Crit Care Med 1995. 1994;152(3):1107–36.
25. Ferris BG Jr, Speizer FE, Bishop Y, Prang G, Weener J. Spirometry for an epidemiologic study: deriving optimum summary statistics for each subject. Bull Eur Physiopathol Respir. 1978;14(2):145–66.
26. Kanner RE, Schenker MB, Munoz A, Speizer FE. Spirometry in children. Methodology for obtaining optimal results for clinical and epidemiologic studies. Am Rev Respir Dis. 1983;127(6):720–4.
27. Brusasco V, Pellegrino R, Rodarte JR. Vital capacities in acute and chronic airway obstruction: dependence on flow and volume histories. Eur Respir J. 1997;10(6):1316–20.
28. Pellegrino R, Crimi E, Gobbi A, Torchio R, Antonelli A, Gulotta C, Baroffio M, Papa GF, Dellaca R, Brusasco V. Severity grading of chronic obstructive pulmonary disease: the confounding effect of phenotype and thoracic gas compression. J Appl Physiol. 2015;118(7):796–802.
29. Conrad DJ, Bailey BA, Hardie JA, Bakke PS, Eagan TML, Aarli BB. Median regression spline modeling of longitudinal FEV1 measurements in cystic fibrosis (CF) and chronic obstructive pulmonary disease (COPD) patients. PLoS One. 2017;12(12):e0190061.
30. Cho O, Oh YT, Chun M, Noh OK, Heo JS. Prognostic implication of FEV1/FVC ratio for limited-stage small cell lung cancer. J Thorac Dis. 2018;10(3):1797–805.
31. Majid A, Sosa AF, Ernst A, Feller-Kopman D, Folch E, Singh AK, Gangadharan S. Pulmonary function and flow-volume loop patterns in patients with tracheobronchomalacia. Respir Care. 2013;58(9):1521–6.
32. Lunn WW, Sheller JR. Flow volume loops in the evaluation of upper airway obstruction. Otolaryngol Clin North Am. 1995;28(4):721–9.
33. Miller RD, Hyatt RE. Obstructing lesions of the larynx and trachea: clinical and physiologic characteristics. Mayo Clin Proc. 1969;44(3):145–61.
34. Pierce R. Spirometry: an essential clinical measurement. Aust Fam Physician. 2005;34(7):535–9.
35. Varga J, Casaburi R, Ma S, Hecht A, Hsia D, Somfay A, Porszasz J. Relation of concavity in the expiratory flow-volume loop to dynamic hyperinflation during exercise in COPD. Respir Physiol Neurobiol. 2016;234:79–84.
36. Vincken WG, Elleker MG, Cosio MG. Flow-volume loop changes reflecting respiratory muscle weakness in chronic neuromuscular disorders. Am J Med. 1987;83(4):673–80.
37. Lu Q, Rouby JJ. Measurement of pressure-volume curves in patients on mechanical ventilation: methods and significance. Crit Care. 2000;4(2):91–100.
38. Liang BM, Lam DC, Feng YL. Clinical applications of lung function tests: a revisit. Respirology. 2012;17(4):611–9.
39. Robinson PD, Latzin P, Verbanck S, Hall GL, Horsley A, Gappa M, Thamrin C, Arets HG, Aurora P, Fuchs SI, et al. Consensus statement for inert gas washout measurement using multiple- and single-breath tests. Eur Respir J. 2013;41(3):507–22.
40. Wrigge H, Sydow M, Zinserling J, Neumann P, Hinz J, Burchardi H. Determination of functional residual capacity (FRC) by multibreath nitrogen washout in a lung model and in mechanically ventilated patients. Accuracy depends on continuous dynamic compensation for changes of gas sampling delay time. Intensive Care Med. 1998;24(5):487–93.
41. Olegard C, Sondergaard S, Houltz E, Lundin S, Stenqvist O. Estimation of functional residual capacity at the bedside using standard monitoring equipment: a modified nitrogen washout/

washin technique requiring a small change of the inspired oxygen fraction. Anesth Analg. 2005;101(1):206–12, table of contents
42. Brewer LM, Orr JA, Sherman MR, Fulcher EH, Markewitz BA. Measurement of functional residual capacity by modified multiple breath nitrogen washout for spontaneously breathing and mechanically ventilated patients. Br J Anaesth. 2011;107(5):796–805.
43. Chiumello D, Cressoni M, Chierichetti M, Tallarini F, Botticelli M, Berto V, Mietto C, Gattinoni L. Nitrogen washout/washin, helium dilution and computed tomography in the assessment of end expiratory lung volume. Crit Care. 2008;12(6):R150.
44. Mitchell RR, Wilson RM, Holzapfel L, Benis AM, Sierra D, Osborn JJ. Oxygen wash-in method for monitoring functional residual capacity. Crit Care Med. 1982;10(8):529–33.
45. Fretschner R, Deusch H, Weitnauer A, Brunner JX. A simple method to estimate functional residual capacity in mechanically ventilated patients. Intensive Care Med. 1993;19(7):372–6.
46. Zinserling J, Wrigge H, Varelmann D, Hering R, Putensen C. Measurement of functional residual capacity by nitrogen washout during partial ventilatory support. Intensive Care Med. 2003;29(5):720–6.
47. Brunner J, Langenstein H, Wolff G. Direct accurate gas flow measurement in the patient: compensation for unavoidable error. Med Prog Technol. 1983;9(4):233–8.
48. Tonga KO, Robinson PD, Farah CS, King GG, Thamrin C. In vitro and in vivo functional residual capacity comparisons between multiple-breath nitrogen washout devices. ERJ Open Res. 2017:3(4).
49. Tang R, Huang Y, Chen Q, Hui X, Li Y, Yu Q, Zhao H, Yang Y, Qiu H. The effect of alveolar dead space on the measurement of end-expiratory lung volume by modified nitrogen wash-out/wash-in in lavage-induced lung injury. Respir Care. 2012;57(12):2074–81.
50. Dellamonica J, Lerolle N, Sargentini C, Beduneau G, Di Marco F, Mercat A, Richard JC, Diehl JL, Mancebo J, Rouby JJ, et al. Accuracy and precision of end-expiratory lung-volume measurements by automated nitrogen washout/washin technique in patients with acute respiratory distress syndrome. Crit Care. 2011;15(6):R294.
51. Heinze H, Eichler W. Measurements of functional residual capacity during intensive care treatment: the technical aspects and its possible clinical applications. Acta Anaesthesiol Scand. 2009;53(9):1121–30.
52. Wood EH. Noninvasive three-dimensional viewing of the motion and anatomical structure of the heart, lungs, and circulatory system by high speed computerized X-ray tomography. CRC Crit Rev Biochem. 1979;7(2):161–86.
53. Ritman EL, Kinsey JH, Robb RA, Gilbert BK, Harris LD, Wood EH. Three-dimensional imaging of heart, lungs, and circulation. Science (New York, NY). 1980;210(4467):273–80.
54. Hoffman EA. Effect of body orientation on regional lung expansion: a computed tomographic approach. J Appl Physiol. 1985;59(2):468–80.
55. Hoffman EA, Ritman EL. Effect of body orientation on regional lung expansion in dog and sloth. J Appl Physiol. 1985;59(2):481–91.
56. Tajik JK, Chon D, Won C, Tran BQ, Hoffman EA. Subsecond multisection CT of regional pulmonary ventilation. Acad Radiol. 2002;9(2):130–46.
57. Hoffman EA, Tajik JK, Kugelmass SD. Matching pulmonary structure and perfusion via combined dynamic multislice CT and thin-slice high-resolution CT. Comput Med Imaging Graph. 1995;19(1):101–12.
58. Gattinoni L, Presenti A, Torresin A, Baglioni S, Rivolta M, Rossi F, Scarani F, Marcolin R, Cappelletti G. Adult respiratory distress syndrome profiles by computed tomography. J Thorac Imaging. 1986;1(3):25–30.
59. Gattinoni L, Pelosi P, Crotti S, Valenza F. Effects of positive end-expiratory pressure on regional distribution of tidal volume and recruitment in adult respiratory distress syndrome. Am J Respir Crit Care Med. 1995;151(6):1807–14.
60. Aliverti A, Pennati F, Salito C, Woods JC. Regional lung function and heterogeneity of specific gas volume in healthy and emphysematous subjects. Eur Respir J. 2013;41(5):1179–88.

61. Galban CJ, Han MK, Boes JL, Chughtai KA, Meyer CR, Johnson TD, Galban S, Rehemtulla A, Kazerooni EA, Martinez FJ, et al. Computed tomography-based biomarker provides unique signature for diagnosis of COPD phenotypes and disease progression. Nat Med. 2012;18(11):1711–5.
62. Pennati F, Salito C, Baroni G, Woods J, Aliverti A. Comparison between multivolume CT-based surrogates of regional ventilation in healthy subjects. Acad Radiol. 2014;21(10):1268–75.
63. Vieira SR, Puybasset L, Richecoeur J, Lu Q, Cluzel P, Gusman PB, Coriat P, Rouby JJ. A lung computed tomographic assessment of positive end-expiratory pressure-induced lung overdistension. Am J Respir Crit Care Med. 1998;158(5 Pt 1):1571–7.
64. Puybasset L, Cluzel P, Gusman P, Grenier P, Preteux F, Rouby JJ. Regional distribution of gas and tissue in acute respiratory distress syndrome. I. Consequences for lung morphology. CT Scan ARDS Study Group. Intensive Care Med. 2000;26(7):857–69.
65. Pennati F, Roach DJ, Clancy JP, Brody AS, Fleck RJ, Aliverti A, Woods JC. Assessment of pulmonary structure-function relationships in young children and adolescents with cystic fibrosis by multivolume proton-MRI and CT. J Magn Reson Imaging. 2018;48(2):531–42.
66. Zapke M, Topf HG, Zenker M, Kuth R, Deimling M, Kreisler P, Rauh M, Chefd'hotel C, Geiger B, Rupprecht T. Magnetic resonance lung function—a breakthrough for lung imaging and functional assessment? A phantom study and clinical trial. Respir Res. 2006;7:106.
67. Petersson J, Sanchez-Crespo A, Larsson SA, Mure M. Physiological imaging of the lung: single-photon-emission computed tomography (SPECT). J Appl Physiol. 2007;102(1):468–76.
68. Simon BA, Kaczka DW, Bankier AA, Parraga G. What can computed tomography and magnetic resonance imaging tell us about ventilation? J Appl Physiol. 2012;113(4):647–57.
69. Malbouisson LM, Muller JC, Constantin JM, Lu Q, Puybasset L, Rouby JJ. Computed tomography assessment of positive end-expiratory pressure-induced alveolar recruitment in patients with acute respiratory distress syndrome. Am J Respir Crit Care Med. 2001;163(6):1444–50.
70. Barber DC, Brown BH. Applied potential tomography. J Br Interplanet Soc. 1989;42(7):391–3.
71. Harris ND, Suggett AJ, Barber DC, Brown BH. Applications of applied potential tomography (APT) in respiratory medicine. Clin Phys Physiol Meas. 1987;8(Suppl A):155–65.
72. Frerichs I, Hahn G, Hellige G. Thoracic electrical impedance tomographic measurements during volume controlled ventilation-effects of tidal volume and positive end-expiratory pressure. IEEE Trans Med Imaging. 1999;18(9):764–73.
73. Karsten J, Stueber T, Voigt N, Teschner E, Heinze H. Influence of different electrode belt positions on electrical impedance tomography imaging of regional ventilation: a prospective observational study. Crit Care. 2016;20:3.
74. Reifferscheid F, Elke G, Pulletz S, Gawelczyk B, Lautenschlager I, Steinfath M, Weiler N, Frerichs I. Regional ventilation distribution determined by electrical impedance tomography: reproducibility and effects of posture and chest plane. Respirology. 2011;16(3):523–31.
75. Krueger-Ziolek S, Schullcke B, Kretschmer J, Muller-Lisse U, Moller K, Zhao Z. Positioning of electrode plane systematically influences EIT imaging. Physiol Meas. 2015;36(6):1109–18.
76. Bachmann MC, Morais C, Bugedo G, Bruhn A, Morales A, Borges JB, Costa E, Retamal J. Electrical impedance tomography in acute respiratory distress syndrome. Crit Care. 2018;22(1):263.
77. Mauri T, Bellani G, Confalonieri A, Tagliabue P, Turella M, Coppadoro A, Citerio G, Patroniti N, Pesenti A. Topographic distribution of tidal ventilation in acute respiratory distress syndrome: effects of positive end-expiratory pressure and pressure support. Crit Care Med. 2013;41(7):1664–73.
78. Frerichs I, Dargaville PA, van Genderingen H, Morel DR, Rimensberger PC. Lung volume recruitment after surfactant administration modifies spatial distribution of ventilation. Am J Respir Crit Care Med. 2006;174(7):772–9.
79. Meier T, Luepschen H, Karsten J, Leibecke T, Grossherr M, Gehring H, Leonhardt S. Assessment of regional lung recruitment and derecruitment during a PEEP trial based on electrical impedance tomography. Intensive Care Med. 2008;34(3):543–50.

80. Frerichs I, Hinz J, Herrmann P, Weisser G, Hahn G, Dudykevych T, Quintel M, Hellige G. Detection of local lung air content by electrical impedance tomography compared with electron beam CT. J Appl Physiol. 2002;93(2):660–6.
81. Victorino JA, Borges JB, Okamoto VN, Matos GF, Tucci MR, Caramez MP, Tanaka H, Sipmann FS, Santos DC, Barbas CS, et al. Imbalances in regional lung ventilation: a validation study on electrical impedance tomography. Am J Respir Crit Care Med. 2004;169(7):791–800.
82. Adler A, Amyot R, Guardo R, Bates JH, Berthiaume Y. Monitoring changes in lung air and liquid volumes with electrical impedance tomography. J Appl Physiol. 1997;83(5):1762–7.
83. Frerichs I, Hahn G, Schiffmann H, Berger C, Hellige G. Monitoring regional lung ventilation by functional electrical impedance tomography during assisted ventilation. Ann N Y Acad Sci. 1999;873:493–505.
84. Mauri T, Eronia N, Turrini C, Battistini M, Grasselli G, Rona R, Volta CA, Bellani G, Pesenti A. Bedside assessment of the effects of positive end-expiratory pressure on lung inflation and recruitment by the helium dilution technique and electrical impedance tomography. Intensive Care Med. 2016;42(10):1576–87.
85. Wrigge H, Zinserling J, Muders T, Varelmann D, Gunther U, von der Groeben C, Magnusson A, Hedenstierna G, Putensen C. Electrical impedance tomography compared with thoracic computed tomography during a slow inflation maneuver in experimental models of lung injury. Crit Care Med. 2008;36(3):903–9.
86. Muders T, Luepschen H, Zinserling J, Greschus S, Fimmers R, Guenther U, Buchwald M, Grigutsch D, Leonhardt S, Putensen C, et al. Tidal recruitment assessed by electrical impedance tomography and computed tomography in a porcine model of lung injury. Crit Care Med. 2012;40(3):903–11.
87. Kobylianskii J, Murray A, Brace D, Goligher E, Fan E. Electrical impedance tomography in adult patients undergoing mechanical ventilation: a systematic review. J Crit Care. 2016;35:33–50.
88. Frerichs I, Amato MB, van Kaam AH, Tingay DG, Zhao Z, Grychtol B, Bodenstein M, Gagnon H, Bohm SH, Teschner E, et al. Chest electrical impedance tomography examination, data analysis, terminology, clinical use and recommendations: consensus statement of the TRanslational EIT developmeNt stuDy group. Thorax. 2017;72(1):83–93.
89. Dargaville PA, Rimensberger PC, Frerichs I. Regional tidal ventilation and compliance during a stepwise vital capacity manoeuvre. Intensive Care Med. 2010;36(11):1953–61.
90. Franchineau G, Brechot N, Lebreton G, Hekimian G, Nieszkowska A, Trouillet JL, Leprince P, Chastre J, Luyt CE, Combes A, et al. Bedside contribution of electrical impedance tomography to setting positive end-expiratory pressure for extracorporeal membrane oxygenation-treated patients with severe acute respiratory distress syndrome. Am J Respir Crit Care Med. 2017;196(4):447–57.

Chapter 5
Extravascular Lung Water Monitoring

Hong-Liang Li

5.1 Definition and a Brief History

Water contributes 80% of the lung components; however, most of them existed in the blood vessels and distributed in a gradient of increasing density from nondependent to dependent regions. By definition, extravascular lung water (EVLW) is the amount of water that is contained in the lungs outside the pulmonary vasculature, composed of the sum of interstitial, intracellular, alveolar, and lymphatic fluid; however, pleural effusions did not include [1]. The EVLW monitoring and evaluation play an essential role in pulmonary edema assessment.

5.2 Physiology of Lung Water

In human beings, about 700 million alveoli are contained in both lungs, with an overall surface area of approximately 100 m^2. The alveoli consist of an epithelial layer, interstitium, and capillaries. The lungs work in a unique engineering fashion since air circulates in the alveoli, while blood circulates in capillary surrounded outside. The extravasation of fluid and solutes from the pulmonary microvessels into the pulmonary interstitial tissue is a physiological phenomenon, which is usually constrained in the interstitium, with little possibility to reach the alveoli due to the intact junctions of the alveolar epithelium. The process of fluid movement across the barrier between pulmonary capillaries and interstitial spaces is determined with the gradient of hydrostatic and oncotic pressure, as well as the filtration coefficient

H.-L. Li (✉)
Department of Critical Care Medicine, Beijing Tiantan Hospital, Capital Medical University, Beijing, China

J. Zhou et al. (eds.), *Respiratory Monitoring in Mechanical Ventilation*,
https://doi.org/10.1007/978-981-15-9770-1_5

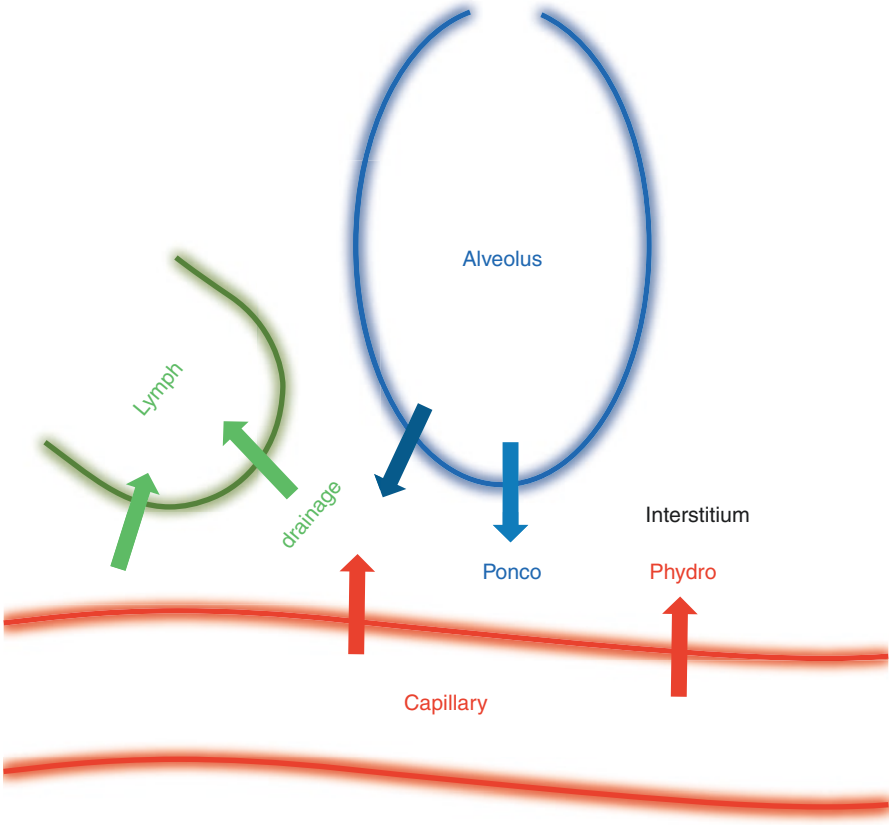

Fig. 5.1 The basic principle of the Starling's law, EVLW is the result of balance between the hydrostatic and oncotic pressure across the capillary and alveolus, and is influenced by drainage of the lymph

of the alveolocapillary barrier, all of which bundled together and known as the Starling's law (Fig. 5.1), which is proposed by Ernest Starling as early as 1896 [2].

The doctrine status of the Starling model has been challenged for a long time. Danielli found there was an endothelial surface layer lining the luminal side of the capillary endothelium in 1940 [3]. Recent studies found a nonlinear relationship between hydrostatic pressure and vascular permeability [4, 5]. Endothelial glycocalyx (EG), which composed of glycosaminoglycans and proteins and coating the surface of endothelial-like a gel, is believed to play a crucial role in extravasation prevention [6]. Acting as a molecular sieve, EG can limit water and solute efflux across the intercellular junction. Furthermore, EG provides scaffolding on which serum plasma proteins accumulate and a layer of ultrafiltrate formed, which pulls fluid to the intravascular compartment with the powerful oncotic force. Additionally, EG transmitting the shear stress from blood flow to the endothelium cytoskeleton and initiating intracellular signaling as a mechanosensor, increasing capillary permeability [7].

The understanding of the pathophysiology of pulmonary edema goes further based on the emerging role of EG. It is well acknowledged now that excessive fluid extravasation could be induced by either a significant increase of capillary hydrostatic pressure or the damage of the EG layer, which is frequently seen in trauma and ischemia/reperfusion injuries.

The pulmonary lymphatics serve as a drainage system, which presents along the peribronchovascular, interlobular septa, and the pleural spaces are responsible for EVLW clearance by actively removing fluid and solutes from the interstitial tissue and poured into the superior vena cava through the thoracic duct continuously. Zarins demonstrated that the lymph flow is about 20 mL/h normally and could increase 5–10 times to compensate for the increase of interstitial pressure [8]. Gee reported that when transpulmonary pressure was increased to 20 cmH_2O, water content contained by the peribronchovascular cuffs increased by 70% [9]. Further extravasation of interstitial fluid is limited due to the progressive decrease of the interstitial compartment compliance. This protection could be destroyed due to the breakdown of interstitial proteoglycans, which caused loss of matrix integrity.

The dynamic equilibrium between the fluid leakage and lymphatic drainage is essential to maintain the dryness of the lungs, and hence preserve the normal function of oxygenation.

In terms of the movement of extravasated fluid into the alveoli from the interstitium, the process is quite faster. The mechanisms of alveolar fluid clearance (AFC) is responsible for the removal of excess fluid from the alveoli to the interstitial tissue across the alveolar epithelial barrier, in which the active ion transport plays a key role. The sodium permeant ion channels expressed in the distal lung epithelium are responsible for actively transport sodium back into the interstitial space, with chlorine and water following. Other molecular transporters including but not limiting the cystic fibrosis transmembrane conductance regulator, Na^+-K^+-ATPase, and several aquaporin water channels. The process of isosmolar fluid transport across the distal lung epithelium is upregulated by both catecholamine-dependent and -independent mechanisms [10].

The AFC rate depends on the species difference. In human beings, roughly on the order of 25% per hour [11], whereas in mice may be as high as 50% per hour [12].

Regulated with the mechanisms described above, EVLW seldom exceeds 500 ml in normal lungs; however, it may be 75–100% higher in the condition of alveolar flooding. Typically, increased interstitial EVLW is caused by increased hydrostatic pressure in the pulmonary capillaries (as occurs in congestive heart failure), decreased oncotic pressure (such as hypoalbuminemia), or the increased permeability of the alveolocapillary barrier (as in the ARDS) [13]. The accumulation of EVLW in interstitial spaces will thicken the blood-air barrier (0.5–2 μm in the normal range), impede the gas exchange under the same alveolar-arterial difference of oxygen, and reduce lung compliance.

It is well known that one of the major pathophysiological characteristics of ARDS is the increase of pulmonary permeability and the increase of hydrostatic pressure also prevalent due to fluid resuscitation. In the early phase of ARDS, the increase in interstitial EVLW could be compensated by the enhancement of lymphatic drainage. Once the speed of drainage is overwhelmed by high filtration rate and fluid enters the alveoli, the impaired active ion transport and lymphatic drainage

network may not clear excess fluid effectively, leading to the accumulation of EVLW, and what is worse is the flood of alveoli. Apart from ARDS, an increase of EVLW is also seen in septic shock [14] and other critically ill patients.

Indexed to the body weight (mL/kg), instead of absolute value (ml), EVLWI is better correlated with the oxygenation and the lung injury score, provide more accurate information in predicting the mortality of patients with ARDS. After screening a series of autopsies in Japan from more than 800 hospitals between 2004 and 2009, Tagami and colleagues compared the postmortem lung weights, and converted to EVLW with the following equation [15]:

$$\mathrm{EVLW}\left(\mathrm{mL}\right) = \left[0.56 \times \text{lung weight}\left(\mathrm{g}\right)\right] - 58.0.$$

Their results showed the mean value of EVLWI was 7.3 ± 2.8 mL/kg in 534 normal lungs, and 13.7 ± 4.5 mL/kg in 1688 lungs with diffuse alveolar damage (DAD), respectively. The cut-off value higher than 10 mL/kg could establish the diagnosis of DAD with a sensitivity of 81.3% and a specificity of 81.2%, therefore lower than 10 mL/kg is regarded as the normal values of EVLWI.

It will be a great value to detect and quantify the EVLW in monitoring the progression of the illness, evaluating the severity, and accessing treatment response accurately and timely. The histologic and gravimetric methods are good for experimental study; however, they could not be used in the clinical scenario. Ideally, a technique that fulfills the advantage of noninvasive, easy to implement, reproducible, and less expensive concomitantly is preferred by clinicians, which may provide enough information with sufficient sensitivity and specificity.

5.3 The Methods of EVLW Measuring

5.3.1 Gravimetry

Gravimetry remains as the golden standard in EVLW measuring. It is a precisely laboratory postmortem technique, which measures the total lung water by weighting the difference of lungs before and after desiccation. The amount of intravascular lung water could be estimated by comparing the hematocrit in systemic blood and lung specimen, assuming red blood cells do not cross the alveolar-capillary barrier, although it is not always true. Subtracting intravascular lung water from total lung water, we could know the EVLW.

5.3.2 Imaging Methods

The information provided by all imaging methods is spatially related, which means that each pixel (picture) or voxel (volume) in a cross-sectional image of the lung corresponding to a specific physical volume. Different from other solid organs, the

lung is air-containing and the parenchyma in a specific region varies with the state of lung inflation. The signal must be integrated over the entire lung to quantify changes in images of EVLW.

It has to be pointed out that imaging methods (except for positron emission tomography) just provide a rough estimation of total water content or concentration, and could neither differentiate extravascular water from vascular water technically, nor extracellular from intracellular water. If the blood volume varies with the hemodynamic status, the data calculated from imaging methods may mislead the estimation of EVLW.

5.3.3 Chest Radiography

Conventional chest roentgenogram is fast and easy to acquire method for detecting the presence of pulmonary edema, describing the overall distribution with the lung, and semi-quantifying the amount of exudate fluid. The typical signs such as pulmonary "congestion," vascular "redistribution," peribronchial cuffing, perihilar "haze," septal (Kerley) lines, and "interstitial" pattern to the radiographic densities may indicate the modest increases in EVLW (more than 35%) [16]. Further increase of EVLW presents with acinar opacities, ground-glass opacities, and frank consolidations. Initially, the distribution of increased radiographic density may be prominent regionally, i.e., gravity-dependent lung regions, and even turned to be opacity with the progression of fluid exudation.

In the clinical environment, the degree of interobserver variability and the lack of sensitivity raised concerns about the accuracy of chest radiography monitoring. For example, the interobserver variability ranged from 36% to 71% in diagnosing ARDS based on the American-European Consensus Conference definition, after reviewing 28 chest radiographs by 21 radiology experts [17]. Compared with CT, the accuracy of chest radiography was only 72% in alveolar-interstitial pulmonary edema assessment [18].

Apart from the limitations mentioned above, sometimes the X-rays are difficult to interpret, which is often the case in supine ICU patients, influenced by the heart and relaxed diaphragm. Besides, repeated radiation exposure brings safety risks to chest X-ray photography, all of which require the use of more sensitive and accurate techniques when evaluating EVLW.

5.3.4 Computed Tomography

Computed tomography (CT) enables the visualization of lung lesions from the apex to the bottom, from the anterior to the posterior regions, and quantify the infiltrate density of the lungs. In transverse sections of CT display, the arbitrary Hounsfield units (HU) calibrated against substances of known density, could easily define the spatial distribution of edema. Normally the value of 0 HU characterizes a voxel with

a density equal to that of water and the value of −1000 HU characterizes a voxel with a density equal to that of air. In isolated canine lungs, CT densitometry can detect modest increases in EVLW [19].

The disadvantages of CT include exposure to large doses of ionizing radiation (i.e., pregnant women or preterm infants), time-consuming, unrepeatable, and facing the risk of critically ill patient's transportation. Different from the previous studies, the most recent study questioned the diagnostic value of quantitative CT analysis for the assessment of pulmonary fluid status in unselected critically ill patients, mainly contribute to the real clinical routine other than a standardized protocol, i.e., without an end-expiratory pause while receiving mechanical ventilation [20].

5.3.5 Lung Ultrasonography

Although echocardiography is widely used in the ICU, the lung was not considered suitable for this imaging technology for a long time. Clinicians started the exploration of lung ultrasound since 1989 and gradually turned it to be a valuable point-of-care (POC) tool in the assessment of acute pulmonary diseases [21]. Healthy lung tissue is poorly penetrated by ultrasound due to the high acoustic impedance of air, which is usually defined as "black" lung. However, in the condition of increased EVLW, the air-fluid interface between collapsed, fluid-filled, and aerated alveoli will result in the acoustic reverberation artifacts, which provide the possibility of transmission of ultrasound deep into the diseased lung tissues.

With multimodal scanning of the anterior and lateral lung at different locations with 5–13 MHz linear array or 1–6 MHz phased array ultrasound probes, a panoramic impression of the complete lung and pleura could be achieved. B-lines (also named lung rockets) are well-defined, hyperechoic artifacts arising from the pleural line fanning down into the far-field of the screen without fading will display more than three in the condition of increased EVLW. In severe pulmonary edema, more B-lines are seen in narrow distance apart, and merge to display ground-glass rockets, also called "white lung." The linear correlation between the quantity of B-lines and the amount of EVLW is well acknowledged and make it possible to a semi-quantitative estimation of EVLW by counting the number of B-lines (Fig. 5.2).

Lung ultrasonography has high sensitivities and specificities in detecting EVLW when compared with other methodologies such as chest radiology, CT, or transpulmonary thermodilution. Combined with advantages of economic, fast, immediate, and dynamic feedback, free of radiation exposure, lung ultrasonography is very useful in daily clinical fluid management. Of course, standardized training is essential to limit the variation of the practitioner.

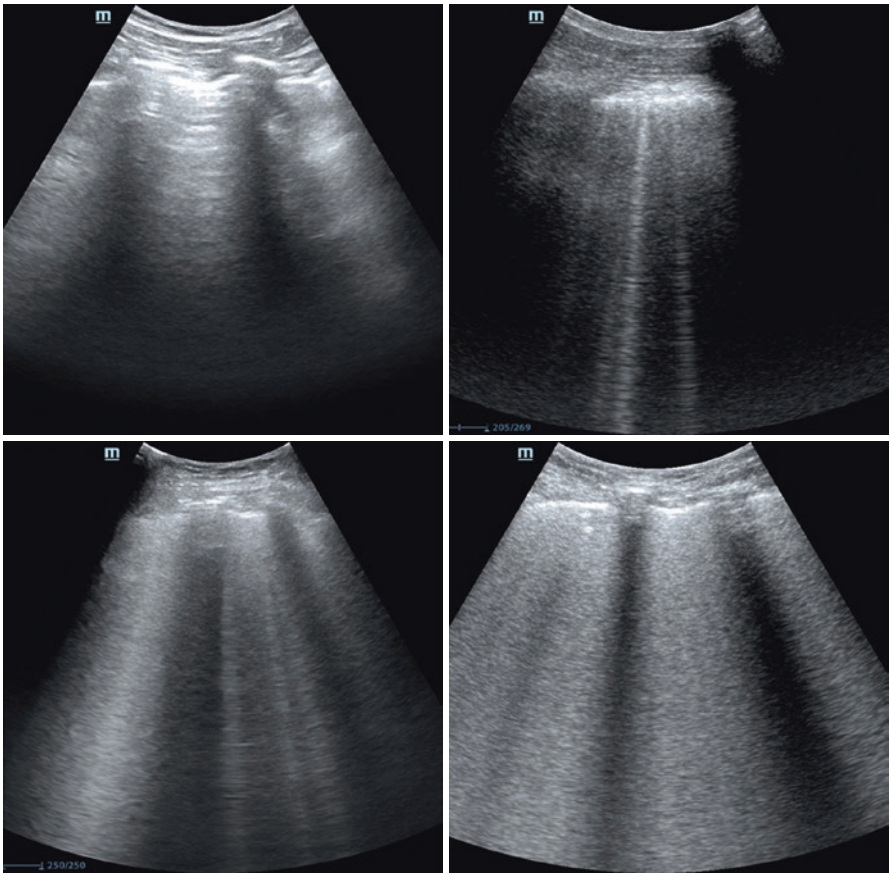

Fig. 5.2 The illustration of the semi-quantitative estimation of EVLW by counting the number of B-lines. In Severe cases, the B-lines almost merged

5.3.6 Nuclear Magnetic Resonance Imaging (MRI)

The principles of using MRI in evaluating EVLW are based on the fact that the signal of any MR image is related to the number of protons present. Under the external magnetic field, the hydrogen nuclei (protons) of water will align and keep in the same direction. Resonance comes from absorption and subsequent release of energy when the subject is irradiated with electromagnetic radiation in the form of a certain radiofrequency pulse, which is applied and discontinued regularly.

Although the lung is difficult to image since the overall density is low and subsequently MR signal is weak, early studies in excised animal lungs have demonstrated excellent correlations between gravimetric and MRI water content [22, 23]. However, it is impractical to use in the human examination due to long imaging

times of T2-decay (>6 min per slice) [24], since it should be completed within a single breath-hold.

The development of rapid imaging techniques such as submillisecond echo time (TE) gradient echo (GRE) imaging makes it possible to measure the proton density of the lung in a single breath-hold [25]. Theilmann et al. adapted GRE sequence to collect 12 images alternating between two closely spaced echoes in a single 9-s breath-hold, and the resulting data were fit with a single exponential decay function to determine T2* and lung water by back-extrapolating signal to an echo time of zero [26]. Albeit absolute values may be overestimated a little bit (errors are systematic and less than 10%, ~10 g), this technique has been proved reliable and valid compared with the ex vivo gravimetric method, regardless of lung volume or density, which enables the assessment of lung water content in a single breath-hold, and thus may offer significant advantages in the study of human lung disease and physiology [27].

5.3.7 Indicator Dilution Methods

5.3.7.1 Transpulmonary Thermo-Dye Dilution

When injected via central venous, freely diffusible (heat/cold) and a non-diffusible (indocyanine green dye which binds to albumin) indicator each have the same flow but through different volumes of distribution. The difference in the mean transit times of the two indicators is, therefore, extravascular thermal volume (ETV). Since compared with the extravascular water content of the lung, the extravascular water content of myocardium and non-pulmonary blood vessels is small, ETV and EVLW are usually considered to be equivalent.

Lewis introduced the thermos-green dye dilution technique in the early 1980 [28] and validated against gravimetry in human beings [29]. In detail, 10 mL of cold (0 °C) indocyanine green dye (4 mg) is injected rapidly into superior vena cava through a central catheter, then withdrawn by syringe pump through a densitometer cuvette attached to the femoral catheter with the speed of 30 mL/min, and recorded the curves of both the thermodilution and dye concentration versus time. The collected data is processed by the computer and EVLW is derived from the difference between the volume of distribution of the indicator diffusing into the extravascular space (cold) and of the green dye remaining in the circulation. As the double indicator dilution technique, thermos-dye dilution has been replaced by the single indicator thermodilution technique and is not available in the market anymore.

5.3.7.2 Transpulmonary Thermodilution (TPTD)

TPTD uses a cold indicator delivered into a central vein and detected by a thermistor tipped catheter in the aorta (either in the femoral or axillary artery), resulting in the recording of a thermodilution curve. During pulmonary transit, the presence of

pulmonary edema will result in the indicator loss by warming the fluid bolus, and this loss of indicator is used to quantify EVLW. The application of TPTD is based on the assumption that the pulmonary blood volume represents 20% of the intrathoracic blood volume (ITBV), or 25% of the global end-diastolic volume (GEDV), which comes from the observations reported by Sakka et al. in 2000 [30]. Due to the individual variability between pulmonary blood volume and ITBV, TPTD is only the best estimation, instead of a precise measure of EVLW [31].

Compelling evidence showed the power of TPTD in early and accurate measuring EVLW. In a porcine model of hydrostatic pulmonary edema conducted by Bongard, a strong linear association exist between ELVW and increase in perivascular cuff width to vessel diameter ratio, interalveolar septal width, and alveolar flooding, and 100% increase of EVLW is required before the onset of hypoxemia or histologic changes [32]. In another porcine study, researchers demonstrated that TPTD could detect a modest increase of EVLW, even only 50 mL of saline is instilled into the trachea [33]. In terms of reliability, the coefficient of variation of EVLW ranging from 4.8 to 8% suggests it is highly reliable [34]. In the case report of ARDS induced by 2009 pandemic influenza A (H1N1) virus, the maximum of EVLWI once reached 33 mL/kg, coincidence with poor respiratory compliance and low PaO_2/FiO_2 ratio, and decreased with the improvement of clinical symptoms and respiratory parameters, showing its high value of monitoring EVLW dynamically [35].

Since the central venous and arterial cannulation are common in ICU, TPTD monitoring is easy to perform. By measuring the cardiac preload concomitantly, it is possible to differentiate increased capillary permeability from the increased hydrostatic pressure, which is typically seen in ARDS and cardiac failure, respectively. It must be pointed out that the TPTD only measures lung water in perfused areas of lung and therefore rely on the homogenous distribution of pulmonary perfusion. Mismatch of ventilation-perfusion will lead to errors in the estimation of EVLW, e.g., pulmonary embolism, lung resection, and high level of positive end-expiratory pressure.

Until now, TPTD is the only methodology available at the bedside to evaluate the amount of EVLW, with the advantage of nonoperator dependent, nurse-performed, and helpful in differentiating the etiology of pulmonary edema. However, the relatively high cost and invasive nature limit its widespread use.

5.4 Conclusion

Assessment of lung water is crucial in pulmonary edema diagnosis and management. Several methodologies are available to quantify lung water, depending not only on the understanding of the unique advantages and limitations of these approaches but also the availability of expertise in each modality's application and interpretation. Currently, gravimetry is deemed as the experimental reference method and transpulmonary thermodilution as the clinical reference method, while lung ultrasonography stands for the promising tool.

References

1. Jozwiak M, Teboul JL, Monnet X. Extravascular lung water in critical care: recent advances and clinical applications. Ann Intensive Care. 2015;5(1):38.
2. Starling EH. On the absorption of fluids from the connective tissue spaces. J Physiol. 1896;19(4):312–26.
3. Danielli JF. Capillary permeability and oedema in the perfused frog. J Physiol. 1940;98(1):109–29.
4. Tarbell JM, Demaio L, Zaw MM. Effect of pressure on hydraulic conductivity of endothelial monolayers: role of endothelial cleft shear stress. J Appl Physiol (Bethesda MD 1985). 1999;87(1):261–8.
5. Collins SR, Blank RS, Deatherage LS, Dull RO. Special article: the endothelial glycocalyx: emerging concepts in pulmonary edema and acute lung injury. Anesth Analg. 2013;117(3):664–74.
6. Rehm M, Bruegger D, Christ F, Conzen P, Thiel M, Jacob M, Chappell D, Stoeckelhuber M, Welsch U, Reichart B, et al. Shedding of the endothelial glycocalyx in patients undergoing major vascular surgery with global and regional ischemia. Circulation. 2007;116(17):1896–906.
7. Weinbaum S, Tarbell JM, Damiano ER. The structure and function of the endothelial glycocalyx layer. Annu Rev Biomed Eng. 2007;9:121–67.
8. Zarins CK, Rice CL, Peters RM, Virgilio RW. Lymph and pulmonary response to isobaric reduction in plasma oncotic pressure in baboons. Circ Res. 1978;43(6):925–30.
9. Gee MH, Williams DO. Effect of lung inflation on perivascular cuff fluid volume in isolated dog lung lobes. Microvasc Res. 1979;17(2):192–201.
10. Matthay MA, Folkesson HG, Clerici C. Lung epithelial fluid transport and the resolution of pulmonary edema. Physiol Rev. 2002;82(3):569–600.
11. Verghese GM, Ware LB, Matthay BA, Matthay MA. Alveolar epithelial fluid transport and the resolution of clinically severe hydrostatic pulmonary edema. J Appl Physiol (Bethesda MD 1985). 1999;87(4):1301–12.
12. Fukuda N, Folkesson HG, Matthay MA. Relationship of interstitial fluid volume to alveolar fluid clearance in mice: ventilated vs. in situ studies. J Appl Physiol (Bethesda MD 1985). 2000;89(2):672–9.
13. Kushimoto S, Taira Y, Kitazawa Y, Okuchi K, Sakamoto T, Ishikura H, Endo T, Yamanouchi S, Tagami T, Yamaguchi J, et al. The clinical usefulness of extravascular lung water and pulmonary vascular permeability index to diagnose and characterize pulmonary edema: a prospective multicenter study on the quantitative differential diagnostic definition for acute lung injury/acute respiratory distress syndrome. Crit Care. 2012;16(6):R232.
14. Martin GS, Eaton S, Mealer M, Moss M. Extravascular lung water in patients with severe sepsis: a prospective cohort study. Crit Care. 2005;9(2):R74–82.
15. Tagami T, Sawabe M, Kushimoto S, Marik PE, Mieno MN, Kawaguchi T, Kusakabe T, Tosa R, Yokota H, Fukuda Y. Quantitative diagnosis of diffuse alveolar damage using extravascular lung water. Crit Care Med. 2013;41(9):2144–50.
16. Snashall PD, Keyes SJ, Morgan BM, McAnulty RJ, Mitchell-Heggs PF, McLvor JM, Howlett KA. The radiographic detection of acute pulmonary oedema. A comparison of radiographic appearances, densitometry and lung water in dogs. Br J Radiol. 1981;54(640):277–88.
17. Rubenfeld GD, Caldwell E, Granton J, Hudson LD, Matthay MA. Interobserver variability in applying a radiographic definition for ARDS. Chest. 1999;116(5):1347–53.
18. Lichtenstein D, Goldstein I, Mourgeon E, Cluzel P, Grenier P, Rouby JJ. Comparative diagnostic performances of auscultation, chest radiography, and lung ultrasonography in acute respiratory distress syndrome. Anesthesiology. 2004;100(1):9–15.
19. Forster BB, Muller NL, Mayo JR, Okazawa M, Wiggs BJ, Pare PD. High-resolution computed tomography of experimental hydrostatic pulmonary edema. Chest. 1992;101(5):1434–7.
20. Saugel B, Wildgruber M, Staudt A, Dieckmeyer M, Holzapfel K, Kaissis G, Kirov MY, Kuzkov VV, Schmid RM, Huber W. Quantitative computed tomography in comparison with

transpulmonary thermodilution for the estimation of pulmonary fluid status: a clinical study in critically ill patients. J Clin Monit Comput. 2019;33(1):5–12.
21. Lichtenstein DA. BLUE-protocol and FALLS-protocol: two applications of lung ultrasound in the critically ill. Chest. 2015;147(6):1659–70.
22. Hayes CE, Case TA, Ailion DC, Morris AH, Cutillo A, Blackburn CW, Durney CH, Johnson SA. Lung water quantitation by nuclear magnetic resonance imaging. Science. 1982;216(4552):1313–5.
23. Cutillo AG, Morris AH, Blatter DD, Case TA, Ailion DC, Durney CH, Johnson SA. Determination of lung water content and distribution by nuclear magnetic resonance. J Appl Physiol Respir Environ Exerc Physiol. 1984;57(2):583–8.
24. Estilaei M, MacKay A, Whittall K, Mayo J. In vitro measurements of water content and T2 relaxation times in lung using a clinical MRI scanner. J Magn Reson Imaging. 1999;9(5):699–703.
25. Hatabu H, Alsop DC, Listerud J, Bonnet M, Gefter WB. T2* and proton density measurement of normal human lung parenchyma using submillisecond echo time gradient echo magnetic resonance imaging. Eur J Radiol. 1999;29(3):245–52.
26. Theilmann RJ, Arai TJ, Samiee A, Dubowitz DJ, Hopkins SR, Buxton RB, Prisk GK. Quantitative MRI measurement of lung density must account for the change in T(2) (*) with lung inflation. J Magn Reson Imaging. 2009;30(3):527–34.
27. Holverda S, Theilmann RJ, Sa RC, Arai TJ, Hall ET, Dubowitz DJ, Prisk GK, Hopkins SR. Measuring lung water: ex vivo validation of multi-image gradient echo MRI. J Magn Reson Imaging. 2011;34(1):220–4.
28. Lewis FR, Elings VB, Hill SL, Christensen JM. The measurement of extravascular lung water by thermal-green dye indicator dilution. Ann N Y Acad Sci. 1982;384:394–410.
29. Mihm FG, Feeley TW, Jamieson SW. Thermal dye double indicator dilution measurement of lung water in man: comparison with gravimetric measurements. Thorax. 1987;42(1):72–6.
30. Sakka SG, Ruhl CC, Pfeiffer UJ, Beale R, McLuckie A, Reinhart K, Meier-Hellmann A. Assessment of cardiac preload and extravascular lung water by single transpulmonary thermodilution. Intensive Care Med. 2000;26(2):180–7.
31. Michard F. Bedside assessment of extravascular lung water by dilution methods: temptations and pitfalls. Crit Care Med. 2007;35(4):1186–92.
32. Bongard FS, Matthay M, Mackersie RC, Lewis FR. Morphologic and physiologic correlates of increased extravascular lung water. Surgery. 1984;96(2):395–403.
33. Fernandez-Mondejar E, Rivera-Fernandez R, Garcia-Delgado M, Touma A, Machado J, Chavero J. Small increases in extravascular lung water are accurately detected by transpulmonary thermodilution. J Trauma. 2005;59(6):1420–3; discussion 1424.
34. Allison RC, Carlile PV Jr, Gray BA. Thermodilution measurement of lung water. Clin Chest Med. 1985;6(3):439–57.
35. Li HL, Wang ZY, Yao GQ, Zhu X. Monitoring extravascular lung water in acute respiratory distress syndrome induced by probable 2009 pandemic influenza a (H1N1) virus: report of two cases. Chin Med J. 2010;123(9):1225–7.

Part II
Applications of Respiratory Monitoring

Chapter 6
Acute Respiratory Distress Syndrome

Yu-Mei Wang and Guang-Qiang Chen

Acute respiratory distress syndrome (ARDS) can be caused by several diseases. The symptoms are characterized as impaired gas exchange, decreased lung compliance, increased lung weight, and widespread involvement of the lung parenchyma. No matter what causes ARDS, the treatment of symptoms is mandatory to save time for the resolution of the underlying process [1]. ARDS patients need mechanical ventilation [2]. The mortality of mechanically ventilated patients remains as high as 30–40% [3]. Despite being life-saving, mechanical ventilation also can be harmful for the lungs as well as the diaphragm [4]. During mechanical ventilation, especially passive ventilation, inappropriate ventilator settings can worsen lung injury, which is called ventilation-induced lung injury (VILI). In the transition to assisted ventilation, harmful patient–ventilator interactions might occur. Understanding the physiology of ARDS and better respiratory monitoring will help clinicians adapt the best available evidence with the ultimate goal of improving morbidity and mortality. This chapter summarizes respiratory monitoring in ARDS to provide more protective ventilation. Most of the physiological concepts are mentioned above.

6.1 Physiology of ARDS

The concept of ARDS was born more than 50 years ago. Ashbaugh and colleagues reported 12 cases of young patients with severe acute respiratory failure with bilateral pulmonary infiltrates, decreased compliance, poor oxygenation refractory to supplemental oxygen, and in some cases impaired carbon dioxide clearance [5].

The current Berlin definition characterizes ARDS by bilateral lung infiltrates on chest imaging due to pulmonary edema [2]. Three main physiological consequences

Y.-M. Wang · G.-Q. Chen (✉)
Department of Critical Care Medicine, Beijing Tiantan Hospital, Capital Medical University, Beijing, China

J. Zhou et al. (eds.), *Respiratory Monitoring in Mechanical Ventilation*,
https://doi.org/10.1007/978-981-15-9770-1_6

are included in ARDS: a defect in oxygenation, a high dead space, and a dramatic reduction in lung volumes as illustrated by a functional residual capacity of around 40% predicted and this reduction is inhomogeneous [6]. In addition, the study of chest computed tomography (CT) reported that the lung was heterogeneous and a small amount of air remained in aerated areas [7]. This led to the popular concept of "baby lung" proposed by Gattinoni and Pesenti, which refers to the small amount of normally aerated lung units [8]. The first CT scan images obtained in ARDS patients, show that densities were preferentially distributed in the dependent lung regions, but relatively less in the independent lung area. This view is in contrast to the commonly accepted lung heterogeneity in ARDS patients. CRS has decreased accordingly not because of stiffer lungs, but due to a small number of aerated lung units with normal compliance. Therefore, with mechanical ventilation, the insufficiency of a given VT in a small aerated lung will generate higher pressures in ARDS than in normal lungs.

These characteristics may have clinical consequences, which is defined as VILI, (1) barotrauma (alveolar air leaks such as pneumothorax, pneumomediastinum, or subcutaneous emphysema) [9]; (2) volutrauma (overdistension of aerated lung regions) [10]; (3) atelectrauma (repeated opening and closing of some lung regions) [11]; (4) decreased cardiac output by means of a decrease in the left ventricular preload [12]; and an increase in right ventricular afterload up [13]. All these consequences are harmful to the patients.

Imbalance of lung ventilation and perfusion is also an important characteristic of ARDS [14]. Because of lung heterogeneity, some lung regions are better ventilated than perfused (such as dead space), whereas others are less ventilated than perfused or nonventilated at all (i.e., intrapulmonary shunt) [15]. Dead space is related to lung microcirculatory occlusion, to a certain extent to shunt and potentially to distension, and is an independent predictor of mortality in ARDS [16]. Impaired CO_2 clearance is the main clinical consequence of dead space and it can be corrected by increasing alveolar ventilation. And the main clinical consequence of intrapulmonary shunt is hypoxemia without significant improvement by an increase of FiO_2 [15].

6.2 Monitoring Gas Exchange

In general, FiO_2 can be monitored by the ventilator to ensure that sufficient concentration of O_2 is delivered to the patient, and then pulse oximetry or by blood gas analyses can be used to monitor the patient's oxygenation status.

The O_2_hemoglobin saturation can quite well be estimated by continuous measurement of pulse oxymetric saturation (SpO_2), which can be easily obtained. But the disadvantage is that there may be an important discrepancy between the blood O_2 saturation (SaO_2) and SpO_2 and that the measurement accuracy is much lower at lower SaO2. In addition, a precondition is that the patient has to have an adequate peripheral perfusion, or it is not so accurate.

PaO_2 might be continuously monitored by blood gas analysis or an arterial catheter. However, continuous PaO_2 required transducers which have to be inserted in an artery and are difficult to maintain if clotting around the catheter tip as well as

measurement drift. Therefore, it is seldom used in the ICU. Henceforth, frequent arterial blood samples and PaO_2 measurement via a blood gas analyzer are required. This is the most common oxygenation monitoring. It is important to consider that PaO_2 is different from tissue oxygenation in interpreting blood gas results. Furthermore, oxygenation, perfusion, and metabolism in different organs and tissues are very different. Thus, mixing different parameters and techniques to estimate the condition of ARDS patients is the key to monitor oxygenation. There are no studies to investigate the level of the lowest acceptable PaO_2. In the ARDSNet trials, they enrolled a large number of patients with the target oxygenation range of 55–80 mmHg. On the contrary, in one study cognitive impairment was found associated with PaO_2 levels <60 mmHg [17]. Thus, PaO_2 >60 mmHg may be adequate for the patients, but some other values need to be assessed including the patient's cardiac output (CO), hemoglobin level as well as metabolic demand. Maybe the oxygen transport (DaO_2) to the tissues is more comprehensive which include CO and hemoglobin level.

In addition, in most cases, mixed venous oxygen partial pressure (PvO_2) may be more important than PaO_2. Because it is primarily related to the oxygen tension in the tissues (but it should be noted that it reflects the mixing of oxygen tension in all organs and tissues).

As the physiologies of ARDS are dead space and intrapulmonary shunt, dead space can be assessed using volumetric capnography [15], while intrapulmonary shunt is related to alveolar flooding or lung atelectasis and can be assessed using the shunt equation requiring a pulmonary artery catheter (Details see above). The amount of CO_2 elimination in the lung is directly proportional to the alveolar ventilation. The elimination of pulmonary CO_2 can be monitored by volumetric exhaled CO_2 measurement (the CO_2 signal is integrated with the expired flow) for in-line or side stream infrared CO_2 analysis [18].

CO_2 elimination is dependent not only on the pulmonary circulation but also on the pulmonary ventilation as well as CO_2 production (i.e., metabolism). Thus, if CO_2 excretion has a sudden decrease at stable ventilation, this may lead to pulmonary perfusion to a sudden decrease, for example, pulmonary emboli or a reduction in cardiac output. Similarly, the reduction in CO_2 excretion without any change in circulation is due to deteriorated ventilation, e.g., at PCV reduced compliance (secretions edema or lung collapse) or increased airway obstruction by secretion.

6.3 Monitoring Respiratory Mechanics

The mechanics of the respiratory system correlate with the airway pressure, the pleural pressure, the flow rate, the lung volume, the tidal volume, and the condition of the lungs and chest wall. As a result, in a very heterogeneous lung in ARDS patients, the local strain (lung tissue deformation or volume change) and the transpulmonary pressure (airway pressure-pleural pressure) are different in different locations [19, 20]. It is important to pay attention that the outcome depends on the condition of the respiratory system and the patient position.

In short, the lung mechanics is the forces (i.e., pressures) required to inflate a certain amount of gas into the lung including two different parts: one is the force needed to overcome the resistance to airflow in the endotracheal tube and in the airways (flow-resistive pressure); the other one is the force requiring to overcome the elastic properties of the lungs and the chest wall (elastic recoil pressure).

6.3.1 Flow Resistance

One important thing is to monitor flow resistance. Although some methods can be used to estimate flow resistance, some principles are important and need to keep in mind. First, resistance is dependent on the flow rate. Secondly, inspiratory resistance is different from expiratory resistance, and resistance depends on the patient's airways and a variable extent on the endotracheal tube resistance. There are two easy monitoring methods to monitor flow resistance: one is a computation of inspiratory resistance under a constant inspiratory flow:

$$\text{Flow resistance} = \frac{\left(\text{Peak pressure} - \text{Plateau pressure}\right)}{\text{Inspiratory flow rate}}$$

the other is an assessment of whether the flow has ceased at end-inspiration (during pressure-controlled ventilation) or at end-expiration. If not, this is because a time constant (resistance × compliance) of the system is too long for inspiratory and expiratory time according to the ventilator settings, respectively. In ARDS patients, this is due to either high resistance or too short expiratory time. Too short expiratory time has been used to induce auto-PEEP in order to keep the lungs open (inverse ratio ventilation) (Auto-PEEP is mentioned above).

6.3.2 Monitoring the Condition of Lung and Chest Wall

Monitoring the condition of the lung and chest wall is the other important thing, such as plateau pressure, elastance, compliance, driving pressure, and so on. Lung and chest wall compliance, elastance can be obtained by all the parameters mentioned above, including VT, plateau pressure, PEEP, and so on (Details are below).

6.3.2.1 Plateau Pressure

Assuming that all alveoli are opened, plateau pressure (Pplat) reflects end-inspiratory alveolar pressure [21]. A short end-inspiratory occlusion (0.3 s) is sufficient to estimate injurious pressure applied to the alveoli, especially in passive breathing. During spontaneous breathing, measuring Pplat might be possible also using an

end-inspiratory occlusion if no effort is detected, but this requires validation [22]. Pplat is strongly correlated with the risk of pneumothorax and other consequences of overdistension [23]. Boussarsar et al. found an increasing risk of pneumothorax when Pplat was greater than 35 cmH_2O [23], and a safety limit of 30 cmH_2O was deemed protective in a large randomized controlled trial [24]. However, Terragni and colleagues found with a Pplat greater than 28 cmH_2O had a higher risk of overdistension on CT scan and higher proinflammatory cytokine levels in bronchoalveolar lavage than those with a lower Pplat [25] at patients in a cohort of patients with ARDS ventilated with a Pplat below 30 cmH_2O. Nowadays, maintaining Pplat at or below 28 cmH_2O as used in a large trial seems to be a reasonable and safe threshold.

6.3.2.2 Elastance and Compliance

Suter and colleagues first used the beat oxygen delivery to titrate the PEEP level [26]. They found that the best oxygen delivery was associated with the best compliance of respiratory system (C_{RS}), suggesting that compliance could be used to set the level of optimal PEEP. Grasso and colleagues reported different effects of high PEEP levels on C_{RS} according to the lung recruitability [27]. The C_{RS} depends on the lung recruitability. However, one major caveat of C_{RS} is that it may be artificially increased by intratidal recruitment. Therefore, repeated lung and airway opening and closing need to be avoided, or setting PEEP according to the best C_{RS} could be very misleading.

6.3.2.3 Driving Pressure (ΔP)

Ventilation with a ΔP value below 20 cmH_2O was associated with a lower risk of pneumothorax as compared with conventional ventilation with large tidal volumes [28]. In a post hoc analysis of large randomized trials, Amato and colleagues found that a ΔP value greater than 14–15 cmH_2O was independently associated with higher mortality [29]. Moreover, beneficial effects of VT reduction or high PEEP levels on mortality were mediated by a decrease in ΔP. However, whether a ventilation strategy according to ΔP would result in better outcomes is still unknown.

6.3.2.4 Transpulmonary Pressure (PL) and Esophageal Pressure

At end-inspiration, PL is a more reliable measurement of the distending pressure of the lung than Pplat. Because Pplat depends not only on PL, but also on pleural pressure (Ppl). Indeed, in some patients, Ecw is responsible for almost 50% of the E_{RS}, while in other cases is approximately 15–20% [30]. Grasso and colleagues [31] enrolled 14 patients with refractory ARDS referred for consideration of extracorporeal membrane oxygenation (ECMO). They were all ventilated with a Pplat greater than 30 cmH_2O. Half of them had PL at end-inspiration (PL,ei) below 25 cmH_2O,

suggesting a significant contribution of the chest wall to the increase Pplat. Increasing PEEP up to a PL,ei of 25 improved oxygenations without the need for ECMO. PL,ei might also be assessed in spontaneous breathing patients with an esophageal balloon catheter doing an end-inspiratory occlusion [32].

PL at end-expiration (PL,ee) is the pressure distending the lungs at end-expiration. Negative PL,ee values are common in ARDS, potentially favoring cyclic reopening and closing of alveoli during ventilation and atelectrauma [33]. In ARDS, setting PEEP to a positive PL,ee was associated with improved physiological parameters and was well tolerated compared with setting PEEP according to an oxygenation Table [34]. However, the absolute value of esophageal pressure reflects the pleural pressure at mid-chest [35]. Different part of the chest has different Ppl, which can be monitored by esophageal pressure (Details are above). In addition, it does not specifically indicate whether the lung is recruitable or not.

Recently, Yoshida and coworkers carried out a study to confirm the validity of the esophageal pressure to assess regional pleural pressure in pigs and human cadavers embalmed to preserve tissue elasticity [35]. The Ppl gradient between the nondependent and the dependent part of the chest was higher in pigs with injured lungs than healthy lungs, which may indicate higher in human cadavers (around 10 cmH_2O) confirm Ppl heterogeneity. PL calculated using esophageal pressure was reliable; however, it was not reliable in calculating the Ppl in the nondependent and the dependent part of the chest cavity [35]. Moreover, the elastance-derived method was a good surrogate to calculate PL,ei for the actual PL in the nondependent part of the chest cavity. Therefore, the use of PL using the elastance-derived method may be used to estimate the risk of overdistension in the nondependent part of the lung, while the use of absolute values reflects pleural pressure at mid-chest.

6.3.2.5 Work of Breathing and Esophageal Pressure–Time Product

Work of breathing (WOB) is the energy expenditure of respiratory muscles to generate a volume. And Campbell diagram can be used to calculate WOB as the area enclosed by the product of the change in Pmus and change in volume. WOB per minute can be calculated (in joules per minute [J/min]) and normalized to the tidal volume (effort per unit of volume displaced, in joules per liter [J/L]). In healthy subjects at rest, WOB ranges from 2.4 to 7.5 J/min and from 0.2 to 0.9 J/L [36].

6.3.2.6 End-Expiratory Lung Volume

It is recommended that end-expiratory lung volume (EELV) can be measured to evaluate whether the lung is collapsed or overinflated and to set or assess the effect of PEEP. EELV could be assessed by CT scan and CT is the golden tool to measure EELV. But CT is cumbersome and has radiation risk at frequent repeated exposure. Therefore, CT cannot be used as a monitoring routine tool at bedside, and especially

for monitoring EELV or its changes, such as recruitment and overdistention by different interventions.

Another way is gas dilution techniques. However, the limitation of the tracer gas dilution techniques is the closed-circuit method, which requires patient disconnecting from the ventilator. This disadvantage makes this technology hardly as a monitor technique. Because of this disadvantage, an improved method, open-circuit multi breathing nitrogen well flushing technology, is proposed. In contrast, it is now incorporated in one ventilator brand is quite easy to handle and gives acceptable estimates of EELV [37]. However, one thing should be considered that the obtained EELV is only the volume in lungs. If EELV increases with PEEP, it is important to determine whether the increase in EELV is due to overinflation of open units, increased in normal lung volume, or recruiting previously collapsed lung units or a combination of all.

6.3.2.7 Mechanical Power

Mechanical power is the combination of pressure, volume, flow, and respiratory rate, which may be a more reliable predictor of VILI. 12 J/min may be a meaningful threshold of VILI, and may be a predictor of mortality and survival. What is more, mechanical power may be a predictor of mortality (For details refer to Chap. 2).

The aim of mechanical ventilation is to provide adequate gas exchange without further injuries to the lungs and other organs. Lung mechanics (such as pressures, volumes, and flow) and lung imaging enable the clinician to ensure they provide as much lung-protective ventilation as possible. Lung mechanics monitoring is very important to avoid VILI.

6.4 Monitoring by Lung Imaging

ARDS lungs are very heterogeneous and it is not possible to assess the regional differences in lung mechanical properties with conventional lung mechanics. Physiological respiratory parameters cannot provide regional information. For this reason, the other choices are chest CT or electrical impedance tomography (EIT). CT is a golden method to provide regional ventilation information. However, CT is an excellent method for diagnosis and understanding of the underlying deterioration in lung morphology, but too demanding for monitoring [38]. It is impossible using CT for monitoring at bedside. On the other hand, EIT is more useful for monitoring and evaluating the regional effects of PEEP, recruitment maneuvers, and ventilation [39]. EIT is no-radiation, dynamic, and simple way for monitoring. And EIT can provide different regional information, including ventilation distribution, the percentage of overdistention and collapse, center of ventilation, and so on.

Another useful method is lung and diaphragm ultrasound, which is suitable to diagnose lung consolidation and pleural conditions [40]. Lung ultrasound is a

bedside method, which is developing rapidly in the recent years. Lung ultrasound is ideal for both diagnosing and intermittent monitoring. What is more, the ultrasound is easy to get and can be used at bedside. Diaphragm ultrasound allows the noninvasive quantification of inspiratory efforts during assisted ventilation using a linear probe (>10 MHz) positioned on the zone of apposition of the diaphragm. The measurement of diaphragm ultrasound has been validated in critically ill patients [41].

6.5 Monitoring of Adequate PEEP by Lung Mechanics Monitoring

PEEP setting is a difficult ventilation element to choose. There are lots of methods for selecting optimal PEEP. An optimal PEEP is a pressure at end-expiratory, which should be set at an end-expiratory pressure that prevents: expiratory collapse, intratidal collapse, and re-expansion (recruitment-derecruitment); and end-expiratory and end-inspiratory overdistension. It is essential to ARDS patient; however, still not set using suitable methods. Also, since in ARDS the lung is very heterogeneous, in other words, lung regions close to each other have extremely different specific lung volumes and compliances [20], the general methods setting PEEP are always a compromise and could never be completely "optimal."

Based on lung mechanics, there are many approaches to select PEEP. Exclued lung imaging methods, the most common methods for PEEP setting all use respiratory mechanics. Static pressure-volume curve is the classical way to set PEEP. PEEP is set at the pressure where inspiratory compliance increases, which can be revealed by the "lower inflection point" (LIP). Ventilation operates on the steep part of P-V curve, between LIP and the pressure at the "upper inflection point" (UIP), when compliance suddenly decreases, indicating excessive expansion. However, the most important pressure is the pressure at which a large number of lung regions begin to collapse, and this pressure occurs on the expiratory limb of the loop, where compliance is maximal.

Another method is based on the oxygenation goal (ARDS network PEEP/FIO_2 table) proposed by ARDSNet. PEEP according to the PEEP/FIO_2 table of the National Institutes of Health ARDS network trial [42] (PEEP/FIO_2 table), PEEP and FIO_2 were titrated to maintain PaO_2 between 55 and 80 mmHg or SpO_2 between 88% and 95%. This is the most common way to select PEEP. However, this method just considers the oxygenation but ignores lung and chest wall condition.

As P-V curve has some limitations, there are some other technologies to select PEEP. A PEEP trial can estimate similar pressure as reducing or increasing PEEP slowly after a maximum recruitment is performed [43]. The pressure with best or highest C_{RS} (or lowest ΔP) is found and the "optimal" PEEP is 2 cmH_2O above the pressure, which is CRS-related method or ΔP-related method. However, this kind of maneuver is only useful if the lungs can be recruited, mainly in early ARDS. Non-recruitment patients may have no highest C_{RS} or lowest ΔP.

Another selection may be stress index (SI). Since time shows a linear volume increase at a constant flow, SI can be considered as a tidal volume/pressure curve,

that is, the instant slope of the curve equaling to the Ers if the resistance is constant. Therefore, the slope (SI > 1) and volume increasing over time indicate that Ers increases, i.e., overinflation. In contrast, a decrease in slope (SI < 1) indicates a decrease in Ers, such as tidal volume recruitment, while a straight line (SI = 1) indicates that Ers is constant. Although physiologically reasonable, it is not clear whether PEEP can reduce VILI or improve outcome.

Except all these methods, there are still some methods according to lung mechanics, such as the ExPress trial [44]: PEEP was adjusted to reach a Pplat between 28 and 30 cmH_2O, transpulmonary pressure, and esophageal pressure. They all have their advantages and disadvantages.

With the development of technology, EIT can be used to select optimal PEEP. And it may be the simplest way at bedside. There are many EIT parameters to select PEEP. The simplest way is to use the center of ventilation (COV) representing the distribution of ventilation across the chest from the ventral to dorsal [45–47]. If most ventilation moves in the ventral region and PEEP increases, a shift of COV from ventral to dorsal regions indicates that PEEP has a positive response. During the decremental PEEP maneuver, another way to assess the risk of atelectasis is to observe the change in end-expiratory lung impedance (ΔEELI) over time [48], or regional ventilation delay (RVD) [49]. When PEEP is reduced, there is always an associated decrease in EELV (and in EELI) which will be much greater if associated with derecruitment. Setting PEEP above the level associated with a decrease in ΔEELI of 10% during a decremental PEEP trial resulted in improved oxygenation and lower ΔP compared with PEEP setting according to the low $PEEP/FIO_2$ table in 16 patients with a baseline PaO_2/FIO_2 below 300 mmHg [48]. RVD is a measure of tidal recruitment in passively breathing patients. Areas of repetitive opening and closing of alveolar units would likely have delays, the higher the value the greater degree of tidal recruitment. Monitoring ventilation distribution now is available to quantify the degree of regional compliance changes when PEEP is titrated. Compliance changes relative to each PEEP is graphically computed to demonstrate compliance loss related to high PEEP (i.e., overdistension) and low PEEP (i.e., collapse), which is so-called Costa's method to calculate the percentage of overdistention and collapse [50]. The lowest sum of collapse and overdistension will be the optimal PEEP, which will lead to less lung injury. This point of intersection may represent the balance of risk versus benefit. Recently, some researches carried out trials using this method selecting optimal PEEP.

6.6 Monitoring Airway Closure

Small airway injury was found in experimental and autopsy studies in ARDS [51]. This can be interpreted as the results of repeated airway opening and closing during tidal breaths at low PEEP levels. Chen and colleagues [52] conducted a study based on the analysis of low-flow inflation *P–V* curves in ARDS. The study gave attention to that in about 1/3 of patients, the initial part of the slope can be superimposed to the *P–V* curve of a blocked circuit indicating complete closure of the airways.

However, the esophageal pressure is unchanged during that period whereas airway pressure increases dramatically [52]. Therefore, this may indicate complete airway closure while the "baby lung" remains aerated on the chest CT scan. Respiratory monitoring can help clinicians discover airway closure as early as possible to avoid lung injury.

6.7 Monitoring Dyssynchrony

Dyssynchrony will occur as an appropriate ventilation setting. It is essential to distinguish all kinds of dyssynchrony. Clinical assessment by visual observation will provide many important information on patient's synchrony. The ventilator's screen displays flow, Paw, and tidal volume waveforms which can be sufficient to diagnose some dyssynchronies [53]. Nevertheless, more precise detection can be obtained using additional monitoring tools such as esophageal balloon or electrical activity of the diaphragm (EAdi). Esophageal pressure is directly dependent on respiratory muscle activity with granting dyssynchrony assessment. EAdi can be displayed on a ventilator screen along with the other waveforms providing useful information on patient's neural respiratory times and its synchrony with ventilator delivery. This is a minimally invasive way to monitor patient–ventilator dyssynchrony as most of the ventilated ICU patients require a feeding tube (details see above).

6.8 Conclusion

Mechanical ventilation is life-saving for ARDS patients and provides a unique window on the lung pathophysiology on which management should be guided. Additional tools such as esophageal pressure monitoring, electrical activity of the diaphragm, or bedside lung imaging by EIT add a lot to our understanding and for delivering a personalized approach to mechanical ventilation. It is possible to prevent VILI and maintain acceptable gas exchange according to the obtained information from respiratory system monitoring, such as gas exchange, lung mechanics, and imaging monitoring. With respiratory monitoring, precise mechanical ventilation will come soon. It can provide an individual ventilation setting in order to avoid unnecessary lung injury.

References

1. Gattinoni L, Quintel M. Fifty years of research in ARDS why is acute respiratory distress syndrome so important for critical care? Am J Respir Crit Care Med. 2011;194(9):1051–2.
2. Definition Task Force ARDS, Ranieri VM, Rubenfeld GD, Thompson BT, et al. Acute respiratory distress syndrome: the Berlin Definition. JAMA. 2012;307(23):2526–33.

3. Bellani G, Laffey JG, Pham T, et al. Epidemiology, patterns of care, and mortality for patients with acute respiratory distress syndrome in intensive care units in 50 countries. JAMA. 2016;315(08):788–800.
4. Slutsky AS, Ranieri VM. Ventilator-induced lung injury. N Engl J Med. 2013;369(22):2126–36.
5. Ashbaugh DG, Bigelow DB, Petty TL, Levine BE. Acute respiratory distress in adults. Lancet. 1967;2(7511):319–23.
6. Falke KJ, Pontoppidan H, Kumar A, Leith DE, Geffin B, Laver MB. Ventilation with end-expiratory pressure in acute lung disease. J Clin Invest. 1972;51(09):2315–23.
7. Maunder RJ, Shuman WP, McHugh JW, Marglin SI, Butler J. Preservation of normal lung regions in the adult respiratory distress syndrome. Analysis by computed tomography. JAMA. 1986;255(18):2463–5.
8. Gattinoni L, Pesenti A. The concept of "baby lung". Intensive Care Med. 2005;31(06):776–84.
9. Gammon RB, Shin MS, Groves RH Jr, Hardin JM, Hsu C, Buchalter SE. Clinical risk factors for pulmonary barotrauma: a multivariate analysis. Am J Respir Crit Care Med. 1995;152(4, Pt1):1235–40.
10. Dreyfuss D, Soler P, Basset G, Saumon G. High inflation pressure pulmonary edema. Respective effects of high airway pressure, high tidal volume, and positive end-expiratory pressure. Am Rev Respir Dis. 1988;137(05):1159–64.
11. Tremblay L, Valenza F, Ribeiro SP, Li J, Slutsky AS. Injurious ventilatory strategies increase cytokines and c-fos m-RNA expression in an isolated rat lung model. J Clin Invest. 1997;99(05):944–52.
12. Dhainaut JF, Devaux JY, Monsallier JF, Brunet F, Villemant D, Huyghebaert MF. Mechanisms of decreased left ventricular preload during continuous positive pressure ventilation in ARDS. Chest. 1986;90(01):74–80.
13. Mekontso Dessap A, Boissier F, Charron C, et al. Acute cor pulmonale during protective ventilation for acute respiratory distress syndrome: prevalence, predictors, and clinical impact. Intensive Care Med. 2016;42(05):862–70.
14. Dantzker DR, Brook CJ, Dehart P, Lynch JP, Weg JG. Ventilation-perfusion distributions in the adult respiratory distress syndrome. Am Rev Respir Dis. 1979;120(05):1039–52.
15. Radermacher P, Maggiore SM, Mercat A. Fifty years of research in ARDS. Gas exchange in acute respiratory distress syndrome. Am J Respir Crit Care Med. 2017;196(08):964–84.
16. Nuckton TJ, Alonso JA, Kallet RH, et al. Pulmonary dead-space fraction as a risk factor for death in the acute respiratory distress syndrome. N Engl J Med. 2002;346(17):1281–6.
17. Mikkelsen ME, Christie JD, Lanken PN, et al. The adult respiratory distress syndrome cognitive outcomes study: long-term neuropsychological function in survivors of acute lung injury. Am J Respir Crit Care Med. 2012;185:1307–15.
18. Suarez-Sipmann F, Bohm SH, Tusman G. Volumetric capnography: the time has come. Curr Opin Crit Care. 2014;20:333–9.
19. Chiumello D, Carlesso E, Cadringher P, et al. Lung stress and strain during mechanical ventilation for acute respiratory distress syndrome. Am J Respir Crit Care Med. 2008;178:346–55.
20. Perchiazzi G, Rylander C, Derosa S, et al. Regional distribution of lung compliance by image analysis of computed tomograms. Respir Physiol Neurobiol. 2014;201:60–70.
21. Loring SH, Topulos GP, Hubmayr RD. Transpulmonary pressure: the importance of precise definitions and limiting assumptions. Am J Respir Crit Care Med. 2016;194(12):1452–7.
22. Bellani G, Grassi A, Sosio S, Foti G. Plateau and driving pressure in the presence of spontaneous breathing. Intensive Care Med. 2019;45(01):97–8.
23. Boussarsar M, Thierry G, Jaber S, Roudot-Thoraval F, Lemaire F, Brochard L. Relationship between ventilatory settings and barotrauma in the acute respiratory distress syndrome. Intensive Care Med. 2002;28(04):406–13.
24. Brower RG, Matthay MA, Morris A, Schoenfeld D, Thompson BT, Wheeler A. Ventilation with lower tidal volumes as compared with traditional tidal volumes for acute lung injury and the acute respiratory distress syndrome. N Engl J Med. 2000;342(18):1301–8.
25. Terragni PP, Rosboch G, Tealdi A, et al. Tidal hyperinflation during low tidal volume ventilation in acute respiratory distress syndrome. Am J Respir Crit Care Med. 2007;175(02):160–6.

26. Suter PM, Fairley B, Isenberg MD. Optimum end-expiratory airway pressure in patients with acute pulmonary failure. N Engl J Med. 1975;292(06):284–9.
27. Grasso S, Fanelli V, Cafarelli A, et al. Effects of high versus low positive end-expiratory pressures in acute respiratory distress syndrome. Am J Respir Crit Care Med. 2005;171(09):1002–8.
28. Amato MB, Barbas CS, Medeiros DM, et al. Effect of a protective ventilation strategy on mortality in the acute respiratory distress syndrome. N Engl J Med. 1998;338(06):347–54.
29. Amato MBP, Meade MO, Slutsky AS, et al. Driving pressure and survival in the acute respiratory distress syndrome. N Engl J Med. 2015;372(08):747–55.
30. Gattinoni L, Pelosi P, Suter PM, Pedoto A, Vercesi P, Lissoni A. Acute respiratory distress syndrome caused by pulmonary and extrapulmonary disease. Different syndromes? Am J Respir Crit Care Med. 1998;158(01):3–11.
31. Grasso S, Terragni P, Birocco A, et al. ECMO criteria for influenza a (H1N1)-associated ARDS: role of transpulmonary pressure. Intensive Care Med. 2012;38(03):395–403.
32. Mezidi M, Guérin C. Complete assessment of respiratory mechanics during pressure support ventilation. Intensive Care Med. 2019;45(04):557–8.
33. Talmor D, Sarge T, O'Donnell CR, et al. Esophageal and transpulmonary pressures in acute respiratory failure. Crit Care Med. 2006;34(05):1389–94.
34. Talmor D, Sarge T, Malhotra A, et al. Mechanical ventilation guided by esophageal pressure in acute lung injury. N Engl J Med. 2008;359(20):2095–104.
35. Yoshida T, Amato MBP, Grieco DL, et al. Esophageal manometry and regional transpulmonary pressure in lung injury. Am J Respir Crit Care Med. 2018;197(08):1018–26.
36. Mancebo J, Isabey D, Lorino H, Lofaso F, Lemaire F, Brochard L. Comparative effects of pressure support ventilation and intermittent positive pressure breathing (IPPB) in non-intubated healthy subjects. Eur Respir J. 1995;8(11):1901–9.
37. Dellamonica J, Lerolle N, Sargentini C, et al. Accuracy and precision of end-expiratory lung-volume measurements by automated nitrogen washout/washin technique in patients with acute respiratory distress syndrome. Crit Care. 2011;15:R294.
38. Simon M, Braune S, Laqmani A, et al. Value of computed tomography of the chest in subjects with ARDS: a retrospective observational study. Respir Care. 2016;61:316–23.
39. Frerichs I, Amato MB, van Kaam AH, et al. Chest electrical impedance tomography examination, data analysis, terminology, clinical use and recommendations: consensus statement of the TRanslational EIT developmeNt stuDy group. Thorax. 2017;72:83–93.
40. Lichtenstein D, Goldstein I, Mourgeon E, et al. Comparative diagnostic performances of auscultation, chest radiography, and lung ultrasonography in acute respiratory distress syndrome. Anesthesiology. 2004;100:9–15.
41. Vivier E, Mekontso Dessap A, Dimassi S, et al. Diaphragm ultrasonography to estimate the work of breathing during noninvasive ventilation. Intensive Care Med. 2012;38(05):796–803.
42. The Acute Respiratory Distress Syndrome Network. Ventilation with lower tidal volumes as compared with traditional tidal volumes for acute lung injury and the acute respiratory distress syndrome. N Engl J Med. 2000;342:1301–8.
43. Marik PE, Cavallazzi R, Vasu T, Hirani A. Dynamic changes in arterial waveform derived variables and fluid responsiveness in mechanically ventilated patients: a systematic review of the literature. Crit Care Med. 2009;37:2642–7.
44. Mercat A, Richard JC, Vielle B, Jaber S, Osman D, Diehl JL, et al. Positive end-expiratory pressure setting in adults with acute lung injury and acute respiratory distress syndrome: a randomized controlled trial. JAMA. 2008;299:646–55.
45. Frerichs I, Dargaville PA, van Genderingen H, Morel DR, Rimensberger PC. Lung volume recruitment after surfactant administration modifies spatial distribution of ventilation. Am J Respir Crit Care Med. 2006;174(07):772–9.
46. Yoshida T, Engelberts D, Otulakowski G, et al. Continuous negative abdominal pressure: mechanism of action and comparison with prone position. J Appl Physiol (1985). 2018;125(01):107–16.

47. Yoshida T, Engelberts D, Otulakowski G, et al. Continuous negative abdominal pressure reduces ventilator-induced lung injury in a porcine model. Anesthesiology. 2018;129(01):163–72.
48. Eronia N, Mauri T, Maffezzini E, et al. Bedside selection of positive end-expiratory pressure by electrical impedance tomography in hypoxemic patients: a feasibility study. Ann Intensive Care. 2017;7(01):76.
49. Blankman P, Hasan D, Erik G, Gommers D. Detection of 'best' positive end-expiratory pressure derived from electrical impedance tomography parameters during a decremental positive end-expiratory pressure trial. Crit Care. 2014;18(03):R95.
50. Costa ELV, Borges JB, Melo A, et al. Bedside estimation of recruitable alveolar collapse and hyperdistension by electrical impedance tomography. In: Pinsky M, Brochard L, Hedenstierna G, Antonelli M, editors. Applied physiology in intensive care medicine, vol. 1. Berlin, Heidelberg: Springer; 2012. p. 165–70.
51. Morales MMB, Pires-Neto RC, Inforsato N, et al. Small airway remodeling in acute respiratory distress syndrome: a study in autopsy lung tissue. Crit Care. 2011;15(01):R4.
52. Chen L, Del Sorbo L, Grieco DL, et al. Airway closure in acute respiratory distress syndrome: an underestimated and misinterpreted phenomenon. Am J Respir Crit Care Med. 2018;197(01):132–6.
53. Georgopoulos D, Prinianakis G, Kondili E. Bedside waveforms interpretation as a tool to identify patient–ventilator asynchronies. Intensive Care Med. 2006;32(01):34–47.

Chapter 7
Obstructive Pulmonary Disease

Jian-Xin Zhou and Hong-Liang Li

Patients with obstructive pulmonary diseases, mainly including chronic obstructive pulmonary disease (COPD) and asthma, compromise a considerable proportion of mechanically ventilated patients in the intensive care unit (ICU) [1]. Mechanically ventilated patients with comorbidity of COPD might have a longer duration of ventilation with difficult weaning. Nowadays, modern ventilators can display pressure-, flow-, and volume-time tracings, as well as pressure-volume and flow-volume curves at the bedside. Additionally, advanced respiratory mechanics monitoring modalities, such as esophageal pressure and electrical activity of the diaphragm, are available to provide sophisticated analysis of breathing efforts and diaphragm function. This information facilitates early identification of abnormalities, detection of patient-ventilator asynchrony, and optimization of mechanical ventilation settings. In this chapter, based on the introduction of the main pathophysiologic alterations in patients with obstructive pulmonary diseases undergoing mechanical ventilation, we will discuss respiratory mechanics monitoring, specifically on the measurement of dynamic hyperinflation and air trapping. In the end, we will briefly introduce the principle for ventilation management in this population.

7.1 Dynamic Hyperinflation and Intrinsic Positive End-Expiratory Pressure

The central pathophysiologic change in patients with obstructive pulmonary disease is the airflow obstruction induced increase in airway resistance, which results in dynamic hyperinflation and intrinsic positive end-expiratory pressure (PEEP).

J.-X. Zhou (✉) · H.-L. Li
Department of Critical Care Medicine, Beijing Tiantan Hospital, Capital Medical University, Beijing, China

J. Zhou et al. (eds.), *Respiratory Monitoring in Mechanical Ventilation*,
https://doi.org/10.1007/978-981-15-9770-1_7

Airflow obstruction occurs as distal airway diameter is constricted by bronchospasm, mucosal and interstitial edema, and dynamic airway collapse during expiration [2, 3]. The cause of airway obstruction during exacerbating COPD is different from that during asthma, with increased airway collapsibility resulted from lung parenchyma devastation and decreased lung elastance in the former, and with increased thickness of airway wall resulted from inflammation and decreased collapsibility in the latter [4, 5].

Normally, lung volume returns to the relaxed volume at the end of passive expiration. This relaxed lung volume is defined as a functional residual capacity (FRC) during spontaneous breathing. In patients with increased expiratory resistance due to airflow obstruction, the end-expiratory lung volume (EELV) may increase above the predicted FRC. This phenomenon is defined as lung hyperinflation, which can be further classified as static hyperinflation induced by the destruction of pulmonary parenchyma and loss of alveolar elastic recoil, and dynamic hyperinflation induced by a slowed lung emptying. Along with the increase in EELV, end-expiratory alveolar pressure increases, which is also called intrinsic PEEP [6].

The mechanical causes of dynamic hyperinflation include:

1. Increased expiratory resistance resulting in longer time constant;
2. Reduced lung elastance resulting in decreased expiratory driving pressure;
3. Expiratory flow limitation defined as the inability of augmentation of expiratory flow regardless of an increased expiratory driving pressure [7];
4. High respiratory rate with short expiratory time impairing complete exhalation to relaxed lung volume;
5. A high tidal volume may occur during mechanical ventilation.

The consequences of hyperinflation and intrinsic PEEP include:

1. The increased inspiratory load threshold

   During assist mechanical ventilation, the patients with intrinsic PEEP have to generate an additional pleural pressure to counterbalance the intrinsic PEEP to trigger the ventilator. This can be considered as a wasted energy cost of breathing because inspiratory muscle contraction to counterbalance intrinsic PEEP does not generate inspiratory flow. The increased inspiratory muscle load tends to result in muscle fatigue and patient-ventilator asynchrony such as ineffective triggering [8, 9].
2. Increased elastic load

   Because of the increase in EELV, inspiratory muscles generate tidal breathing at a higher lung volume, which represents the flattened part of the pressure-volume curve. A greater effort is needed to produce a given tidal volume.
3. Decreased capacity of pressure generated by inspiratory muscles

   The elevated EELV and intrinsic PEEP push diaphragm downward, resulting in shortened muscular fibers and decreased diaphragm moving amplitude [10]. The rib cage expanding action is also reduced due to the hyperinflation induced rib cage distortion. Additionally, respiratory muscle blood flow is worsened by

intrinsic PEEP and dynamic hyperinflation. Consequently, the capacity of inspiratory muscles to generate inspiratory pressure decreases.

4. Impaired gas exchange

   Several factors contribute to gas exchange impairment [11]. Airway obstruction produces regional hypoventilation. Emphysema results in loss of the capillary bed and hyperinflated alveoli compresses the pulmonary capillaries. These factors tend to increase dead space. Besides, concomitant pneumonia and congestive heart failure also contribute to ventilation-perfusion mismatch and hypoxemia.

5. Cardiovascular dysfunction

   Positive intrathoracic pressure due to intrinsic PEEP reduces venous return and thereafter cardiac output [12]. Dynamic hyperinflation compresses alveolar capillaries increasing pulmonary vascular resistance and right ventricular afterload, ultimately inducing right heart failure. The initiation of mechanical ventilation and the use of sedatives during endotracheal intubation produce hypotension.

7.2 Respiratory Mechanics Monitoring in Passive Patients Without Spontaneous Breathing

In relaxed patients undergoing passive ventilation, the observation of flow-time tracing can reliably identify dynamic hyperinflation by a far from zero end-expiratory flow, which indicates an end-expiratory alveolar pressure higher than the atmospheric pressure or the applied PEEP (Fig. 7.1). The flow-volume loop can also

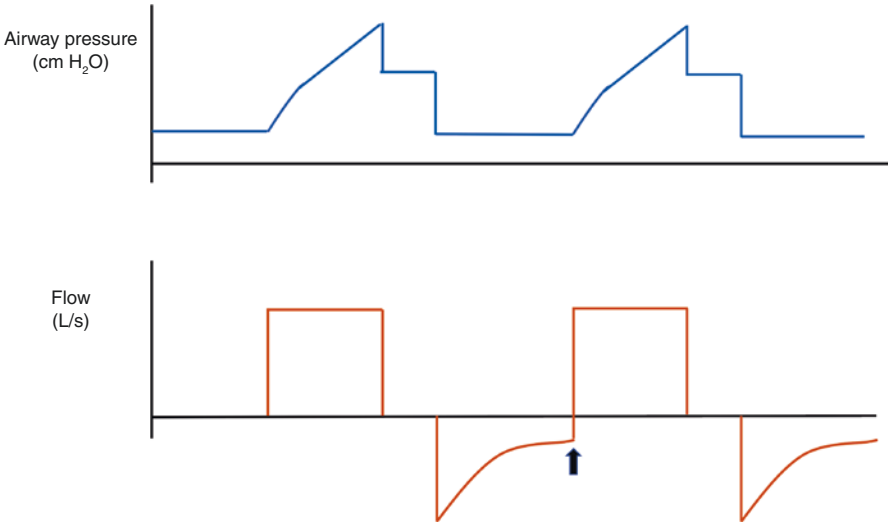

Fig. 7.1 The expiratory flow does not return to the baseline at the beginning of the next initiation of inspiratory effort observed from the flow-time curve

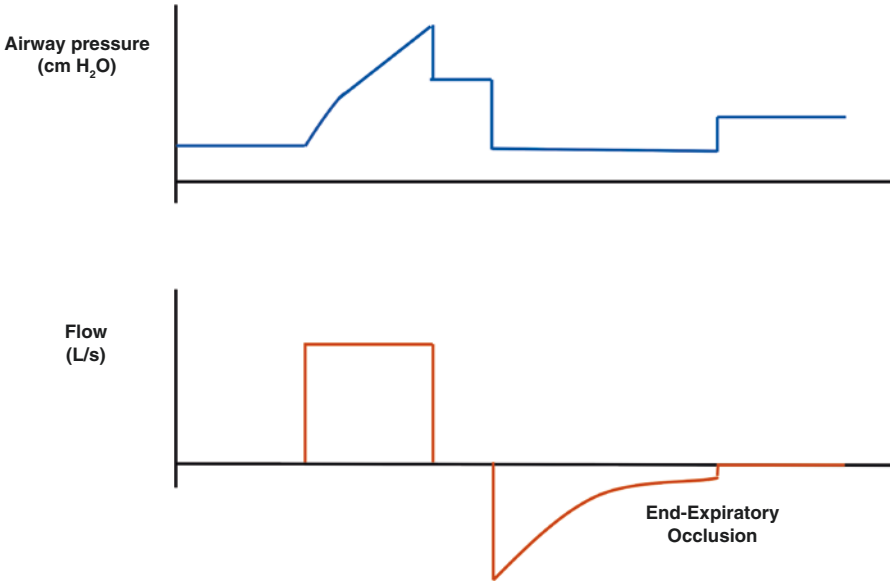

Fig. 7.2 The measuring of intrinsic PEEP by performing an end-expiratory occlusion

provide similar information (Please refer to Fig. 2.14b) (for detail please see Chap. 2, Sect. 2.8: flow-volume loop). By conducting end-expiratory occlusion, static intrinsic PEEP can be measured (Fig. 7.2). In combination with end-inspiratory occlusion, the static compliance of the respiratory system can be obtained. In patients with dynamic hyperinflation and intrinsic PEEP, the calculation of static compliance should be calibrated by intrinsic PEEP, otherwise, the true compliance will be underestimated [13]. However, it has to be noted that, in patients with severe asthma, measured intrinsic PEEP may underestimate end-expiratory alveolar pressure because of prevalent airway closure [14].

Tidal airway closure represents the cyclic opening and closing of peripheral airways, which is commonly observed in COPD and asthma [15]. Low-flow pressure-volume curves can be used to detect airway closure [16]. The initial portion of the pressure–volume curve presents an extremely low slope, corresponding to the compliance of the ventilator circuit. Later, the slope abruptly changes above a given level of airway opening pressure (Please refer to Fig. 2.11). Simultaneous use of electrical impedance tomography with a pressure-volume curve maneuver can be used to support the diagnosis of airway closure [17]. Electrical impedance tomography images show that almost no gas enters the lung during the initial period of inflation even in the non-dependent lung region [17]. Additionally, electrical impedance tomography can also provide information about regional airway closure.

Expiratory flow limitation can be evaluated in passive patients by externally applying augmentation of driving pressure, including abdominal compression and negative expiratory pressure technique [7]. During a tested breath, a negative

pressure is applied during expiration to create an increase in driving pressure. The obtained flow-volume loop is compared with the breath without negative expiratory pressure. For a detailed description, please see Chap. 2, Sect. 2.8.

Dynamic hyperinflation-induced elevation of EELV can be measured at the bedside using release and prolonged expiration maneuver [18]. Pneumotachograph is used to perform flow rate measurement and volume integration. During end-expiratory occlusion, a release maneuver can be conducted by disconnecting the patient from the ventilator with the pneumotachograph remaining on the artificial airway, until the flow tracing reaches zero, which indicates a completed expiration to the relaxed volume (Fig. 7.3). The volume passively exhales during the release maneuver is defined as the lung volume change induced by external and intrinsic PEEP. The measurement performed without the application of PEEP corresponds to the increase in EELV due to dynamic hyperinflation.

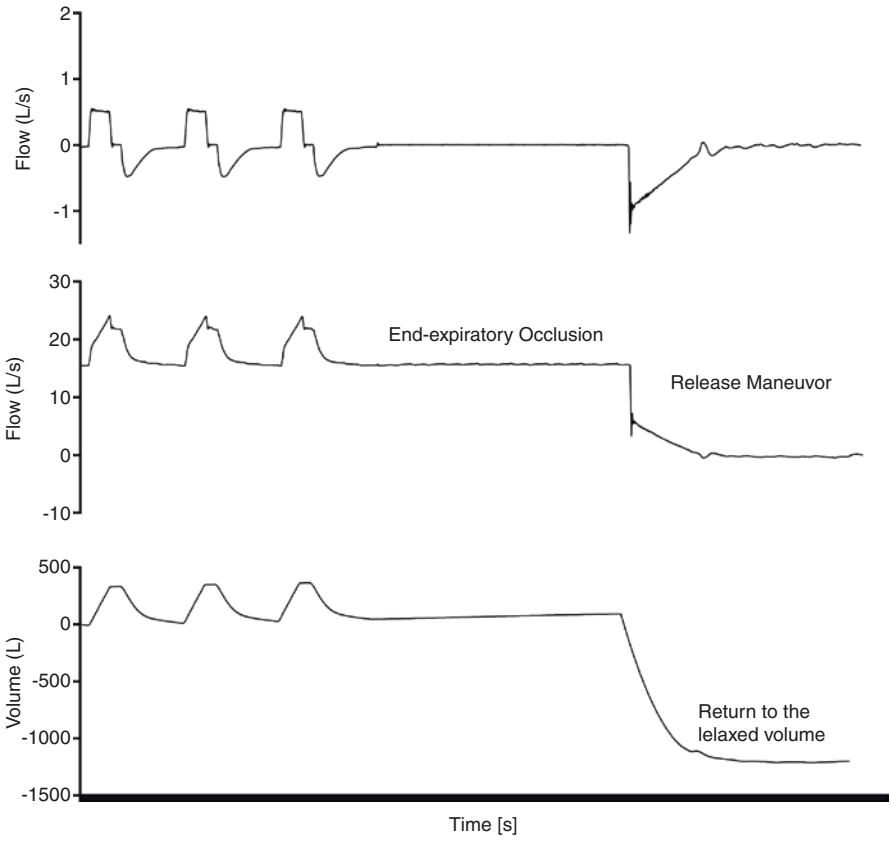

Fig. 7.3 At the end-expiratory occlusion, a release maneuver by disconnect the patient from the ventilator leading to further exhalation from end-expiratory lung volume to functional lung volume

7.3 Respiratory Mechanics Monitoring in Patients with Spontaneous Breathing

Intrinsic PEEP can be measured using esophageal pressure in spontaneously breathing patients undergoing assist ventilation [13]. The detailed method of measurement is presented in Chap. 2, Sect. 2.2.

Quasi compliance of the respiratory system can also be measured during pressure support ventilation [19]. A brief inspiratory hold during inspiration results in a satisfactory plateau pressure measurement, and thus provides driving pressure to calculate compliance (Fig. 7.4).

In clinical settings, it is not easy to measure intrinsic PEEP at the bedside, since the use of an end-expiratory occlusion is not always suitable due to incomplete patient's relaxation and Pes measurement is not frequently used. In this term, NAVA has a great advantage since the ventilator is triggered by the electrical activity of the diaphragm (Eadi) instead of airflow and pressure change, which avoid the delay of flow delivering due to the existence of intrinsic PEEP. At the same time, the intrinsic PEEP could be estimated correctly, by multiplying the value of Eadi at the onset of inspiratory flow (auto-Eadi) and the occlusion Pmusc/Eadi index, a calculated value which is named as the auto-$PEEP_{Eadi}$ could provide a clinically acceptable estimation of intrinsic PEEP derived from Pes monitoring. Since the Pmusc/Eadi index is about 1.5-fold larger in occlusion than dynamic condition, usually a 1.5 should be divided, which means the equation should be expressed as [20]:

$$\text{Auto} - \text{PEEP}_{\text{Eadi}} = \text{auto} - \text{Eadi} \times \text{dynamic Pmusc / Eadi index / 1.5}$$

7.4 Principle for Ventilation Management

The initial objective of mechanical ventilation in patients with obstructive pulmonary diseases is to preserve gas exchange. Studies have shown that the use of noninvasive ventilation in exacerbated COPD patients decreases the intubation rate and length of stay in hospitals [21]. However, some patients, especially those with severe respiratory acidosis, will not succeed for noninvasive ventilation and will need invasive ventilation via artificial airway. For noninvasive ventilation, please see Chap. 9.

For asthmatic patients, the decision to intubate is based on the patient's condition and response to bronchodilators. Progressive exhaustion and fatigue in spite of maximal therapy, as well as consciousness alteration, are an indication for intubation.

The major principle of mechanical ventilation in obstructive pulmonary disease should be avoiding or attenuating dynamic hyperinflation and intrinsic PEEP [22, 23]. Adequate expiratory time is essential for the settings of mechanical ventilation.

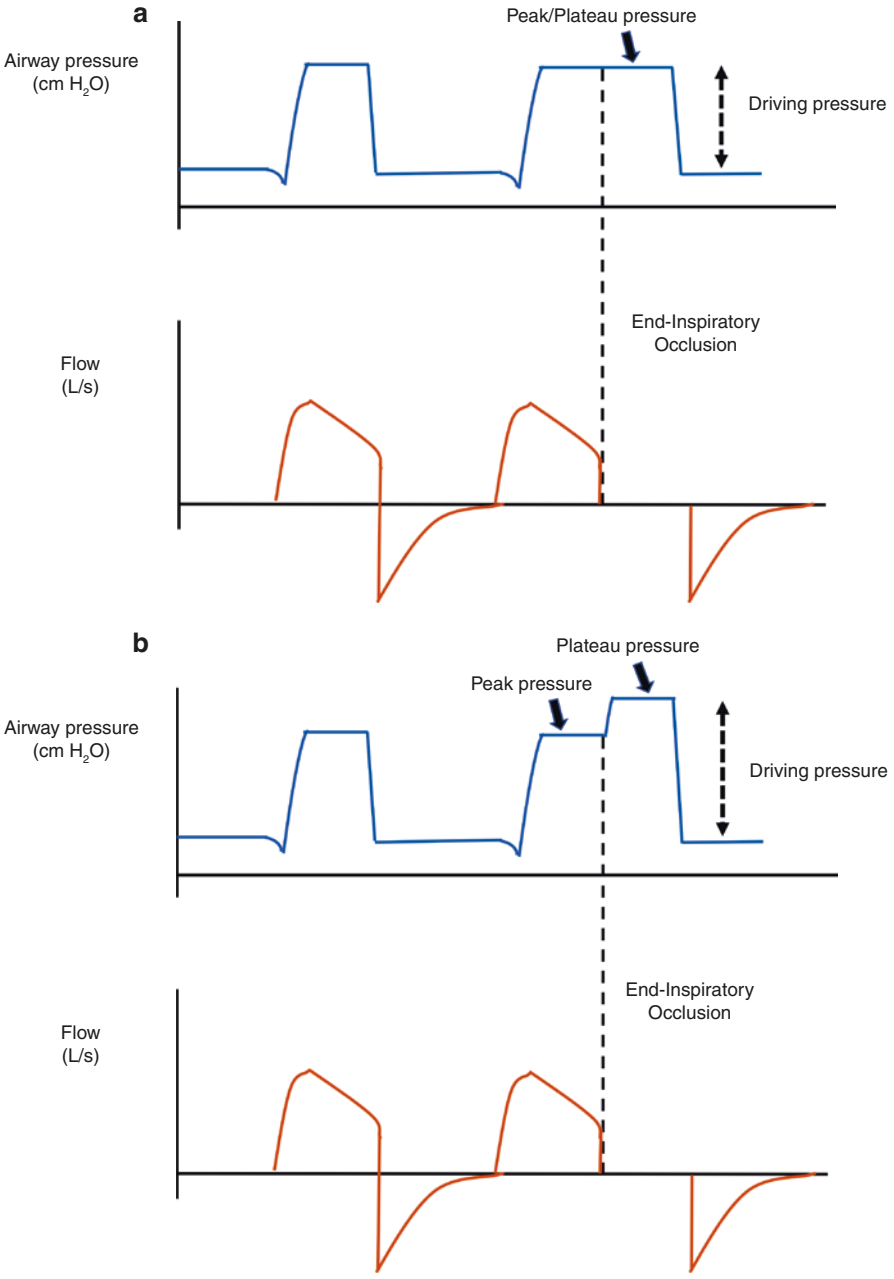

Fig. 7.4 Plateau pressure could be measured by perform inspiratory occlusion during pressure support ventilation. Panels **a**, **b**, **c** demonstrated three possible conditions respectively

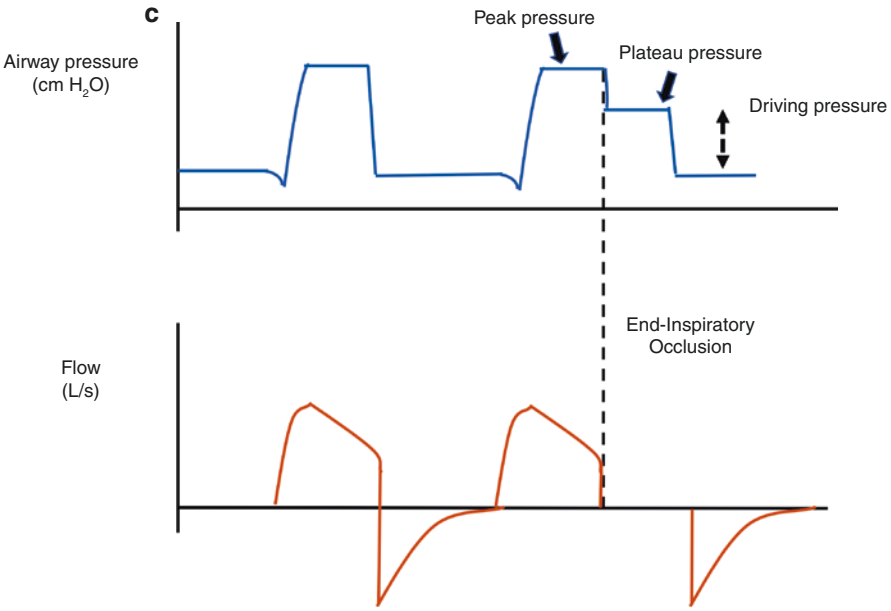

Fig. 7.4 (continued)

For example, in a patient with exacerbation of COPD undergoing volume-controlled ventilation with the constant inspiratory flow, the mean maximal expiratory flow is 250 mL/s. When respiratory rate and inspiratory to expiratory ratio are set as 20 breaths/min and 1:2, the patient has 2 s to exhale 500 mL. Thus, if tidal volume is set higher than 500 mL, dynamic hyperinflation will occur iatrogenically. No matter what ventilation model is selected, monitoring of expiration should be performed periodically to allow lung emptying. For severe asthmatic patients, a relatively small tidal volume and a higher inspiratory flow have been recommended to preserve expiratory time and minimize dynamic hyperinflation.

To counterbalance intrinsic PEEP during ventilator triggering, PEEP may be applied in patients with COPD. The PEEP level is usually set as 80% of baseline intrinsic PEEP, which has been explained by the waterfall analogy [6]. However, for patients with severe asthma, applying PEEP may be dangerous because dynamic hyperinflation is due to fixed airflow obstruction.

The Eadi signal is a promising tool for monitoring and calculating intrinsic PEEP, and help to titrate the external PEEP level. During NAVA mode, the inspiratory effort necessary to overcome intrinsic PEEP is significantly lower than flow or pressure triggered ventilatory mode and less affected by the decrease of external PEEP. What's more important, if used in noninvasive ventilation, NAVA improves patient-ventilator interaction, both in terms of more accurate triggering, cycling-off, and proportionality of assist to patient's effort [24].

References

1. Esteban A, Frutos-Vivar F, Muriel A, Ferguson ND, Penuelas O, Abraira V, Raymondos K, Rios F, Nin N, Apezteguia C, Violi DA, Thille AW, Brochard L, Gonzalez M, Villagomez AJ, Hurtado J, Davies AR, Du B, Maggiore SM, Pelosi P, Soto L, Tomicic V, D'Empaire G, Matamis D, Abroug F, Moreno RP, Soares MA, Arabi Y, Sandi F, Jibaja M, Amin P, Koh Y, Kuiper MA, Bulow HH, Zeggwagh AA, Anzueto A. Evolution of mortality over time in patients receiving mechanical ventilation. Am J Respir Crit Care Med. 2013;188:220–30.
2. Blanch L, Bernabe F, Lucangelo U. Measurement of air trapping, intrinsic positive end-expiratory pressure, and dynamic hyperinflation in mechanically ventilated patients. Respir Care. 2005;50:110–23; discussion 123–114.
3. Dhand R. Ventilator graphics and respiratory mechanics in the patient with obstructive lung disease. Respir Care. 2005;50:246–61; discussion 259–261.
4. McFadden ER Jr. Acute severe asthma. Am J Respir Crit Care Med. 2003;168:740–59.
5. Rabe KF, Watz H. Chronic obstructive pulmonary disease. Lancet. 2017;389:1931–40.
6. Tobin MJ, Lodato RFPEEP. Auto-PEEP, and waterfalls. Chest. 1989;96:449–51.
7. Koutsoukou A, Pecchiari M. Expiratory flow-limitation in mechanically ventilated patients: a risk for ventilator-induced lung injury? World J Crit Care Med. 2019;8:1–8.
8. Fernandez R, Benito S, Blanch L, Net A, Intrinsic PEEP. A cause of inspiratory muscle ineffectivity. Intensive Care Med. 1988;15:51–2.
9. Nava S, Bruschi C, Fracchia C, Braschi A, Rubini F. Patient-ventilator interaction and inspiratory effort during pressure support ventilation in patients with different pathologies. Eur Respir J. 1997;10:177–83.
10. De Troyer A. Effect of hyperinflation on the diaphragm. Eur Respir J. 1997;10:708–13.
11. Young IH, Bye PT. Gas exchange in disease: asthma, chronic obstructive pulmonary disease, cystic fibrosis, and interstitial lung disease. Compr Physiol. 2011;1:663–97.
12. MacDonald MI, Shafuddin E, King PT, Chang CL, Bardin PG, Hancox RJ. Cardiac dysfunction during exacerbations of chronic obstructive pulmonary disease. Lancet Respir Med. 2016;4:138–48.
13. Rossi A, Polese G, Brandi G, Conti G. Intrinsic positive end-expiratory pressure (PEEPi). Intensive Care Med. 1995;21:522–36.
14. Leatherman JW, Ravenscraft SA. Low measured auto-positive end-expiratory pressure during mechanical ventilation of patients with severe asthma: hidden auto-positive end-expiratory pressure. Crit Care Med. 1996;24:541–6.
15. Milic-Emili J, Torchio R, D'Angelo E. Closing volume: a reappraisal (1967-2007). Eur J Appl Physiol. 2007;99:567–83.
16. Chen L, Del Sorbo L, Grieco DL, Shklar O, Junhasavasdikul D, Telias I, Fan E, Brochard L. Airway closure in acute respiratory distress syndrome: an underestimated and misinterpreted phenomenon. Am J Respir Crit Care Med. 2018;197:132–6.
17. Sun XM, Chen GQ, Zhou YM, Yang YL, Zhou JX. Airway closure could be confirmed by electrical impedance tomography. Am J Respir Crit Care Med. 2018;197:138–41.
18. Patroniti N, Bellani G, Cortinovis B, et al. Role of absolute lung volume to assess alveolar recruitment in acute respiratory distress syndrome patients. Crit Care Med. 2010;38:1300–7.
19. Bellani G, Grassi A, Sosio S, Foti G. Plateau and driving pressure in the presence of spontaneous breathing. Intensive Care Med. 2019;45:97–8.
20. Bellani G, Coppadoro A, Patroniti N, Turella M, Arrigoni Marocco S, Grasselli G, Mauri T, Pesenti A. Clinical assessment of auto-positive end-expiratory pressure by diaphragmatic electrical activity during pressure support and neurally adjusted ventilatory assist. Anesthesiology. 2014;121(3):563–71.
21. Viniol C, Vogelmeier CF. Exacerbations of COPD. Eur Respir Rev. 2018;27:170103.
22. Jolliet P, Tassaux D. Clinical review: patient-ventilator interaction in chronic obstructive pulmonary disease. Crit Care. 2006;10:236.

23. Oddo M, Feihl F, Schaller MD, Perret C. Management of mechanical ventilation in acute severe asthma: practical aspects. Intensive Care Med. 2006;32:501–10.
24. Beck J, Emeriaud G, Liu Y, Sinderby C. Neurally-adjusted ventilatory assist (NAVA) in children: a systematic review. Minerva Anestesiol. 2016;82(8):874–83.

Chapter 8
Patient-Ventilator Asynchrony

Xu-Ying Luo and Jian-Xin Zhou

8.1 Definition and Epidemiology

Mechanical ventilation is one of the most important life-supporting strategies for patients with critical illnesses, which aims to improve gas exchange and decrease the patient's work of breathing and unload the respiratory muscles [1–3]. Optimal patient-ventilator interaction is essential to achieve these goals. Therefore, neuromuscular blockade was always administrated to eliminate the patient's respiratory efforts and controlled ventilation was used in the old days. As assisted ventilatory modalities are employed and new generation ventilators are developed, neuromuscular blockade prescription is decreasing and the interaction between the patient and the ventilation attracts more attention.

Patient-ventilator asynchrony (PVA) is defined as a mismatch between the patient and ventilator in terms of inspiratory and expiration times [4]. Although a variety of new ventilator modalities such as assist controlled ventilation (ACV), pressure-regulated volume control (PRVC), pressure support ventilation (PSV), and proportional assist ventilation (PAV) were developed, and more ventilator settings could also be adjusted for the needs of patients, including triggering sensitivity, rise time of ventilator delivery and cycling criteria, asynchronies are still very common, especially in critically ill patients.

PVA has been evaluated in some studies, with incidence varied from 16% to 80%, due to the differences in the detection methods used, evaluation periods, and population studied [5–7]. It occurs in all kinds of mechanical ventilation modes and all stages of mechanical ventilation, including the trigger phase, breath delivery phase, termination of inspiration, and expiratory phase, which is influenced by the condition

X.-Y. Luo · J.-X. Zhou (✉)
Department of Critical Care Medicine, Beijing Tiantan Hospital, Capital Medical University, Beijing, China

J. Zhou et al. (eds.), *Respiratory Monitoring in Mechanical Ventilation*,
https://doi.org/10.1007/978-981-15-9770-1_8

of the patient (patient's inspiratory drive, disease process), ventilator settings (trigger, sensitivity, flow delivery, and cycling criteria), and sedation levels [3, 8, 9]. PVA could be evaluated by an asynchrony index, defined as the number of asynchrony events divided by the total respiratory rate, which is the sum of ventilator cycles and wasted efforts and expressed as a percentage [10]. And a high prevalence of asynchrony (AI >10%) may be associated with adverse outcomes, such as prolonged duration of mechanical ventilation and hospital stay and increased mortality [9, 10].

$$\text{Asynchrony Index} = \text{number of asynchrony events} / \text{total respiratory rate}\left(\text{ventilator cycles} + \text{wasted efforts}\right) \times 100\%$$

8.2 Detection Methods

There have been a lot of studies that evaluated the prevalence of patient-ventilator asynchrony, and airway pressure and flow signals were the most frequently used, which has been proved to be reliable [10]. However, there are still some limitations. The interpretation of these waveforms depends on the experience of clinicians, type of asynchronies [11], and the reliance on the internal measurements of the ventilator. Some types of asynchronies may be missed or misread even by experienced clinicians [11–13]. Esophageal pressure, respiratory muscle electromyograms, transdiaphragmatic pressure measurement, and electrical activity of the diaphragm (EAdi) have also been used to detect asynchronies, which are more accurate but invasive and not routinely used during daily clinical practice.

8.2.1 Airway Pressure and Flow Waveforms

As a noninvasive method, interpretation of airway pressure and flow waveforms could help clinicians to recognize patient-ventilator asynchronies, and its accuracy and validity of detection of ineffective triggering and double triggering have been demonstrated comparable with esophageal pressure signals [10]. Airway pressure and flow signals could be obtained at the bedside, and the clinicians could make proper adjustments in time. However, its validity of detection of auto-triggering, reverse triggering, and cycling asynchrony remains uncertain [12, 14].

8.2.2 Esophageal Pressure

Esophageal pressure (Pes) has been used as a surrogate for pleural pressure to monitor the patient's respiratory drive and inspiratory effort, which could be obtained at the bedside. Usually, a negative Pes swing indicates an inspiratory effort, which triggers the ventilator to deliver one breath cycle. Asynchrony could be identified by

comparing the time occurrence of the change in Pes with that of the airway pressure and flow. As a negative Pes swing indicates an inspiratory effort, which could also help to identify auto-triggering, reverse triggering, and cycling asynchronies accurately [3, 15].

Pes could be obtained by a specific catheter with a balloon. To obtain accurate Pes measurements, the esophageal balloon should be placed in the lower two-thirds of the intrathoracic esophagus, which is determined by an occlusion test [16]. However, the results could also be influenced by mediastinal loading, variations of esophageal elastance, and amplitude of the cardiac oscillations [17]. Despite Pes monitoring is a minimally invasive procedure with accurate detection of asynchronies, it is not routinely used in the clinical setting.

8.2.3 Electrical Activity of the Diaphragm

The electrical activity of the diaphragm (EAdi) represents the patient's neural respiratory drive, which could be used to monitor the onset of neural inspiration and expiration. EAdi could be obtained easily through a nasogastric tube with multiple electrodes and recorded by the software. Some studies have used EAdi to detect patient-ventilator asynchronies, which is more accurate and sensitive than airway pressure and flow waveforms only, especially in the detection of auto-triggering, reverse triggering, premature and delayed termination [18, 19]. It could also help to differentiate reverse triggering from double triggering, depending on the first inspiration that is triggered by the patient or the ventilator [20]. However, considering its invasiveness, cost, technical challenges, and contraindications, such as severe coagulopathy, diagnosed or suspected esophageal varices, and history of esophageal or gastric surgery, EAdi is not routinely used to monitor asynchronies in the clinical practice. Some authors have demonstrated the linear relationship between EAdi and respiratory muscle surface electromyography (EMG), which may also be used to detect the activity of inspiratory muscles in patients under ventilation [21].

8.3 Classification

Patient-ventilator asynchrony could be classified based on the phases of the ventilator breathing cycle, including triggering phase, flow delivery, cycling off phase, and expiratory phase. Asynchrony can happen at every phase of breath [3, 8, 22]. Airway pressure, flow, Pes, and EAdi signals can be used to detect and classify different types of asynchronies (Table 8.1).

Table 8.1 Definition of different types of patient-ventilator asynchronies was based on flow, airway pressure, and esophageal pressure waveforms

Respiratory phase	Asynchrony	Definition
Triggering	Ineffective triggering	Refers to a patient's inspiratory effort but not followed by a ventilator cycle, indicated by a decrease in pressure drop ($\geq$0.5 cm H_2O) associated with a simultaneous increase in the flow [10]
	Double triggering	Refers to two cycles separated by a very short expiratory time, defined as less than one-half of the mean inspiratory time, and the first cycle being patient-triggered [10]
	Reverse triggering	Refers to inspiratory efforts triggered by the ventilator in a repetitive and consistent manner [16]
	Auto-triggering	Refers to an assisted breath delivered by the ventilator that is not triggered by the patient (without a prior airway pressure decrease) [10]
Flow delivery	Insufficient flow	Refers to the ventilator's flow setting is lower than patient's demand, indicated by a dish-out of pressure waveform [23]
	Excessive flow	Refers to the ventilator's flow setting is higher than the patient's demand, indicated by a peaking of pressure waveform (overshoot) at the beginning of the inspiration [23]
Cycling off	Premature termination	Refers to the termination of the ventilator cycle despite the patient's effort continued, indicated by a sharp decrease in the expiratory flow followed by an increase and then a decrease gradually to the baseline [23]
	Delayed termination	Refers to a patient's expiratory effort starting before the ventilator switch to the expiratory phase, indicated by a spike in the airway pressure waveform and a rapid decrease of the inspiratory flow towards the end of mechanical inspiration [23]
Expiratory	Intrinsic PEEP	Refers to the magnitude of the end-expiratory pressure in excess of the set extrinsic PEEP, indicated by a sudden onset of inspiratory flow prior to the expiratory flow curve returning to zero [34]

8.3.1 Triggering Asynchrony

Triggering asynchronies include ineffective triggering, double triggering, reverse triggering, and auto-triggering.

1. Ineffective triggering refers to a patient's inspiratory effort but not followed by a ventilator cycle, defined as a decrease in pressure drop ($\geq$0.5 cm H_2O) associated with a simultaneous increase in the flow [10]. Ineffective triggering usually occurred among patients with chronic obstructive pulmonary disease (COPD), asthma, and those with intrinsic PEEP (PEEPi), as well as diminished respiratory drives, such as deep sedation and patients with brain stem injuries. Additionally, improper triggering thresholds of the ventilator could also lead to ineffective triggering. It can occur during both mechanical inspiratory phase and expiratory phase, under both pressure support ventilation and mandatory ventila-

tion (Fig. 8.1). Most of the ineffective triggering can be detected by airway pressure and flow waveforms. Combined with pes or EAdi signals can improve the accuracy and sensitivity of detecting ineffective triggering than airway pressure and flow waveforms only [18, 19]. Ineffective triggering may be eliminated by reducing pressure support or inspiratory duration to decrease tidal volume and applying extrinsic PEEP to decrease the patient's inspiratory effort to trigger the ventilator [23, 24].

2. Double triggering was defined as two cycles separated by a very short expiratory time, defined as less than one-half of the mean inspiratory time, the first cycle being patient-triggered [10]. For most patients, there is a pressure drop and flow change in the pre-inspiratory phase, which indicates an inspiratory effort of the patient (Fig. 8.2). Some authors classified three types of DT according to the first breath, including patient-triggered, auto-triggered, and ventilator-triggered [25]. Double triggering is usually caused by a greater inspiratory effort and an insufficient level of pressure support [10]. It may lead to hyperinflation, even ventilator-induced lung injury [26]. Double triggering could be reduced by prolonging the inspiratory time, decreasing the expiratory flow-cycle threshold, switching to PSV mode, and decreasing the patient's respiratory effort through sedation medication [25].
3. Reverse triggering refers to those inspiratory efforts triggered by the ventilator in a repetitive and consistent manner [15]. Pes and EAdi, as an indicator of the patient's inspiratory effort, combined with the flow and airway pressure, can be used to identify reverse triggering (Fig. 8.3). It has been observed in deeply sedated patients, brain-dead patients, and those with ARDS [15, 20, 27]. Reverse triggering may cause diaphragmatic muscle fiber damage, increase of work of breathing and oxygen consumption, enlarged tidal volume, and increased transpulmonary pressure [9]. There have been several hypotheses on pathophysiological mechanisms, such as Hering-Breuer reflex, vagal nervous fibers, and cortical and subcortical influences [20], which are still unclear. Similar to double triggering, reverse triggering may lead to hyperinflation, even ventilator-induced lung injury, due to enlarged tidal volume and higher plateau pressure in volume-control ventilation. Some authors reported that reverse triggering might be eliminated by adjustment of the mechanical rate or tidal volume and neuromuscular blockers, which need further study [15, 28].
4. Auto-triggering refers to an assisted breath delivered by the ventilator that is not triggered by the patient (without a prior airway pressure decrease) [10]. It can be caused by inappropriately triggering sensitivity, flow change produced by the cardiac oscillations, and leaks of the ventilator circuit. Auto-triggering may lead to hyperventilation, misjudgment of the patient's spontaneous breath leading to hypoventilation, even wrong clinical decisions [29]. Under pressure support ventilation, auto-triggering could be detected by an absence of airway pressure decrease before inspiration, and could also be distinguished by trigger sensitivity adjustment. Therefore, careful evaluation of the patient and inspection of the airway pressure and flow signals are important to detect auto-triggering. Besides, Pes and EAdi monitoring could help in the detection of auto-triggering.

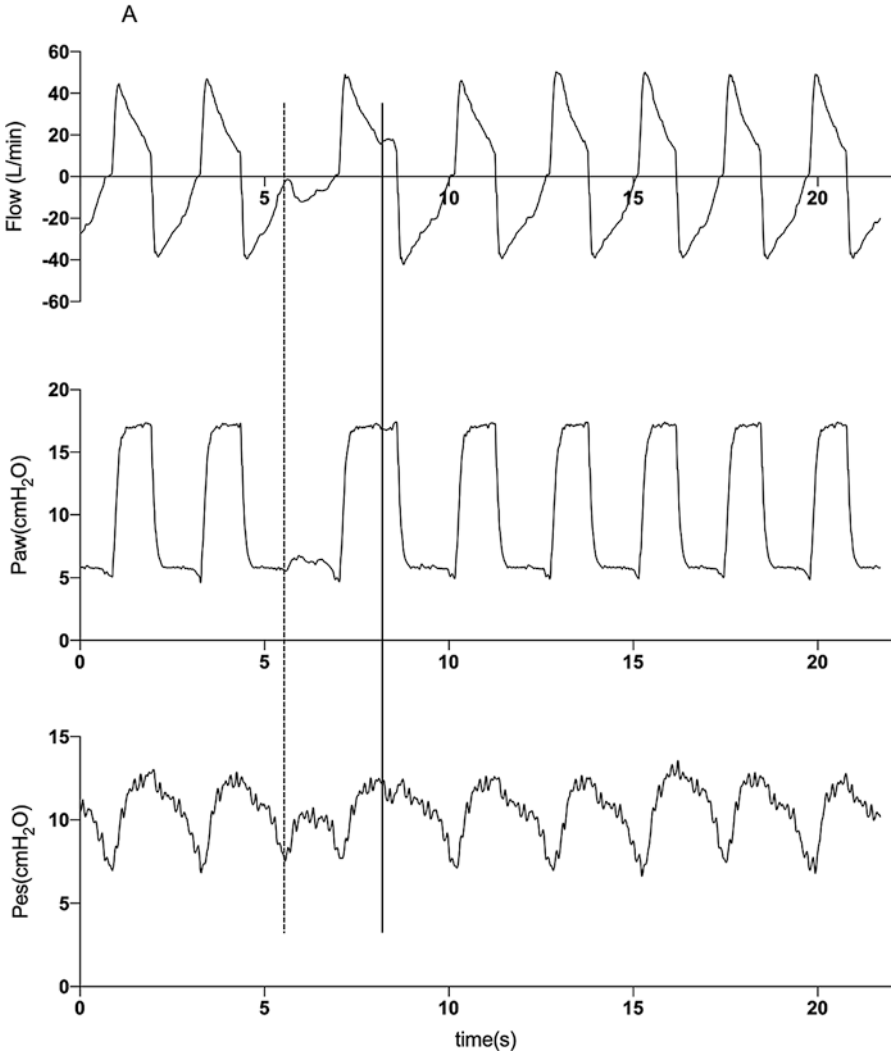

Fig. 8.1 Flow, airway pressure, and esophageal pressure recordings showing ineffective triggering occurring both during the expiratory phase (dotted line) and during the inspiratory phase (solid line); during pressure support ventilation (PSV) (**a**) and during pressure assist-control ventilation (PA/C) (**b**)

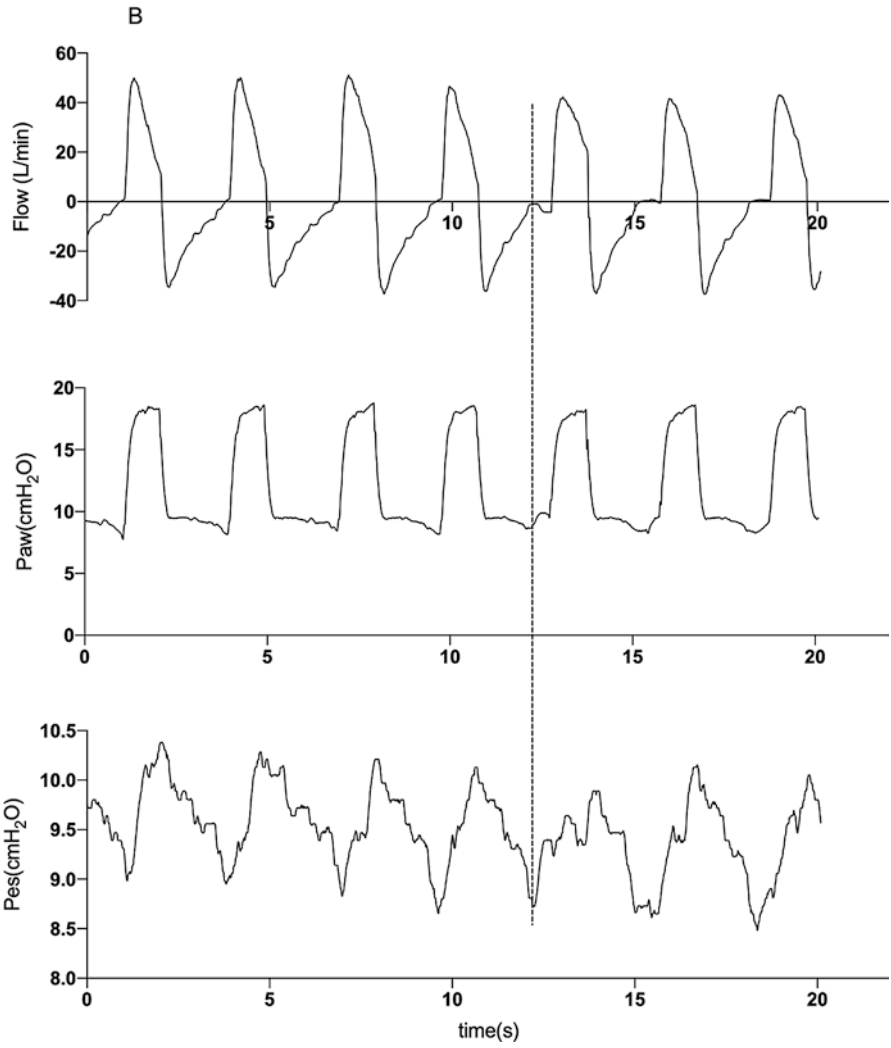

Fig. 8.1 (continued)

8.3.2 Flow Asynchrony

Flow asynchrony refers to a mismatch between ventilator flow and patient's inspiratory demand, including insufficient inspiratory flow (dish-out of pressure waveform) and excessive flow (overshoot of pressure waveform). It may occur during either flow-targeted breaths or pressure-targeted breaths [22].

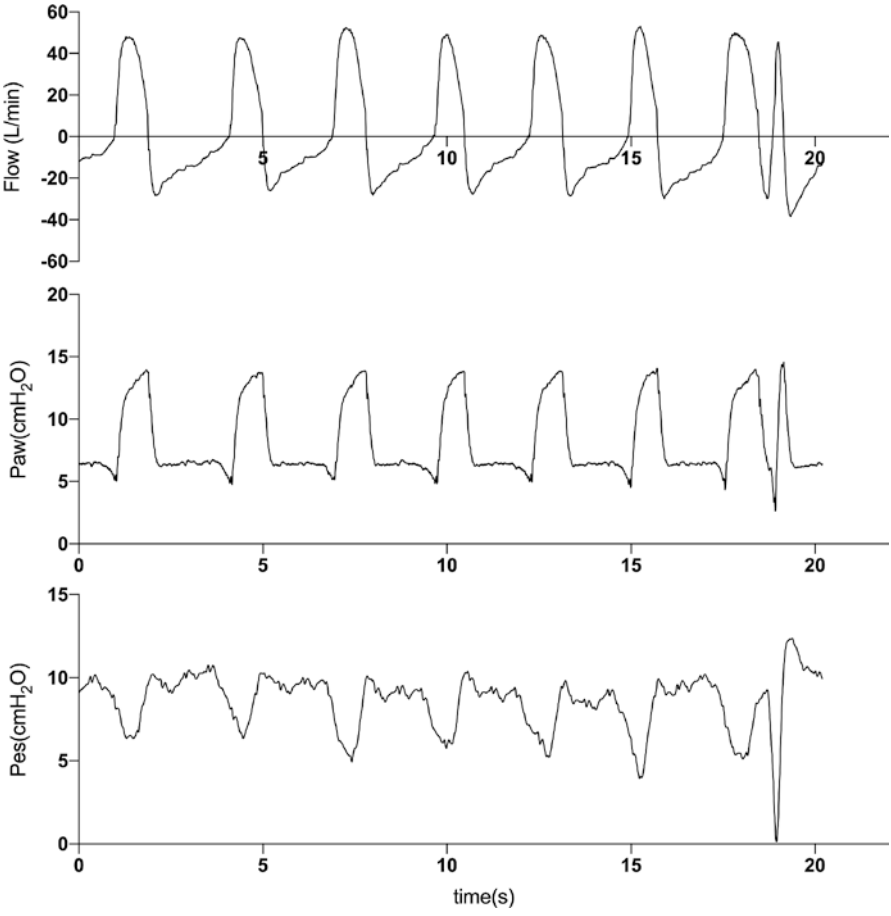

Fig. 8.2 Flow, airway pressure, and esophageal pressure recordings showing double triggering occurring during pressure support ventilation (PSV)

8.3.2.1 Insufficient Flow

When the ventilator's flow setting is lower than the patient's demand, a dish-out of pressure waveform could be observed. Under flow-targeted breaths, such as volume-control ventilation, the inspiratory flow or peak flow is usually set by the clinician. When the patient's inspiratory demand is higher than the peak flow of the ventilator, a downward deflection of pressure-time waveform could be observed (Fig. 8.4). The accessory respiratory muscle of the patient may be used. It could be resolved by increasing the peak flow of the ventilator, changing to pressure mode, or decreasing the patient's inspiratory demand [22]. On pressure-targeted breaths, such as pressure support and pressure control ventilation, the speed of flow delivery depends on the rise time set by the clinician. When the patient's respiratory demand is higher, a

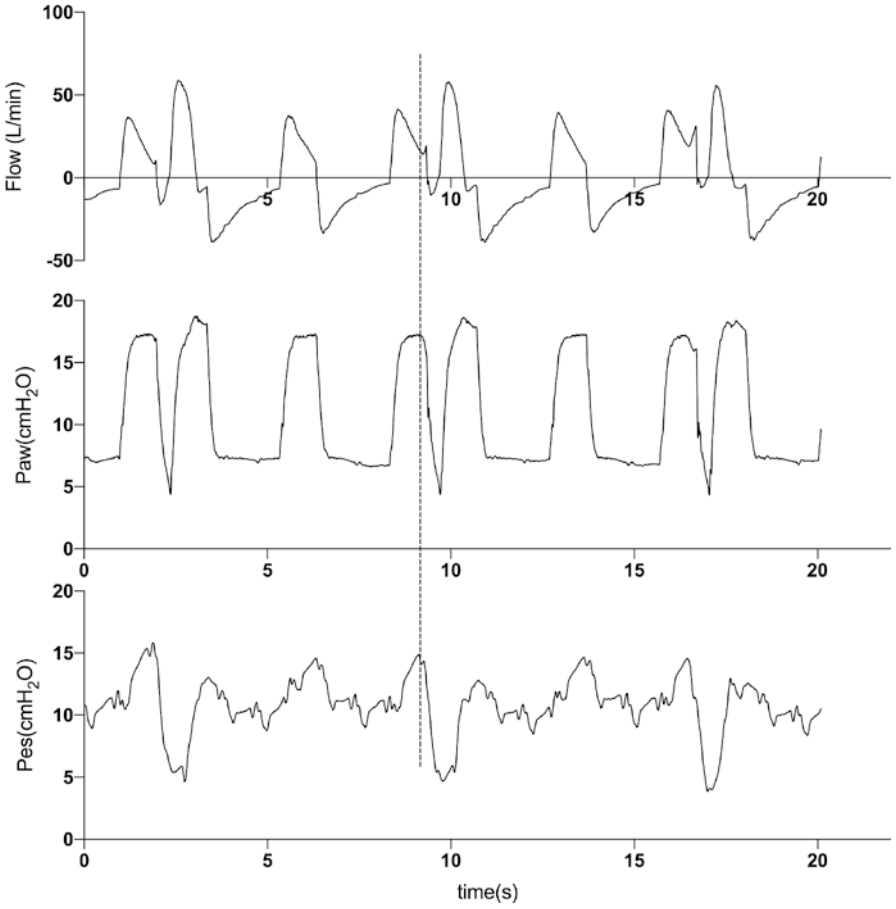

Fig. 8.3 Flow, airway pressure, and esophageal pressure recordings showing reverse triggering occurring during pressure assist/control ventilation (PA/C)

drop of pressure-time waveform could be seen [22] (Fig. 8.5). It could be resolved by shortening the rise time, increasing applied pressure, or decreasing the patient's respiratory demand.

8.3.2.2 Excessive Flow

When the ventilator flow setting is higher than the patient's demand, a peaking of pressure waveform (overshoot) at the beginning of the inspiration could be observed (Fig. 8.6). It could be resolved by reducing the inspiratory flow in the volume-control ventilation, reducing the applied pressure or prolonging the rise time in the pressure mode [3, 22].

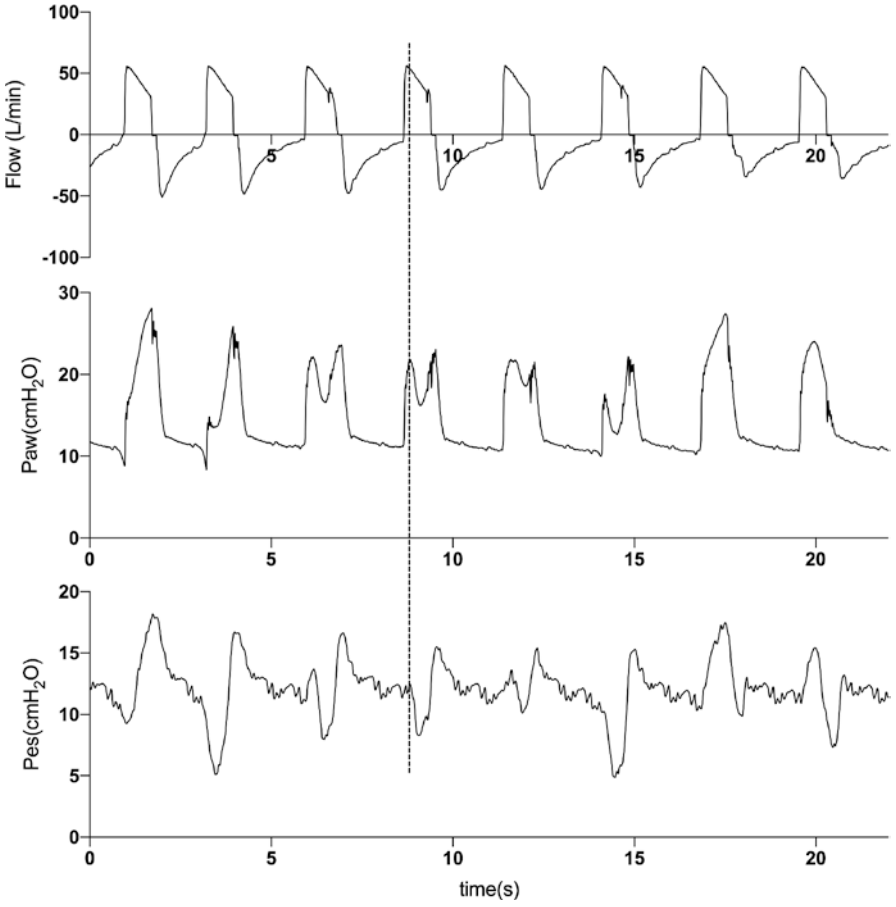

Fig. 8.4 Flow, airway pressure, and esophageal pressure recordings showing insufficient flow delivery occurring during volume assist/control ventilation (VA/C)

8.3.3 Cycling Asynchrony

As the inspiratory phase ceases, the exhalation valve opens and the expiration phase begins. This process is termed as cycling. There are four cycle variables, including pressure cycling, time cycling, volume cycling, and flow cycling [30]. Cycling asynchrony is defined as a mismatch between the patient and the ventilator in terms of expiratory times starting, including premature termination and delayed termination. Both can occur during pressure support ventilation and mandatory ventilation.

1. Premature termination refers to the termination of the ventilator cycle despite the patient's effort continued [22]. The inspiratory muscles continue to contract after the end of ventilator inspiration. A sharp decrease in the expiratory flow followed

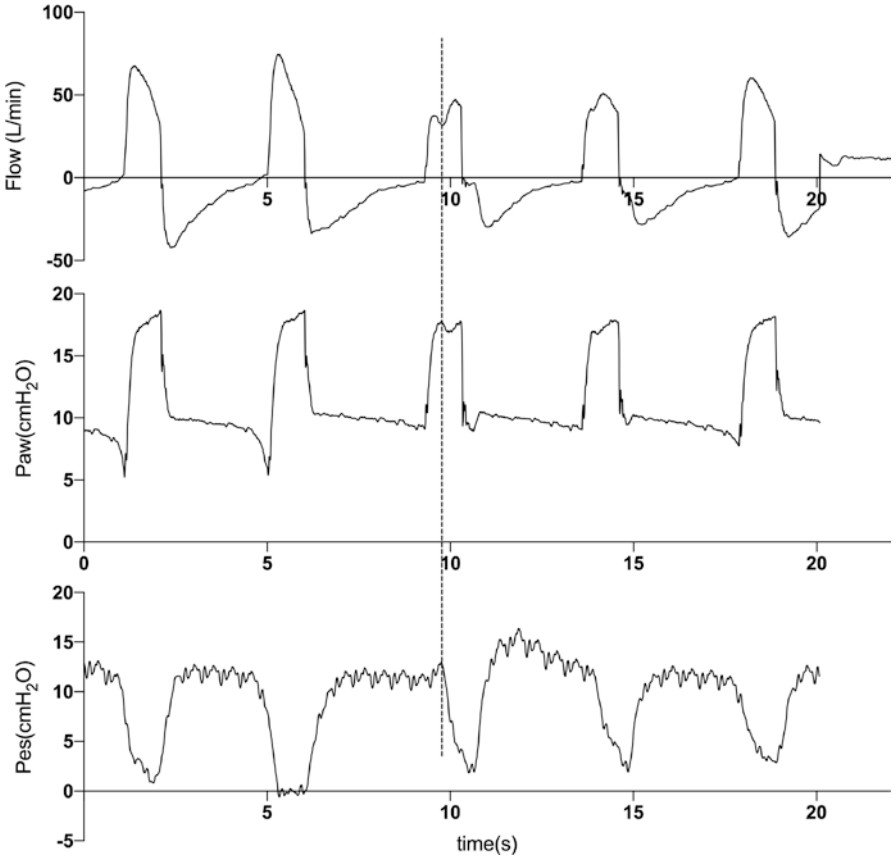

Fig. 8.5 Flow, airway pressure, and esophageal pressure recordings showing insufficient flow delivery occurring during pressure assist/control ventilation (PA/C)

by an increase and then a decrease gradually to the baseline may be observed [31] (Fig. 8.7). For some patients, the inspiratory muscle contraction may cause the ventilator to deliver a second breath, which is identified as double triggering.

Sometimes, it is difficult to distinguish from ineffective triggering. While Pes and EAdi signals may help to identify the deflection at the beginning of the expiratory phase is caused by either the unfinished inspiratory effort or another new inspiratory effort that fails to trigger the ventilator. Premature termination is usually caused by the patient's high inspiratory demand, short ventilator inspiratory time, and high flow-cycling percentage. It may cause decreased tidal volume; while, if a second ventilator breath is triggered (double triggering), it may result in a larger tidal volume and even lung injury [32]. Premature termination could usually be eliminated by prolonging ventilator inspiratory time, increasing pressure support, lowering flow-cycling percentage, and decreasing the patient's respiratory demand.

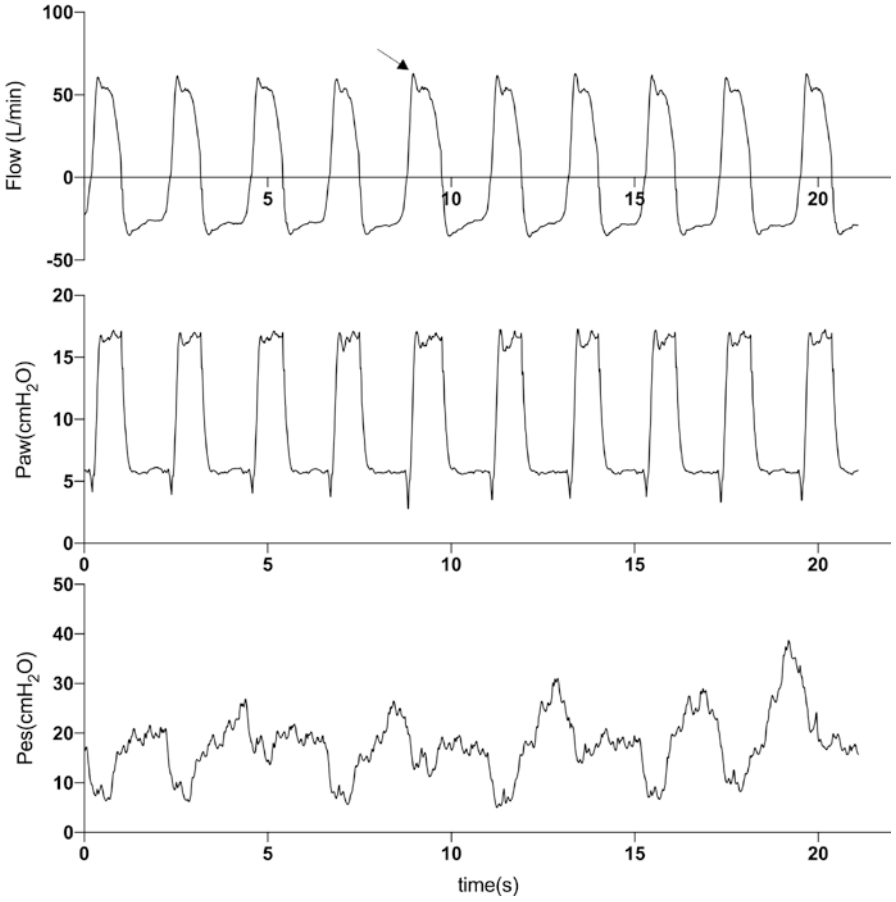

Fig. 8.6 Flow, airway pressure, and esophageal pressure recordings showing excessive flow delivery (overshoot) occurring during pressure support ventilation (PSV)

2. Delayed termination refers to a patient's expiratory effort starting before the ventilator switch to the expiratory phase, which is indicated by a spike in the airway pressure waveform and a rapid decrease of the inspiratory flow towards the end of mechanical inspiration [22] (Fig. 8.8). It may be difficult to detect depending on the pressure and flow waveforms only when there is no patient's expiratory muscle contraction. We also need Pes and EAdi signals indicating the patient's neural expiratory starting. Usually, it could be caused by excessive support, long inspiratory time, and large tidal volume, and lead to insufficient expiratory time, large tidal volume, air-trapping, and PEEPi. Delayed termination could be resolved by adjusting cycling off threshold, including reducing inspiratory time, decreasing applied pressure, and increasing flow-cycling percentage, as well as switching to pressure support mode. Additionally, the optimal cycling setting may need to be adjusted according to the patient's demand.

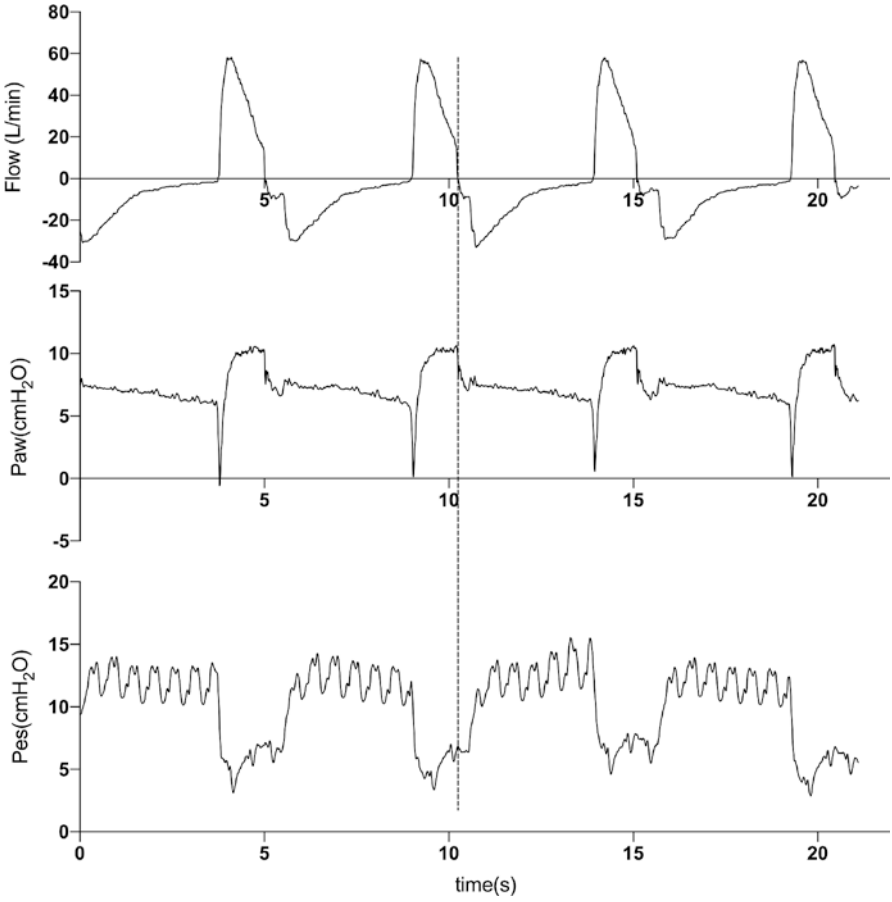

Fig. 8.7 Flow, airway pressure, and esophageal pressure recordings showing premature termination occurring during pressure support ventilation (PSV)

8.3.4 Expiration

At the end of expiration, airway pressure should decrease to PEEP and flow gradually decrease to zero in normal condition. For patients with PEEPi, a sudden onset of inspiratory flow before the expiratory flow curve returning to zero can be observed (Fig. 8.9). PEEPi is usually caused by dynamic hyperinflation and air-trapping, due to large tidal volumes, rapid respiratory rates, and insufficient expiratory time. It could be measured by a pause maneuver at end-expiration under mandatory ventilation without a patient's inspiratory effort. However, when there is significant airway closure, it may be difficult to detect through airway pressure and flow waveforms, which is common in patients with COPD, asthma, and sometimes in those with ARDS [33]. PEEPi may lead to hemodynamic disorders, such as bradycardia, hypotension, and

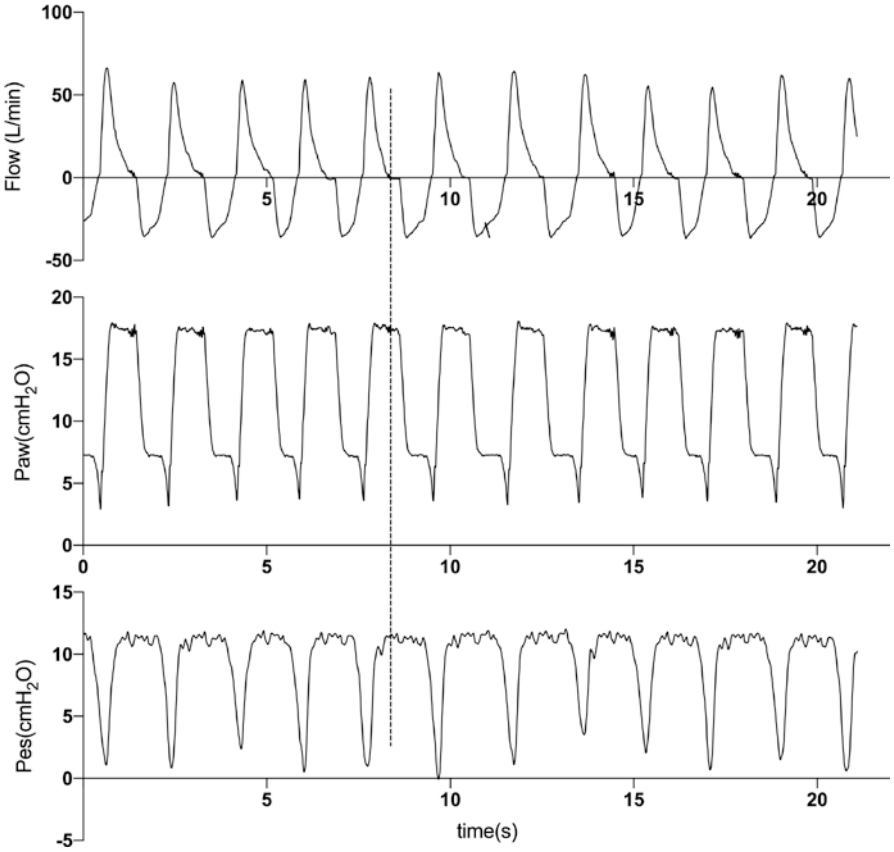

Fig. 8.8 Flow, airway pressure, and esophageal pressure recordings showing delayed termination occurring during pressure assist/control ventilation (PA/C)

even cardiac arrest. Additionally, the patient has to overcome the PEEPi to trigger the ventilator, which may cause triggering delay and ineffective triggering, and increase work of breathing. In most situations, it could be reduced by several measures, including decreasing the set respiratory rate to prolong the expiratory time, increasing the set extrinsic PEEP to decrease the patient's work to trigger the ventilator, and appropriate sedation to prevent the patient triggering the ventilator [34].

8.3.5 Automated Detection of Asynchrony

Airway pressure and flow waveforms, combined with Pes and EAdi monitoring could detect most types of asynchronies. However, it is time-consuming, dependent on experienced physicians, and cannot provide real-time information. Some authors

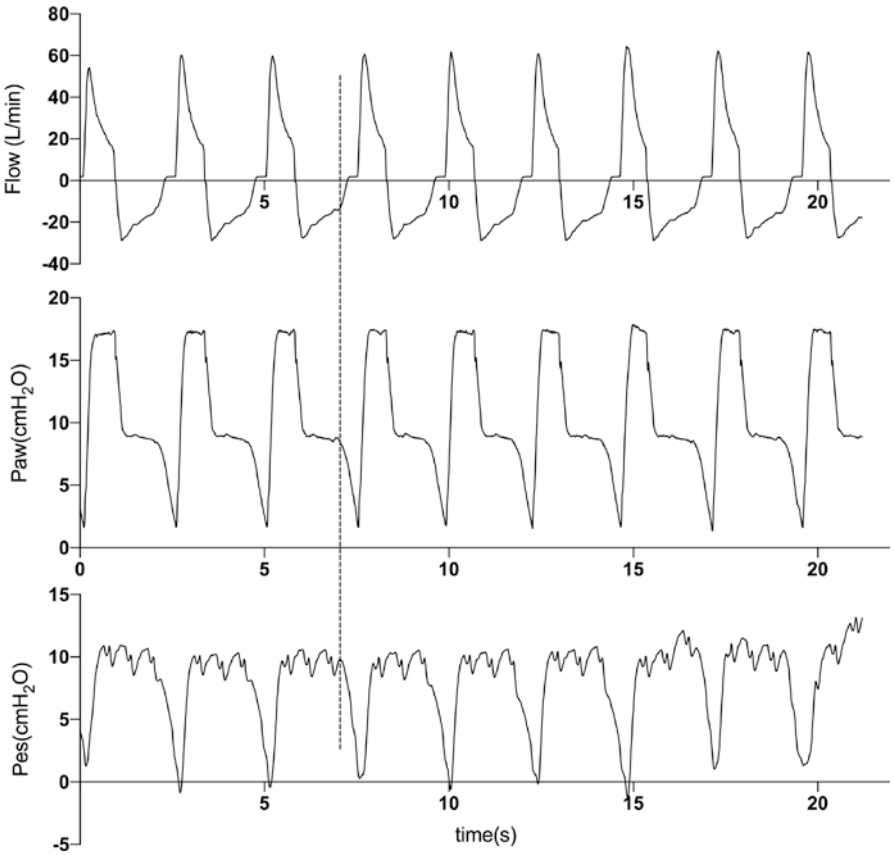

Fig. 8.9 Flow, airway pressure, and esophageal pressure recordings showing intrinsic PEEP occurring during pressure support ventilation (PSV)

reported the ability to recognize asynchrony through ventilator waveforms was associated with clinicians' experiences [11]. Therefore, automatic detecting methods have been developed, which make it possible to continuously monitor asynchrony, detect asynchrony in a large population, analyze risk factors, and improve patient-ventilator interaction. Mulqueeny et al. [35] developed an algorithm embedded in a ventilator system that could accurately detect ineffective triggering and double triggering in real-time. Sinderby et al. [36] introduced another automated algorithm, by analyzing the ventilator pressure and EAdi waveforms and comparing their timings, to detect asynchrony, and the efficiency and accuracy were comparable with experienced clinicians. Blanch et al. [9] used the software (Better Care TM, Barcelona, Spain) to detect asynchronies, including ineffective triggering during expiration (IEE), double triggering, aborted inspirations, and short and prolonged cycling. Sottile et al. developed a computerized algorithm, based on Python and the SciPy scientific stack, which could accurately detect double triggered breaths,

ineffective triggering, premature ventilator termination, and flow-limited breaths [37]. However, they used only airway pressure, flow, and volume waveforms of the ventilator, whose validity and accuracy remains uncertain [12, 14].

In brief, automated systems could detect some frequent types of asynchronies. They could not detect all asynchronies unless combined with Pes or EAdi. However, through these automated systems, it is feasible to detect some frequent types of asynchronies continuously, including ineffective triggering, double triggering, and premature termination at the bedside. It may also be able to alert clinicians in real-time and make adjustments accordingly in the future.

8.4 Summary

Patient-ventilator asynchrony is very common in critically ill patients. Patients with a high incidence of asynchrony were found to have a longer duration of mechanical ventilation, longer ICU stays, and possibly higher hospital mortality. Most asynchronies could be detected by airway pressure, flow, and volume waveforms. Pes and EAdi monitoring as minimally invasive procedures that could help identify asynchrony more accurately; however, they are not routinely used in the clinical setting. As some automated systems have been developed, it is feasible to detect some frequent types of asynchronies continuously in real-time. It could also be embedded in a ventilator system that could accurately detect asynchronies and alert clinicians to make appropriate adjustments to reduce patient-ventilator asynchronies.

References

1. Brochard L, Harf A, Lorino H, et al. Inspiratory pressure support prevents diaphragmatic fatigue during weaning from mechanical ventilation. Am Rev Respir Dis. 1989;139:513–21.
2. Sassoon CS, Foster GT. Patient-ventilator asynchrony. Curr Opin Crit Care. 2001;7:28–33.
3. Georgopoulos D, Prinianakis G, Kondili E. Bedside waveforms interpretation as a tool to identify patient-ventilator asynchronies. Intensive Care Med. 2006;32:34–47.
4. Tobin MJ, Jubran A, Laghi F. Patient-ventilator interaction. Am J Respir Crit Care Med. 2001;163:1059–63.
5. Chao DC, Scheinhorn DJ, Stearn- Hassenpflug M. Patient-ventilator trigger asynchrony in prolonged mechanical ventilation. Chest. 1997;112:1592–9.
6. Unroe M, MacIntyre N. Evolving approaches to assessing and monitoring patient-ventilator interactions. Curr Opin Crit Care. 2010;16:261–8.
7. Nava S, Bruschi C, Fracchia C, et al. Patient-ventilator interaction and inspiratory effort during pressure support ventilation in patients with different pathologies. Eur Respir J. 1997;10:177–83.
8. Nilsestuen JO, Hargett KD. Using ventilator graphics to identify patient-ventilator asynchrony. Respir Care. 2005;50:202–34.
9. Blanch L, Villagra A, Sales B, et al. Asynchronies during mechanical ventilation are associated with mortality. Intensive Care Med. 2015;41:633–41.

10. Thille AW, Rodriguez P, Cabello B, et al. Patient-ventilator asynchrony during assisted mechanical ventilation. Intensive Care Med. 2006;32:1515–22.
11. Colombo D, Cammarota G, Alemani M, et al. Efficacy of ventilator waveforms observation in detecting patient-ventilator asynchrony. Crit Care Med. 2011;39:2452–7.
12. Chen CW, Lin WC, Hsu CH. Pseudo-double-triggering. Intensive Care Med. 2007;33:742–3.
13. Haynes JM. Patient-ventilator asynchrony and standard waveforms: looks can be deceiving. Respir Care. 2017;62:1004.
14. Parthasarathy S, Jubran A, Tobin MJ. Cycling of inspiratory and expiratory muscle groups with the ventilator in airflow limitation. Am J Respir Crit Care Med. 1998;158:1471–8.
15. Akoumianaki E, Lyazidi A, Rey N, et al. Mechanical ventilation-induced reverse-triggering breaths: a frequently unrecognized form of neuromechanical coupling. Chest. 2013;143:927–38.
16. Baydur A, Behrakis PK, Zin WA, et al. A simple method for assessing the validity of the esophageal balloon technique. Am Rev Respir Dis. 1982;126:788–91.
17. Van de Woestijne KP, Trop D, Clement J. Influence of the mediastinum on the measurement of esophageal pressure and lung compliance in man. Pflugers Arch. 1971;323:323–41.
18. Piquilloud L, Vignaux L, Bialais E, et al. Neurally adjusted ventilatory assist improves patient-ventilator interaction. Intensive Care Med. 2011;37:263–71.
19. Mauri T, Bellani G, Grasselli G, et al. Patient-ventilator interaction in ARDS patients with extremely low compliance undergoing ECMO: a novel approach based on diaphragm electrical activity. Intensive Care Med. 2013;39:282–91.
20. Delisle S, Charbonney E, Albert M, et al. Patient-ventilator asynchrony due to reverse triggering occurring in brain-dead patients: clinical implications and physiological meaning. Am J Respir Crit Care Med. 2016;194:1166–8.
21. Bellani G, Bronco A, Arrigoni Marocco S, et al. Measurement of diaphragmatic electrical activity by surface electromyography in intubated subjects and its relationship with inspiratory effort. Respir Care. 2018;63:1341–9.
22. de Wit M. Monitoring of patient-ventilator interaction at the bedside. Respir Care. 2011;56:61–72.
23. Nava S, Bruschi C, Rubini F. et la. Respiratory response and inspiratory effort during pressure support ventilation in COPD patients. Intensive Care Med. 1995;21:871–9.
24. Thille AW, Cabello B, Galia F, et al. Reduction of patient-ventilator asynchrony by reducing tidal volume during pressure-support ventilation. Intensive Care Med. 2008;34:1477–86.
25. Liao KM, Ou CY, Chen CW, et al. Classifying different types of double triggering based on airway pressure and flow deflection in mechanically ventilated patients. Respir Care. 2011;56:460–6.
26. Beitler JR, Sands SA, Loring SH, et al. Quantifying unintended exposure to high tidal volumes from breath stacking dyssynchrony in ARDS: the BREATHE criteria. Intensive Care Med. 2016;42:1427–36.
27. Yonis H, Gobert F, Tapponnier R, et al. Reverse triggering in a patient with ARDS. Intensive Care Med. 2015;41:1711–2.
28. He X, Luo XY, Chen GQ, et al. Detection of reverse triggering in a 55-year-old man under deep sedation and controlled mechanical ventilation. J Thorac Dis. 2018;10:E682–5.
29. Imanaka H, Nishimura M, Takeuchi M, et al. Autotriggering caused by cardiogenic oscillation during flow triggered mechanical ventilation. Crit Care Med. 2000;28:402–7.
30. Gentile MA. Cycling of the mechanical ventilation breath. Respir Care. 2011;56:52–60.
31. Kondili E, Xirouchaki N, Georgopoulos D. Modulation and treatment of patient-ventilator dyssynchrony. Curr Opin Crit Care. 2007;13:84–9.
32. Tokioka H, Tanaka T, Ishizu T, et al. The effect of breath termination criterion on breathing patterns and the work of breathing during pressure support ventilation. Anesth Analg. 2001;92:161–5.
33. Marini JJ. Dynamic hyperinflation and auto-positive end-expiratory pressure: lessons learned over 30 years. Am J Respir Crit Care Med. 2011;184:756–62.
34. Berlin D. Hemodynamic consequences of auto-PEEP. J Intensive Care Med. 2014;29:81–6.

35. Mulqueeny Q, Ceriana P, Carlucci A, et al. Automatic detection of ineffective triggering and double triggering during mechanical ventilation. Intensive Care Med. 2007;33:2014–8.
36. Sinderby C, Liu S, Colombo D, et al. An automated and standardized neural index to quantify patient-ventilator interaction. Crit Care. 2013;17:R239.
37. Sottile PD, Albers D, Higgins C, et al. The association between ventilator dyssynchrony, delivered tidal volume, and sedation using a novel automated ventilator dyssynchrony detection algorithm. Crit Care Med. 2018;46:e151–7.

Chapter 9
Noninvasive Ventilation

Hao-Ran Gao, Rui Su, and Hong-Liang Li

Noninvasive ventilation (NIV) refers to mechanical ventilation without invasive artificial airways. There have been many noninvasive methods of assisted ventilation in the past, including negative pressure ventilator, rocking bed, pneumobelt, diaphragm pacing, and high-frequency oscillatory ventilation. However, in comparison to other noninvasive methods, noninvasive positive pressure ventilation (NIPPV) has become the dominant positive pressure ventilation method in the world due to its effectiveness and convenience, the use of a mask (or interface) to transfer gas from a positive pressure ventilator to the nose or mouth.

9.1 Noninvasive Positive Pressure Ventilation (NIPPV)

Mechanical ventilation that delivers gas to the airway through a mask or "interface" is called noninvasive positive pressure ventilation (NIPPV). It allows air leaks through the mouth or around the mask. The optimization of patient comfort and acceptance and effective management of air leaks are the keys to NIPPV's success [1].

Indications for noninvasive positive pressure ventilation [2]:

Strong evidence (Level A):

1. Acute exacerbations of COPD
2. To facilitate weaning in COPD
3. Acute cardiogenic pulmonary edema (use of CPAP)

H.-R. Gao
Weifang Medical University, Weifang, Shandong, China

R. Su · H.-L. Li (✉)
Department of Critical Care Medicine, Beijing Tiantan Hospital, Capital Medical University, Beijing, China

J. Zhou et al. (eds.), *Respiratory Monitoring in Mechanical Ventilation*,
https://doi.org/10.1007/978-981-15-9770-1_9

4. Immunocompromised patients

Reasonable evidence (Level B):

1. Postoperative respiratory failure
2. Asthma
3. Not intubating patients
4. Obstructive sleep apnea
5. Obesity hypoventilation

Cohort series, case reports (Level C):

1. During bronchoscopy
2. Cystic fibrosis
3. Restrictive lung diseases
4. Upper airway obstruction
5. Acute respiratory distress syndrome

The exclusion criteria for NIPPV:

1. Cardiac arrest
2. Hemodynamic shock
3. Life-threatening myocardial ischemia
4. Dangerous arrhythmias
5. Patients who do not cooperate
6. Airway surgery

9.2 Human-Ventilator Interface

Interfaces are devices that connect ventilator tubing to the face, facilitating the pressurized gas into the lung through the entry of the airway. Appropriate interfaces can provide accurate target airway pressure, optimize patient comfort, and achieve the best treatment results. In determining the optimal pressure level, patients should be encouraged to try several different interfaces to determine the one with the best overall comfort and effect, that is, the most comfortable mask may not be the most suitable, and the most suitable mask may not be the most comfortable.

Currently available interfaces include a nasal mask, nasal pillow, full face mask (oronasal mask), and oral interface. An oronasal mask for acute and short-term diseases, and in cases of chronic and prolonged cases, a nasal mask; and if the patient does not cooperate well, full face masks are recommended. For some patients, an oronasal mask usually requires higher pressure and poorer control than a nasal mask, and in practice, the best choice of the interface varies from person-to-person. Many experts agree that the best interface is “the one the patient is willing to use” [3, 4].

9.3 Complications

9.3.1 Mask Intolerance

Mask intolerance is the most common problem encountered by patients in adapting to NIPPV. Trying different types of interfaces can help. Do not force patients to wear a mask for longer than they can tolerate, and encourage patients to try at least weeks or months to get used to noninvasive ventilation before considering giving up.

9.3.2 Nasal Congestion and Dry Nose

These symptoms are often seasonal. Increasing humidity and heat often improve the comfort and acceptance of airflow through the airways. The application of saline or nasal gel may also be effective for dry nose.

9.3.3 Redness or Ulcers on the Bridge of the Nose

When the mask puts too much pressure on the bridge of the nose causes the symptoms. Minimizing the tension of the straps or use another type of mask can often alleviate this problem. Some patients experience a rash where the mask comes in contact with the skin. It may be helpful to use glucocorticoid cream or to wash your face with a mild cleansing soap before using the mask.

9.3.4 Bloating

The symptom is usually tolerable and transient without the need to adjust the settings.

9.3.5 Oral Leak

Patients are usually well ventilated in the presence of air leaks, and no special measures are required. The pressure-limited ventilation can maintain mask pressure by maintaining airflow to compensate for leaks. While volume-restricted ventilation, tidal volume needs to be adjusted to up to the compensation for leaks.

9.3.6 Failure to Improve Daytime Gas Exchange

If the gas exchange did not improve within a few weeks, considering the following factors: application time, air leaks accidentally, obstructive pulmonary diseases, human–ventilator asynchronization, and insufficient minute ventilation. By adjusting the inspiratory pressure or tidal volume, the frequency and the application time, or these parameters in combination, gas exchange may be improved. If there is evidence that the patient cannot trigger the ventilator, adjusting the trigger sensitivity or increasing the backup rate may be helpful [5].

9.3.7 The Deterioration of Gas Exchange after Initial Stabilization

In cases of progressive neuromuscular disease, the deterioration of gas exchange after initial stabilization often occurs. Pulmonary function tests and arterial blood gas analysis should be done periodically to assess the conditions. The frequency of follow-up depends on whether the patient has just started the treatment (every few weeks), or in a stable period of treatment (twice a year), or is experiencing clinical deterioration (more frequent follow-up). To improve the worsening of the lung function, it is often necessary to gradually increase inspiratory pressure, tidal volume, respiratory rates, or the application time of the ventilator.

9.4 Main Ventilation Techniques

9.4.1 CPAP (Continuous Positive Airway Pressure)

By delivering constant pressure during both inspiration and expiration, the variation ranges within 1–2 cm H_2O, CPAP can increase functional residual capacity and prevent the alveoli from collapsing. CPAP can also decrease afterload and increase cardiac output. This method does not provide additional pressure above the CPAP level, the patients must trigger the ventilator spontaneously.

9.4.2 BiPAP (Bilevel Positive Airway Pressure)

BiPAP provides different levels of positive airway pressure during inspiration and expiration. The pressure level during inspiration is called inspirational positive airway pressure (IPAP), and the pressure level during expiration is called expiratory positive airway pressure (EPAP) [6].

Recommendations for Conducting CPAP and BPAP Titrations.

1. The recommended minimum starting CPAP should be 4 cm H_2O, and the recommended minimum starting IPAP and EPAP should be 8 cm H_2O and 4 cm H_2O, respectively, for on BPAP.
2. The recommended maximum CPAP should be 15 cm H_2O (or recommended maximum IPAP of 20 cm H_2O if on BPAP) for patients less than 12 years and 20 cm H_2O (or recommended maximum IPAP of 30 cm H_2O if on BPAP) for patients older than 12 years.
3. The recommended minimum IPAP-EPAP difference is 4 cm H_2O and the recommended maximum IPAP-EPAP difference is 10 cm H_2O.
4. EPAP is initially set on a lower level, it can be set on the maximum of 10–12 cm H_2O, the IPAP-EPAP difference is called PS [7, 8].

Procedure for noninvasive positive pressure ventilation (Fig. 9.1) [9]

9.5 Summary and Recommendations

Noninvasive positive pressure ventilation (NIPPV) has some difficulties in the adapting process, but most patients can successfully adapt within a few weeks. Solving the problems caused by NIPPV actively, continuing the use of NIPPV is the key to the treatment.

9.6 Other Aspects

1. Negative Pressure Ventilation (NPV)

   NPV has been shown to relax respiratory muscles in patients with COPD and ARF, thereby improving gas exchange. NPV can be used for home mechanical ventilation in patients with chronic respiratory failure who cannot tolerate mask ventilation. Negative pressure ventilation can be used for all causes of respiratory failure in children, and can effectively reduce complications, with an effective rate of 70%. In addition, the use of both NPV and mask ventilation in most patients can avoid endotracheal intubation and its complications thus expanding the application of noninvasive ventilator technology [10].
2. The Rocking Bed and Pneumobelt

   Both the rocking bed and pneumobelt rely on gravity to assist diaphragm movement and are suitable for patients with severe diaphragm muscle weakness or paralysis. However, it is less functional in patients who are obese, overly lean, and severely kyphotic. Therefore, these two methods have great limitations and are not suitable for the treatment of acute respiratory failure. They are now rarely used [11].

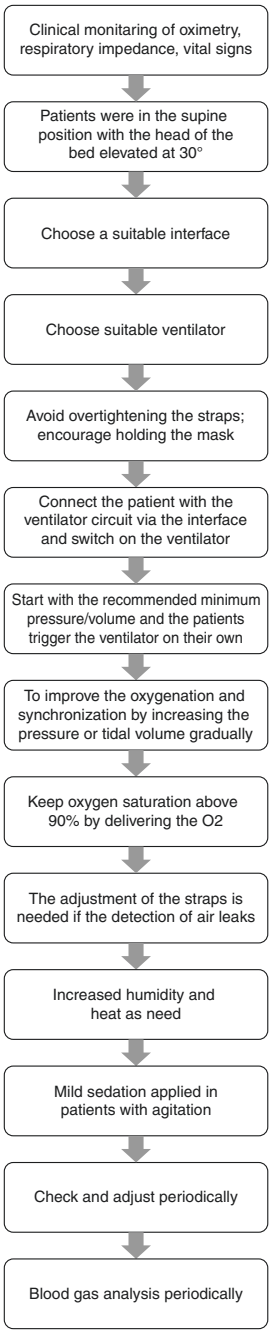

Fig. 9.1 Procedures for noninvasive positive pressure ventilation (NIPPV)

3. Diaphragm Pacing

   DP is primarily suitable for patients with high-level spinal cord injuries (SCI) and central hypoventilation syndromes (CHS). There are two different technologies, the first method is to place electrodes directly around the phrenic nerve, called intrathoracic diaphragm pacing (IT-DP). and the second method involves laparoscopic implantation of a nonconductive electrode, called intraperitoneal diaphragm pacing (IP-DP). DP has many benefits, including increased mobility, reduced anxiety and embarrassment, improved comfort, assistance in weaning, reduced incidence of respiratory infections, and reduced total cost. But there are also phrenic nerve mechanical injuries, technical failure, infection, and other complications [12, 13].

4. High-frequency Oscillatory Ventilation (HFOV)

   High-frequency oscillatory ventilation (HFOV) is a new type of mechanical ventilation developed in the 1980s, which can effectively improve oxygenation without increasing barotrauma. In adult patients, HFOV may be used when increased inhaled oxygen concentration and airway pressure do not improve gas exchange. And in patients with severe acute respiratory distress syndrome, HFOV can be used to prevent lung damage caused by ventilators. In neonates and children, HFOV can improve oxygenation [14–16].

5. High-Flow Nasal Cannula Oxygen Therapy (HFNC)

   High-flow nasal cannula oxygen therapy (HFNC) is an oxygen therapy method that directly delivers a certain oxygen concentration of air-oxygen mixed high-flow gas to a patient through a nasal obstruction catheter without sealing, as noninvasive breathing The form of support, which can rapidly improve oxygenation, can currently be applied to patients with acute hypoxic respiratory failure, patients after surgery, patients with respiratory failure who have not undergone intubation, immunosuppressed patients, and patients with heart failure [17]. High-flow nasal cannula oxygen therapy (HFNC) uses a flow rate of 60 liters per minute and FIO2 = 21–100% [18]. Its main advantage is that it can increase oxygenation without a ventilator. Its main disadvantage is the lack of ventilation support [19].

References

1. Ambrosino N, Vitacca M. The patient needing prolonged mechanical ventilation: a narrative review. Multidiscip Respir Med. 2018;13:6.
2. Seyfi S, Amri P, Mouodi S. New modalities for non-invasive positive pressure ventilation: a review article. Caspian J Intern Med. 2019;10(1):1–6.
3. Rochwerg B, et al. Official ERS/ATS clinical practice guidelines: noninvasive ventilation for acute respiratory failure. Eur Respir J. 2017;50(2)
4. Deshpande S, et al. Oronasal masks require a higher pressure than nasal and nasal pillow masks for the treatment of obstructive sleep apnea. J Clin Sleep Med. 2016;12(9):1263–8.
5. Aboussouan LS. Sleep-disordered breathing in neuromuscular disease. Am J Respir Crit Care Med. 2015;191(9):979–89.

6. Wedzicha JAEC-C, et al. Management of COPD exacerbations: a European Respiratory Society/American Thoracic Society guideline. Eur Respir J. 2017;49(3)
7. Kushida CA, et al. Clinical guidelines for the manual titration of positive airway pressure in patients with obstructive sleep apnea. J Clin Sleep Med. 2008;4(2):157–71.
8. Ozsancak Ugurlu A, et al. Use and outcomes of noninvasive positive pressure ventilation in acute care hospitals in Massachusetts. Chest. 2014;145(5):964–71.
9. Mehta S, Hill NS. Noninvasive ventilation. Am J Respir Crit Care Med. 2001;163(2):540–77.
10. Hassinger AB, et al. Negative-pressure ventilation in pediatric acute respiratory failure. Respir Care. 2017;62(12):1540–9.
11. Hill NS. Clinical applications of body ventilators. Chest. 1986;90(6):897–905.
12. Le Pimpec-Barthes F, et al. Diaphragm pacing: the state of the art. J Thorac Dis. 2016;8(Suppl 4):S376–86.
13. DiMarco AF. Diaphragm pacing. Clin Chest Med. 2018;39(2):459–71.
14. Fan E, Mehta S. High-frequency oscillatory ventilation and adjunctive therapies: inhaled nitric oxide and prone positioning. Crit Care Med. 2005;33(3 Suppl):S182–7.
15. Kinsella JP, et al. Inhaled nitric oxide in premature neonates with severe hypoxaemic respiratory failure: a randomised controlled trial. Lancet. 1999;354(9184):1061–5.
16. Kinsella JP, Abman SH. Recent developments in the pathophysiology and treatment of persistent pulmonary hypertension of the newborn. J Pediatr. 1995;126(6):853–64.
17. Masip J, et al. Indications and practical approach to non-invasive ventilation in acute heart failure. Eur Heart J. 2018;39(1):17–25.
18. Hernandez G, et al. Effect of postextubation high-flow nasal cannula vs conventional oxygen therapy on reintubation in low-risk patients: a randomized clinical trial. JAMA. 2016;315(13):1354–61.
19. Spoletini G, et al. Heated humidified high-flow nasal oxygen in adults: mechanisms of action and clinical implications. Chest. 2015;148(1):253–61.

Chapter 10
Brain Injury with Increased Intracranial Pressure

Han Chen and Linlin Zhang

10.1 Introduction

Mechanical ventilation is frequently applied in the daily management of brain injury patients. The purposes of mechanical ventilation are to protect the airway from the risk of aspiration and to prevent both hypoxemia and hypercapnia, which are two probable causes of secondary brain damage. There are concerns about the potential adverse effects of mechanical ventilation to the brain; for instance, an elevated airway pressure (Paw) may impede the venous return of the brain, which could increase cerebral blood volume (CBV) and intracranial pressure (ICP), especially in the case that a high positive end-expiratory pressure (PEEP) is applied to improve oxygenation. However, recent data suggest that it is not always the case, ICP can increase, unchanged, or even decreased [1–5]. The impact of PEEP on the brain is complicated and there are several factors involved in the brain–lung interaction including respiratory mechanics [2, 4, 5], lung recruitability and $PaCO_2$ [6], baseline ICP or cerebral compliance [7, 8], etc.

In addition, although the impact of tidal volume setting in patients with lung injury has been extensively investigated, showing that low tidal volume (e.g., the lung-protective ventilation strategy) can reduce ventilator-induced lung injury (VILI) and thus mortality [9, 10]. It is still unclear whether it should also be applied in brain injury patients. Although some ventilation targets had been provided in the recent guideline, it did not detail the setting of tidal volume or PEEP in brain injury patients [11]. Moreover, impaired consciousness in brain injury patients makes the decisions of both weaning from mechanical ventilation and extubation challenging

H. Chen
Surgical Intensive Care Unit, Fujian Provincial Hospital, Fuzhou, China

L. Zhang (✉)
Department of Critical Care Medicine, Beijing Tiantan Hospital, Capital Medical University, Beijing, China

J. Zhou et al. (eds.), *Respiratory Monitoring in Mechanical Ventilation*,
https://doi.org/10.1007/978-981-15-9770-1_10

issues. In recent years, some new tools to predict successful weaning have been proposed [12–16]; however, no clear recommendations are currently available owing to the lack of robust evidence in the literature.

In this chapter, the (patho) physiology basis of brain-lung interaction will be discussed, including the impact of positive pressure ventilation on hemodynamics, $PaCO_2$ and its physiological effects on cerebral vessels, and the role of the intracranial Starling resistor and its anatomic basis. The data available in the neurocritical care field regarding respiratory management, from the early phase of mechanical ventilation to the weaning and extubation will be reviewed.

10.2 Physiology and Pathophysiology

10.2.1 Monro–Kellie Doctrine

It was in the seventeenth century when Edinburgh physician Alexander Monro and his student George Kellie first proposed the "science" of ICP, that the skull as a rigid structure containing incompressible brain, and the volume of blood must remain constant unless: "water or other matter is effused or secreted from the blood vessels" in which case "a quantity of blood, equal in bulk to the effused matter will be pressed out of the cranium" [17].

This doctrine is usually summarized in this way today: with an intact skull, the sum of the volume of intracranial contents (i.e., brain tissue, blood, and cerebrospinal fluid) is constant, an increase in one (e.g., edema, tumor, hematoma, hydrocephalus, etc.) causes a "shifting" in one or both of the remaining two (i.e., some degree of compensation). In this compensated state, the increase in intracranial volume is offset by shifting venous blood out of the intracranial space and cerebrospinal fluid into the spinal subarachnoid space. However, once the capacity to displace cerebrospinal fluid and blood is exhausted, additional increases in any of the intracranial contents are associated with precipitous increases in ICP.

Allied to the Monro-Kellie doctrine is the intracranial compliance that describes the capacity of the intracranial contents to compensate for volume changes. Similar to the calculation of respiratory compliance, it can be calculated as the ratio between the change in ICP (ΔICP) to the change in intracranial volume (ΔV). A high compliance represents a good reserve to increase in intracranial volume; in the contrast, compromised intracranial compliance means the corresponding change in ICP to a given increase in intracranial volume becomes greater. Hence, when compliance is reduced, even minor changes in intracranial volume, which can be caused by mechanical ventilation (e.g., increase PEEP, altered tidal volume or respiratory rate that increases $PaCO_2$, etc.; see below for detail), can lead to a rapid increase in ICP.

10.2.2 Transmission of Pressure

Right atrial is the end of venous system and the right atrial pressure (Pra) is thus the downstream pressure of the whole venous system. The driving force of venous return is the pressure gradient between upstream venous pressure (which is the mean systemic pressure of the circulation (Pms) for the whole body and the cranial venous pressure for the brain) and Pra. In this point of view, venous return would decrease for any cause which increases Pra (e.g., increasing PEEP) while the upstream unchanged [18]. In the simplest analysis, the decreased venous return from the brain would thus increase CBV and ICP. In other words, the increased downstream pressure can somehow be "transmitted" into cranium and thus increase ICP. An elevated Paw during positive pressure ventilation can increase pleural pressure (Ppl) and thus Pra, and eventually ICP. It has been suggested by observational data that neurological patients received lower PEEP levels than non-neurological patients [19]. The concern of the potential impact of PEEP on cerebral venous return and ICP might be the reason why physicians prefer lower PEEP levels.

However, the transmission of elevated Paw into cranium is not always fully efficient: the effectiveness of the transmission of Paw to the pleural space and the intrathoracic veins is determined by the relative compliance of the lung and chest wall [20]; while the transmission of pressure from the right atrial to the neck and cranial veins can be impeded by the effect of an intracranial "Starling resistor."

10.2.2.1 Compliance of the Lung and the Chest Wall

It has been reported that respiratory system compliance may help in predicting how PEEP influences ICP [2, 4, 5, 21, 22]. The effects of PEEP may become evident only in patients with both decreased intracranial compliance and normal lung compliance [22]. In other words, lung disease per se could be a protective factor because less compliant lungs poorly transmit the increased pressure to the pleural cavity. Similarly, cerebral hemodynamics and ICP may be minimally influenced by the application of PEEP in patients whose lung compliance is impaired [2].

In contrast, a large retrospective study reported a significant relationship between PEEP and ICP only in patients with severe lung injury [21]; however, these data are retrospective and, in some cases, "respiratory system compliance" is termed "lung compliance." Indeed, a given decrease in respiratory system compliance might reflect impaired lung compliance (e.g., acute respiratory distress syndrome (ARDS), pulmonary fibrosis), or decreased chest wall compliance (e.g., intra-abdominal hypertension, pleural effusion). Studies differentiated compliance of the lung and the chest wall using esophageal manometry demonstrated that the impact of PEEP on ICP was greater in the subjects (patients or pigs) with lower chest wall compliance [4, 5].

10.2.2.2 Starling Resistor

A Starling resistor is a collapsible tube in which the pressure external to the tube exceeds the outflow pressure. The external pressure determines the degree of collapse of the tube, thereby providing a variable resistor. The anatomic basis for the intracranial Starling resistor is the rigid cranium (sealed box that determines the external pressure) and the rigid artery (upstream tube) and superior sagittal sinus (downstream tube), and the intervening collapsible cerebral veins [23]. This phenomenon is supported by both hemodynamic [7, 24, 25] and imaging studies [26, 27]. Luce and collages conducted a series of studies in dogs [7, 25] in which they measured the pressure in cerebral vein and sagittal sinus with an intravascular catheter. An abrupt drop in pressure was found when the catheter was advanced into the sinus from the cerebral vein [25] suggested the presence of a Starling resistor between the sagittal sinus and the cerebral veins.

In an imaging study using magnetic resonance venography in intracranial hypertension patients, narrowing of the distal part of brain-bridging veins is clearly displayed [23]. This is exactly the behavior of a Starling resistor: the collapse always begins at the distal end of the flexible tube, and thereby generates an increase in the flow velocity at the level of the partially collapsed segment (so-called Venturi effect), results in the loss of the magnetic resonance venography signal (termed "void sign").

Luce and collages suggested that this "resistor" regulates cerebral venous outflow when sagittal sinus pressure is increased by PEEP [25]. In this setting, an elevated ICP would occlude the resistor, thereby preventing the transmission of Pra into the cranium; thus, increases in airway pressure will not be transmitted and will not increase ICP. However, steadily elevating the airway pressure will progressively increase Pra and this will eventually open the resistor. In this way, when the resistor is open, a direct (venous) communication exists between the thorax and the ICP, and here, elevating airway pressure would effectively elevate the ICP.

10.2.3 Impact of Mechanical Ventilation on the Arterial Side

10.2.3.1 Cerebral Autoregulation

Cerebral autoregulation is the intrinsic ability of the cerebral vascular to maintain cerebral blood flow (CBF) constant to a fluctuation of blood pressure [28, 29]. Vasoconstriction or dilation of the cerebral vascular in response to elevated or decreased blood pressure helps to maintain a constant CBF across a wide range of systemic arterial pressures (50–160 mmHg) in healthy individuals [29]. However, in a variety of acute neurologic disorders, cerebral autoregulation is impaired or absent. In this case, CBF may simply change parallelly to cerebral perfusion pressure (CPP, defined as the difference between mean arterial pressure and ICP), and results in either inadequate tissue perfusion (in hypotension) or hyperemia (in hypertension). In a recent review, a conceptual framework of the integrated

regulation of brain perfusion has been proposed, suggesting that multiple factors rather than blood pressure alone are involved in the regulation of CBF including sympathetic activity, renin–angiotensin action, cardiac output, blood pressure, metabolic products, nitric oxide, etc. [30].

Elevated Ppl induced by positive pressure ventilation would not only (to some extend) impede the venous return of the brain, but also the global venous return, which determines preload and thus cardiac output. If a high Ppl reduces systemic arterial pressure, CPP decreases. In the case that cerebral autoregulation is intact, CBF may be maintained despite a lower CPP; but if impaired, decreased CPP may lower CBF and CBV, and thereby decrease ICP. In a recent experimental study, the authors reported that ICP is reduced by gradual increases of PEEP, probably due to the lowered CPP [5]. It is worth pointing out that although ICP can be decreased by elevated Paw, it is actually in the price of decreased CBF. If hypoperfusion/ischemia is sustained, secondary brain injury is inevitable, and the outcome would be poor.

10.2.3.2 Impact of CO_2 and pH

$PaCO_2$ is a powerful physiological modulator of ICP via intracranial vasodilation. The relationship between $PaCO_2$ and CBF is an asymmetric sigmoid curve that is approximately linear within a physiological range of $PaCO_2$ [31]. Hypercapnia increases CBF and CBV, leading to an increase in ICP, whereas hypocapnia results in vasoconstriction and decrease ICP. While deliberate hyperventilation is applied to reduce elevated intracranial hypertension, the vasoconstrictive effects of hypocapnia may result in cerebral hypoxia and ischemia. Adaptation can occur and the vasoconstrictive effects dissipate within hours [32, 33], but it seems clear that the effects of hypocapnia on intracranial blood volume are even more short-lived than its effects on CBF (possibly due to differential effects of hypocapnia on intracranial resistance and capacitance vessels) [34]. In addition, rebound elevation of ICP may occur once hyperventilation is discontinued [33]. Standard guidelines on the management of traumatic brain injury recommend hyperventilation as a temporizing measure only for the emergency reduction of acute neurologic deterioration (e.g., herniation, sudden ICP elevation, etc) only; in addition, prolonged "prophylactic" hyperventilation is no longer recommended [11].

A contrasting concern is that hypercapnia may increase ICP, especially in those who are receiving lung-protective ventilation involving permissive hypercapnia. Petridis et al. reported despite hypercapnia ($PaCO_2$ 50–60 mmHg) there was no increase in ICP in patients with subarachnoid hemorrhage who were ventilated with lung-protective ventilation [35]. However, the dominant cause of intracranial hypertension in many patients with subarachnoid hemorrhage is hydrocephalus, and once this is treated with CSF diversion, the intracranial compliance may be much less of a problem; indeed, in the series from Petridis et al., the ICP was 10–18 mmHg following CSF drainage [35]. Consequently, these results cannot be safely extrapolated to patients in whom the primary cause of intracranial hypertension is cerebral edema or a space-occupying lesion. Another study suggested that ICP increased

significantly only in patients with non-recruitable lung where PEEP was associated with increased $PaCO_2$ due to alveolar overdistension [6].

Collectively, the impact of positive pressure ventilation on CBV and ICP is determined by multiple factors [23]. In brief, an increment in Paw will transmit to pleural cavity and intrathoracic major vessels, elevating both Ppl and Pra, where the effectiveness of the transmission is determined by the relative compliance of the lung and the chest wall. The elevated Pra impedes the venous return from both cerebral veins, which decreases cerebral venous outflow and results in an increase in CBV (Starling resistor involved here) and the whole body, which reduces cardiac preload and output. Reduced cardiac output (and blood pressure) may result in a decrease in CBV due to decreased cerebral artery inflow, and this is regulated by cerebral autoregulation. An increment in Paw may also result in hypocapnia, which can cause cerebral vasoconstriction and reduce CBV. Consequently, the net impact on ICP reflects the balance of changes in CBV caused by altered (venous) outflow and (arterial) inflow, and here, the intracranial compliance is another key determinant.

10.3 Management of Mechanical Ventilation

In the early phase following brain injury, hypoxemia and hyper/hypocapnia lead to secondary brain insults, which alter the outcome [36]. Traditional ventilation strategy in brain injury patients, especially those with intracranial hypertension, includes airway protection (intubation), optimization of brain oxygen delivery, strict control of $PaCO_2$, and minimizing the postulated adverse effects of positive pressure ventilation on ICP. Such a brain-centered ventilation strategy lead to the use of larger tidal volumes, high inspired O_2, and low or zero PEEP [19].

Treatment of hypoxemia can be modulated via increasing the inspired oxygen fraction (FiO_2) to ensure a PaO_2 >60 mmHg [11]. Moreover, PaO_2 could be further modulated if brain hypoxia is diagnosed with low tissue oxygen tension ($PtiO_2$) and jugular venous oxygen saturation ($SvjO_2$) [37]. However, it has also been shown that a supranormal PaO_2 level may aggravate secondary brain damage after both severe traumatic brain injury [38] and cardiac arrest [39]. In addition, the optimal setting of tidal volume and PEEP is still controversial, and the recent guideline did not provide any recommendation on this [11]. Nonetheless, no consensus is available to set the tidal volume and PEEP, and in daily practice, one should always assess the risk/benefit relationship before altering any mechanical ventilation setting.

10.3.1 Tidal Volume

The effectiveness of lung-protective ventilation strategy, including lower tidal volume to attenuate VILI, limiting plateau pressure, and using PEEP to limit atelectasis [9, 40], has been well-established in the treatment of ARDS patients. Such

ventilation strategy even also has shown benefits in patients without lung injury (but non-brain injury) [41].

Recently, the safety and efficacy of lung-protective ventilation in brain injury patients were tested in two studies [42, 43]. One study included 499 patients with TBI, SAH, and stroke, and tidal volume was set to 6–8 mL/kg predicted body weight combined with a PEEP level of >3 cmH_2O [42]. A significant increase in the number of ventilatory-free days was observed [42]. In the other study that included 749 brain injury patients, tidal volume was set to ≤7 mL/kg of predicted body weight and PEEP was set between 6 and 8 cmH_2O. No differences in ventilatory-free days were observed [43]. Nonetheless, in both studies [42, 43] lung-protective ventilation did not lead to clinically relevant effects on ICP. It also should be noted that the level of $PaCO_2$ was carefully monitored and manipulated within normal ranges in both studies. These data highly suggest that protective ventilation with a moderate tidal volume (6–8 mL/kg predicted body weight) could be safely applied in brain injury patients, with the careful monitoring and manipulation of $PaCO_2$ within normal range by adjusting the respiratory rate.

10.3.2 PEEP

Another issue regarding the ventilatory settings is the level of PEEP. Clinical studies investigating the effects of PEEP (or other patterns that mimic the effect of PEEP) are summarized in Table 10.1. Disparate reports exist on the responses of ICP to increases in PEEP. Some studies report that increased PEEP may have no impact on ICP if not initially elevated, but may have an impact if initially elevated [44]. However, the opposite has also been reported: raised PEEP had no impact on already elevated ICP, but increased it if initially normal [8]. Finally, increased PEEP may decrease ICP [3, 5].

In attempting to interpret these disparate reports, several issues should be noted. First, individual intracranial compliance may vary even with the same ICP numbers. However, the ability to perform interventional testing in patients with intracranial hypertension is limited, as such patients are vulnerable. Second, assessment is confounded by concomitant medical management such as analgesics, sedatives, and anticonvulsants, as well as deliberate control of blood pressure, blood gases, and temperature [11, 59–61]. Third, intracranial veins can behave as either veins in series without threshold flow characteristics [62], or as a "Starling Resistor" [7, 25]. Finally, because PEEP affects the respiratory and cardiovascular systems simultaneously, there is "interdependence" among the involved parameters and no single parameter can be considered in isolation. Therefore, the net impact of PEEP may be difficult to predict.

Consequently, due to its multifactor-determining nature, PEEP can either increase ICP or conversely have no significant effects. The impact is generally unpredictable, and thus individualized monitoring and titration are key. In addition, in the case of brain injury with concomitant ARDS, which is a clinical situation that a high PEEP is required in a brain injury patient, current studies suggest that PEEP

Table 10.1 Impacts of positive end-expiratory pressure on intracranial pressure in patients with brain injury

Author (#)	Year	Subjects	Interventions	Measurements	Main results
PEEP increases ICP					
Apuzzo [44]	1977	Neurosurgery (n = 25)	0 vs. 10 PEEP	CPP SjO_2	Increase in ICP was only observed in the patients who manifested decreased cerebral compliance.
Burchiel [22]	1981	TBI (n = 16), SAH (n = 2)	Individualized PEEP	ICP CPP	PEEP increased ICP and decreased CPP in patients with abnormal cerebral compliance and normal lung compliance. No impact in patients with normal cerebral compliance or those who with both decreased cerebral and lung compliance.
Chen [4]	2018	Neurosurgery (n = 30)	5 vs 15 PEEP	ICP	Patients with greater increment in ICP had lower chest wall compliance.
Cooper [45]	1985	TBI (n = 33)	Baseline vs. additional 5–15 PEEP	ICP	PEEP increases ICP, but patients with elevated baseline ICP experienced no significant increase.
Cunitz [46]	1979	Neurosurgery (n = 24)	Between different PEEP levels	ICP	PEEP increased ICP.
Lima [47]	2011	ICH (n = 25)	Between different PEEP levels (from 0 to 14 cm H2O)	ICP CPP	PEEP increased ICP. No impact on CPP.
Lodrini [48]	1989	Neurosurgery (n = 10)	0/5/10/15 PEEP	ICP	PEEP increased ICP but without intracranial hypertension. In patients with increased ICP, the combination of head flexion and rotation with institution of PEEP caused a dangerous increase in ICP.
Ludwig [49]	2000	TBI (n = 10)	Between different Paw levels	ICP CPP VmMCA	Elevated Paw increased ICP; increasing peak Paw increased variability of ICP, CPP and VmMCA

Table 10.1 (continued)

Author (#)	Year	Subjects	Interventions	Measurements	Main results
Mascia [6]	2005	TBI & ARDS (n = 20)	0/5/10 PEEP	ICP VmMCA SjO_2	ICP, VmMCA, and SjO_2 remained constant in recruiters but increased in non-recruiters.
McGuire [8]	1997	Neurosurgery (n = 18)	5/10/15 PEEP	ICP CPP	In patients with normal ICP, PEEP increased ICP. In patients with increased baseline ICP, PEEP did not change ICP or CPP.
Muench [50]	2005	SAH (n = 10)	Baseline to 20 PEEP	ICP rCBF $PtiO_2$	Stepwise elevation of PEEP increased ICP; decreased rCBF and $PtiO_2$.
Shapiro [51]	1978	TBI (n = 12)	0 vs. 4–8 PEEP	ICP CPP	In six patients PEEP increased ICP. CPP was less than 50 mmHg in six patients given PEEP.
Videtta [52]	2002	Neurosurgery (n = 20)	5/10/15 PEEP	ICP CPP	PEEP increased ICP. No impact on CPP.
No impact on ICP					
Caricato [2]	2005	TBI, SAH (n = 21)	0/4/8/12 PEEP	ICP CPP VmMCA SjO_2	PEEP reduces CPP and VmMCA only in patients with normal respiratory system compliance. No impact on ICP or SjO_2.
Frost [53]	1977	Coma (n = 7)	0 to up to 40 PEEP	ICP	PEEP did not increase ICP in patients with either normal or low intracranial compliance and did not increase ICP in the absence of pulmonary disease.
Martinez-Perez [54]	2004	TBI & ARDS (n = 7)	Standard ventilation vs. mid to end expiratory tracheal gas insufflation	CPP SjO_2	No changes in hemodynamic or cerebral parameters
Nemer [55]	2015	TBI & ARDS (n = 20)	5/10/15 PEEP	$PtiO_2$ ICP CPP	PEEP increases $PtiO_2$, no impact on ICP or CPP
Pulitano [56]	2013	Pedeatric brain tumor (n = 21)	0/4/8 PEEP	ICP CPP VmMCA	No change in ICP, CPP or VmMCA

(continued)

Table 10.1 (continued)

Author (#)	Year	Subjects	Interventions	Measurements	Main results
Solodov [57]	2016	ICH (n = 39)	Baseline vs. 15 PEEP	ICP CPP	PEEP had no adverse effect on CPP and led only to clinical insignificant increase in ICP.
Zhang [1]	2011	TBI & ARDS (n = 9)	RMs using different PEEP levels	ICP CPP	No impact on ICP and CPP 5 min after RMs
Other effects					
Georgiadis [58]	2001	Neurosurgery (n = 20)	4/8/12/4 PEEP	ICP CPP VmMCA	CPP significantly changed depending on the various PEEP levels. Three distinct reaction patterns of ICP and other parameters observed

Abbreviations: ARDS Acute respiratory distress syndrome, *CPP* Cerebral perfusion pressure, *ICH* Intracranial hemorrhage, *ICP* Intracranial pressure, *Paw* Airway pressure, *PEEP* Positive end-expiratory pressure, *$PtiO_2$* Brain tissue oxygenation, *rCBF* Regional cerebral blood flow, *RMs* Recruitment maneuvers, *SAH* Subarachnoid hemorrhage, *SjO_2* Jugular saturation of oxygen, *TBI* Traumatic brain injury, *VmMCA* Mean blood flow velocity, middle cerebral artery

has basically no or mild impact on ICP [1, 54, 55]. The transmission of PEEP is lessened if lung compliance is low; however, it could become "efficient" in the case of coexisting decreased chest wall compliance (e.g., intra-abdominal hypertension). Monitoring and individualization are definitely necessary in such cases.

Unlike the impact on ICP which is extensively explored, there are few reports of the effects of increased PEEP on cerebral perfusion or oxygenation, likely in part, because of the lack of available equipment at bedside. Experimental studies using intracranial flow probes [50], radioactive microspheres [63, 64], or arterial flow probes [65] for direct measurement of CBF suggest decreased [65] or unchanged [50, 63, 64] CBF following increases in PEEP. In patients with subarachnoid hemorrhage, increased PEEP decreases mean arterial pressure, regional CBF, and brain tissue oxygenation [50]. In contrast, Nemer et al. reported that increased PEEP improves brain tissue oxygenation in severe traumatic brain injury patients with ARDS [55]. Moreover, it should be noted that an increase in PEEP may change cerebral perfusion or oxygenation before any change in ICP can be observed. In summary, such effects have not been extensively investigated and, at the bedside, are likely under-recognized.

10.4 Weaning from Mechanical Ventilation in Brain Injury

It is important to recognize at what point mechanical ventilation can be reduced and discontinued from a brain injury patient since timely weaning from mechanical ventilation and extubation reduce the risk of VILI, ventilator-associated pneumonia and

the length of ICU stay [14, 15, 66]. The level of conscious status is the major concern for physicians to decide when to safely perform extubation. One study using algorithm-based extubation protocol including a Glasgow coma scale (GCS) ≥8 significantly reduces the rate of reintubation [67]. Namen et al. showed that the odds of successful extubation rose by 39% for every 1-point increase in GCS, and a GCS >8 had the highest area under the receiver operating curve for predicting successful extubation [68]. Surprisingly, however, there are also studies showing that higher GCS was not associated with extubation success [15, 16]. A possible explanation is that GCS is never validated in intubated patients. One should keep in mind that it is impossible to quantify the verbal component of GCS in intubated patients and it is therefore often arbitrarily scored [14]. This could explain why using GCS in isolation has been inconsistently identified as a predictor of successful extubation.

In attempting to improve the accuracy of the screening tool for extubation in brain injury patients, specific neurologic features associated with safe extubation have been identified. In a recent multicenter study, age <40 years old, visual pursuit, attempts to swallow, and a GCS >10 were independent markers of successful extubation; thereby, a screening tool termed VISAGE score was built [14]. When three items out of the four are present, the score predicts more than 90% of extubation success [14]. Similar clinical signs are also identified in other studies (visual pursuit [15], younger age [16]). In addition, negative fluid balance preserved upper airway reflexes and the presence of cough are also predictors of successful extubation (Table 10.2) [13, 15, 16, 69].

In the case of a complicated weaning process, tracheostomy appears as an interesting therapeutic alternative. The potential advantages of tracheostomy include decreased risk for sinusitis, reduced airway resistance and dead space resulting in decreased work of breathing, better subjective tolerance, less need for sedation, and decreased duration of mechanical ventilation [70]. Debate remains over the benefit of early versus late tracheostomy: a number of recent retrospective studies favored early tracheostomy with less pneumonia, lower mechanical ventilation duration, ICU length of stay, and medical cost [71–73]; however, in a randomized, controlled study in stroke patients, early tracheostomy did not result in a reduction in the ICU length of stay [74]. But early tracheostomy did improve survival in this study [74]. To date, there is no guideline regarding the management of tracheostomy in patients with brain injury. In clinical practice, early tracheostomy is not

Table 10.2 Predictive factors of successful extubation in patients with brain injury

Presence of cough
Positive gag reflex
Negative fluid balance VISAGE score
– Age < 40
– Glasgow coma score > 10
– Swallowing attempts
– Visual pursuit

recommended to all patients but could be considered in situations with a high risk of extubation failure, prolonged mechanical ventilation, or in patients with poor neurological recovery.

10.5 Conclusion

The effect of positive pressure mechanical ventilation on ICP is determined by several factors, and the net impact may be unpredictable, which calls for individualized titration to optimize care, especially in patients with concomitant severe brain injury and respiratory failure. Mechanical ventilation may change cerebral perfusion or oxygenation before any change in ICP can be observed; such effects have not been extensively investigated. Impaired conscious status and neurologic reflexes may hinder the successful weaning; using protocolized weaning strategies integrating assessments of respiratory ability, conscious status, and neurologic reflexes may lead to expeditious and safe liberation from mechanical ventilation in brain injury patients.

References

1. Zhang XY, Yang ZJ, Wang QX, Fan HR. Impact of positive end-expiratory pressure on cerebral injury patients with hypoxemia. Am J Emerg Med. 2011;29(7):699–703. https://doi.org/10.1016/j.ajem.2010.01.042.
2. Caricato A, Conti G, Della Corte F, Mancino A, Santilli F, Sandroni C, Proietti R, Antonelli M. Effects of PEEP on the intracranial system of patients with head injury and subarachnoid hemorrhage: the role of respiratory system compliance. J Trauma. 2005;58(3):571–6.
3. Huynh T, Messer M, Sing RF, Miles W, Jacobs DG, Thomason MH. Positive end-expiratory pressure alters intracranial and cerebral perfusion pressure in severe traumatic brain injury. J Trauma. 2002;53(3):488–92.; discussion 492–483. https://doi.org/10.1097/01.ta.0000025657.37314.2f.
4. Chen H, Chen K, Xu JQ, Zhang YR, Yu RG, Zhou JX. Intracranial pressure responsiveness to positive end-expiratory pressure is influenced by chest wall elastance: a physiological study in patients with aneurysmal subarachnoid hemorrhage. BMC Neurol. 2018;18(1):124. https://doi.org/10.1186/s12883-018-1132-2.
5. Chen H, Zhou J, Lin YQ, Zhou JX, Yu RG. Intracranial pressure responsiveness to positive end-expiratory pressure in different respiratory mechanics: a preliminary experimental study in pigs. BMC Neurol. 2018;18(1):183. https://doi.org/10.1186/s12883-018-1191-4.
6. Mascia L, Grasso S, Fiore T, Bruno F, Berardino M, Ducati A. Cerebro-pulmonary interactions during the application of low levels of positive end-expiratory pressure. Intensive Care Med. 2005;31(3):373–9. https://doi.org/10.1007/s00134-004-2491-2.
7. Huseby JS, Luce JM, Cary JM, Pavlin EG, Butler J. Effects of positive end-expiratory pressure on intracranial pressure in dogs with intracranial hypertension. J Neurosurg. 1981;55(5):704–5. https://doi.org/10.3171/jns.1981.55.5.0704.
8. McGuire G, Crossley D, Richards J, Wong D. Effects of varying levels of positive end-expiratory pressure on intracranial pressure and cerebral perfusion pressure. Crit Care Med. 1997;25(6):1059–62.

9. Fan E, Del Sorbo L, Goligher EC, Hodgson CL, Munshi L, Walkey AJ, Adhikari NKJ, Amato MBP, Branson R, Brower RG, Ferguson ND, Gajic O, Gattinoni L, Hess D, Mancebo J, Meade MO, McAuley DF, Pesenti A, Ranieri VM, Rubenfeld GD, Rubin E, Seckel M, Slutsky AS, Talmor D, Thompson BT, Wunsch H, Uleryk E, Brozek J, Brochard LJ. An official American Thoracic Society/European Society of Intensive Care Medicine/Society of Critical Care Medicine clinical practice guideline: mechanical ventilation in adult patients with acute respiratory distress syndrome. Am J Respir Crit Care Med. 2017;195(9):1253–63. https://doi.org/10.1164/rccm.201703-0548ST.
10. The Acute Respiratory Distress Syndrome Network. Ventilation with lower tidal volumes as compared with traditional tidal volumes for acute lung injury and the acute respiratory distress syndrome. N Engl J Med. 2000;342(18):1301–8. https://doi.org/10.1056/nejm200005043421801.
11. Carney N, Totten AM, O'Reilly C, Ullman JS, Hawryluk GW, Bell MJ, Bratton SL, Chesnut R, Harris OA, Kissoon N, Rubiano AM, Shutter L, Tasker RC, Vavilala MS, Wilberger J, Wright DW, Ghajar J. Guidelines for the management of severe traumatic brain injury, fourth edition. Neurosurgery. 2017;80(1):6–15. https://doi.org/10.1227/neu.0000000000001432.
12. Perin C, Meroni R, Rega V, Braghetto G, Cerri CG. Parameters influencing tracheostomy decannulation in patients undergoing rehabilitation after severe acquired brain injury (sABI). Int Arch Otorhinolaryngol. 2017;21(4):382–9. https://doi.org/10.1055/s-0037-1598654.
13. Dos Reis HFC, Gomes-Neto M, Almeida MLO, da Silva MF, Guedes LBA, Martinez BP, de Seixas Rocha M. Development of a risk score to predict extubation failure in patients with traumatic brain injury. J Crit Care. 2017;42:218–22. https://doi.org/10.1016/j.jcrc.2017.07.051.
14. Asehnoune K, Seguin P, Lasocki S, Roquilly A, Delater A, Gros A, Denou F, Mahe PJ, Nesseler N, Demeure-Dit-Latte D, Launey Y, Lakhal K, Rozec B, Malledant Y, Sebille V, Jaber S, Le Thuaut A, Feuillet F, Cinotti R. Extubation success prediction in a multicentric cohort of patients with severe brain injury. Anesthesiology. 2017;127(2):338–46. https://doi.org/10.1097/aln.0000000000001725.
15. Godet T, Chabanne R, Marin J, Kauffmann S, Futier E, Pereira B, Constantin JM. Extubation failure in brain-injured patients: risk factors and development of a prediction score in a preliminary prospective cohort study. Anesthesiology. 2017;126(1):104–14. https://doi.org/10.1097/aln.0000000000001379.
16. McCredie VA, Ferguson ND, Pinto RL, Adhikari NK, Fowler RA, Chapman MG, Burrell A, Baker AJ, Cook DJ, Meade MO, Scales DC. Airway management strategies for brain-injured patients meeting standard criteria to consider extubation. A prospective cohort study. Ann Am Thorac Soc. 2017;14(1):85–93. https://doi.org/10.1513/AnnalsATS.201608-620OC.
17. Wilson MH. Monro-Kellie 2.0: the dynamic vascular and venous pathophysiological components of intracranial pressure. J Cereb Blood Flow Metab. 2016;36(8):1338–50. https://doi.org/10.1177/0271678x16648711.
18. Funk DJ, Jacobsohn E, Kumar A. The role of venous return in critical illness and shock-part I: physiology. Crit Care Med. 2013;41(1):255–62. https://doi.org/10.1097/CCM.0b013e3182772ab6.
19. Pelosi P, Ferguson ND, Frutos-Vivar F, Anzueto A, Putensen C, Raymondos K, Apezteguia C, Desmery P, Hurtado J, Abroug F, Elizalde J, Tomicic V, Cakar N, Gonzalez M, Arabi Y, Moreno R, Esteban A. Management and outcome of mechanically ventilated neurologic patients. Crit Care Med. 2011;39(6):1482–92. https://doi.org/10.1097/CCM.0b013e31821209a8.
20. Chapin JC, Downs JB, Douglas ME, Murphy EJ, Ruiz BC. Lung expansion, airway pressure transmission, and positive end-expiratory pressure. Arch Surg. 1979;114(10):1193–7.
21. Boone MD, Jinadasa SP, Mueller A, Shaefi S, Kasper EM, Hanafy KA, O'Gara BP, Talmor DS. The effect of positive end-expiratory pressure on intracranial pressure and cerebral hemodynamics. Neurocrit Care. 2017;26(2):174–81. https://doi.org/10.1007/s12028-016-0328-9.
22. Burchiel KJ, Steege TD, Wyler AR. Intracranial pressure changes in brain-injured patients requiring positive end-expiratory pressure ventilation. Neurosurgery. 1981;8(4):443–9.

23. Chen H, Menon DK, Kavanagh BP. Impact of altered airway pressure on intracranial pressure, perfusion, and oxygenation: a narrative review. Crit Care Med. 2019;47(2):254–63. https://doi.org/10.1097/ccm.0000000000003558.
24. Nakagawa Y, Tsuru M, Yada K. Site and mechanism for compression of the venous system during experimental intracranial hypertension. J Neurosurg. 1974;41(4):427–34. https://doi.org/10.3171/jns.1974.41.4.0427.
25. Luce JM, Huseby JS, Kirk W, Butler J. A Starling resistor regulates cerebral venous outflow in dogs. J Appl Physiol Respir Environ Exerc Physiol. 1982;53(6):1496–503.
26. Si Z, Luan L, Kong D, Zhao G, Wang H, Zhang K, Yu T, Pang Q. MRI-based investigation on outflow segment of cerebral venous system under increased ICP condition. Eur J Med Res. 2008;13(3):121–6.
27. R DES, Ranieri A, Bonavita V. Starling resistors, autoregulation of cerebral perfusion and the pathogenesis of idiopathic intracranial hypertension. Panminerva Med. 2017;59(1):76–89. https://doi.org/10.23736/s0031-0808.16.03248-1.
28. McBryde FD, Malpas SC, Paton JF. Intracranial mechanisms for preserving brain blood flow in health and disease. Acta Physiol (Oxf). 2017;219(1):274–87. https://doi.org/10.1111/apha.12706.
29. Lassen NA. Cerebral blood flow and oxygen consumption in man. Physiol Rev. 1959;39(2):183–238. https://doi.org/10.1152/physrev.1959.39.2.183.
30. Meng L, Hou W, Chui J, Han R, Gelb AW. Cardiac output and cerebral blood flow: the integrated regulation of brain perfusion in adult humans. Anesthesiology. 2015;123(5):1198–208. https://doi.org/10.1097/aln.0000000000000872.
31. Reivich M. Arterial PCO2 and cerebral hemodynamics. Am J Phys. 1964;206:25–35.
32. Diringer MN, Videen TO, Yundt K, Zazulia AR, Aiyagari V, Dacey RG Jr, Grubb RL, Powers WJ. Regional cerebrovascular and metabolic effects of hyperventilation after severe traumatic brain injury. J Neurosurg. 2002;96(1):103–8. https://doi.org/10.3171/jns.2002.96.1.0103.
33. Muizelaar JP, van der Poel HG, Li ZC, Kontos HA, Levasseur JE. Pial arteriolar vessel diameter and CO2 reactivity during prolonged hyperventilation in the rabbit. J Neurosurg. 1988;69(6):923–7. https://doi.org/10.3171/jns.1988.69.6.0923.
34. Steiner LA, Balestreri M, Johnston AJ, Czosnyka M, Coles JP, Chatfield DA, Smielewski P, Pickard JD, Menon DK. Sustained moderate reductions in arterial CO2 after brain trauma time-course of cerebral blood flow velocity and intracranial pressure. Intensive Care Med. 2004;30(12):2180–7. https://doi.org/10.1007/s00134-004-2463-6.
35. Petridis AK, Doukas A, Kienke S, Maslehaty H, Mahvash M, Barth H, Mehdorn HM. The effect of lung-protective permissive hypercapnia in intracerebral pressure in patients with subarachnoid haemorrhage and ARDS. A retrospective study. Acta Neurochir. 2010;152(12):2143–5. https://doi.org/10.1007/s00701-010-0761-z.
36. Rosenfeld JV, Maas AI, Bragge P, Morganti-Kossmann MC, Manley GT, Gruen RL. Early management of severe traumatic brain injury. Lancet. 2012;380(9847):1088–98. https://doi.org/10.1016/s0140-6736(12)60864-2.
37. Longhi L, Pagan F, Valeriani V, Magnoni S, Zanier ER, Conte V, Branca V, Stocchetti N. Monitoring brain tissue oxygen tension in brain-injured patients reveals hypoxic episodes in normal-appearing and in peri-focal tissue. Intensive Care Med. 2007;33(12):2136–42. https://doi.org/10.1007/s00134-007-0845-2.
38. Quintard H, Patet C, Suys T, Marques-Vidal P, Oddo M. Normobaric hyperoxia is associated with increased cerebral excitotoxicity after severe traumatic brain injury. Neurocrit Care. 2015;22(2):243–50. https://doi.org/10.1007/s12028-014-0062-0.
39. Wang HE, Prince DK, Drennan IR, Grunau B, Carlbom DJ, Johnson N, Hansen M, Elmer J, Christenson J, Kudenchuk P, Aufderheide T, Weisfeldt M, Idris A, Trzeciak S, Kurz M, Rittenberger JC, Griffiths D, Jasti J, May S. Post-resuscitation arterial oxygen and carbon dioxide and outcomes after out-of-hospital cardiac arrest. Resuscitation. 2017;120:113–8. https://doi.org/10.1016/j.resuscitation.2017.08.244.

40. Slutsky AS, Ranieri VM. Ventilator-induced lung injury. N Engl J Med. 2013;369(22):2126–36. https://doi.org/10.1056/NEJMra1208707.
41. Guay J, Ochroch EA, Kopp S. Intraoperative use of low volume ventilation to decrease postoperative mortality, mechanical ventilation, lengths of stay and lung injury in adults without acute lung injury. Cochrane Database Syst Rev. 2018;7:Cd011151. https://doi.org/10.1002/14651858.CD011151.pub3.
42. Roquilly A, Cinotti R, Jaber S, Vourc'h M, Pengam F, Mahe PJ, Lakhal K, Demeure Dit Latte D, Rondeau N, Loutrel O, Paulus J, Rozec B, Blanloeil Y, Vibet MA, Sebille V, Feuillet F, Asehnoune K. Implementation of an evidence-based extubation readiness bundle in 499 brain-injured patients. A before-after evaluation of a quality improvement project. Am J Respir Crit Care Med. 2013;188(8):958–66. https://doi.org/10.1164/rccm.201301-0116OC.
43. Asehnoune K, Mrozek S, Perrigault PF, Seguin P, Dahyot-Fizelier C, Lasocki S, Pujol A, Martin M, Chabanne R, Muller L, Hanouz JL, Hammad E, Rozec B, Kerforne T, Ichai C, Cinotti R, Geeraerts T, Elaroussi D, Pelosi P, Jaber S, Dalichampt M, Feuillet F, Sebille V, Roquilly A. A multi-faceted strategy to reduce ventilation-associated mortality in brain-injured patients. The BI-VILI project: a nationwide quality improvement project. Intensive Care Med. 2017;43(7):957–70. https://doi.org/10.1007/s00134-017-4764-6.
44. Apuzzo JL, Wiess MH, Petersons V, Small RB, Kurze T, Heiden JS. Effect of positive end expiratory pressure ventilation on intracranial pressure in man. J Neurosurg. 1977;46(2):227–32. https://doi.org/10.3171/jns.1977.46.2.0227.
45. Cooper KR, Boswell PA, Choi SC. Safe use of PEEP in patients with severe head injury. J Neurosurg. 1985;63(4):552–5. https://doi.org/10.3171/jns.1985.63.4.0552.
46. Cunitz G, Danhauser I, Gruss P. Change of intracranial pressure in neurosurgical patients by hyperventilation, positive negative pressure ventilation and PEEP (author's transl). Anaesthesist. 1979;28(3):142–51.
47. Lima WA, Campelo AR, Gomes RL, Brandao DC. The impact of positive end-expiratory pressure on cerebral perfusion pressure in adult patients with hemorrhagic stroke. Rev Bras Ter Intensiva. 2011;23(3):291–6.
48. Lodrini S, Montolivo M, Pluchino F, Borroni V. Positive end-expiratory pressure in supine and sitting positions: its effects on intrathoracic and intracranial pressures. Neurosurgery. 1989;24(6):873–7.
49. Ludwig HC, Klingler M, Timmermann A, Weyland W, Mursch K, Reparon C, Markakis E. The influence of airway pressure changes on intracranial pressure (ICP) and the blood flow velocity in the middle cerebral artery (VMCA). Anasthesiol Intensivmed Notfallmed Schmerzther. 2000;35(3):141–5. https://doi.org/10.1055/s-2000-13008.
50. Muench E, Bauhuf C, Roth H, Horn P, Phillips M, Marquetant N, Quintel M, Vajkoczy P. Effects of positive end-expiratory pressure on regional cerebral blood flow, intracranial pressure, and brain tissue oxygenation. Crit Care Med. 2005;33(10):2367–72.
51. Shapiro HM, Marshall LF. Intracranial pressure responses to PEEP in head-injured patients. J Trauma. 1978;18(4):254–6.
52. Videtta W, Villarejo F, Cohen M, Domeniconi G, Santa Cruz R, Pinillos O, Rios F, Maskin B. Effects of positive end-expiratory pressure on intracranial pressure and cerebral perfusion pressure. Acta Neurochir Suppl. 2002;81:93–7.
53. Frost EA. Effects of positive end-expiratory pressure on intracranial pressure and compliance in brain-injured patients. J Neurosurg. 1977;47(2):195–200. https://doi.org/10.3171/jns.1977.47.2.0195.
54. Martinez-Perez M, Bernabe F, Pena R, Fernandez R, Nahum A, Blanch L. Effects of expiratory tracheal gas insufflation in patients with severe head trauma and acute lung injury. Intensive Care Med. 2004;30(11):2021–7. https://doi.org/10.1007/s00134-004-2439-6.
55. Nemer SN, Caldeira JB, Santos RG, Guimaraes BL, Garcia JM, Prado D, Silva RT, Azeredo LM, Faria ER, Souza PC. Effects of positive end-expiratory pressure on brain tissue oxygen pressure of severe traumatic brain injury patients with acute respiratory distress syndrome: a pilot study. J Crit Care. 2015;30(6):1263–6. https://doi.org/10.1016/j.jcrc.2015.07.019.

56. Pulitano S, Mancino A, Pietrini D, Piastra M, De Rosa S, Tosi F, De Luca D, Conti G. Effects of positive end expiratory pressure (PEEP) on intracranial and cerebral perfusion pressure in pediatric neurosurgical patients. J Neurosurg Anesthesiol. 2013;25(3):330–4. https://doi.org/10.1097/ANA.0b013e31828bac4d.
57. Solodov AA, Petrikov SS, Krylov VV. Positive end-expiratory pressure (PEEP) influences on intracranial pressure, systemic hemodynamics and pulmonary gas exchange in patients with intracranial hemorrhage in critical state. Anesteziol Reanimatol. 2016;61(2):115–20.
58. Georgiadis D, Schwarz S, Baumgartner RW, Veltkamp R, Schwab S. Influence of positive end-expiratory pressure on intracranial pressure and cerebral perfusion pressure in patients with acute stroke. Stroke. 2001;32(9):2088–92.
59. Taccone FS, Baar I, De Deyne C, Druwe P, Legros B, Meyfroidt G, Ossemann M, Gaspard N. Neuroprognostication after adult cardiac arrest treated with targeted temperature management: task force for Belgian recommendations. Acta Neurol Belg. 2017;117(1):3–15. https://doi.org/10.1007/s13760-017-0755-1.
60. Carteron L, Taccone FS, Oddo M. How to manage blood pressure after brain injury? Minerva Anestesiol. 2017;83(4):412–21. https://doi.org/10.23736/s0375-9393.16.11696-7.
61. Buitrago Blanco MM, Prashant GN, Vespa PM. Cerebral metabolism and the role of glucose control in acute traumatic brain injury. Neurosurg Clin N Am. 2016;27(4):453–63. https://doi.org/10.1016/j.nec.2016.05.003.
62. Le Roux P. Invasive neurological and multimodality monitoring in the neuroICU. In: Layon JA, Gabrielli A, Friedman WA, editors. Textbook of Neurointensive care. 2nd ed. London: Springer; 2013. p. 127–45.
63. Toung TJ, Miyabe M, McShane AJ, Rogers MC, Traystman RJ. Effect of PEEP and jugular venous compression on canine cerebral blood flow and oxygen consumption in the head elevated position. Anesthesiology. 1988;68(1):53–8.
64. Walfisch S, Weksler N, Fisher A, Shapira Y. Effects of oleic acid lung injury and positive end-expiratory pressure on central hemodynamics and regional blood flow. Isr J Med Sci. 1997;33(1):14–7.
65. Doblar DD, Santiago TV, Kahn AU, Edelman NH. The effect of positive end-expiratory pressure ventilation (PEEP) on cerebral blood flow and cerebrospinal fluid pressure in goats. Anesthesiology. 1981;55(3):244–50.
66. Coplin WM, Pierson DJ, Cooley KD, Newell DW, Rubenfeld GD. Implications of extubation delay in brain-injured patients meeting standard weaning criteria. Am J Respir Crit Care Med. 2000;161(5):1530–6. https://doi.org/10.1164/ajrccm.161.5.9905102.
67. Navalesi P, Frigerio P, Moretti MP, Sommariva M, Vesconi S, Baiardi P, Levati A. Rate of reintubation in mechanically ventilated neurosurgical and neurologic patients: evaluation of a systematic approach to weaning and extubation. Crit Care Med. 2008;36(11):2986–92. https://doi.org/10.1097/CCM.0b013e31818b35f2.
68. Namen AM, Ely EW, Tatter SB, Case LD, Lucia MA, Smith A, Landry S, Wilson JA, Glazier SS, Branch CL, Kelly DL, Bowton DL, Haponik EF. Predictors of successful extubation in neurosurgical patients. Am J Respir Crit Care Med. 2001;163(3 Pt 1):658–64. https://doi.org/10.1164/ajrccm.163.3.2003060.
69. Cinotti R, Bouras M, Roquilly A, Asehnoune K. Management and weaning from mechanical ventilation in neurologic patients. Ann Transl Med. 2018;6(19):381. https://doi.org/10.21037/atm.2018.08.16.
70. Stevens RD, Lazaridis C, Chalela JA. The role of mechanical ventilation in acute brain injury. Neurol Clin. 2008;26(2):543–63. https://doi.org/10.1016/j.ncl.2008.03.014.
71. Alali AS, Scales DC, Fowler RA, Mainprize TG, Ray JG, Kiss A, de Mestral C, Nathens AB. Tracheostomy timing in traumatic brain injury: a propensity-matched cohort study. J Trauma Acute Care Surg. 2014;76(1):70–6; discussion 76–78. https://doi.org/10.1097/TA.0b013e3182a8fd6a.
72. Shibahashi K, Sugiyama K, Houda H, Takasu Y, Hamabe Y, Morita A. The effect of tracheostomy performed within 72 h after traumatic brain injury. Br J Neurosurg. 2017;31(5):564–8. https://doi.org/10.1080/02688697.2017.1302071.

73. Hyde GA, Savage SA, Zarzaur BL, Hart-Hyde JE, Schaefer CB, Croce MA, Fabian TC. Early tracheostomy in trauma patients saves time and money. Injury. 2015;46(1):110–4. https://doi.org/10.1016/j.injury.2014.08.049.
74. Bosel J, Schiller P, Hook Y, Andes M, Neumann JO, Poli S, Amiri H, Schonenberger S, Peng Z, Unterberg A, Hacke W, Steiner T. Stroke-related early tracheostomy versus prolonged orotracheal intubation in neurocritical care trial (SETPOINT): a randomized pilot trial. Stroke. 2013;44(1):21–8. https://doi.org/10.1161/strokeaha.112.669895.

Chapter 11
Ventilator-Induced Diaphragm Dysfunction

Hong-Liang Li

11.1 Definition and Brief History

It was Vassilakopoulos and Petrof who first proposed the concept of ventilator-induced diaphragm dysfunction (VIDD) in 2004, which refers to the loss of diaphragmatic force-generating capacity that is specifically related to the use of mechanical ventilation [1]. As early as 1988, it has been recognized that the phenomenon of diaphragm atrophy or failure of normal growth in ventilated neonates, which may contribute to difficulties in weaning [2]. In 1994, the loss of diaphragm mass and a large reduction in maximal diaphragmatic-specific force production induced by 48 h of controlled mechanical ventilation (MV) were documented in rodent study [3] and supported by the following primate study, which also showed the decrease of diaphragmatic endurance [4].

Although the numerous animal studies indicated that MV promotes VIDD repeatedly, it was highlighted until 2008, Levine has first shown the evidence of rapid disuse atrophy of diaphragm fibers in human beings with prolonged MV [5]. Great efforts have been put in to explore the mechanisms responsible for VIDD and trying to identify the biological target for drug intervention, all of which promote the birth of the strategy of diaphragm-protective mechanical ventilation.

11.2 Anatomy of Diaphragm

The diaphragm is the musculotendinous boundary between the thoracic cavity and abdominal cavity, which is thin (2–3 mm in healthy adults), dome-shaped, and composed of two parts: noncontractile central tendon that separates the right and left

H.-L. Li (✉)
Department of Critical Care Medicine, Beijing Tiantan Hospital, Capital Medical University, Beijing, China

J. Zhou et al. (eds.), *Respiratory Monitoring in Mechanical Ventilation*,
https://doi.org/10.1007/978-981-15-9770-1_11

sides and extends to the dome of each hemidiaphragm, and the contracting muscle fibers: the costal and crural muscle groups, distinguished with each other in composition and function too. The costal muscle group is thin and forms the diaphragmatic leaflets, the contraction of fibers will lead to flattening of the diaphragm and lowers the ribs. Although the crural muscle groups are thicker, it contributes little to the displacement of the diaphragm. The continuation of the medial tendinous margins of the crura forms the median arcuate ligament anterior to the aortic hiatus. The aorta, inferior vena cava, thoracic duct, esophagus, vagus, and phrenic nerves, traverse the diaphragm through aortic, caval, and esophageal apertures separately.

The left and right sides of the diaphragm are innervated by the ipsilateral phrenic nerves, which originates from the anterior branches of the cervical spinal cord of segments 3–5 and traverses the neck and mediastinum before inserting into the diaphragm centrally. Each nerve divides into four trunks that innervate the anterolateral, posterolateral, sternal, and crural portions of the diaphragm on that side.

The outer rim of the diaphragmatic muscle is innervated laterally from the thoracic spinal cord of 7 through 12 and recently, the study found that the crural diaphragm also receives innervation from the vagus nerve [6]. In terms of blood supply, it mainly comes from the phrenic artery below and the pericardiophrenic arteries above the diaphragm.

About 55% of the diaphragm fibers are of the slow-twitch, oxidative type (highly resistant to fatigue), 25% are of the fast-twitch, oxidative glycolytic type (relatively resistant to fatigue), and the remaining 20% of the fibers are of the fast-twitch glycolytic variety (susceptible to fatigue) [7].

11.3 The Physiological Function of the Diaphragm

The respiratory system consists essentially of two vital parts: the gas exchanging organ (lung) and the pump that drive the ventilation (respiratory muscles). The diaphragm plays an important role in respiratory mechanics. As the most powerful of the respiratory muscles, the diaphragm performs up to 75% of the work of breathing alone and assisted by accessory inspiratory muscles (e.g., scalene, parasternal portions of the internal and external intercostal muscles, and sternomastoids). The simultaneous contraction of inspiratory muscles elevates and expands the upper ribcage, increasing negative intrapleural pressure, and driving air into the lungs. Apart from the role of the respiratory pump, the diaphragm also serves as a mechanical barrier between the abdominal and thoracic cavities and maintains the pressure gradient between the cavities.

11.4 Ventilator-Induced Diaphragm Dysfunction

Although mechanical ventilation is life-saving in respiratory failure supporting, prolonged ventilator use associated with difficult weaning. Among the variety of impact factors, diaphragm weakness is believed to be the leading cause [8].

Compared with assist modes that allow the respiratory muscles to remain active, controlled mechanical ventilation increases the risk of diaphragm dysfunction by abolishing the effort of inspiration. We will discuss the two most important reasons: ventilator-induced diaphragm atrophy and contractile dysfunction in the following.

11.5 Ventilator-Induced Diaphragm Atrophy and Responsible Mechanisms

Numerous animal and human experiments consistently demonstrate that prolonged MV promotes a reduction in diaphragm mass, a surrogate of diaphragm atrophy. With high anatomy and fiber type composition similar to human beings, the rat is selected as the most frequently used animal model to study VIDD. Studies showed that 10–15% reduction in the cross-sectional area of rat diaphragm fiber types (specifically, type I, type IIa, and type IIx/b) happened, even as less as 12 h with fully controlled ventilation mode [9, 10], and 30% reduction following 18–24 h of prolonged ventilatory support [11, 12].

In human studies, Levine demonstrated that 18–69 h of fully controlled MV results in the magnitude of diaphragmatic atrophy (about 50% reduction in fiber cross-sectional area) of both type I (slow) and type II (fast) muscle fibers in the costal diaphragm. This finding was confirmed by the following studies, not only limited in controlled ventilation [13] but also in partial support mode [14]. On average, a rate of 6% loss of diaphragm thickness per ventilated day was detected [14].

Keeping the balance of protein degradation and synthesis is the basis of maintaining skeletal muscle fiber size. During controlled MV, increased proteolysis and depressed protein synthesis developed rapidly in the diaphragm fibers, all of which contribute to the net loss of protein and diaphragm fiber atrophy [15, 16].

11.6 Decrease of Protein Diaphragmatic Synthesis

In rat studies, controlled MV promotes a rapid decrease of diaphragmatic protein synthesis, both mixed and myosin heavy chain [16, 17]. On the contrary, partial support ventilation does not promote a significant decrease in diaphragm protein synthesis compared with spontaneous breathing [17]. We have known that keeping the skeletal muscle contractile activity is essential to maintain protein synthesis. During the controlled MV, the initial decrease of diaphragm protein synthesis was likely caused by decreased protein translation, which enrolled the Akt/mammalian target of rapamycin (mTOR) signaling pathway [18].

11.7 Increase of Diaphragmatic Proteolysis

It is reasonable to speculate that increased proteolysis, other than decreased protein synthesis, is responsible for the rapid diaphragm atrophy which occurs as early as 12 h after controlled MV. The increased activity of four major proteolytic systems was well demonstrated, i.e., macroautophagy (autophagy), calpains, caspase-3, and the ubiquitin-proteasome system [19]. In partial support MV, conflicting results in limited studies may be originated from the differences in the levels of ventilatory support [17, 20].

Compelling evidence confirmed that reactive oxygen species (ROS) induced by MV is responsible for the activation of the key protease, and the dominating site of oxidant production is the mitochondrion [10, 21]. Oxidative stress could promote the increase of gene expression of key proteins involved in both autophagy and the ubiquitin-proteasome system, increase the activity of 20S proteasome, calpain, and caspase-3 in the diaphragm. Oxidative modification of myofibrillar proteins further increases their susceptibility to proteolytic degradation [22] (Fig. 11.1). However, the theory of oxidative stress was seriously challenged with negative evidence from biopsies [23].

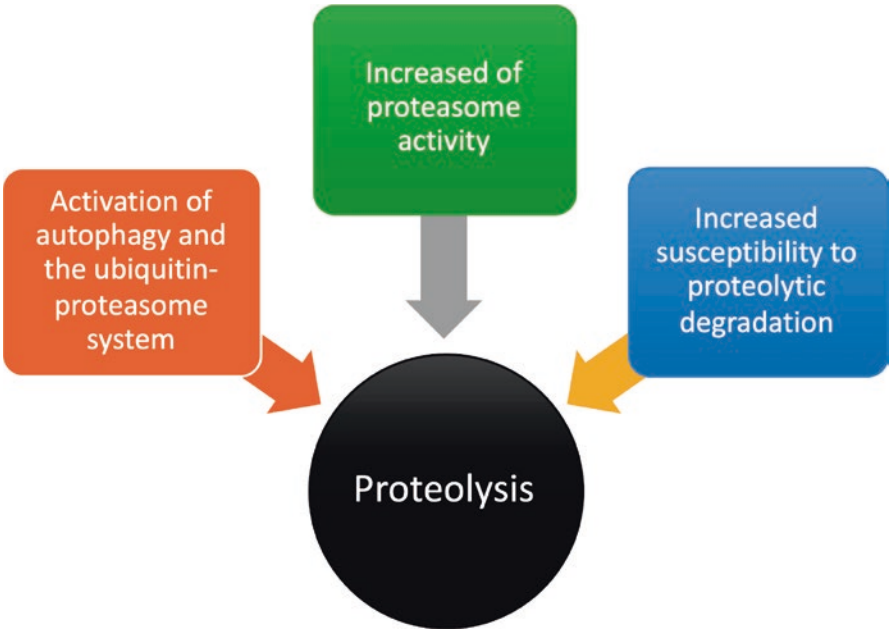

Fig. 11.1 The mechanisms responsible for the increased proteolysis and diaphragm atrophy mediated by reactive oxygen species (ROS)

Pharmacological inhibition of calpain and caspase-3 activity in rats decreases the rate of proteolysis and offers protection against MV-induced diaphragmatic atrophy [24, 25], and there is a regulatory cross-talk between calpain and caspase-3 activity [25]. It is promising for medication therapy in diaphragm protection during MV.

11.8 Ventilator-Induced Diaphragm Contractile Dysfunction and Responsible Mechanisms

Not only the atrophy but also the contractile dysfunction is prevalent in diaphragm with prolonged MV, which only occurs at the level of the peripheral muscle, independent with the phrenic nerve conduction and neuromuscular transmission [26]. This reduction of maximal diaphragmatic-specific force production is rapid and time-dependent, about 15–20% with 12 h, and 50% with 48 h of controlled MV [3, 27]. This could be alleviated by keeping spontaneous breathing during controlled MV [28], ventilated with assisted modes [29, 30], or short periods of bilateral phrenic nerve stimulation (10 min/h) [31].

Aging, neuromuscular blockers, and/or glucocorticoids are independent risk factors of diaphragm dysfunction. Particularly in severe ARDS patients, nondepolarizing neuromuscular-blocking agents are commonly used to minimize patient agitation, improve ventilator-patient asynchrony, and reduce oxygen consumption. Both skeletal muscle and diaphragm weakness are anticipated and confirmed [32, 33]. Corticosteroids are useful in treating lung underlying disease or inflammation; however, steroid-induced myopathy of both limb muscles and respiratory were well documented [34, 35]. Conflicting results still exist in terms of VIDD, and it is unclear whether the species or mode of MV selected were responsible for this difference [36, 37].

The basic functional element of diaphragm muscle fibers is the sarcomere, and the fundamental unit to generate force production is the interaction between the sarcomeric proteins (actin and myosin). The relationship between cytosolic free calcium, cross-bridge attachment/cross-bridge cycling rate, and sarcomere length determined the mechanical properties of diaphragm muscle fibers [38]. Although the precise mechanisms responsible for diaphragm contractile dysfunction caused by MV remains unclear, oxidative stress, by decreasing calcium sensitivity [39], or promote calpain activation [21], combined with the loss of myosin heavy chain protein [40], contribute to the damage of sarcomere structure. There is a linear relationship between the prevalence of the ultrastructure damage and the time on the ventilator. Studies shown that the average magnitude of sarcomeric injury varied from 10% of the total fiber area for patients ventilated 24 h, to 20% for ventilated 50 h, and 30–80% for ventilated 100–249 h [13].

11.9 Other Mechanisms Responsible for VIDD

Although the disuse atrophy caused by the suppression of inspiratory effort is the main culprit, other mechanisms may contribute to VIDD either. Concentric or eccentric load-induced injury, which refers to the acute diaphragm injury, inflammation, and weakness, occurs when the diaphragm contract against excessive load during muscular shorting or lengthening [41–45] and heightened in the existence of sepsis and systemic inflammation.

During the ventilation of patients with acute exacerbation of the chronic obstructive pulmonary disease, insufficient assist expose diaphragm to the high load and induce a rapid rise in diaphragm thickness, which believed to be a unique form of injury (i.e., inflammation and fiber swelling), instead of the reflection of hypertrophy. In patients with decreased end-expiratory lung volume (EELV) and atelectasis, the diaphragm contract during expiration trying to maintain lung volume, also known as "expiratory braking" [46]. In the case of certain types of patient-ventilator asynchronies, such as ineffective efforts, reverse triggering, and premature cycling, the diaphragm contracts even as lung volume decreases leading to eccentric myotrauma. Additionally, the fiber length was reduced with the application of positive end-expiratory pressure (PEEP). Decreased PEEP level abruptly such as withdrawn from ventilator may lead to the diaphragm overstretched and impaired its performance [47, 48].

11.10 VIDD: Evidence for Impact on Patient Outcomes

Among the numerous etiologies, the depressed strength and endurance of diaphragm play a crucial role in difficult weaning. When critically ill patients were ready to extubate, 63% of them had diaphragm dysfunction, almost twice as frequently as limb muscle weakness [8]. Compared with the patients that are successfully weaned, the inspiratory muscle endurance, the maximal inspiratory pressure generation, and diaphragmatic contractile function decreased in patients that experience prolonged weaning [49–51]. Diaphragm weakness at the time of extubation increased the risk of ICU readmission and the risk of mortality within the year after ICU discharge [52, 53]. Diaphragm dysfunction should be suspected in the setting of difficult weaning or repeated episodes of respiratory failure. On the other hand, inspiratory muscle training helped the patients who failed repeated weaning attempts to remove from the ventilator successfully [54–56].

11.11 Diaphragm-Protective Mechanical Ventilation

The harmful effects of mechanical ventilation on the lungs are well recognized, and ventilator-induced lung injury (VILI) directly lead to the development of lung-protective ventilation strategies. After decades of research on ventilator-induced

diaphragm dysfunction, and deep understanding of the various potential mechanisms, Heunks proposed the concept of diaphragm-protective mechanical ventilation in 2018, highlight the priority of this new approach to ventilatory management [57].

Maintaining the appropriate level of inspiratory effort is paramount in the performance of diaphragm-protective mechanical ventilation, by avoiding over- and under-assist combined with titrating the dose of sedatives carefully. This should be monitored and targeted as early as possible since the VIDD occurs within mere hours of initiating ventilation. Partial support modes (e.g., pressure support, neutrally adjusted ventilatory assist, proportional assist), other than controlled modes, may help to alleviate disuse atrophy; however, insufficient assist should be avoided.

Unfortunately, the optimal effort level to prevent VIDD remains unclear. A relatively low effort similar to the healthy breathing at rest is recommended since both excessive and insufficient levels of effort lead diaphragm to fatigue and successful weaning patients exhibit inspiratory effort levels in the resting range [58] (Fig. 11.2). The study illustrated that the thickening fraction of 15–30% (similar to healthy status at rest) during the first 3 days of ventilation had stable diaphragm thickness and the shortest duration of ventilation [59].

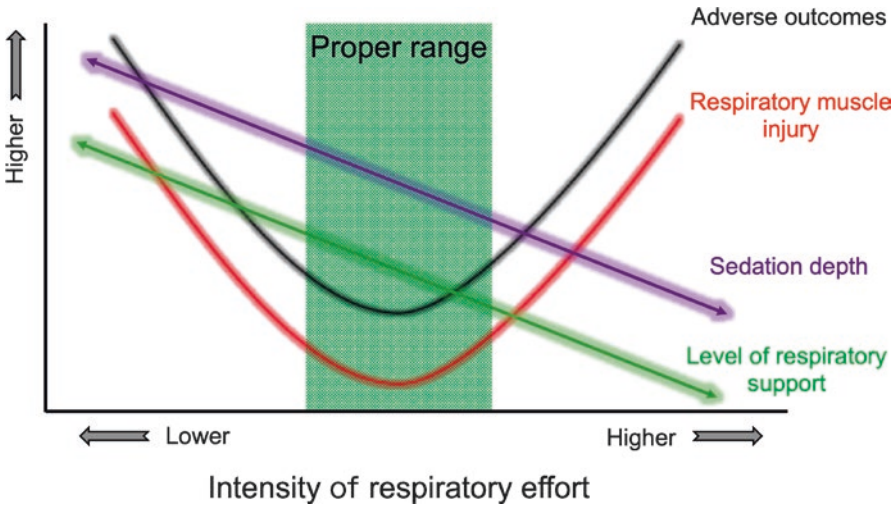

Fig. 11.2 The rationale to perform diaphragm-protective ventilation in clinical ventilator management

11.12 Monitoring Tools in the Diaphragm-Protective Mechanical Ventilation

Until now, limited methodologies to monitor the diaphragm thickness, electricity, and function are available, and a brief description of these techniques follows.

Airway occlusion pressure, $P_{0.1}$ or maximum negative inspiratory pressure, is highly reliable to evaluate the respiratory drive and is easy to acquire by the performance of expiratory hold on the ventilator. For technical details please refer Chap. 2.

Esophageal manometry is the gold-standard method to measure esophageal or transdiaphragmatic pressure, which offers continuous, less invasive, and direct measurement of inspiratory effort. The accuracy and reliability rely on the correct placement of the balloon catheter and expertise in data interpretation. Theoretical and empirical considerations favor targeting the esophageal pressure of 5–10 cm H2O [58]. For technical details please refer Chap. 2.

Diaphragm ultrasound permits imaging of diaphragm thickness with a linear high-frequency probe at the bedside. The thickening fraction is the percentage increase in thickness during inspiration, which is a good noninvasive parameter to evaluate diaphragm contractile effort [60], and around 40% should be achieved. Intermittent instead of continuous monitoring is the drawback of this technique; however, offset by the advantage of easy to manipulate and instruments widely available. For technical details please refer Chap. 3.

The electrical activity of the diaphragm (Edi) is a surrogate parameter to monitor the performance of diaphragm, by acquiring signals from the nasogastric catheter mounted with surface electrodes [61]. The normal values have not been established since there is a big variance of Edi values individually. 8% of maximum Edi may be an appropriate target for the specific patients [62]. For technical details please refer Chap. 2.

11.13 Summary

Mechanical ventilation results in diaphragm atrophy and contractile dysfunction, with a rapid and time-dependent fashion. Damage of diaphragmatic fiber architecture, impaired mitochondrial respiration, oxidative damage of diaphragmatic proteins and lipids, decreased protein synthesis, and activation of the proteolytic system are responsible for the occurrence of VIDD. It is a novel approach to initiate the diaphragm-protective ventilation strategy, with the potential to substantially improve patient outcomes. Meticulous titrate ventilator settings to avoid both excessive and insufficient inspiratory effort with appropriate monitoring is encouraged in clinical mechanical ventilation management.

References

1. Vassilakopoulos T, Petrof BJ. Ventilator-induced diaphragmatic dysfunction. Am J Respir Crit Care Med. 2004;169(3):336–41.
2. Knisely AS, Leal SM, Singer DB. Abnormalities of diaphragmatic muscle in neonates with ventilated lungs. J Pediatr. 1988;113(6):1074–7.
3. Le Bourdelles G, Viires N, Boczkowski J, Seta N, Pavlovic D, Aubier M. Effects of mechanical ventilation on diaphragmatic contractile properties in rats. Am J Respir Crit Care Med. 1994;149(6):1539–44.
4. Anzueto A, Peters JI, Tobin MJ, de los Santos R, Seidenfeld JJ, Moore G, Cox WJ, Coalson JJ. Effects of prolonged controlled mechanical ventilation on diaphragmatic function in healthy adult baboons. Crit Care Med. 1997;25(7):1187–90.
5. Levine S, Nguyen T, Taylor N, Friscia ME, Budak MT, Rothenberg P, Zhu J, Sachdeva R, Sonnad S, Kaiser LR, et al. Rapid disuse atrophy of diaphragm fibers in mechanically ventilated humans. N Engl J Med. 2008;358(13):1327–35.
6. Young RL, Page AJ, Cooper NJ, Frisby CL, Blackshaw LA. Sensory and motor innervation of the crural diaphragm by the vagus nerves. Gastroenterology. 2010;138(3):1091–101.
7. Rochester DF. The diaphragm: contractile properties and fatigue. J Clin Invest. 1985;75(5):1397–402.
8. Dres M, Dube BP, Mayaux J, Delemazure J, Reuter D, Brochard L, Similowski T, Demoule A. Coexistence and impact of limb muscle and diaphragm weakness at time of liberation from mechanical ventilation in medical intensive care unit patients. Am J Respir Crit Care Med. 2017;195(1):57–66.
9. Smuder AJ, Min K, Hudson MB, Kavazis AN, Kwon OS, Nelson WB, Powers SK. Endurance exercise attenuates ventilator-induced diaphragm dysfunction. J Appl Physiol (Bethesda, MD1985). 2012;112(3):501–10.
10. Powers SK, Hudson MB, Nelson WB, Talbert EE, Min K, Szeto HH, Kavazis AN, Smuder AJ. Mitochondria-targeted antioxidants protect against mechanical ventilation-induced diaphragm weakness. Crit Care Med. 2011;39(7):1749–59.
11. Gayan-Ramirez G, De Paepe K, Cadot P, Decramer M. Detrimental effects of short-term mechanical ventilation on diaphragm function and IGF-I mRNA in rats. Intensive Care Med. 2003;29(5):825–33.
12. Shanely RA, Zergeroglu MA, Lennon SL, Sugiura T, Yimlamai T, Enns D, Belcastro A, Powers SK. Mechanical ventilation-induced diaphragmatic atrophy is associated with oxidative injury and increased proteolytic activity. Am J Respir Crit Care Med. 2002;166(10):1369–74.
13. Jaber S, Petrof BJ, Jung B, Chanques G, Berthet JP, Rabuel C, Bouyabrine H, Courouble P, Koechlin-Ramonatxo C, Sebbane M, et al. Rapidly progressive diaphragmatic weakness and injury during mechanical ventilation in humans. Am J Respir Crit Care Med. 2011;183(3):364–71.
14. Grosu HB, Lee YI, Lee J, Eden E, Eikermann M, Rose KM. Diaphragm muscle thinning in patients who are mechanically ventilated. Chest. 2012;142(6):1455–60.
15. Powers SK, Kavazis AN, Levine S. Prolonged mechanical ventilation alters diaphragmatic structure and function. Crit Care Med. 2009;37(10 Suppl):S347–53.
16. Shanely RA, Van Gammeren D, Deruisseau KC, Zergeroglu AM, McKenzie MJ, Yarasheski KE, Powers SK. Mechanical ventilation depresses protein synthesis in the rat diaphragm. Am J Respir Crit Care Med. 2004;170(9):994–9.
17. Futier E, Constantin JM, Combaret L, Mosoni L, Roszyk L, Sapin V, Attaix D, Jung B, Jaber S, Bazin JE. Pressure support ventilation attenuates ventilator-induced protein modifications in the diaphragm. Crit Care (London, England). 2008;12(5):R116.
18. Bodine SC, Stitt TN, Gonzalez M, Kline WO, Stover GL, Bauerlein R, Zlotchenko E, Scrimgeour A, Lawrence JC, Glass DJ, et al. Akt/mTOR pathway is a crucial regulator of skeletal muscle hypertrophy and can prevent muscle atrophy in vivo. Nat Cell Biol. 2001;3(11):1014–9.

19. Powers SK, Wiggs MP, Sollanek KJ, Smuder AJ. Ventilator-induced diaphragm dysfunction: cause and effect. Am J Physiol Regul Integr Comp Physiol. 2013;305(5):R464–77.
20. Hudson MB, Smuder AJ, Nelson WB, Bruells CS, Levine S, Powers SK. Both high level pressure support ventilation and controlled mechanical ventilation induce diaphragm dysfunction and atrophy. Crit Care Med. 2012;40(4):1254–60.
21. Whidden MA, McClung JM, Falk DJ, Hudson MB, Smuder AJ, Nelson WB, Powers SK. Xanthine oxidase contributes to mechanical ventilation-induced diaphragmatic oxidative stress and contractile dysfunction. J Appl Physiol (Bethesda, MD: 1985). 2009;106(2):385–94.
22. Smuder AJ, Kavazis AN, Hudson MB, Nelson WB, Powers SK. Oxidation enhances myofibrillar protein degradation via calpain and caspase-3. Free Radic Biol Med. 2010;49(7):1152–60.
23. van den Berg M, Hooijman PE, Beishuizen A, de Waard MC, Paul MA, Hartemink KJ, van Hees HWH, Lawlor MW, Brocca L, Bottinelli R, et al. Diaphragm atrophy and weakness in the absence of mitochondrial dysfunction in the critically ill. Am J Respir Crit Care Med. 2017;196(12):1544–58.
24. McClung JM, Kavazis AN, DeRuisseau KC, Falk DJ, Deering MA, Lee Y, Sugiura T, Powers SK. Caspase-3 regulation of diaphragm myonuclear domain during mechanical ventilation-induced atrophy. Am J Respir Crit Care Med. 2007;175(2):150–9.
25. Nelson WB, Smuder AJ, Hudson MB, Talbert EE, Powers SK. Cross-talk between the calpain and caspase-3 proteolytic systems in the diaphragm during prolonged mechanical ventilation. Crit Care Med. 2012;40(6):1857–63.
26. Radell PJ, Remahl S, Nichols DG, Eriksson LI. Effects of prolonged mechanical ventilation and inactivity on piglet diaphragm function. Intensive Care Med. 2002;28(3):358–64.
27. Powers SK, Shanely RA, Coombes JS, Koesterer TJ, McKenzie M, Van Gammeren D, Cicale M, Dodd SL. Mechanical ventilation results in progressive contractile dysfunction in the diaphragm. J Appl Physiol (Bethesda, MD: 1985). 2002;92(5):1851–8.
28. Sassoon CS, Zhu E, Caiozzo VJ. Assist-control mechanical ventilation attenuates ventilator-induced diaphragmatic dysfunction. Am J Respir Crit Care Med. 2004;170(6):626–32.
29. Jung B, Constantin JM, Rossel N, Le Goff C, Sebbane M, Coisel Y, Chanques G, Futier E, Hugon G, Capdevila X, et al. Adaptive support ventilation prevents ventilator-induced diaphragmatic dysfunction in piglet: an in vivo and in vitro study. Anesthesiology. 2010;112(6):1435–43.
30. Gayan-Ramirez G, Testelmans D, Maes K, Racz GZ, Cadot P, Zador E, Wuytack F, Decramer M. Intermittent spontaneous breathing protects the rat diaphragm from mechanical ventilation effects. Crit Care Med. 2005;33(12):2804–9.
31. Yang M, Wang H, Han G, Chen L, Huang L, Jiang J, Li S. Phrenic nerve stimulation protects against mechanical ventilation-induced diaphragm dysfunction in rats. Muscle Nerve. 2013;48(6):958–62.
32. Testelmans D, Maes K, Wouters P, Gosselin N, Deruisseau K, Powers S, Sciot R, Decramer M, Gayan-Ramirez G. Rocuronium exacerbates mechanical ventilation-induced diaphragm dysfunction in rats. Crit Care Med. 2006;34(12):3018–23.
33. Testelmans D, Maes K, Wouters P, Powers SK, Decramer M, Gayan-Ramirez G. Infusions of rocuronium and cisatracurium exert different effects on rat diaphragm function. Intensive Care Med. 2007;33(5):872–9.
34. Sassoon CS, Zhu E, Pham HT, Nelson RS, Fang L, Baker MJ, Caiozzo VJ. Acute effects of high-dose methylprednisolone on diaphragm muscle function. Muscle Nerve. 2008;38(3):1161–72.
35. Lieu FK, Powers SK, Herb RA, Criswell D, Martin D, Wood C, Stainsby W, Chen CL. Exercise and glucocorticoid-induced diaphragmatic myopathy. J Appl Physiol (Bethesda, MD: 1985). 1993;75(2):763–71.
36. Sassoon CS, Zhu E, Fang L, Ramar K, Jiao GY, Caiozzo VJ. Interactive effects of corticosteroid and mechanical ventilation on diaphragm muscle function. Muscle Nerve. 2011;43(1):103–11.
37. Maes K, Agten A, Smuder A, Powers SK, Decramer M, Gayan-Ramirez G. Corticosteroid effects on ventilator-induced diaphragm dysfunction in anesthetized rats depend on the dose administered. Respir Res. 2010;11:178.
38. Edman KA. Contractile performance of striated muscle. Adv Exp Med Biol. 2010;682:7–40.

39. Ochala J, Radell PJ, Eriksson LI, Larsson L. EMD 57033 partially reverses ventilator-induced diaphragm muscle fibre calcium desensitisation. Pflugers Arch. 2010;459(3):475–83.
40. van Hees HW, Schellekens WJ, Andrade Acuna GL, Linkels M, Hafmans T, Ottenheijm CA, Granzier HL, Scheffer GJ, van der Hoeven JG, Dekhuijzen PN, et al. Titin and diaphragm dysfunction in mechanically ventilated rats. Intensive Care Med. 2012;38(4):702–9.
41. Orozco-Levi M, Lloreta J, Minguella J, Serrano S, Broquetas JM, Gea J. Injury of the human diaphragm associated with exertion and chronic obstructive pulmonary disease. Am J Respir Crit Care Med. 2001;164(9):1734–9.
42. Jiang TX, Reid WD, Belcastro A, Road JD. Load dependence of secondary diaphragm inflammation and injury after acute inspiratory loading. Am J Respir Crit Care Med. 1998;157(1):230–6.
43. Hillas G, Perlikos F, Toumpanakis D, Litsiou E, Nikolakopoulou S, Sagris K, Vassilakopoulos T. Controlled mechanical ventilation attenuates the systemic inflammation of severe chronic obstructive pulmonary disease exacerbations. Am J Respir Crit Care Med. 2016;193(6):696–8.
44. Proske U, Morgan DL. Muscle damage from eccentric exercise: mechanism, mechanical signs, adaptation and clinical applications. J Physiol. 2001;537(Pt 2):333–45.
45. Gea J, Zhu E, Galdiz JB, Comtois N, Salazkin I, Fiz JA, Grassino A. Functional consequences of eccentric contractions of the diaphragm. Arch Bronconeumol. 2009;45(2):68–74.
46. Pellegrini M, Hedenstierna G, Roneus A, Segelsjo M, Larsson A, Perchiazzi G. The diaphragm acts as a brake during expiration to prevent lung collapse. Am J Respir Crit Care Med. 2017;195(12):1608–16.
47. Lindqvist J, van den Berg M, van der Pijl R, Hooijman PE, Beishuizen A, Elshof J, de Waard M, Girbes A, Spoelstra-de Man A, Shi ZH, et al. Positive end-expiratory pressure ventilation induces longitudinal atrophy in diaphragm fibers. Am J Respir Crit Care Med. 2018;198(4):472–85.
48. Gorman RB, McKenzie DK, Pride NB, Tolman JF, Gandevia SC. Diaphragm length during tidal breathing in patients with chronic obstructive pulmonary disease. Am J Respir Crit Care Med. 2002;166(11):1461–9.
49. Cader SA, de Souza Vale RG, Zamora VE, Costa CH, Dantas EH. Extubation process in bedridden elderly intensive care patients receiving inspiratory muscle training: a randomized clinical trial. Clin Interv Aging. 2012;7:437–43.
50. Cader SA, Vale RG, Castro JC, Bacelar SC, Biehl C, Gomes MC, Cabrer WE, Dantas EH. Inspiratory muscle training improves maximal inspiratory pressure and may assist weaning in older intubated patients: a randomised trial. J Physiother. 2010;56(3):171–7.
51. Chang AT, Boots RJ, Brown MG, Paratz J, Hodges PW. Reduced inspiratory muscle endurance following successful weaning from prolonged mechanical ventilation. Chest. 2005;128(2):553–9.
52. Adler D, Dupuis-Lozeron E, Richard JC, Janssens JP, Brochard L. Does inspiratory muscle dysfunction predict readmission after intensive care unit discharge? Am J Respir Crit Care Med. 2014;190(3):347–50.
53. Medrinal C, Prieur G, Frenoy E, Robledo Quesada A, Poncet A, Bonnevie T, Gravier FE, Lamia B, Contal O. Respiratory weakness after mechanical ventilation is associated with one-year mortality—a prospective study. Crit Care (London, England). 2016;20(1):231.
54. Aldrich TK, Karpel JP, Uhrlass RM, Sparapani MA, Eramo D, Ferranti R. Weaning from mechanical ventilation: adjunctive use of inspiratory muscle resistive training. Crit Care Med. 1989;17(2):143–7.
55. Martin AD, Smith BK, Davenport PD, Harman E, Gonzalez-Rothi RJ, Baz M, Layon AJ, Banner MJ, Caruso LJ, Deoghare H, et al. Inspiratory muscle strength training improves weaning outcome in failure to wean patients: a randomized trial. Crit Care (London, England). 2011;15(2):R84.
56. Martin AD, Davenport PD, Franceschi AC, Harman E. Use of inspiratory muscle strength training to facilitate ventilator weaning: a series of 10 consecutive patients. Chest. 2002;122(1):192–6.

57. Heunks L, Ottenheijm C. Diaphragm-protective mechanical ventilation to improve outcomes in ICU patients? Am J Respir Crit Care Med. 2018;197(2):150–2.
58. Jubran A, Grant BJ, Laghi F, Parthasarathy S, Tobin MJ. Weaning prediction: esophageal pressure monitoring complements readiness testing. Am J Respir Crit Care Med. 2005;171(11):1252–9.
59. Goligher EC, Dres M, Fan E, Rubenfeld GD, Scales DC, Herridge MS, Vorona S, Sklar MC, Rittayamai N, Lanys A, et al. Mechanical ventilation-induced diaphragm atrophy strongly impacts clinical outcomes. Am J Respir Crit Care Med. 2018;197(2):204–13.
60. Vivier E, Mekontso Dessap A, Dimassi S, Vargas F, Lyazidi A, Thille AW, Brochard L. Diaphragm ultrasonography to estimate the work of breathing during non-invasive ventilation. Intensive Care Med. 2012;38(5):796–803.
61. Hutten GJ, van Thuijl HF, van Bellegem AC, van Eykern LA, van Aalderen WM. A literature review of the methodology of EMG recordings of the diaphragm. J Electromyogr Kinesiol. 2010;20(2):185–90.
62. Sinderby C, Beck J, Spahija J, Weinberg J, Grassino A. Voluntary activation of the human diaphragm in health and disease. J Appl Physiol (Bethesda, MD: 1985). 1998;85(6):2146–58.

Chapter 12
Weaning from Ventilation

Xu-Ying Luo and Guang-Qiang Chen

12.1 Introduction

Mechanical ventilation (MV) is a life-saving strategy for critically ill patients, while unnecessarily prolonged ventilation is also associated with risks of ventilator-associated pneumonia (VAP), respiratory muscle weakness, prolonged duration of MV, and increase of hospital mortality [1]. Therefore, weaning from the ventilator should be at the earliest possible time. As an important part of MV, weaning accounts for approximately 40% of the time patients spend on invasive ventilation [2]. It usually refers to discontinuation of MV and extubating of any artificial airway (coma patients excluded), which has been a challenging problem faced by clinicians in the intensive care unit (ICU). Both premature and delay of weaning is associated with adverse outcome [3]. To identify the appropriate time for weaning, some procedures have been proposed, including a screening test of the patient's readiness to weaning and an unassisted breathing trial [4]. Approximately two-thirds of patients could be extubated after their first successful spontaneous breathing trial, and those who failed may need other gradual approaches [5].

12.2 Readiness to Wean from Mechanical Ventilation

It is important to recognize the proper time when patients are ready to be weaned from MV and weaning protocols are associated with a reduction in total time spent on ventilators and ICU stay, compared with usual care [6]. And the weaning process should be started as soon as the patient meets the following criteria [4]:

X.-Y. Luo · G.-Q. Chen (✉)
Department of Critical Care Medicine, Beijing Tiantan Hospital, Capital Medical University, Beijing, China

J. Zhou et al. (eds.), *Respiratory Monitoring in Mechanical Ventilation*,
https://doi.org/10.1007/978-981-15-9770-1_12

- Recovery from the disease for which the patient was ventilated;
- Hemodynamic stability with no need or minimal vasopressors;
- No continuous sedation that may affect the patient's ability to protect the airway;
- Adequate oxygenation defined as PaO_2/FiO_2 ≥150 mmHg requiring positive end-expiratory pressure (PEEP) ≤8 cmH_2O.

Daily screening is commonly recommended as standard care [7]. While, a study conducted by Burns et al. found that more frequent screening was associated with a nonsignificantly shorter time to successful extubation, more successful extubations, and a trend toward shorter hospital stay [8].

Moreover, some parameters have been proposed to predict weaning outcomes, such as rapid shallow breathing test (respiratory frequency/tidal volume, f/VT), maximal inspiratory pressure (MIP), occlusion pressure at 100 ms (P 0.1), respiratory rate, tidal volume, minute volume, and so on. Rapid shallow breathing test is the most commonly used, and a high ratio (f/VT >100–105 breaths/min/L) is associated with a weaning failure [9]. MIP is commonly used to assess the inspiratory muscle strength, and a value of ≤−20 ~ −25 cmH_2O could predict successful weaning. However, the result may be affected by many factors, which may lead to underestimating patients' strength [10, 11]. P 0.1 is related with inspiratory effort: P 0.1 value = 3.5 cmH_2O corresponds to an inspiratory effort of approximately 0.75 J/L. Inspiratory effort values lower than 0.75 J/L could predict successful weaning [12]. While, the accuracy of these predictors remains controversial, and they are not recommended as routine clinical practice [13–15]. Decision-making should be based on the evaluation of the patients.

12.3 Spontaneous Breathing Trials

Spontaneous breathing trials (SBT) are used to evaluate patients' ability to breathe with low-level or without an assist from ventilators. As physicians usually tend to underestimate the possibility of successful weaning, weaning protocols could be used to help to make a decision, which could reduce the time spent on mechanical ventilation and ICU stay [16]. There are four SBT strategies commonly used in the clinical practice, shown as following [17]:

- Synchronized intermittent mechanical ventilation (SIMV);
- Low-level pressure support ventilation (PSV ≤ 7 mmHg);
- Continuous positive airway pressure ventilation (CPAP);
- Unassisted breathing through a T-piece circuit.

The duration of SBT should be at least 30 min and can last up to 120 min to test the patient's tolerance to spontaneous breathing [1, 2]. Theoretically, the endotracheal tube has a respiratory resistance which may increase the patient's breathing work. The use of low-level PSV or CPAP could compensate for the resistance to

breathing through the endotracheal tube [18]. However, Straus et al. reported that a 120-min breathing trial through an endotracheal tube did not increase breathing work [19]. The rate of successful extubation was similar between 30 and 120 min with either T-piece or PSV [3, 20]. It has been recently reported that the success rates of both SBT and extubation in patients with PSV mechanical ventilation mode are higher than that in patients with T-piece ventilation, without increasing the risk of reintubation. This proposes a shorter and less demanding strategy for SBT [18, 21]. For patients with chronic obstructive pulmonary disease (COPD) or heart failure, applying PEEP could decrease both the effort and capillary pulmonary pressure, suggesting that weaning trials without PEEP may expose underlying lung and cardiac dysfunction [22]. So far, the optimal strategy of weaning patients from the ventilator is controversial, which may depend on the condition of patients.

It is important to recognize a failed weaning trial, which may cause cardiopulmonary distress and impairment of respiratory muscles, and ventilator support should be promptly reestablished. The criteria for terminating SBT are shown as following [4, 5, 23, 24]:

- Agitation or anxiety;
- Hypoxemia ($PaO_2 \leq 50$–60 mmHg and $FiO_2 > 0.5$, or $SPO_2 < 90\%$);
- Hypercapnia ($PaCO_2 \geq 50$ mmHg or an increase in $PaCO_2 > 8$ mmHg);
- pH <7.32 or reduced by ≥0.07;
- Tachypnea (respiratory rate >35 breaths/min or increased by ≥20% for more than 5 min);
- Tachycardia (heart rate >140 beats/min; or increased by ≥20%);
- Bradycardia (sustained heart rate decrease ≥20%);
- Hypertension (systolic BP >180 mmHg or increased by ≥20%);
- Hypotension (systolic BP <90 mmHg);
- Severe cardiac arrhythmias.

12.4 Failure of Weaning from the Ventilator

Weaning failure is identified as the failure of SBT or the need for reintubation within 48 h after extubation, occurring in 10–20% of patients [5, 25]. According to the results of the first SBT and length of the weaning process, patients could be classified as following [4]:

Simple Weaning: patient successfully passes the first SBT and is extubated on the first attempt (70% of weaning patients);

Difficult Weaning: patient fails the first SBT, and requires up to three SBT or not more than 7 days from the first SBT to achieve successful weaning (15% of weaning patients);

Prolonged Weaning: The patient requires more than three SBT or more than 7 days of weaning after the first SBT (15% of weaning patients).

It has been proven that prolonged weaning was associated with increased mortality and morbidity in the ICU [26, 27]. Weaning failure is usually caused by the imbalance between the respiratory load and the patient's ability to cope with it [28, 29].

Excess respiratory loads can be caused by an increase of respiratory resistance due to the endotracheal tube and heat and moisture exchange devices in patients undergoing a T-piece SBT, and which could be compensated by the use of low-level PSV or CPAP strategy of SBT [18].

Diaphragmatic dysfunction leading to reduced inspiratory muscle strength is one of the major causes of weaning failure [30, 31]. The diaphragm is the major inspiratory muscle, and its function can be assessed by diaphragm ultrasonography, including diaphragmatic excursion (DE) and diaphragm thickening fraction (DTF). DE is defined as the distance that diaphragm moves during the respiratory cycle [32, 33]. Values of DE ranged from 10 to 14 mm during normal spontaneous breathing and 25 mm for maximal inspiratory effort indicate diaphragmatic dysfunction [34]. DTF reflects the magnitude of diaphragmatic effort and could predict successful weaning. It can be calculated as (thickness at the end-inspiration—thickness at the end-expiration)/thickness at the end of the expiration [35]. A cutoff of DTF more than 30–36% was associated with successful weaning [36, 37].

Cardiac dysfunction can cause a decrease of aeration of the pulmonary parenchyma and pulmonary compliance, and lead to weaning failure. Discontinuation from a ventilator may cause a decrease of the intrathoracic pressure, an increase in the systemic venous pressure gradient, preload and afterload, and result in cardiac dysfunction [38]. An increase of B-type natriuretic peptides (BNP) after discontinuing from the ventilator usually indicates cardiac dysfunction. The BNP-guided weaning strategy could shorten the weaning process compared with the usual medical strategy, although it did not change ICU mortality [39]. Echocardiography could help assess the cardiac function, and pulmonary echography could help assess the status of aeration of the pulmonary parenchyma [40].

Considering the heterogeneity of patients, causes of weaning failure varied. The clinician should comprehensively evaluate the patient and find out reasons. For patients experiencing difficult or prolonged weaning, gradual reduction of ventilatory support could be attempted.

Noninvasive ventilation (NIV) is suggested as an alternative to invasive ventilation for those with COPD, which may reduce the duration of invasive ventilation and mortality [41, 42]. While among other patients the use of NIV remains controversial [43]. Besides, NIV may cause aspiration, gastric distension, and facial skin breakdown, and efficiency is dependent on patients' cooperation. Therefore, NIV is not generally recommended as prophylactic use after extubation [44].

The high-flow nasal cannula (HFNC) can deliver humidified and heated gas at a maximum flow of 50–60 L/min (inspired oxygen fractions up to 95–100%) thereby generate a low level of PEEP, which may reduce breathing work and improve oxygenation compared with conventional oxygen therapy [45]. Patients with hypercapnic respiratory failure and heart dysfunction may benefit from HFNC therapy [46].

However, the evidence supporting its use remains limited, and HFNC is not recommended as a routine therapy.

12.5 Protocolized Weaning

Considering the variation of clinical practice in different ICUs, protocolized weaning is proposed intending to facilitate and standardize the weaning process and reduce MV duration and ICU mortality. Protocolized weaning refers to a written list used to guide discontinuation from the ventilator, including the first two of the following criteria, with or without the third one [6].

A list of criteria for assessing the patient's readiness to discontinue from the ventilator, which should be screened daily.

Structured guidelines for reducing ventilatory support such as SBT or gradual reduction in ventilator support to achieve weaning.

A list of criteria for assessing the patient's readiness to be extubated.

Protocolized weaning could reduce the duration of mechanical ventilation and the length of ICU stay, compared with usual weaning practice [6]. However, the efficiency of weaning protocols may be influenced by the differences in weaning protocols and different healthcare providers, including nurses, respiratory therapists (RTs), and physicians. Considering the wide variety of patient populations, it is necessary to make appropriate weaning protocols for specific types of patients. Furthermore, optimized sedation strategies can also reduce the duration of MV. Therefore, protocolized sedation, daily interruption of sedatives, and intermittent use of sedatives have been recommended [47].

12.6 Extubation

Patients without brain injuries are usually extubated after a successful SBT. Extubation failure is defined as a need for reintubation or ventilatory support within 48 h after scheduled extubation [48]. It may be associated with age, chronic comorbidities, altered consciousness, upper airway function, and lower airway protection [48, 49]. Approximately 10–25% of patients require reintubation or mechanical ventilation after a successful SBT and reintubation is associated with prolonged duration of mechanical ventilation and ICU stay, as well as higher mortality.

Upper airway obstruction after extubation, usually due to laryngeal edema, is one of the main causes of reintubation, occurring in approximately 5–15% of patients [50, 51]. A cuff-leak test (cuff-leak volume <130 mL or 12%) and the presence of risk factors could help identify high-risk patients [52]. Although a positive cuff-leak test could screen for high-risk patients, a negative cuff-leak test cannot rule out the occurrence of upper airway obstruction.

References

1. Esteban A, Anzueto A, Frutos F, et al. Characteristics and outcomes in adult patients receiving mechanical ventilation: a 28-day international study. JAMA. 2002;287:345–55.
2. Esteban A, Ferguson ND, Meade MO, et al. Evolution of mechanical ventilation in response to clinical research. Am J Respir Crit Care Med. 2008;177:170–7.
3. Esteban A, Alia I, Gordo F, et al. Extubation outcome after spontaneous breathing trials with T-tube or pressure support ventilation. Am J Respir Crit Care Med. 1997;156:459–65.
4. Boles JM, Bion J, Connors A, et al. Weaning from mechanical ventilation. Eur Respir J. 2007;29:1033–56.
5. Esteban A, Frutos F, Tobin MJ, et al. A comparison of four methods of weaning patients from mechanical ventilation. N Engl J Med. 1995;332:345–50.
6. Blackwood B, Burns KE, Cardwell CR, et al. Protocolized versus non-protocolized weaning for reducing the duration of mechanical ventilation in critically ill adult patients. Cochrane Database Syst Rev. 2014;11:CD006904.
7. Burns KEA, Raptis S, Nisenbaum R, et al. International practice variation in weaning critically ill adults from invasive mechanical ventilation. Ann Am Thorac Soc. 2018;15:494–502.
8. Burns KEA, Wong JTY, Dodek P, et al. Frequency of screening for weaning from mechanical ventilation: two contemporaneous proof-of-principle randomized controlled trials. Crit Care Med. 2019;47(6):817–25.
9. Yang KL, Tobin MJ. A prospective study of indexes predicting the outcome of trials of weaning from mechanical ventilation. N Engl J Med. 1991;324(21):1445–50.
10. Caruso P, Friedrich C, Denari SD, et al. The unidirectional valve is the best method to determine maximal inspiratory pressure during weaning. Chest. 1999;115:1096–101.
11. Multz AS, Aldrich TK, Prezant DJ, et al. Maximal inspiratory pressure is not a reliable test of inspiratory muscle strength in mechanically ventilated patients. Am Rev Respir Dis. 1990;142:529–32.
12. Laghi F. Assessment of respiratory output in mechanically ventilated patients. Respir Care Clin N Am. 2005;11:173–99.
13. Truwit JD, Marini JJ. Validation of a technique to assess maximal inspiratory pressure in poorly cooperative patients. Chest. 1992;102:1216–9.
14. Tanios MA, Nevins ML, Hendra KP, et al. A randomized, controlled trial of the role of weaning predictors in clinical decision-making. Crit Care Med. 2006;34:2530–5.
15. Conti G, Montini L, Pennisi MA, Cavaliere F, Arcangeli A, Bocci MG, et al. A prospective, blinded evaluation of indexes proposed to predict weaning from mechanical ventilation. Intensive Care Med. 2004;30:830–6.
16. Blackwood B, Alderdice F, Burns K, et al. Use of weaning protocols for & reducing duration of mechanical ventilation in critically ill adult patients: Cochrane systematic review and meta-analysis. BMJ. 2011;342:c7237.
17. Peñuelas Ó, Thille AW, Esteban A. Discontinuation of ventilatory support: new solutions to old dilemmas. Curr Opin Crit Care. 2015;21:74–81.
18. Burns KEA, Soliman I, Adhikari NKJ, et al. Trials directly comparing alternative spontaneous breathing trial techniques: a systematic review and meta-analysis. Crit Care. 2017;21:127.
19. Straus C, Louis B, Isabey D, et al. Contribution of the endotracheal tube and the upper airway to breathing workload. Am J Respir Crit Care Med. 1998;157:23–30.
20. Perren A, Domenighetti G, Mauri S, et al. Protocol-directed weaning from mechanical ventilation: clinical outcome in patients randomized for a 30-min or 120-min trial with pressure support ventilation. Intensive Care Med. 2002;28:1058–63.
21. Subirà C, Hernández G, Vázquez A, et al. Effect of pressure support vs T-piece ventilation strategies during spontaneous breathing trials on successful extubation among patients receiving mechanical ventilation a randomized clinical trial. JAMA. 2019;321:2175–82.
22. Cabello B, Thille AW, Roche-Campo F, et al. Physiological comparison of three spontaneous breathing trials in difficult-to-wean patients. Intensive Care Med. 2010;36:1171–9.

23. Hess D. Ventilator modes used in weaning. Chest. 2001;120:474S–6S.
24. Esteban E, Alia I, Tobin MJ, et al. Effect of spontaneous breathing trial duration on outcome of attempts to discontinue mechanical ventilation. Am J Respir Crit Care Med. 1999;159:512–8.
25. MacIntyre NR, Cook DJ, Ely EW, et al. Evidence-based guidelines for weaning and discontinuing ventilatory support. Chest. 2001;120(6):375S–95S.
26. Peñuelas O, Frutos-Vivar F, Fernández C, et al.; for the Ventila Group. Characteristics and outcomes of ventilated patients according to time to liberation from mechanical ventilation. Am J Respir Crit Care Med. 2011;184:430–7.
27. Sellares J, Ferrer M, Cano E, et al. Predictors of prolonged weaning and survival during ventilator weaning in a respiratory ICU. Intensive Care Med. 2011;37:775–84.
28. Frazier SK, Stone KS, Moser D, Schlanger R, Carle C, Pender L, Widener J, Brom H. Hemodynamic changes during discontinuation of mechanical ventilation in medical intensive care unit patients. Am J Crit Care. 2006;15:580–93.
29. Vassilakopoulos T, Zakynthinos S, Roussos C. Respiratory muscles and weaning failure. Eur Respir J. 1996;9:2383–400.
30. Tobin MJ, Laghi F, Brochard L. Role of the respiratory muscles in acute respiratory failure of COPD: lessons from weaning failure. J Appl Physiol. 2009;107:962–70.
31. Matamis D, Soilemezi E, Tsagourias M, et al. Sonographic evaluation of the & diaphragm in critically ill patients. Technique and clinical applications. Intensive Care Med. 2013;39:801–10.
32. Boussuges A, Gole Y, Blanc P. Diaphragmatic motion studied by M-mode ultrasonography: methods, reproducibility, and normal values. Chest. 2009;135:391–400.
33. Petrof BJ, Jaber S, Matecki S. Ventilator-induced diaphragmatic dysfunction. Curr Opin Crit Care. 2010;16:19–25.
34. Zambon M, Greco M, Bocchino S. Assessment of diaphragmatic dysfunction in the critically ill patient with ultrasound: a systematic review. Intensive Care Med. 2017;43:29–38.
35. Summerhill EM, El-Sameed YA, Glidden TJ, et al. Monitoring recovery from diaphragm paralysis with ultrasound. Chest. 2008;133(3):737–43.
36. Ferrari G, De Filippi G, Elia F, et al. Diaphragm ultrasound as a new index of discontinuation from mechanical ventilation. Crit Ultrasound J. 2014;6:8.
37. DiNino E, Gartman EJ, Sethi JM, et al. Diaphragm ultrasound as a predictor of successful extubation from mechanical ventilation. Thorax. 2014;69:423–7.
38. Pinsky MR. Heart lung interactions during mechanical ventilation. Curr Opin Crit Care. 2012;18:256–60.
39. Mekontso Dessap A, Roche-Campo F, Kouatchet A, et al. Natriuretic peptide-driven fluid management during ventilator weaning: a randomized controlled trial. Am J Respir Crit Care Med. 2012;186:1256–63.
40. Bouhemad B, Brisson H, Le-Guen M, et al. Bedside ultrasound assessment of positive end-expiratory pressure-induced lung recruitment. Am J Respir Crit Care Med. 2011;183:341–7.
41. Girault C, Bubenheim M, Abroug F, et al.; VENISE Trial Group Noninvasive ventilation and weaning in patients with chronic hypercapnic respiratory failure: a randomized multicenter trial Am J Respir Crit Care Med. 2011;184:672–679.
42. Ferrer M, Esquinas A, Arancibia F, et al. Noninvasive ventilation during persistent weaning failure: a randomized controlled trial. Am J Respir Crit Care Med. 2003;168:70–6.
43. Perkins GD, Mistry D, Gates S, et al. Effect of protocolized weaning with early extubation to noninvasive ventilation vs invasive weaning on time to liberation from mechanical ventilation among patients with respiratory failure: the breathe randomized clinical trial. JAMA. 2018;320:1881–8.
44. Rochwerg B, Brochard L, Elliott MW, et al. Official ERS/ATS clinical practice guidelines: noninvasive ventilation for acute respiratory failure. Eur Respir J. 2017;50:1602426.
45. Rochwerg B, Granton D, Wang DX, et al. High flow nasal cannula compared with conventional oxygen therapy for acute hypoxemic respiratory failure: a systematic review and meta-analysis. Intensive Care Med. 2019;45:563–72.

46. Roca O, Gonzalo H, Salvador DL, et al. Current evidence for the effectiveness of heated and humidified high flow nasal cannula supportive therapy in adult patients with respiratory failure. Crit Care. 2016;20:109.
47. Barr J, Fraser GL, Puntillo K, et al. Clinical practice guidelines for the management of pain, agitation, and delirium in adult patients in the intensive care unit. Crit Care Med. 2013;41:263–306.
48. Epstein SK, Ciubotaru RL, Wong JB. Effect of failed extubation on the outcome of mechanical ventilation. Chest. 1997;112:186–92.
49. Vallverdu I, Calaf N, Subirana M, et al. Clinical characteristics, respiratory functional parameters, and outcome of a two-hour T-piece trial in patients weaning from mechanical ventilation. Am J Respir Crit Care Med. 1998;158:1855–62.
50. François B, Bellissant E, Gissot V, et al. 12-h pretreatment with methylprednisolone versus placebo for prevention of postextubation laryngeal oedema: a randomised double-blind trial. Lancet. 2007;369:1083–9.
51. Miller RL, Cole RP. Association between reduced cuff leak volume and postextubation stridor. Chest. 1996;110:1035–40.
52. Jaber S, Chanques G, Matecki S, et al. Postextubation stridor in intensive care unit patients. Risk factors evaluation and importance of the cuff-leak test. Intensive Care Med. 2003;29:69–74.